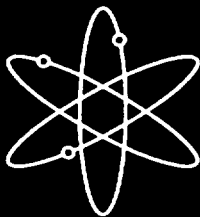


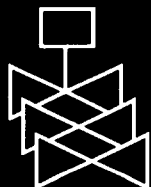
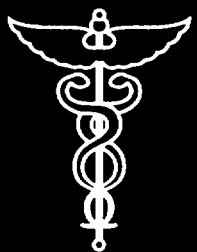
MELCOR Computer Code Manuals



Reference Manuals
Version 1.8.5



Sandia National Laboratories



**Office of Nuclear Regulatory Research
U.S. Nuclear Regulatory Commission
Washington, DC 20555-0001**



NUREG/CR-6119, Vol. 2
Rev. 2
SAND2000-2417/1

MELCOR Computer Code Manuals

Reference Manuals
Version 1.8.5

Manuscript Completed: October 2000
Date Published: December 2000

Prepared by
R.O. Gauntt, R.K. Cole, C.M. Erickson, R.G. Gido,
R.D. Gasser, S.B. Rodriguez, M.F. Young

Sandia National Laboratories
Albuquerque, NM 87185-0744

Division of Systems Analysis and Regulatory Effectiveness
Office of Nuclear Regulatory Research
U.S. Nuclear Regulatory Commission
Washington, DC 20555-0001
NRC Job Code W6203



AVAILABILITY OF REFERENCE MATERIALS IN NRC PUBLICATIONS

NRC Reference Material

As of November 1999, you may electronically access NUREG-series publications and other NRC records at NRC's Public Electronic Reading Room at www.nrc.gov/NRC/ADAMS/index.html.

Publicly released records include, to name a few, NUREG-series publications; *Federal Register* notices; applicant, licensee, and vendor documents and correspondence; NRC correspondence and internal memoranda; bulletins and information notices; inspection and investigative reports; licensee event reports; and Commission papers and their attachments.

NRC publications in the NUREG series, NRC regulations, and *Title 10, Energy*, in the Code of *Federal Regulations* may also be purchased from one of these two sources.

1. The Superintendent of Documents
U.S. Government Printing Office
P. O. Box 37082
Washington, DC 20402-9328
www.access.gpo.gov/su_docs
202-512-1800
2. The National Technical Information Service
Springfield, VA 22161-0002
www.ntis.gov
1-800-533-6847 or, locally, 703-805-6000

A single copy of each NRC draft report for comment is available free, to the extent of supply, upon written request as follows:

Address: Office of the Chief Information Officer,
Reproduction and Distribution
Services Section
U.S. Nuclear Regulatory Commission
Washington, DC 20555-0001

E-mail: DISTRIBUTION@nrc.gov

Facsimile: 301-415-2289

Some publications in the NUREG series that are posted at NRC's Web site address www.nrc.gov/NRC/NUREGS/indexnum.html are updated periodically and may differ from the last printed version. Although references to material found on a Web site bear the date the material was accessed, the material available on the date cited may subsequently be removed from the site.

Non-NRC Reference Material

Documents available from public and special technical libraries include all open literature items, such as books, journal articles, and transactions, *Federal Register* notices, Federal and State legislation, and congressional reports. Such documents as theses, dissertations, foreign reports and translations, and non-NRC conference proceedings may be purchased from their sponsoring organization.

Copies of industry codes and standards used in a substantive manner in the NRC regulatory process are maintained at—

The NRC Technical Library
Two White Flint North
11545 Rockville Pike
Rockville, MD 20852-2738

These standards are available in the library for reference use by the public. Codes and standards are usually copyrighted and may be purchased from the originating organization or, if they are American National Standards, from—

American National Standards Institute
11 West 42nd Street
New York, NY 10036-8002
www.ansi.org
212-642-4900

The NUREG series comprises (1) technical and administrative reports and books prepared by the staff (NUREG-XXXX) or agency contractors (NUREG/CR-XXXX), (2) proceedings of conferences (NUREG/CP-XXXX), (3) reports resulting from international agreements (NUREG/IA-XXXX), (4) brochures (NUREG/BR-XXXX), and (5) compilations of legal decisions and orders of the Commission and Atomic and Safety Licensing Boards and of Directors' decisions under Section 2.206 of NRC's regulations (NUREG-0750).

DISCLAIMER: This report was prepared as an account of work sponsored by an agency of the U.S. Government. Neither the U.S. Government nor any agency thereof, nor any employee, makes any warranty, expressed or implied, or assumes any legal liability or responsibility for any third party's use, or the results of such use, of any information, apparatus, product, or process disclosed in this publication, or represents that its use by such third party would not infringe privately owned rights.

Abstract

MELCOR is a fully integrated, engineering-level computer code that models the progression of severe accidents in light water reactor nuclear power plants. MELCOR is being developed at Sandia National Laboratories for the U.S. Nuclear Regulatory Commission as a second-generation plant risk assessment tool and the successor to the Source Term Code Package. A broad spectrum of severe accident phenomena in both boiling and pressurized water reactors is treated in MELCOR in a unified framework. These include thermal-hydraulic response in the reactor coolant system, reactor cavity, containment, and confinement buildings; core heatup, degradation, and relocation; core-concrete attack; hydrogen production, transport, and combustion; fission product release and transport behavior. Current uses of MELCOR include estimation of severe accident source terms and their sensitivities and uncertainties in a variety of applications.

This publication of the MELCOR computer code manuals corresponds to MELCOR 1.8.5, released to users in October 2000. Volume 1 contains a primer that describes MELCOR's phenomenological scope, organization (by package), and documentation. The remainder of Volume 1 contains the MELCOR User's Guides, which provide the input instructions and guidelines for each package. Volume 2 contains the MELCOR Reference Manuals, which describe the phenomenological models that have been implemented in each package. A new volume, Volume 3 of this publication presents a portfolio of test and sample problems consisting of both analyses of experiments and of full plant problems.

Contents

Volume 2: Reference Manuals

The following chapters are found in Volume 2 of this code manual set.

BWR Bottom Head (BH) Package Reference Manual

Burn (BUR) Package Reference Manual

Cavity (CAV) Package Reference Manual

Condenser (CND) Package Reference Manual

Core (COR) Package Reference Manual

Control Volume Hydrodynamics-Flow Path (CVH/FL) Package Reference Manual

Control Volume Thermodynamics (CVT) Package Reference Manual

Decay Heat (DCH) Package Reference Manual

Fan Cooler (FCL) Package Reference Manual

Fuel Dispersal (FDI) Package Reference Manual

Heat Structures (HS) Package Manual

Material Properties (MP) Package Manual

NonCondensable Gas (NCG) and Water (H₂O) Package Reference Manual

Passive Autocatalytic Hydrogen Recombiner (PAR) Package Manual

RadioNuclide (RN) Package Reference Manual

Containment Sprays (SPR) Package Reference Manual

Executive Summary

MELCOR is a fully integrated, engineering-level computer code whose primary purpose is to model the progression of accidents in light water reactor nuclear power plants. A broad spectrum of severe accident phenomena in both boiling and pressurized water reactors is treated in MELCOR in a unified framework. Current uses of MELCOR include estimation of fission product source terms and their sensitivities and uncertainties in a variety of applications.

The MELCOR code is composed of an executive driver and a number of major modules, or packages, that together model the major systems of a reactor plant and their generally coupled interactions. Reactor plant systems and their response to off-normal or accident conditions include:

- thermal-hydraulic response of the primary reactor coolant system, the reactor cavity, the containment, and the confinement buildings,
- core uncovering (loss of coolant), fuel heatup, cladding oxidation, fuel degradation (loss of rod geometry), and core material melting and relocation,
- heatup of reactor vessel lower head from relocated fuel materials and the thermal and mechanical loading and failure of the vessel lower head, and transfer of core materials to the reactor vessel cavity,
- core-concrete attack and ensuing aerosol generation,
- in-vessel and ex-vessel hydrogen production, transport, and combustion,
- fission product release (aerosol and vapor), transport, and deposition
- behavior of radioactive aerosols in the reactor containment building, including scrubbing in water pools, and aerosol mechanics in the containment atmosphere such as particle agglomeration and gravitational settling, and,
- impact of engineered safety features on thermal-hydraulic and radionuclide behavior.

The various code packages have been written using a carefully designed modular structure with well-defined interfaces between them. This allows the exchange of complete and consistent information among them so that all phenomena are explicitly coupled at every step. The structure also facilitates maintenance and upgrading of the code.

Initially, the MELCOR code was envisioned as being predominantly parametric with respect to modeling complicated physical processes (in the interest of quick code execution time and a general lack of understanding of reactor accident physics). However, over the years

as phenomenological uncertainties have been reduced and user expectations and demands from MELCOR have increased, the models implemented into MELCOR have become increasingly best estimate in nature. The increased speed (and decreased cost) of modern computers (including PCs) has eased many of the perceived constraints on MELCOR code development. Today, most MELCOR models are mechanistic, with capabilities approaching those of the most detailed codes of a few years ago. The use of models that are strictly parametric is limited, in general, to areas of high phenomenological uncertainty where there is no consensus concerning an acceptable mechanistic approach.

Current uses of MELCOR often include uncertainty analyses and sensitivity studies. To facilitate these uses, many of the mechanistic models have been coded with optional adjustable parameters. This does not affect the mechanistic nature of the modeling, but it does allow the analyst to easily address questions of how particular modeling parameters affect the course of a calculated transient. Parameters of this type, as well as such numerical parameters as convergence criteria and iteration limits, are coded in MELCOR as sensitivity coefficients, which may be modified through optional code input.

MELCOR modeling is general and flexible, making use of a "control volume" approach in describing the plant system. No specific nodalization of a system is forced on the user, which allows a choice of the degree of detail appropriate to the task at hand. Reactor-specific geometry is imposed only in modeling the reactor core. Even here, one basic model suffices for representing either a boiling water reactor (BWR) or a pressurized water reactor (PWR) core, and a wide range of levels of modeling detail is possible. For example, MELCOR has been successfully used to model East European reactor designs such as the Russian VVER, and RMBK-reactor classes.

This update of the MELCOR computer code manuals corresponds to MELCOR version 1.8.5, released to users in October 2000. The new version contains many new modeling features as well as improvements to existing models. New models include an iodine chemistry model, a passive autocatalytic recombiner model, many improvements to the core degradation modeling, updates to several of the code default values, improvements to the hygroscopic aerosol model, and enhancements to both the user control function feature and plotting features.

While the new MELCOR release provides many improvements over the previous version, post-MELCOR 1.8.5 development activities continue, with a particular focus on further improvements to the core degradation modeling, including incorporating the core/baffle structure into the COR package and improving the modeling of crusts and molten pool regions, both to achieve a better simulation for the TMI-2 accident progression. Core reflood modeling is also in progress.

The MELCOR 1.8.5 code manuals are contained in two volumes. Volume 1 contains a primer that describes MELCOR's phenomenological scope, organization (by package), and

documentation. The remainder of Volume 1 contains the MELCOR User's Guides, which provide the input instructions and guidelines for each package. Volume 2 contains the MELCOR Reference Manuals, which describe the phenomenological models that have been implemented in each package. A new volume to this publication is added with the MELCOR 1.8.5 release that contains a portfolio of sample demonstration problems. These problems are a combination of experiment analyses, which illustrate code model performance against data, and full plant analyses showing MELCOR's performance on larger realistic problems.

Acknowledgments

The current authors of these revised MELCOR manuals would like to acknowledge the substantial contributions made over the past 15 years by the many previous MELCOR project members. The complete list of historical participants and contributors is far too lengthy to repeat here, and no such attempt will be made. The current release of MELCOR 1.8.5 was achieved with the help and participation of the following individuals:

Randall K. Cole	code development and testing	SNL
Salvador Rodriguez	code development and testing	SNL
Michael F. Young	code development and testing	SNL
Christine Erickson	configuration management	SNL
Ronald D. Gasser	code application and user support	SNL
Richard Gido	configuration management and user support	SNL
Mary Lou Garcia	secretarial support	SNL
Randall O. Gauntt	project leader and technical manager	SNL

Bottom Head (BH) Package Reference Manual

The Bottom Head (BH) package calculates the thermal response of the lower plenum debris, the heatup of the reactor vessel bottom head, and the release of core and structural materials from the reactor vessel to the drywell. Calculations are initiated for most accident sequences when sufficient core debris is present in the lower plenum to establish a debris bed. Materials subsequently relocated downward from the core region (solids and liquids) are added to the upper surface of the bed. Materials released from the lower plenum via penetration failures or bottom head creep rupture are transferred to the containment drywell. Metal/water reactions within the bed due to the entrance of steam are calculated.

The basic BH package models were originally developed by Larry J. Ott at Oak Ridge National Laboratory (ORNL) for use with the Boiling Water Reactor Severe Accident Response (BWRSAR) Code. In this form, they have been applied in accident analyses for the Containment Performance Improvement (CPI) Program and the Mark I shell survivability study, and in assessments of candidate accident management strategies (NUREG/CR-5869). Subsequently, these models have been modified first to operate independently and then to operate (with restart capability) while driven directly by MELCOR in an interactive mode. When exercised with MELCOR, these models constitute the working level routines of the BH package.

This document provides a description of the physical models employed in the BH package. Section 1 discusses the control volume arrangement for the lower plenum debris bed and the nodalization of the bottom head wall. Section 2 describes the method of setting composition-dependent properties for the debris bed control volumes. Section 3 addresses the calculation of heat transfer and metal oxidation within the debris.

Information concerning the formation of eutectic mixtures and the relocation of molten materials within the bed is provided in Section 4. Section 5 describes the models for failure of the bottom head penetrations or creep rupture of the vessel wall. Some examples of calculated results are discussed in Section 6.

BH Package Reference Manual

Section 7 describes the special BH package models that have been developed for use in cases where water is present in the lower plenum together with a debris bed.

Section 8 explains the basic organization of the BH package and the arrangements for exchange of information between this package and MELCOR. Section 9 describes the organization and operation of the MELCOR interface subroutines and discusses special logic provided for interface transactions when the BH package is operational. These include movement of materials associated with shroud melting, debris relocations from the reactor vessel to the containment, and accurate representation of fission product releases within the lower plenum debris bed.

Arrangements to extend applicability of the BH package to the Simplified Boiling Water Reactor (SBWR) design are discussed in Section 10. This involves the use of several special subroutines that include proprietary information. Accordingly, none of these special routines are included with the general MELCOR releases.

The operations of the automatic mass and energy balances, both internal to the BH package and for the other packages of MELCOR when the BH package is used, are described in Section 11.

The BH package may also be applied to PWR designs. The differences in code logic and special guidelines with respect to the preparation of BH package input are discussed in Section 12.

The references cited in the text are listed in Section 13.

Some special measures must be taken in order to run MELGEN and MELCOR with the BH package activated. Procedures for accomplishing this and a description of the associated user-input quantities are provided in the BH Package Users' Guide.

Contents

1.	Introduction	9
1.1	Structure of the Debris Bed	19
1.1.1	Arrangement of Control Volumes.....	21
1.1.2	Initial Setup of Layers One and Two.....	22
1.1.3	The Special Case of Bottom Head LOCA.....	23
1.1.4	Establishing the Third Debris Layer	25
1.2	The Vessel Bottom Head Wall	26
2.	Composition-Dependent Properties	32
2.1	Debris Porosity	32
2.2	Density	32
2.3	Specific Heat	37
2.4	Thermal Conductivity.....	41
2.5	Properties of Alloy Constituents	46
3.	Debris Heat Transfer and Oxidation.....	47
3.1	Heat Transfer Between Bed Control Volumes	47
3.2	Heat Transfer with the Vessel Atmosphere.....	51
3.2.1	Surface Heat Transfer Coefficients.....	51
3.2.2	Establishing the Debris Bed Surface Temperatures	54
3.2.3	Exposed Vessel Wall Nodes.....	55
3.3	Radiation to the Lower Plenum Structures.....	56
3.3.1	Heat Transfer Coefficients for Radiation to the Vessel Wall	58
3.3.2	Direct Radiation Exchange	59
3.3.3	After Downcomer Dryout.....	63
3.3.4	Shroud Melting and Relocation.....	63
3.4	Metal-Steam Reaction in the Debris Bed	64
3.4.1	Oxidation of Zirconium	66
3.4.2	Oxidation of Stainless-Steel.....	68
3.4.3	Treatment of Excess Liquids.....	73
3.4.4	User Controls	74
3.4.5	General Effects of Metals Oxidation	74
4.	Debris Melting and Relocation	76
4.1	Material Relocation.....	76
4.2	Formation of Eutectic Mixtures	77
4.3	Adjustment of Control Volume Dimensions.....	86
4.4	Merging of Bed Control Volumes	89
4.4.1	Merging Criteria	90
4.4.2	Merging Process	91
5.	Failure of the Bottom Head	91

BH Package Reference Manual

5.1	Penetration Welds	92
5.2	Instrument Guide Tubes	94
5.3	Ablation Induced by Flow of Molten Material	94
5.3.1	Ablation of the Wall	95
5.3.2	Ablation of the Bottom Debris Layer	100
5.4	Creep Rupture of the Vessel Wall	105
5.5	Gas Blowdown from Vessel	107
6.	Examples of Calculated Results	108
6.1	Initial Debris Bed Configuration	108
6.2	Formation of the Third Debris Layer	110
6.3	Lower Plenum and Bottom Head Response	112
6.4	The Case with Penetration Failures	115
6.5	Tabulated Output	117
6.6	Special Messages	121
7.	Models for Water in the Lower Plenum	122
7.1	Water Depths	124
7.2	Dryout Heat Flux	126
7.2.1	Calculation	127
7.2.2	Application to Bed Radial Zones	129
7.2.3	Limited Water Availability	133
7.2.4	Experimental Evidence for Oxidic Debris Bed Quenching	133
7.3	Effects of Hydrogen Generation	135
7.3.1	Metal-Steam Reaction Rate	135
7.3.2	Effect on Dryout Heat Flux	137
7.4	Heat Transfer at the Bed Surface	138
7.4.1	Critical Heat Flux	138
7.4.2	Film Boiling Coefficient	139
7.4.3	Nucelate Boiling Coefficient	140
7.5	Heat Transfer at Exposed Wall Nodes	143
7.6	The Case of Lower Plenum Water with Penetration Failures	143
7.6.1	Water Flow	144
7.6.2	Steam Generation	145
7.6.3	Hydrogen Generation	146
7.6.4	Exit Conditions	147
7.7	Interaction of Water with Late Debris Pours	148
7.8	Special Printed Output	151
8.	Package Organization	151
8.1	Arrangement of Subroutines and Commons	152
8.2	Information Exchange with MELCOR	161
8.2.1	Calls to BHQSLU	161
8.2.2	Calls to BHPENF	170

8.2.3	Special Requirements for MELCOR Input	171
8.2.4	Deactivating the BH Package	173
9.	The MELCOR Interface	174
9.1	Interface Organization	174
9.2	MELCOR Core Boundary Modeling Enhancements	175
9.2.1	Introduction	175
9.2.2	Core Boundary Model Prior to Lower Plenum Dryout	176
9.2.3	Core Boundary Model After Lower Plenum Dryout	177
9.2.4	Core Boundary Model After Lower Core Shroud Failure	179
9.3	Interface Modifications for Debris Relocations from the Vessel to Containment	186
9.4	Fission Product Release from the BH Package Debris Bed	188
9.5	Interface Modifications for the MELCOR Energy Balances	190
10.	Application to the SBWR	190
11.	Mass and Energy Balances	191
11.1	Debris Mass Balance	191
11.2	Wall Energy Balance	193
11.3	Bed Energy Balance	196
11.4	Energy Balances External to the BH Package	199
11.4.1	Purpose	199
11.4.2	COR Package	200
11.4.3	HS Package	206
11.4.4	Implementation of the BH Package Global Energy Balance	212
11.4.5	EXEC Package	214
12.	PWR Applications	215
12.1	PWR Materials	216
12.2	Special Logic	217
12.3	Guidance for Package Input	218
13.	References	220

List of Figures

Figure 1.1	Identification of BWR Reactor Vessel Internal Components. The Core Plate (Q) Separates the Core Region from the Lower Plenum	12
Figure 1.2	Arrangement of BWR Core, Core Plate, Control Rod Guide Tubes, and Supporting Components	13
Figure 1.3	Mechanical Arrangement of One of the 43 Local Power Range Detector Assemblies. The Annular Gap Clearance Between the In-core Housing Guide Tube and the Instrument Tube Is Specified as 0.40 inches (1.02 cm)	14

BH Package Reference Manual

Figure 1.4	Mechanical Arrangement of the Four Source Range and Eight Intermediate Range Detector In-Core Instrument Assemblies	15
Figure 1.5	Control Rod Guide Tube Spacing and Available Open Flow Area in the BWR Reactor Vessel Lower Plenum.....	16
Figure 1.6	Description of Models and Illustration of Control Volume Structure Employed for the BWR Reactor Vessel Bottom Head Debris Bed	17
Figure 1.7	The BWR Reactor Vessel Bottom Head Accommodates 241 Penetrations and, Therefore, Is Thicker than the Remainder of the Reactor Vessel Pressure Boundary	18
Figure 1.8	The BWR Control Rod Drive Mechanism Assemblies Are Held in Place by Stainless-Steel-to-Inconel Welds at the Upper Ends of the Stub Tubes, whereas the In-Core Instrument Tubes Are Supported by Stainless-Steel-to-Inconel Welds at the Vessel Wall.....	19
Figure 1.9	A Representation (to scale) of the Control Volume Arrangement for the Lower Plenum Debris Bed as Established for a Short-Term Station Blackout Calculation Based upon the Peach Bottom Plant (The Entire Core Has Relocated into the Lower Plenum.).....	20
Figure 1.10	The Reactor Vessel Bottom Head Is Divided into Calculational Nodes Extending to the Downcomer Region	30
Figure 1.11	Each Reactor Vessel Bottom Head Wall Node Is Divided into Three Radial Segments for the Temperature Calculation.....	31
Figure 1.12	The Baffle Plate and Lower Core Shroud Separate the Downcomer Region from the Reactor Vessel Lower Plenum.....	31
Figure 2.1	Material Densities Considered in Calculation of Debris Bed Control Volume Representative Density [9].....	34
Figure 2.2	Material Specific Heats Considered in Calculation of Debris Bed Control Volume Mass-Averaged Specific Heat (from EGG-CDD-5801).....	38
Figure 2.3	Material Thermal Conductivities Considered in Calculation of Debris Bed Control Volume Mass-Averaged Thermal Conductivity [9]	43
Figure 3.1	Arrangement of BWR Reactor Vessel Lower Plenum Structures.....	57
Figure 3.2	Typical Nodalization of the Upper Structures for the Radiative Heat Transfer Within the BWR Lower Plenum	61
Figure 6.1	Initial Configuration of the Lower Plenum Debris Bed and the Initial Bottom Head Wall Temperatures	109
Figure 6.2	Lower Plenum Debris Bed and Vessel Wall Response for the Example Calculation at the Time that Debris Layer Three Is Established.....	111
Figure 6.3	Lower Plenum Debris Bed and Vessel Wall Response at Time 196 Minutes after Scram for the Example Calculation.....	113
Figure 6.4	The Calculated Situation Just Before Bottom Head Creep Rupture for the Case Without Penetration Failures.....	114
Figure 6.5	Results for a Case with Penetration Failures.....	116
Figure 11.1	Energy Transfers Considered in the Energy Balance for the BWR Vessel Bottom Head Wall	195

List of Tables

Table 1.1	Reactor Vessel Control Volumes Considered in the Lower Plenum Debris Bed Calculation	20
Table 1.2	Material Masses (kg) included in the Initial Setup of the Debris Bed Layers for Peach Bottom Short-term Station Blackout.....	22
Table 2.1	Array Elements for Material Densities.....	33
Table 2.2	Array Elements for Solid Material Specific Heats	41
Table 2.3	Array Elements for Material Thermal Conductivities	46
Table 3.1	Surfaces Considered for Heat Transfer with the Vessel Atmosphere.....	52
Table 3.2	Mixture Parameters Returned by subroutine BHST2P	52
Table 3.3	Values of C_1 and C_2 (Reference 12).....	53
Table 3.4	Lower Plenum Debris-to-Wall Heat Transfer Pathways Calculated by the BH Package.....	58
Table 3.5	Lower Plenum Structure Indices.....	60
Table 3.6	Heats of Reaction at 1,700 K.....	69
Table 3.7	Heats of Reaction for FeO Two-Step Pathway	72
Table 4.1	Eutectic Mixture Compositions Determined for the Lower Plenum Debris Bed	78
Table 4.2	Debris Constituents Considered in a Typical Calculation	78
Table 4.3	Constituent Series Employed by Subroutine BHEUTK with Example of Use of Cross-Reference Index for a Pure Species.....	84
Table 4.4	Constituent Series Employed by Subroutine BHEUTK with Example of Use of Cross-Reference Index for a Eutectic Mixture.....	86
Table 4.5	Cylindrical Coordinates of Boundary Points for Debris Bed Control Volume (I,J)	87
Table 4.6	Heat Transfer Geometric Parameters Recalculated in BHDCHA Whenever the Debris Bed Is Reconfigured	89
Table 5.1	User-Input Parameters Affecting the Vessel Wall Temperature Calculation ..	95
Table 6.1	Material Masses (kg) Included in the Initial Setup of the Debris Bed Layers for Peach Bottom Short-Term Station Blackout.....	110
Table 6.2	Material Masses (kg) at the Initial Setup of Debris Bed Layer Three for Peach Bottom Short-Term Station Blackout.....	112
Table 6.3	Material Masses Included in Debris Bed.....	115
Table 6.4	Example Showing Format of Second Page of Printed Output.....	120
Table 7.1	Typical Values of the IT and IVLP Arrays after Bed Settling and Control Volume Merging	125
Table 7.2	Example Results for the Dryout Heat Flux Calculation	128
Table 7.3	Effect of Debris Temperature Upon Boiling Power	130
Table 7.4	Empirical Fits for the Critical Heat Flux.....	139
Table 7.5	Empirical Fits for the Nucleate Boiling Calculation	141
Table 7.6	Surface Heat Transfer Parameters and Calculated Results.....	141
Table 7.7	Example Results for Water Cooling of the Central Radial Zone.....	142
Table 8.1	BH Package Subroutine Organization	152

BH Package Reference Manual

Table 8.2 Purpose of BH Package Subroutines	155
Table 8.3 Cross-Reference Index of Subroutines and Commons	157
Table 8.4 Cross-reference Index of Commons and Subroutines.....	159
Table 8.5 The User Must Override MELCOR Default COR Package Input to Permit Lower Plenum Dryout	173
Table 9.1 Purpose of BH Package Interface Subroutines	175
Table 9.2 BH to CAV Material Mapping	187
Table 10.1 BH Package Subroutine Equivalents for Application to Conventional BWRs and to the SBWR	190
Table 12.1 BH Package Subroutine Equivalents for Lower Plenum Response Calculations	216
Table 12.2 Component Mass Fractions for Stainless-steel and the TMI-2 Iconel	216
Table 12.3 Guidance for Use of Certain BH Package Input Parameters for PWR Applications	218

1. Introduction

Boiling Water Reactors (BWRs) have unique features (Figure 1.1 and Figure 1.2) for which special models must be provided if best-estimate accident calculations are to be performed. The Boiling Water Reactor Severe Accident Technology (BWRSAT) Program at ORNL has developed and incorporated into its BWRSAR code several advanced models for application to BWR accident analyses [1, 2, 3]. All of these models have been made publicly available as they were developed, tested, and used in ongoing BWR accident studies at Oak Ridge. Many, particularly the earlier models applicable to the period of the accident sequence before relocation of core material into the lower plenum, have been incorporated into other codes such as MELCOR. The lower plenum debris bed formation and behavior models, however, have remained unique to the BWRSAR code until recently.

It is the purpose of this section to explain the operation of the models that establish the lower plenum debris bed from the materials and associated energies passed from the core region through the core plate. The discussion begins with a brief description of the structures within the BWR lower plenum and the numerous penetrations of the bottom head itself. The illustrative dimensions are those applicable to the 6.38 m (251 in.) ID BWR-4 reactor vessel installed at 1067 MWe plants such as Peach Bottom and Browns Ferry.

The portion of the BWR reactor vessel below the elevation of the core plate is formed by a cylindrical section joined with a hemispherical section of radius 3.19 m (125-1/2 in.). As shown in Figure 1.1 and Figure 1.2, much of the volume immediately beneath the core plate is occupied by the control rod guide tubes. Also passing through this volume are source range, intermediate range, and power range detector assemblies as indicated on Figure 1.3 and Figure 1.4.

Fortunately, the development of BWR reactor vessel lower plenum debris bed models can proceed without the necessity for prior resolution of the numerous uncertainties regarding the means by which relocating core and structural material might pass through the core plate boundary. This is true because the lower plenum models have been established in such a manner that they can be driven by information provided by a separate and independent calculation of material relocation from the core region. This is the approach that has been taken with the lower plenum debris bed and bottom head response models, which in effect are driven by the masses and associated energies entering from the region at and above the core plate. The operation of these models when driven by MELCOR in an interactive mode [4] is described in this Reference Manual.

It is important to recognize, however, that these models are initiated at the time that sufficient solid debris has accumulated within the lower plenum. The argument that the falling heated masses of core debris would be quenched in the reactor vessel lower plenum is buttressed by the geometry of the structures and the large water mass initially

present in the BWR lower head. For the Peach Bottom example, there are 185 control rod guide tubes of 28 cm (11 in.) outer diameter on a 30.5 cm (12 in.) pitch in the vessel lower plenum; thus, within a unit cell, the debris must pass through a 0.032 m^2 (0.340 ft^2) opening (see Figure 1.5) that is 3.66 m (12 ft) in length. This, plus the fact that the initial water mass in the lower plenum (73000–95000 kg [160,000–210,000 lbs], depending on the temperature) is sufficient to completely quench more than one molten core, leads to the conclusion that the relocating debris would be quenched as it falls through the water.

The rate of quench of the relocating debris is determined by algorithms within the MELCOR Core (COR) package. The user must override the default COR package input in order to permit the calculation of lower plenum dryout; this requirement plus other special requirements for user input when using the BH package are described in Section 8.2.3.

As the relocated core material accumulates in the BWR reactor vessel lower plenum, it is expected that the composition of the quenched debris bed would vary with height. Lowermost in the bed would be the debris first relocated into the lower plenum. This normally would comprise mostly metallic debris (control blades, canisters, candled clad and dissolved fuel) that had either accumulated on the core plate before local plate failure or had subsequently relocated downward within the same local region before fuel pellet stack collapse. Higher, within the middle region of the bed, would be the collapsed fuel and ZrO_2 from the central region of the core. The initial local core plate structural failures would cause temporary bursts of steaming as the relocating metallic debris was quenched; however, with the collapse of the central core fuel pellet stacks, a constant heat source (the decay heat associated with the pellets) would be introduced to the lower plenum reservoir, initiating a continuous boiloff of the remaining water.

After lower plenum dryout, the debris bed temperature would increase, causing thermal attack and failure of the control rod guide tube and instrument tube structures in the lower plenum, which the debris would completely surround to a depth of about 3 m (10 ft). Since the control rod drive mechanism assemblies and the control rod guide tubes support the core, the remaining standing outer regions of the core would be expected to collapse into the vessel lower plenum when these support columns fail. Thus, the uppermost portion of the completed lower plenum debris bed should primarily consist of the collapsed metallic and fuel material from the relatively undamaged outer regions of the core. The stainless-steel of the control rod guide tubes and mechanism assemblies, the instrument tubes, and other lower plenum structures would be subsumed into the surrounding debris as they become molten.

The lower plenum debris bed control volume arrangement is illustrated in Figure 1.6 together with a brief summary listing of the models employed for the calculation of the bed response. The vessel bottom head is represented at each debris bed control volume in contact with the wall, while the wall itself is sectioned into three radial segments with the outer segment capable of transferring heat to the containment atmosphere or water pool (for the case of drywell flooding). The debris bed and bottom head representations are described in greater detail in the following sections.

There are more than 200 bottom head penetrations as necessary to accommodate the 185 control rod drive mechanism assembly penetrations, 55 instrument guide tube penetrations, and a 5.1 cm (2 in.) drain line penetration near the low point of the bottom head. The general arrangement of the in-core instrument housings and the stub tubes for the control rod drive mechanism assemblies is indicated in Figure 1.7.

The BWR bottom head is clad with Inconel (thickness 0.32 cm [0.125 in.]), while the control rod drive mechanism assembly and instrument guide tube penetrations are stainless-steel. Cross-sections of the control rod drive mechanism assembly and instrument tube penetrations and their weldments are illustrated in Figure 1.8. Each in-core instrument tube is held in place by an Inconel-to-stainless-steel weld located at the inner surface of the bottom head wall, whereas the control rod drive mechanism assemblies are held in place by similar welds at the upper ends of the Inconel stub tubes. These latter welds would be located about 10 cm (4 in.) within the lower plenum debris bed expected to be formed during an unmitigated BWR accident.

Given the perforated status of the BWR bottom head, it is reasonable to expect that the initial pressure boundary failure after lower plenum debris bed dryout might occur through the vessel penetrations and not by failure of the 21 cm (8-7/16 in.) thick bottom head itself. The question of the mode of bottom head penetration failure will be addressed in Section 5.

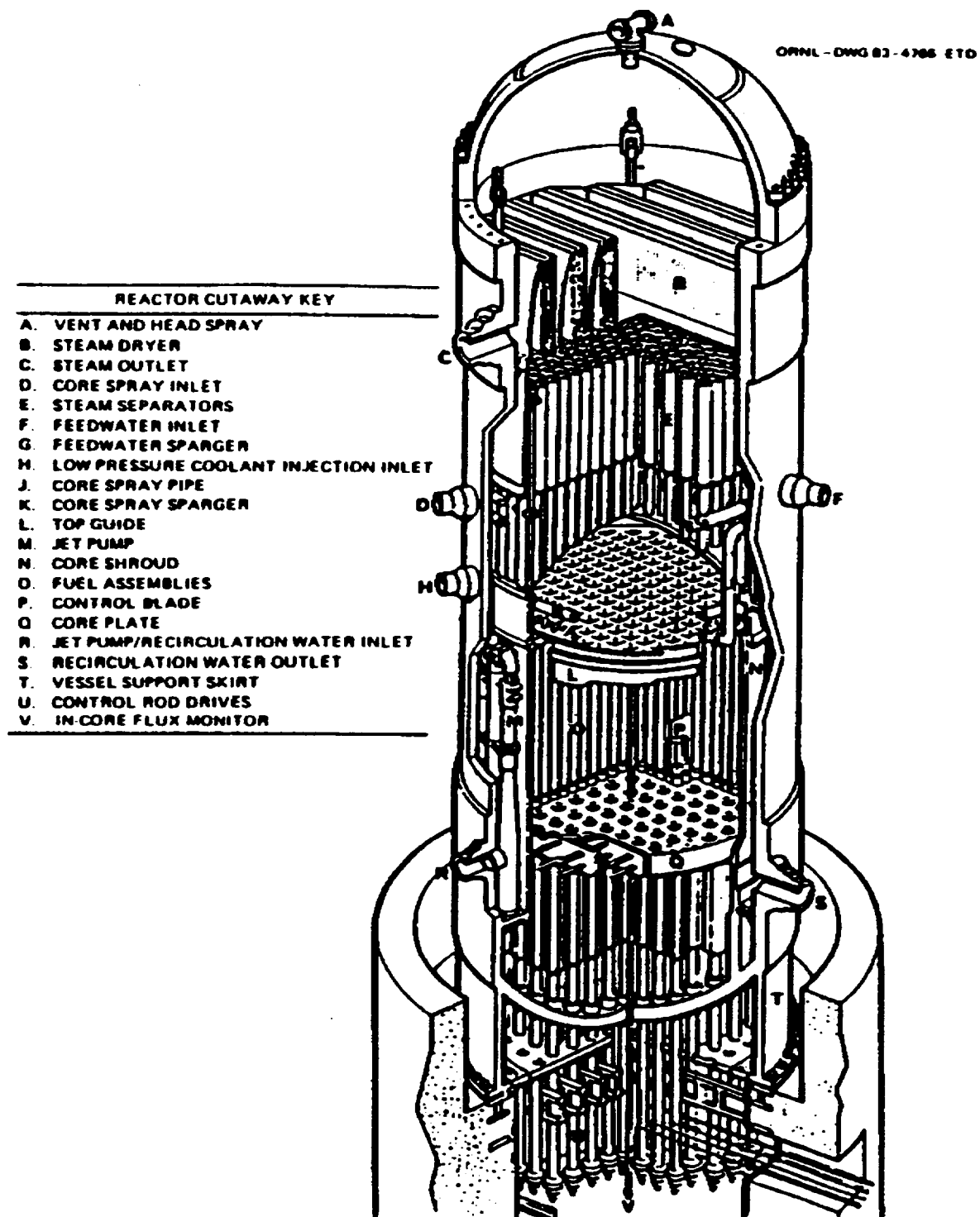


Figure 1.1 Identification of BWR Reactor Vessel Internal Components. The Core Plate (Q) Separates the Core Region from the Lower Plenum

ORNL-DWG 87-4583B ETD

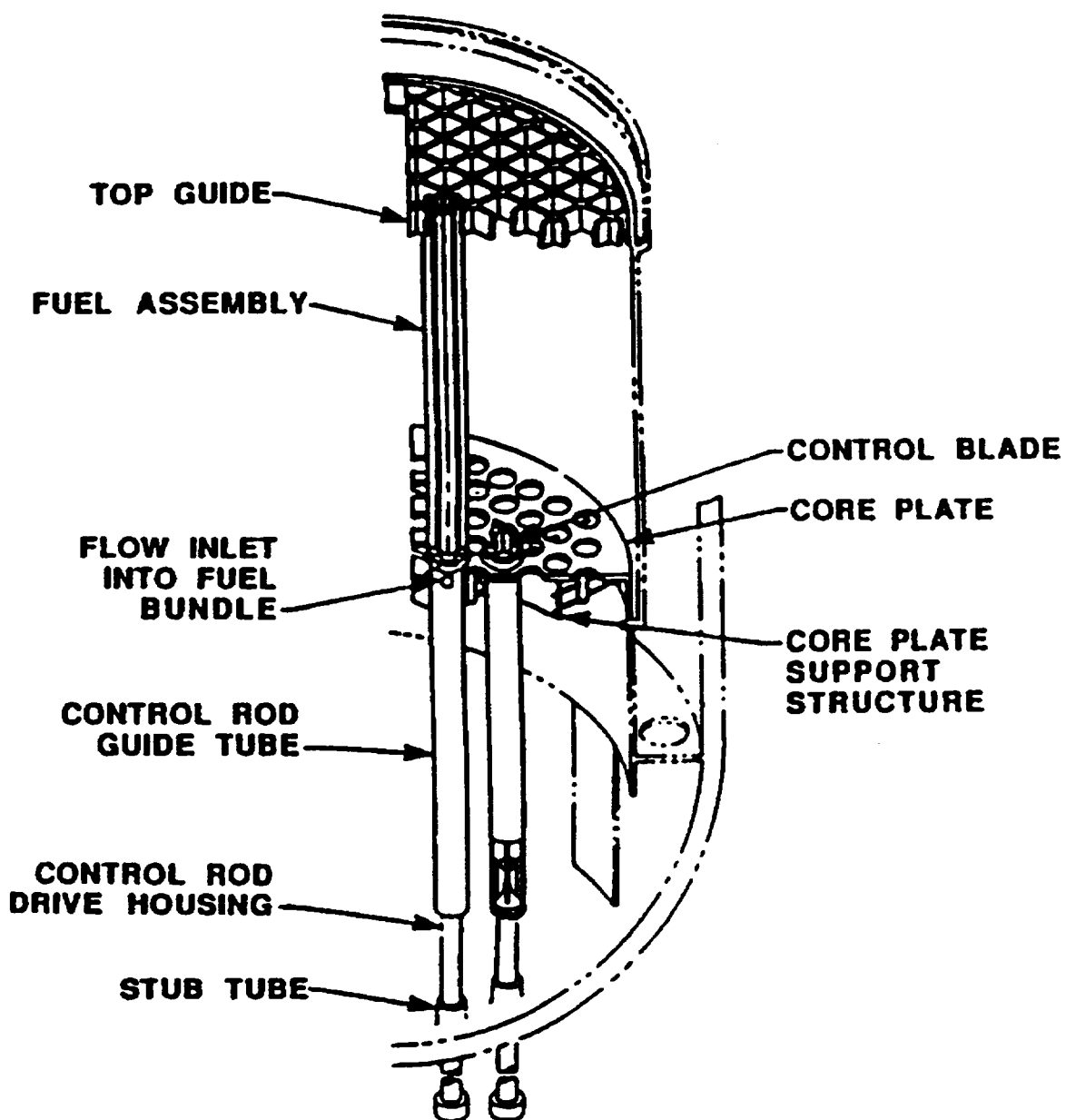


Figure 1.2 Arrangement of BWR Core, Core Plate, Control Rod Guide Tubes, and Supporting Components

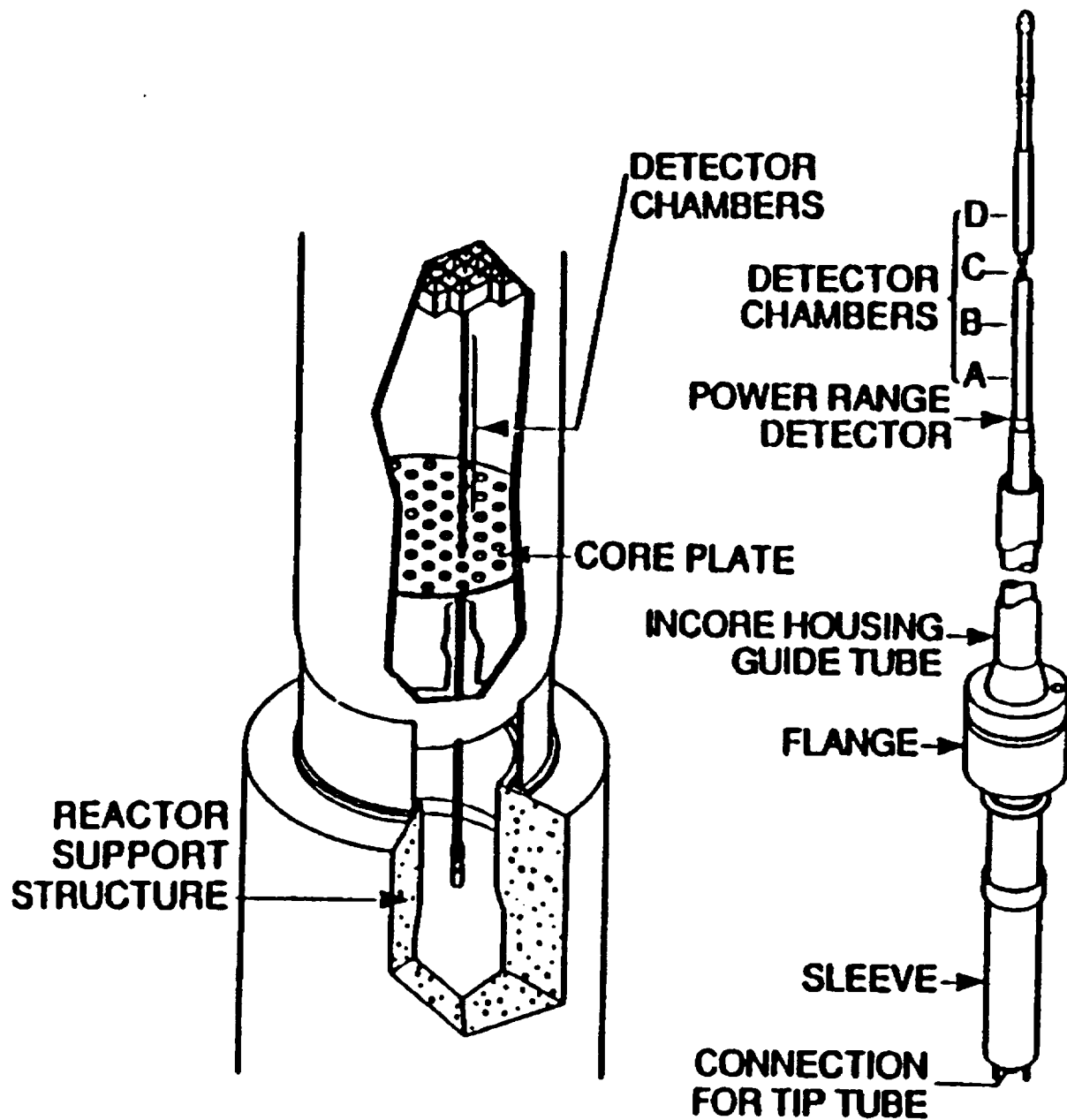


Figure 1.3 Mechanical Arrangement of One of the 43 Local Power Range Detector Assemblies. The Annular Gap Clearance Between the In-core Housing Guide Tube and the Instrument Tube Is Specified as 0.40 inches (1.02 cm)

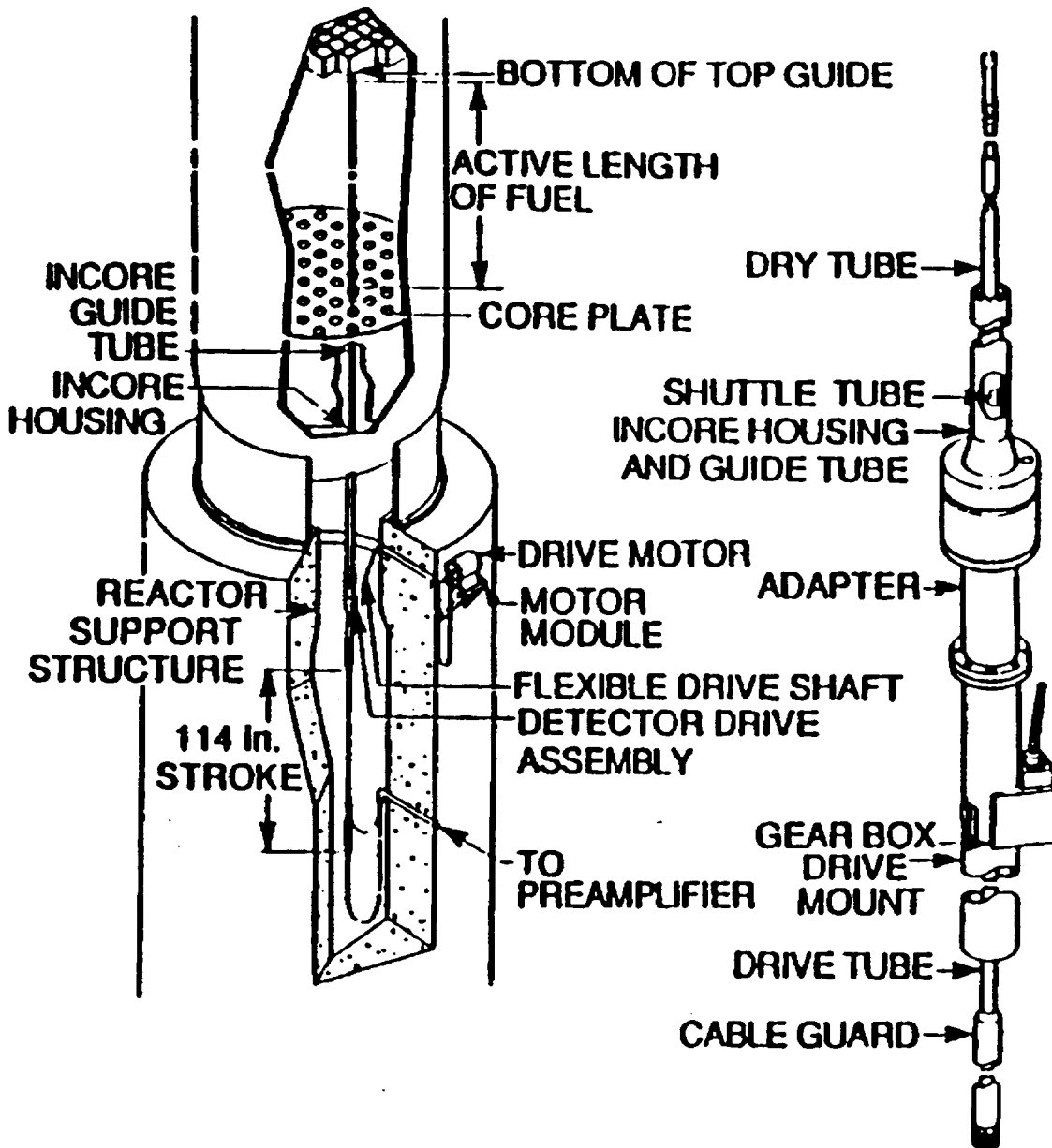


Figure 1.4 Mechanical Arrangement of the Four Source Range and Eight Intermediate Range Detector In-Core Instrument Assemblies

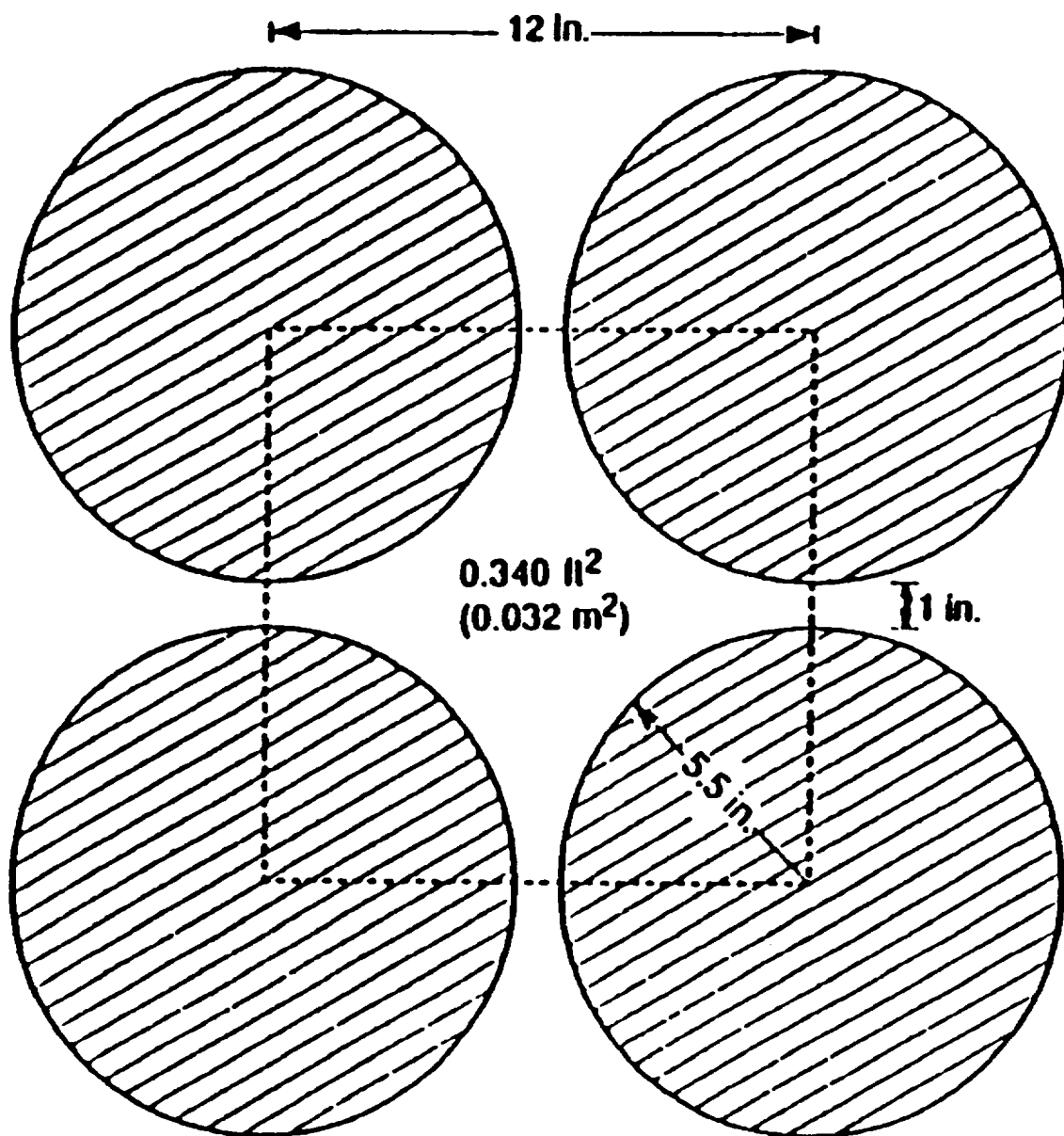


Figure 1.5 Control Rod Guide Tube Spacing and Available Open Flow Area in the BWR Reactor Vessel Lower Plenum

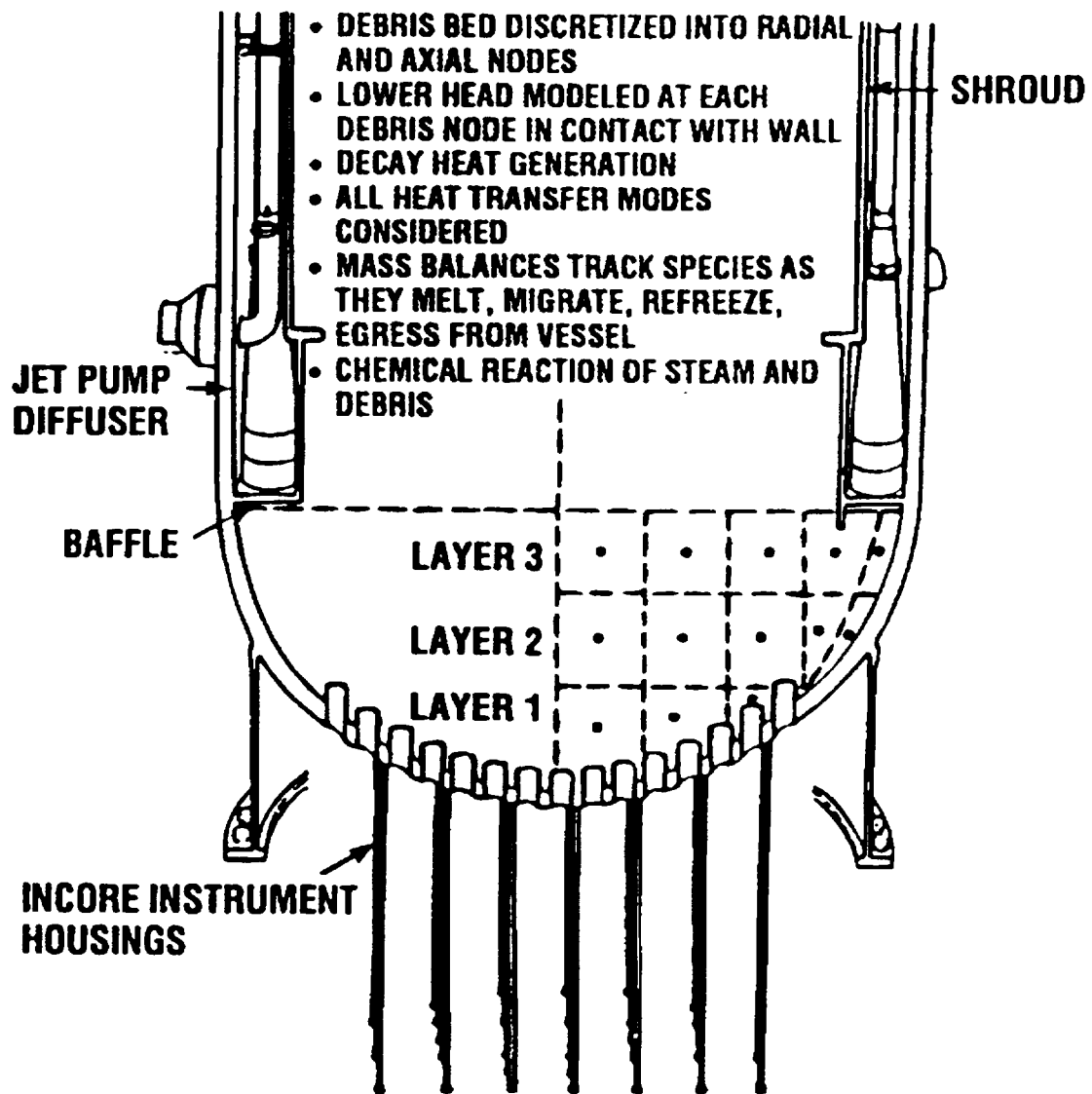


Figure 1.6 Description of Models and Illustration of Control Volume Structure Employed for the BWR Reactor Vessel Bottom Head Debris Bed

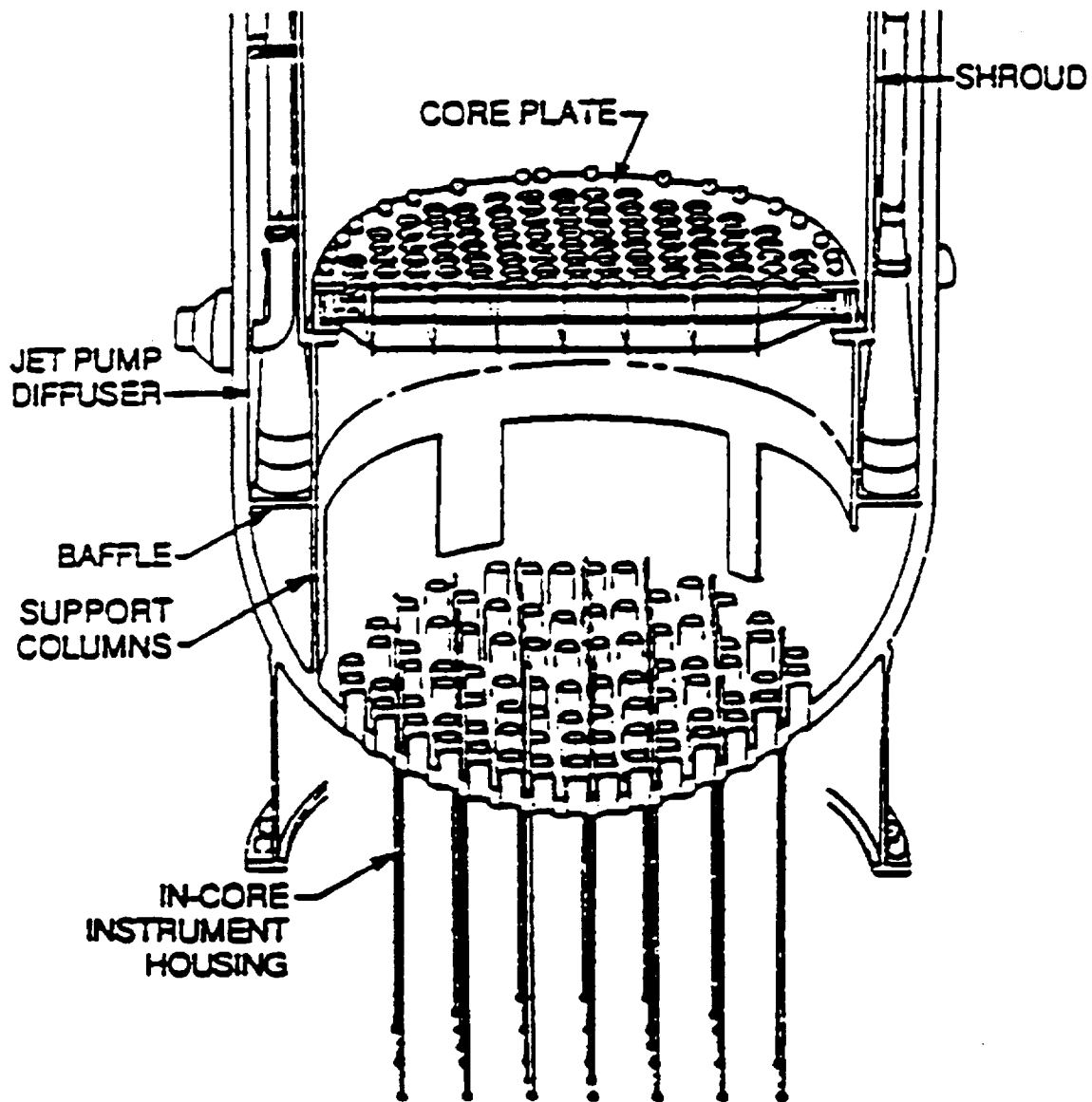


Figure 1.7 The BWR Reactor Vessel Bottom Head Accommodates 241 Penetrations and, Therefore, Is Thicker than the Remainder of the Reactor Vessel Pressure Boundary

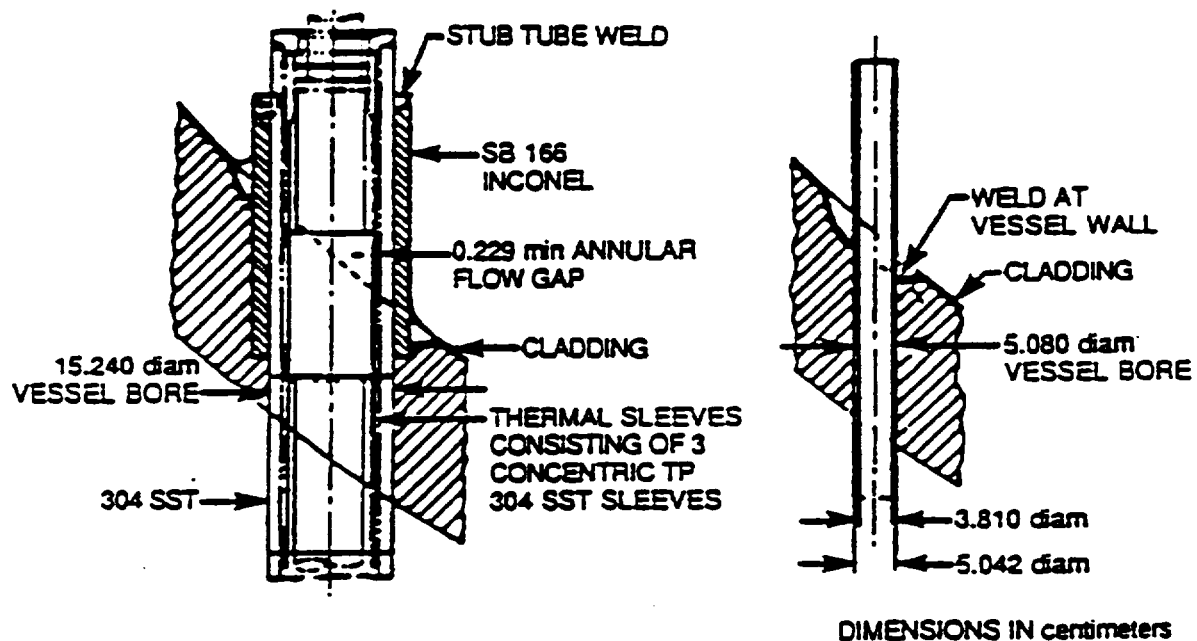


Figure 1.8 The BWR Control Rod Drive Mechanism Assemblies Are Held in Place by Stainless-Steel-to-Inconel Welds at the Upper Ends of the Stub Tubes, whereas the In-Core Instrument Tubes Are Supported by Stainless-Steel-to-Inconel Welds at the Vessel Wall

1.1 Structure of the Debris Bed

The initial structure of the lower plenum debris bed is established in subroutine BHEDN. A drawing of the debris bed control volumes initially employed for a calculation of the late phase of a short-term blackout accident sequence is provided in Figure 1.9. In this calculation, the debris relocations from the core region were predicted by the BWRSAR code. The initial debris bed temperatures were sufficiently high to cause failure of the control rod guide tubes so that the remaining standing portions of the core entered the lower plenum immediately after lower plenum dryout. While this is not expected to be predicted by MELCOR calculations, the results demonstrate a typical arrangement of a whole-core debris bed. The drawing is to-scale, correctly indicating the relative sizes of the calculational control volumes as initially established. These volumes (surfaces of revolution) are listed in Table 1.1.

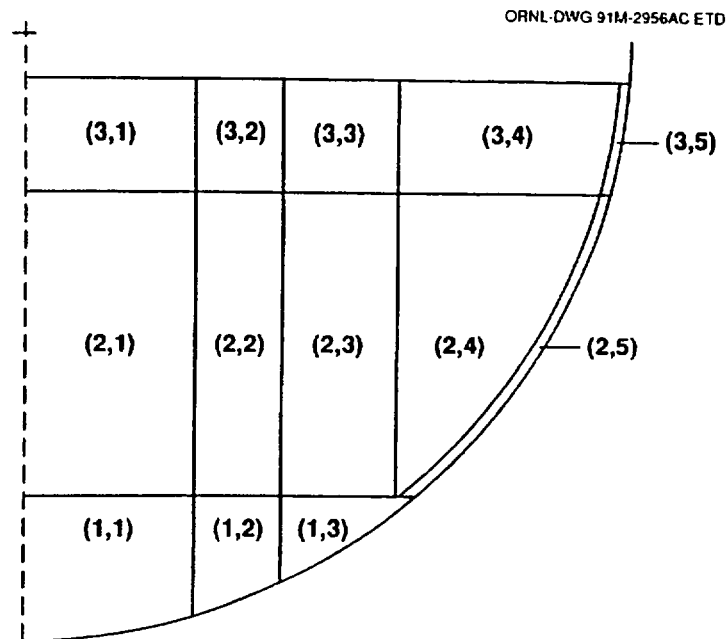


Figure 1.9 A Representation (to scale) of the Control Volume Arrangement for the Lower Plenum Debris Bed as Established for a Short-Term Station Blackout Calculation Based upon the Peach Bottom Plant (The Entire Core Has Relocated into the Lower Plenum.)

Table 1.1 Reactor Vessel Control Volumes Considered in the Lower Plenum Debris Bed Calculation

Nodal Designation	Volume	
	m ³	ft ³
(1,1)	1.784	63.0
(1,2)	1.784	63.0
(1,3)	1.784	63.0
(2,1)	4.117	145.4
(2,2)	5.273	186.2
(2,3)	10.109	357.0
(2,4)	15.889	561.1
(2,5)	1.625	57.4
(3,1)	1.515	53.5
(3,3)	1.937	68.4
(3,2)	3.715	131.2
(3,4)	10.568	373.2
(3,5)	0.597	21.1
TOTAL	60.697	2143.5

It should be noted that the entire debris bed is contained below the center of curvature of the bottom head hemisphere. The volume occupied by the debris is of course dependent upon the assumed bed porosity, which is user-input. Normally, a porosity of 0.40 is employed for the solid oxides and a porosity of 0.34 is employed for the metals; these are considered to be reasonable values based upon the available data [5].

1.1.1 Arrangement of Control Volumes

The lower plenum debris bed model constructs the bed control volumes in the following manner. Record is kept of the accumulation of the different material species as they relocate into the lower plenum, and of their associated internal energies. As many as 20 different material species can be considered.

The first debris layer is intended to comprise the control blade, channel box, and candling clad material that relocates prior to any fuel pellet relocation. While the composition of the first debris layer should be primarily metallic, it includes the small amount of ZrO_2 and UO_2 that was predicted to be carried downward with the candling clad as a eutectic mixture. For this calculation, layers one and two were established at the time of lower plenum dryout. A maximum (lower) height for the first layer can be set by the user, and material present within the lower plenum at the time of dryout that is not included within layer one is used to initiate layer two.

Figure 1.9 shows that the first layer is divided into three control volumes. The vertical interfaces are established so that these three volumes are equal, as indicated in Table 1.1.

The second debris layer begins to be formed at the time that layer one is established and comprises material relocated into the lower plenum from that time forward (until the third layer is initiated [Section 1.1.3]). If, however, the user has chosen to limit the height of the first layer, the excess material above that height that would otherwise have been included with the first layer is instead used to initiate the second layer inventory.

The second layer consists of five control volumes, as shown on Figure 1.9. The vertical interfaces between control volumes (2,1), (2,2), and (2,3) are simple extensions of the interfaces between control volumes (1,1), (1,2), and (1,3). As indicated in Table 1.1, volumes (2,1) and (2,2) are not equal.

Control volume (2,5) is intended to represent the cooler mass of oxidic debris expected to exist close to the heat sink of the bottom head wall. (Such a provision is not considered necessary for the bottom debris layer, since it is relatively small and is intended to represent primarily metallic debris.) User input determines the width of control volume (2,5) perpendicular to the wall.

Finally, the vertical interface between control volumes (2,3) and (2,4) is established so that these volumes are equal. There is, however, a restriction that the radial separation between this vertical (cylindrical) interface and the point of intersection of the inner boundary of control volume (2,5) with the upper surface of layer one must be at least 2.5 cm (1 in.). This is to provide a minimum floor area for control volume (2,4); this restriction is invoked whenever the user chooses to limit the height of layer one, as in this example. As indicated in Table 1.1, control volumes (2,3) and (2,4) are the largest within the second layer of the debris bed.

The vertical interfaces between the layer three control volumes are extensions of the interfaces between the layer two control volumes, as shown on Figure 1.9. The vessel structural masses as they existed at the initiation of the lower plenum debris bed for the recent calculation of Peach Bottom short-term station blackout are outlined in Table 1.2. (Layer three was established immediately after lower plenum dryout in this calculation.)

Table 1.2 Material Masses (kg) included in the Initial Setup of the Debris Bed Layers for Peach Bottom Short-term Station Blackout

Material	Layer 1	Layer 2	Layer 3	Total
Zr	12147.	32349.	5398.	49894.
Fe	12724.	38412.	41797.	92933.
Cr	3095.	9344.	10167.	22605.
Ni	1378.	4164.	4519.	10061.
B ₄ C	269.	753.	84.	1106.
ZrO ₂	837.	11850.	4337.	17024.
FeO	24.	84.	0.	108.
Fe ₃ O ₄	41.	197.	23.	261.
Cr ₂ O ₃	17.	74.	6.	97.
NiO	3.	14.	2.	19.
B ₂ O ₃	6.	15.	0.	20.
UO ₂	892.	120757.	40298.	161947.
Totals	31432.	218013.	106631.	356076.

1.1.2 Initial Setup of Layers One and Two

Now that the control volume arrangement for the whole-core debris bed has been explained, the actual time-dependent debris bed structure that emerges during a typical MELCOR calculation will be described. The following discussion is based upon a short-term station blackout accident sequence with actuation of the automatic depressurization system (ADS). (The special case of accident sequences involving early drainage of the reactor vessel lower plenum will be described in Section 1.1.3.) The modeled plant is Grand Gulf.

MELCOR typically predicts for short-term station blackout that about two-thirds of the core and structural debris has relocated into the lower plenum at the time of bottom head dryout. This debris consists of mixed metals and oxides, since MELCOR does not predict an early series of primarily metallic relocations. This material is apportioned between the bottom and middle debris bed layers; the upper layer is not yet defined. The user can limit the amount of debris included in the bottom layer by use of the input parameter H1MAX (BH0500), which is the maximum permitted height (above vessel zero) of the upper surface of the bottom layer. The size of the lower layer should be limited for MELCOR calculations, since these three bottom control volumes in effect serve as a crust layer.

A reasonable value for H1MAX is 0.6096 m (24 in.) for the Grand Gulf reactor vessel (about 17.5% of the bottom head radius). This causes the middle layer to initially extend from 0.6096 m (24 in.) to 1.8796 m (74 in.) above vessel zero. Should the user choose not to limit the size of the lower layer by setting a large value of H1MAX, then the code logic will still reserve 1% of the debris present at the time of lower plenum dryout to initiate the middle (second) layer.

Thus, the bottom debris layer is completely established at the time of lower plenum dryout and the middle layer is initiated. The bottom head pressure boundary is intact and all debris is in the solid phase. The calculation proceeds to determine the response of these two debris layers and of the vessel bottom head. As additional material (solid or liquid) is relocated downward from the core region, it is added to the middle layer, which continues to grow. Meanwhile, the temperature of the debris within both layers increases, under the impetus of decay heating.

1.1.3 The Special Case of Bottom Head LOCA

For most BWR accident sequences, bottom head dryout would occur only after a lengthy process of heat transfer from quenched debris to water, driven by the decay heating provided by the relocated fission products. Thus a large amount of quenched debris would be present within the lower plenum at the time of dryout to serve as the solid foundation for a lower plenum debris bed, whose size would increase as additional materials (both solid and liquid) were relocated downward from the core region.

It is necessary, however, for the lower plenum debris bed models to also have the capability to calculate the progression of events for accident sequences in which an initiating break occurs in the bottom head penetration assembly welds or the vessel drain lines such that lower plenum dryout occurs before any debris has relocated from the core region. For these scenarios, the MELCOR calculation (with use of the BH package permitted) proceeds as follows:

1. Dryout of the lower plenum due to LOCA.
2. Debris relocates into lower plenum.

BH Package Reference Manual

3. Depending upon user input, the MELCOR COR package may predict release of debris through failed bottom head drain or other penetration failures.
4. When (and if) sufficient solid debris accumulates in the lower plenum to form a debris bed, the BH package is called to perform the lower plenum debris bed and bottom head response calculation for the remainder of the accident sequence.

It should be noted that the lower plenum debris bed and bottom head models will never be called if the loss of debris from the lower plenum as calculated by the MELCOR COR package is such that sufficient solid debris to form a bed does not accumulate within the lower plenum. The operating requirements of the BH package are such that roughly one-fourth of the core mass is required to be present within the lower plenum to permit the debris bed calculation to be initiated. It should be noted, however, that the BH package no longer requires dryout of the lower plenum for transition to the BH package models. The transition is predicated entirely on the debris bed mass criterion.

Certain special features of subroutine BHHEDN address the status of the control rod guide tubes, instrument tubes, and other lower plenum structural steel at the time the lower plenum debris bed is initially established. If MELCOR has predicted that some of this lower plenum structural steel is in the liquid phase at the time the BH package is initiated, then all structural steel beneath the surface of the debris bed will be initially liquid within the BH package. If, in this case, the liquid structural steel mass predicted by MELCOR differs from the structural steel mass underneath the debris bed surface in the BH package initialization, then an adjustment is made in the initial debris temperature as necessary to preserve the debris energy balance.

It is virtually certain that the MELCOR prediction and the BH package determination of the amount of liquid structural steel will differ when the BH package is initiated because MELCOR has no representation of the debris as a bed filling the volume within a portion of the bottom head hemisphere. As an example from an actual calculation, if MELCOR predicts that 7975 kg of structural steel is molten within a debris mass of 105,493 kg then the BH package will determine that the debris will extend to a height of 105 cm within the lower plenum, surrounding 13,679 kg of structural steel, which is in the liquid phase (since the debris temperature is greater than the melting temperature of steel). The debris temperature, 2011 K in the MELCOR calculation will, therefore, be adjusted downward to represent the energy removal necessary to melt 5704 kg of steel. In this case, the temperature difference is 72 K so the BH package is initiated with a debris temperature of 1939 K and with all 13,679 kg of submerged steel in the liquid phase.

If the initial debris temperature provided by MELCOR is below the steel melting temperature (1733 K), then both MELCOR and the BH package consider the lower plenum structural steel to be in the solid phase and no adjustment is necessary. As indicated in the previous section, this is the usual case for non-LOCA accident sequence calculations, where the BH package is initiated at the time of bottom head dryout and all debris present within the lower plenum at that time has been quenched.

Returning to the bottom head LOCA case, if some of the lower plenum structural steel is considered by MELCOR to have escaped from the reactor vessel via the bottom head drain or other penetration failure, then this is recognized when the BH package lower plenum debris bed model is initiated. Specifically, an appropriate amount of additional void is introduced into the debris in place of the steel that would normally be introduced, thereby increasing the local bed porosity. The released steel is considered to have been taken from the bottom of the lower plenum structures upward and the associated voids are introduced into the bottom, middle, and upper debris bed layers, in that order, to the extent necessary to account for the total escaped mass.

Modifications to the BH package associated with MELCOR version 1.8.5 have removed the dry plenum requirement for transition to BH. Therefore, the comments above regarding the quantity of debris resident in the lower plenum volume at the time of transition to BH may no longer be appropriate. The quantity of debris present in the lower plenum at the point of transition to the BH package will essentially be only marginally greater than the minimum required for transition.

1.1.4 Establishing the Third Debris Layer

The upper (third) debris layer will be formed at the time that the temperature of any middle layer control volume exceeds TFAIL2. This temperature parameter is user-input, but subsequently modified (reduced) by code logic as necessary to not exceed the lowest melting temperature of any pure species or eutectic mixture (input record series BH08LL). This modification is necessary since the middle (second) layer must be complete in order to properly account for the movement of liquids within the bed. Note that liquids will be present within the bed upon initial setup for the bottom head LOCA cases discussed in Section 1.1.3; for other cases, the user can also cause the upper layer to be established immediately after lower plenum dryout by setting a low value of TFAIL2 in input (BH0700).

MELCOR does not provide for collapse of all remaining standing portions of the core when temperature TFAIL2 is exceeded. Therefore, the upper layer will initially comprise all of the stainless-steel structure within the lower plenum above the surface of the middle debris layer (as given by the steel volume versus height table entered on Input Record BH04LL), plus any debris that happens to be relocated downward from the core region during the timestep in which the upper layer is established. Subsequently, all relocating debris is added to the third layer. Whether the surface of the upper layer rises or falls as the calculation proceeds depends upon the relative rates of debris addition from the core region and bed settling as a result of material melting and relocation or escape from the vessel via penetration failures. If the bed has settled, debris relocating from the core region is preferentially added to the sunken regions so that the tendency is to restore a level surface. Relocating liquids run into any available interstitial pores of the third layer solid debris whereas relocating solids (with their inherent porosity) are added to the layer surface.

1.2 The Vessel Bottom Head Wall

The nodalization employed for the reactor vessel bottom head wall and the placement of these nodes relative to the debris bed boundary control volumes are shown in Figure 1.10. To facilitate the explanation of the wall configuration, debris bed control volumes (2,5) and (3,5) are shown oversized on Figure 1.10, and the interfaces between control volumes (2,3) and (2,4) and between control volumes (3,3) and (3,4) have been deleted. (The location of these interfaces is shown to scale on Figure 1.9.)

The eight wall nodes placed adjacent to debris bed layer one are allocated as three abutting control volume (1,1), two abutting control volume (1,2), and three abutting control volume (1,3). Bed control volume (2,5) forms the entire wall boundary for debris layer two, and six wall nodes abut this narrow crust control volume. Similarly, bed control volume (3,5) forms the wall (crust) boundary for the relatively small upper debris layer and two wall nodes (numbered 15 and 16 on Figure 1.10) abut this control volume. This arrangement is intended to provide wall nodes of approximately equal length along the wall. Once layer three is established, the wall nodalization does not change during a calculation.

Wall node 17 represents the portion of the wall between the top of debris layer three and the bottom of the shroud baffle. One wall node (node 18 in Figure 1.10) represents the wall adjacent to the water trapped above the shroud baffle in the downcomer region; the upper surface of this last node is at the elevation of the center of curvature of the hemispherical bottom head. (Special provision is made for cases in which the shroud baffle is located less than 0.076 m [three inches] below the center of curvature. Here the length of node 18 is set to 0.076 m and some [or all] of node 18 will extend above the center of curvature.)

Logic within subroutine BHEDN continues to adjust the structure of the second debris layer and the nodal divisions of the adjacent wall until the third layer is established. During the period before the third debris layer is formed, the lower plenum debris bed model simply divides the bottom head wall volume extending from the (moving) upper surface of debris layer two to the bottom of the shroud baffle into three equal nodes. The total number of nodes and the placement of the uppermost wall node adjacent to the downcomer region above the shroud baffle remain the same.

For the purpose of calculating the bottom head wall temperatures, each wall node is divided into three equal-volume segments as shown in Figure 1.11. Heat is transferred from the adjacent debris bed control volumes into the inner segment of each wall node by conduction. Heat transport along and across the wall by conduction from segment-to-segment is also calculated. Exposed inner wall segments above the elevation of the upper debris bed surface receive heat transfer by radiation and convection from the lower plenum atmosphere and by radiation from the upper surfaces of the bed control volumes.

Although not indicated in Figure 1.11, the thickness of the BWR reactor vessel wall increases at some point (plant-specific) between the cylindrical section of the vessel and

the lower portion of the bottom head where the penetrations are located. The vessel wall nodalization established for the bottom head within subroutine BHHEDN recognizes the user-input location of this transition point (HD1D2 [BH0500]) and adjusts the thickness of the wall nodes above and below this location accordingly. Furthermore, the lengths of the two adjacent wall nodes are adjusted (one shortened, one lengthened) so that the transition point falls exactly on their nodal boundary.

The rate of heat transfer from the inner segment of the uppermost wall node (number 18 in Figure 1.10 and Figure 1.11) to the water in the downcomer region is governed by nucleate boiling and conduction through the wall. While water remains, this rate is calculated in subroutine BHHED2 as

$$AH \left[\frac{\frac{TMASJP - THD}{1}}{\frac{HNB}{HNB} + \frac{LH}{2 \times BHAKCS}} \right] \text{ Watts}$$

where

- AH = AHEAD(1,NWALL), inner surface area of wall node NWALL, m²
- HNB = nucleate boiling heat transfer coefficient, W/(m²·K)
- NWALL = index of uppermost wall node
- TMASJP = temperature of downcomer water, K
- THD = THDWO(1,NWALL), temperature of the inner segment of wall node NWALL, K
- LH = XLHEAD(1,NWALL), radial thickness of the inner segment of wall node NWALL, m
- BHAKCS = function BHAKCS(THD), temperature-dependent conductivity of carbon steel, W/(m·K)

The nucleate boiling coefficient HNB is determined by a fit to results calculated by the Rohsenow correlation based upon current pressure and the wall inner surface temperature. This approximate solution is considered adequate since the majority of the resistance to heat transfer lies in the carbon steel conduction path.

Water remains in the downcomer region because of the method of reactor vessel depressurization. Boiling water reactors have an Automatic Depressurization System (ADS) that, upon actuation, causes rapid opening of several (five at Peach Bottom) of the

reactor vessel safety/relief valves (SRVs). The BWR Emergency Procedure Guidelines [6] direct the operators, under accident conditions, to manually actuate the ADS when the core has become partially uncovered (but before any significant core damage has occurred). The flashing attendant to the resulting rapid depressurization of the reactor vessel provides temporary core cooling while causing rapid loss of all water from the core region and core plate dryout. However, much of the cooler water in the downcomer region between the lower core shroud and the vessel wall would not be flashed during this maneuver.

After lower plenum debris bed dryout, the water surrounding the jet pump assemblies in the downcomer region is the only water remaining in the reactor vessel. The proximity of the baffle plate and lower core shroud boundaries of this water-filled region to the bottom head hemisphere is illustrated in Figure 1.12.

In the lower plenum debris bed energy balances, heat transfer by conduction is calculated between the bed control volumes and from the outer bed control volumes to the vessel wall. Additionally, radiation and convection from the bed upper surface to the vessel atmosphere and to intact structures above the bed are considered. Radiation to the lower core shroud from the bed surface, radiation and convection to the lower core shroud from the vessel atmosphere, and axial conduction along the vessel wall all contribute to heating and evaporation of the water trapped in the downcomer region.

While water remains in the downcomer region, the lower core shroud would be maintained at a temperature close to the saturation temperature of the water, which, with the reactor vessel depressurized, would be in the neighborhood of 420 K (296°F). Since this is much lower than the temperature of the upper surface of the debris bed, it is obvious that the core shroud would constitute a major heat sink for radiation from the upper bed.

While the reactor vessel bottom head remained intact, steam generated within the downcomer region would escape from the reactor vessel to the wetwell pressure suppression pool via the SRVs. Reactor vessel bottom head penetration failure would, however, create a leakage pathway from the vessel to the drywell atmosphere via the lower plenum debris bed. The pathway for the steam generated from the water surrounding the jet pumps would be up through the downcomer region, down through the core region, and out through the debris bed, reacting with any available zirconium metal during its passage. Representation of the associated energy release is important in determining the thermal response of the debris bed control volumes, as described in Section 3.4.

In general, dryout of the reactor vessel downcomer region will not be predicted for calculations in which bottom head penetration failures are permitted to occur. As described in Section 5.3, ablation of the vessel bottom head by the flowing debris will induce early failure of the wall and release of all remaining lower plenum debris into the drywell.

For calculations in which bottom head penetration failures are not permitted to occur, however, all liquid debris will be retained within the lower plenum until some portion of the reactor vessel bottom head has been heated (by conduction) to a temperature sufficient to induce local failure by creep rupture. This is a much slower process, and dryout of the downcomer region will be predicted for this case. After the water in the downcomer region has boiled away, the shroud temperature would increase to its melting temperature (1672 K [2550 °F]) and the shroud would melt. The resulting liquid stainless-steel would then enter the debris bed, providing a cooling effect while increasing the volume of the molten pool.

Heat transfer from the outer segment of each wall node to the drywell atmosphere is calculated by the application of convective heat transfer coefficients determined within the Heat Structures (HS) package of MELCOR. Different drywell atmosphere temperatures are used for the portions of the vessel wall above and below the attachment point of the vessel support skirt (shown at the base of node 13 in Figure 1.11 and as item T in Figure 1.1). This is because the temperature of the atmosphere within the pedestal region of the drywell would be much higher than the temperature in the remainder of the drywell, especially after molten debris had begun to leave the vessel. The skirt attachment point (height above vessel zero) is identified by user input HSKIRT (BH0600).

Provision has also been made for use of the BH package to study the effects of drywell flooding as an accident mitigation technique. Briefly, drywell flooding to surround the vessel bottom head with water has been proposed [7,8] as a means to maintain the core debris within the reactor vessel throughout an accident progression that includes formation of a lower plenum debris bed. If the MELCOR calculation predicts that water comes into contact with the outer surface of the reactor vessel, then the pool heat transfer coefficient for the outer surface of each covered wall node is determined as described in the HS Package Reference Manual.

The local heat transfer coefficient and the local heat sink temperature for each wall node outer surface are passed from MELCOR to the BH package by means of array HTCT (2,20) of Common /BHCHED/. Here

$$\text{HTCT}(1,J) = \text{heat transfer coefficient [W/(m}^2\cdot\text{K)]}$$

and

$$\text{HTCT}(2,J) = \text{heat sink temperature (K) at the outer surface of wall node J.}$$

The calculated energy transfer from the outer vessel surface to the drywell atmosphere or surrounding pool is appropriately introduced into the MELCOR calculation of containment response.

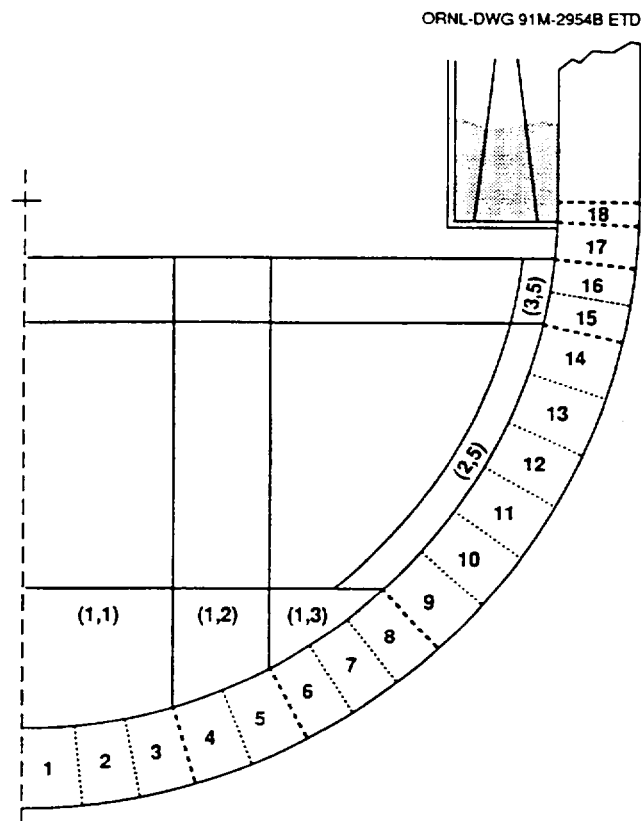


Figure 1.10 The Reactor Vessel Bottom Head Is Divided into Calculational Nodes Extending to the Downcomer Region

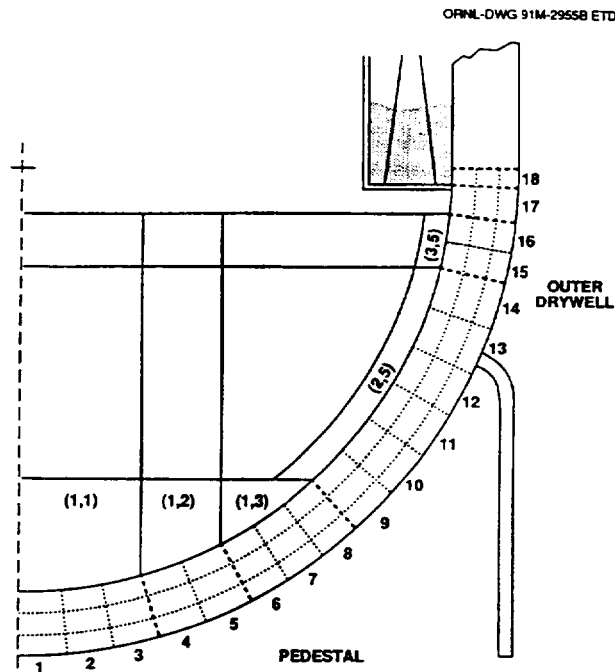


Figure 1.11 Each Reactor Vessel Bottom Head Wall Node Is Divided into Three Radial Segments for the Temperature Calculation

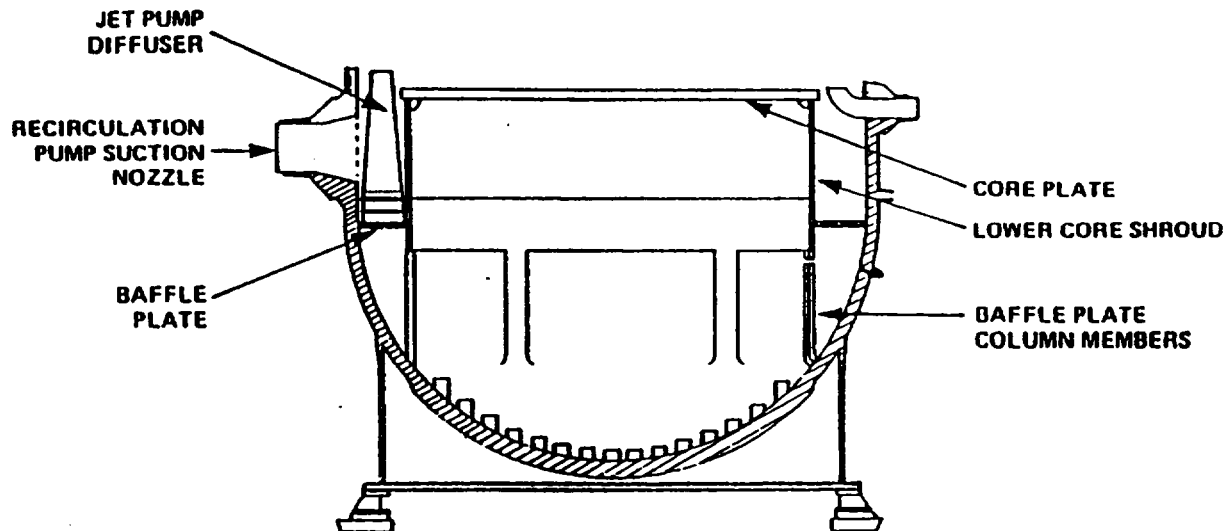


Figure 1.12 The Baffle Plate and Lower Core Shroud Separate the Downcomer Region from the Reactor Vessel Lower Plenum

2. Composition-Dependent Properties

This section provides a discussion of the improvements to the BWR lower plenum debris bed model that have been implemented for use with MELCOR to determine composition-dependent properties for each calculational control volume each timestep. As described previously, the lower-melting temperature metals in the upper portion of the debris bed are predicted to melt during the course of the calculation and to relocate downward into the interstitial voids of the still-solid debris of the bottom layer. Therefore, with the passage of time, the metals-to-oxides ratio decreases in the upper portion of the debris bed and increases in the lower portion. Accordingly, it is the purpose of the code modifications described in the following sections to account for this shifting composition by establishing the representative material properties within each control volume each timestep.

2.1 Debris Porosity

The porosity of the debris within each calculational control volume is established each timestep as derived from the relative masses of solid metals and solid oxides within the volume. The user provides input values (BH0500) of PORBM and PORBOX as the porosities of metallic and oxidic debris, respectively. The representative porosity for an individual control volume is then

$$\varepsilon = \frac{\text{oxide mass} \times \text{PORBOX} + \text{metals mass} \times \text{PORBM}}{\text{oxide mass} + \text{metals mass}}$$

which is the mass-averaged value.

Typical input values are PORBOX = 0.40 and PORBM = 0.34. The effect of these input quantities upon the total calculated debris bed volume is substantial.

The individual control volume mass-averaged porosities are calculated in subroutine BHED2 and stored in the array PORB(I,J), where I is the index of the debris layer (I = 1,3) and J is the index of the control volume within the layer (J = 1,5). (It should be noted from Figure 1.9 that the debris bed model considers five control volumes in the upper layer, five control volumes in the middle layer, and three control volumes in the bottom layer for a total of thirteen. Thus, there are no control volumes [1,4] or [1,5].) If liquid material exists within a control volume, the (available) porosity for the solid material within that control volume is appropriately reduced.

2.2 Density

A representative density is calculated each timestep for each debris bed control volume, based upon the relative masses of each debris constituent within the control volume.

The mass of each debris constituent within a bed control volume (I,J) is contained within the array

AML*P*(I,J,K,M)

where

K = the constituent index (K = 1,20) and

M = the phase index (M = 1,2).

As indicated, there are 20 slots (index K) reserved within this array to identify the various materials making up the debris within a control volume (I,J). The material species currently represented are listed in the second column of Table 2.1. It should be noted that five slots (K = 5, 8, 9, 19, 20) are available for future addition of other material species to be considered in the calculation.

Table 2.1 Array Elements for Material Densities

Material Index K	Material	RHOSOL(K) ^a kg/m ³	RHOLIQ(K) ^b kg/m ³
1	Zr	6420.2	6184.7
2	Fe	7259.0	7015.0
3	Cr	6578.0	6280.0
4	Ni	8187.0	7905.0
5	—	0.0	0.0
6	Ag	10050.0	9475.0
7	CdIn	8450.0	8400.0
8	—	0.0	0.0
9	—	0.0	0.0
10	B ₄ C	2399.6	2349.9
11	ZrO ₂	5859.6	5989.3
12	FeO	5699.8	5699.8
13	Fe ₂ O ₃	0.0	0.0
14	Fe ₃ O ₄	5177.2	5177.2
15	Cr ₂ O ₃	5125.9	5125.9
16	NiO	6666.9	6666.9
17	B ₂ O ₃	1848.5	1848.5
18	UO ₂	10008.3	7999.6
19	—	0.0	0.0
20	—	0.0	0.0

^a The RHOSOL Array is provided via DATA statements in subroutines BHHED2 and BHQSLU.

^b The RHOLIQ Array is provided in subroutines BHHED2, BHDBME, BHDBMX, and BHQSLU.

The array elements Ag (K = 6) and CdIn (K = 7) represent the PWR control rod materials. As indicated, silver (Ag) is treated as an independent species, but cadmium (Cd) and Indium (In) are lumped together under the label CdIn. It is also important to note that although a slot has been reserved within the array for Fe_2O_3 (K = 13), the presence of this material species is not currently calculated by MELCOR.

The phase index M is used to indicate the mass of constituent K that is solid (M = 1) or liquid (M = 2).

The report "Materials Properties Models for Severe Core Damage Analysis" [9] provides information concerning the temperature-dependent densities of Zircaloy, stainless-steel, boron carbide, and the oxides ZrO_2 and UO_2 . The associated plots from this report are shown in Figure 2.1. Based upon this information, the arrays RHOSOL(K) and RHOLIQ(K) have been defined within the lower plenum debris bed model to provide single values for the densities of the solid and liquid phases of each constituent. The values assigned within these arrays are listed for each constituent in Table 2.1.

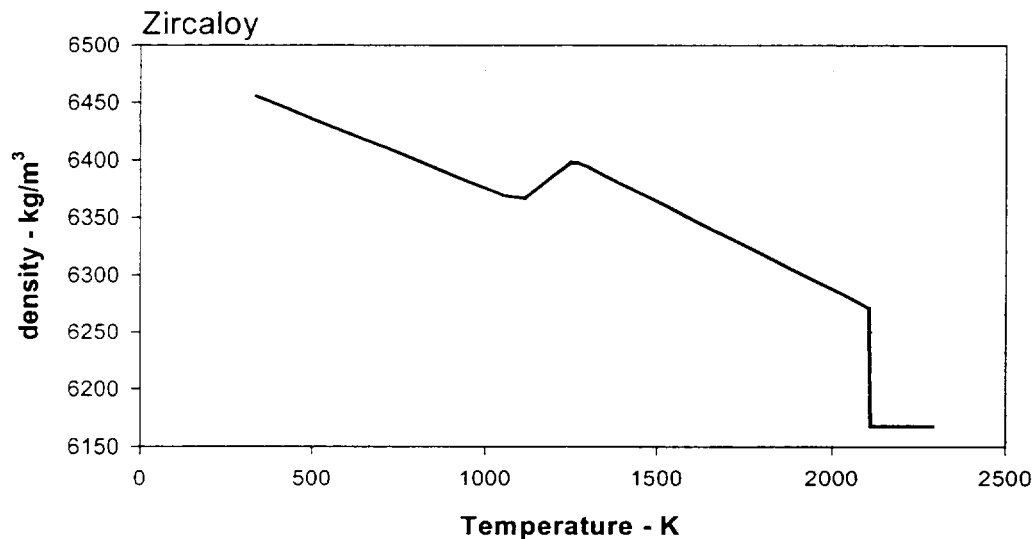


Figure 2.1 Material Densities Considered in Calculation of Debris Bed Control Volume Representative Density [9].

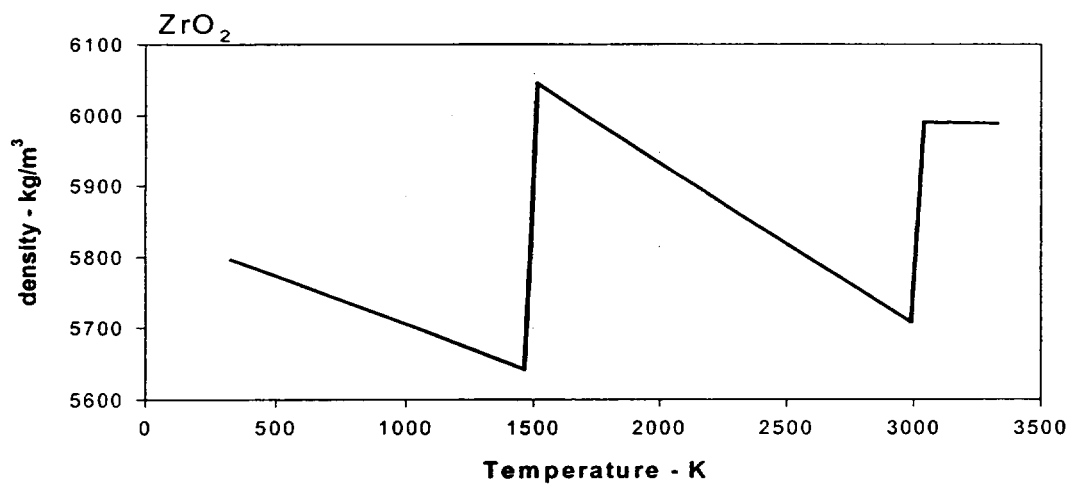
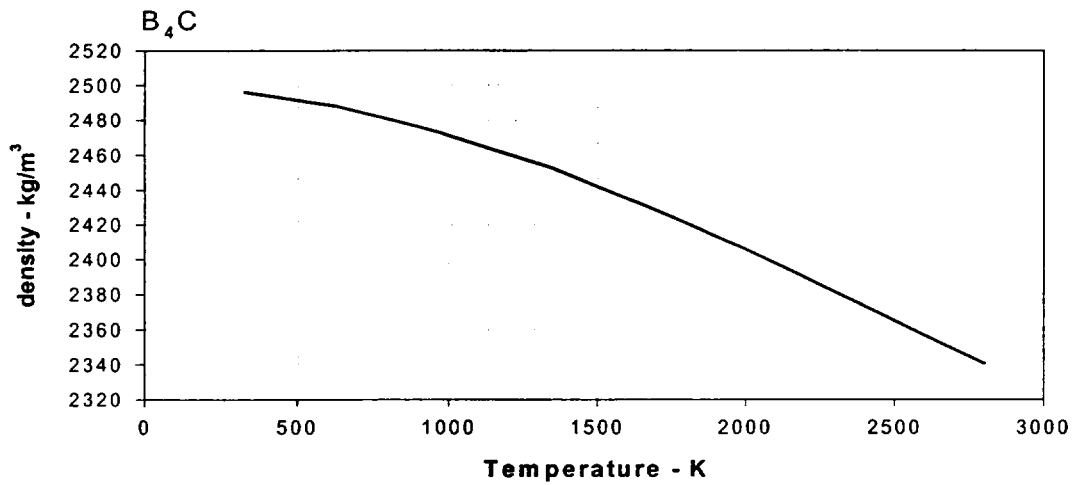
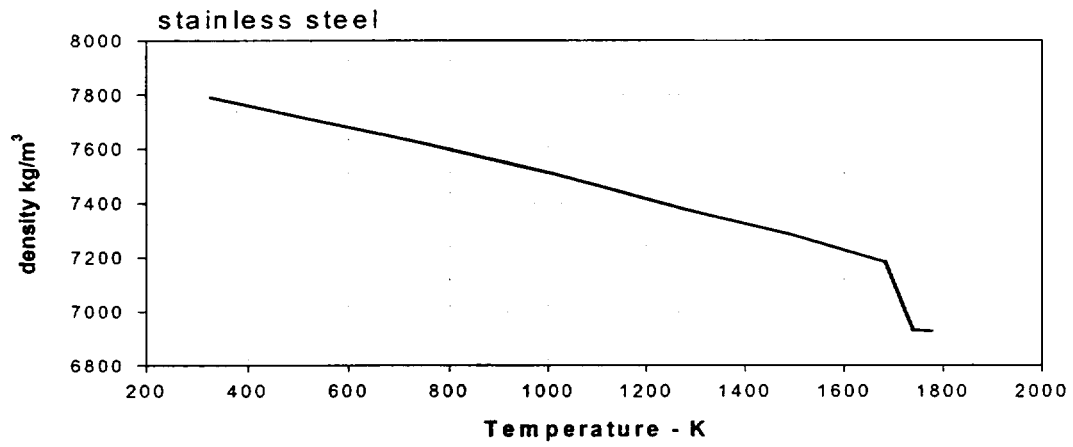


Figure 2.1 (continued)

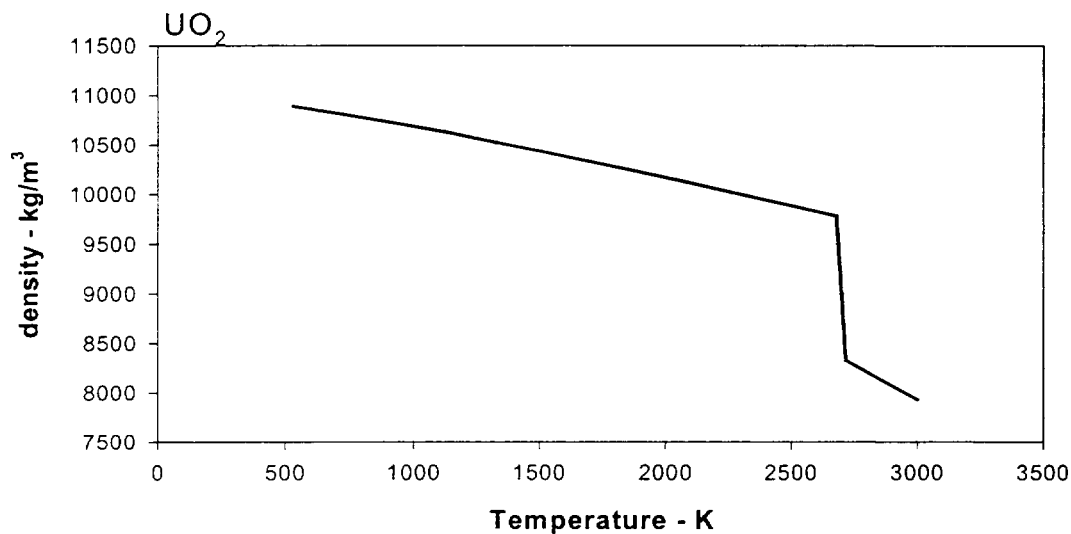


Figure 2.1 (continued)

The RHOSOL and RHOLIQ arrays are used in subroutine BHQSLU as the constituent densities for each new debris pour and within subroutine BHHED2 to calculate volume-averaged and phase-averaged values of the representative density within each debris bed control volume. The representative density for a bed control volume (I,J) is

$$\frac{\sum_{K=1}^{20} [AML P(I,J,K,1) + AML P(I,J,K,2)]}{\sum_{K=1}^{20} [AML P(I,J,K,1)/RHOSOL(K) + AML P(I,J,K,2)/RHOLI Q(K)]}$$

The calculated representative control volume densities are stored within the array RHODB(I,J).

The RHOLI Q array is also used within subroutines BHDBME and BHDBMX. Subroutine BHDBME provides for the movement (both downward relocation to a lower layer and horizontal spreading within the same layer) of molten material species within the bed. Subroutine BHDBMX calculates the release of flowing liquids from the debris bed by means of failed reactor vessel penetration assemblies.

2.3 Specific Heat

A representative specific heat is calculated each timestep for each debris bed control volume, based upon the relative masses of each debris constituent.

The temperature dependencies of the specific heats of Zircaloy, stainless-steel, boron carbide, and the oxides ZrO_2 and UO_2 as provided by Reference 9 are shown in Figure 2.2. Based upon this information and considering the temperature range of interest for the debris bed calculations, the array CPMAT(K) has been placed within the lower plenum debris bed model to provide values of the specific heat for each control volume constituent. Each of the stainless-steel and Ag-Cd-In components is assigned the specific heat of the alloy. These values are listed in Table 2.2.

As indicated in footnote b to Table 2.2, the variations in the specific heats of the stainless-steel components and of ZrO_2 and UO_2 with temperature are considered significant over the range of interest for the debris bed response calculations so temperature is considered in the setting of the representative specific heat for these materials.

The specific heat for the stainless-steel components is, according to Hagrman [9],

$$326.0 + \text{TF} \times (0.298 - 0.0000956 \times \text{TF})$$

where TF is the temperature (K) of interest. This relation follows the stainless steel curve of Figure 2.2.

The specific heat for the local mass of ZrO_2 is

$$600.0 + 0.226316 \times (\text{TF} - 2000.)$$

where TF is the current control volume temperature (K). This simple relation has been developed as a fit to the portion of the curve of Figure 2.2 lying between 2000K (3140 °F) and 2950K (4850 °F). The ZrO_2 specific heat is further constrained to lie between 600.0 and 815.0 J/(kg·K), which follows the curve of Figure 2.2 for temperatures below and above this range.

The specific heat of the local mass of UO_2 within each bed control volume is also calculated as a temperature-dependent value. This dependence, shown in Figure 2.2, is approximated over the range of interest as

$$360.0 + 0.184615 \times (\text{TF} - 2100.)$$

and the UO_2 specific heat is constrained to not be less than 330.0 J/(kg·K).

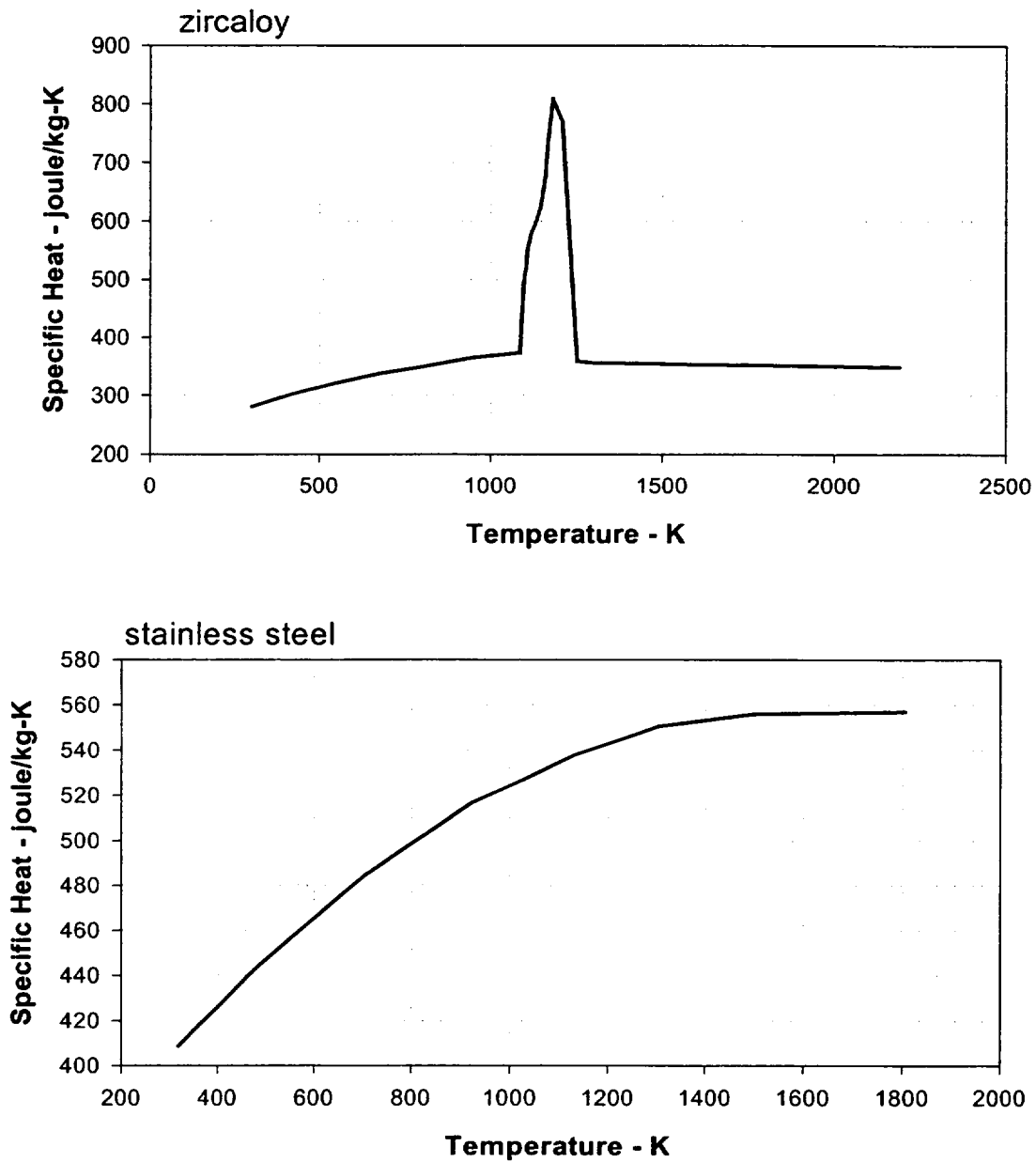


Figure 2.2 Material Specific Heats Considered in Calculation of Debris Bed Control Volume Mass-Averaged Specific Heat (from EGG-CDD-5801)

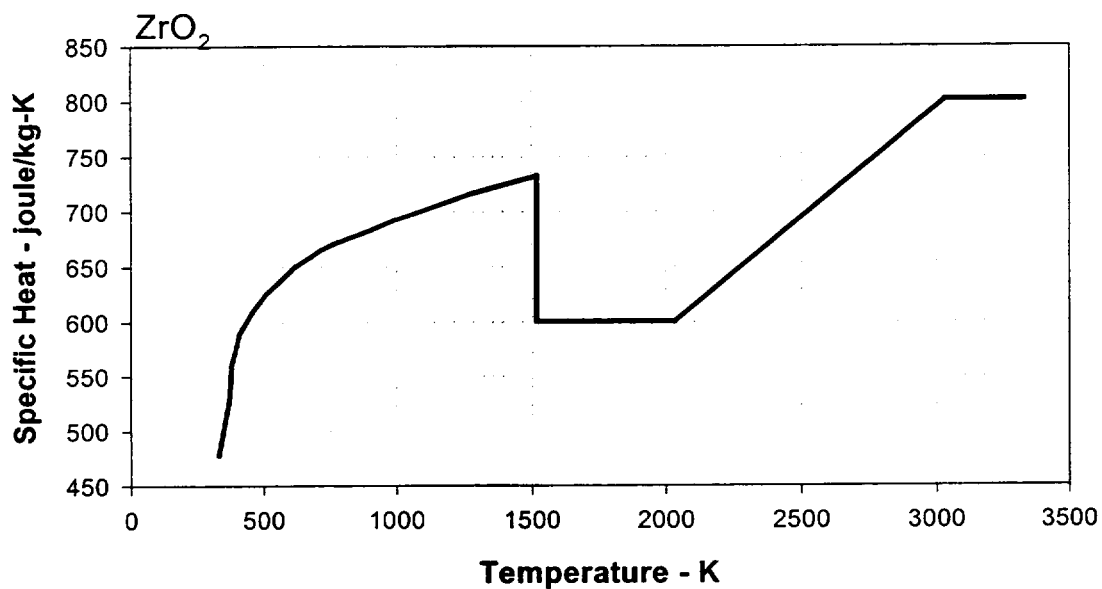
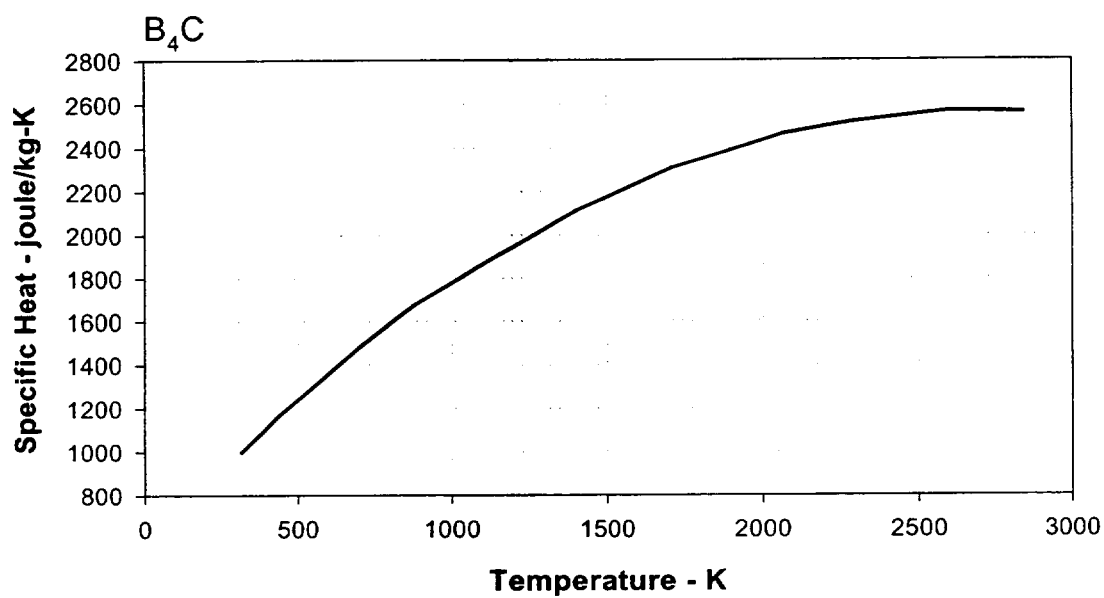


Figure 2.2 (continued)

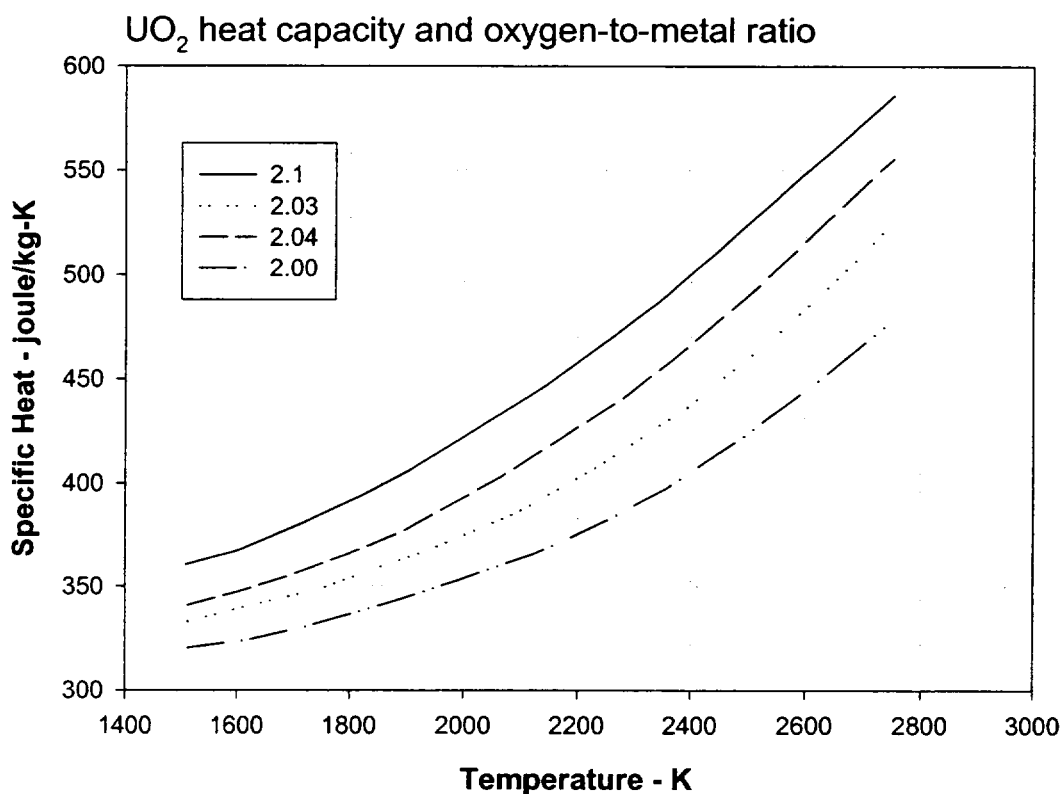


Figure 2.2 (continued)

The material specific heats obtained by calls to subroutine BHMENT are used within subroutine BHED2 to calculate mass-averaged values of the representative specific heat for each bed control volume. Based upon the plotted trends shown in Figure 2.2, a phase correction is not required. These representative specific heats are stored within the array CPDEB(I,J).

Material specific heats obtained by calls to BHMENT are also used within subroutine BHDBME, which calculates the movement of molten debris liquids within the bed, and subroutine BHDBMX, which calculates the release of debris liquids from the lower plenum after penetration failures are predicted to have occurred. Other subroutines calling BHMENT are listed in Table 8.1.

The heat of fusion associated with melting or freezing for each constituent is entered separately and is considered to be consumed or liberated at the melting temperature. The heat of fusion, the melting temperature, and the molecular weight of each constituent are entered on input record BH02JJ.

Table 2.2 Array Elements for Solid Material Specific Heats

Material Index K	Material	CPMAT(K) ^a J/(kg·K)
1	Zr	355.88
2	Fe	558.10
3	Cr	558.10 temperature-dependent ^b
4	Ni	558.10
5	—	0.0
6	Ag	250.00
7	Cd-In	250.00
8	—	0.0
9	—	0.0
10	B ₄ C	2499.94
11	ZrO ₂	816.43 temperature-dependent ^b
12	FeO	837.36
13	Fe ₂ O ₃	0.0
14	Fe ₃ O ₄	1130.44
15	Cr ₂ O ₃	1130.44
16	NiO	782.93
17	B ₂ O ₃	1842.19
18	UO ₂	481.48 temperature-dependent ^b
19	—	0.0
20	—	0.0

^a The CPMAT array is provided via a DATA statement in subroutine BHMENT.

^b The table entries listed here are for the material near the melting point. Within subroutine BHMENT, temperature-dependent values are substituted for these materials each timestep (see text).

2.4 Thermal Conductivity

Since heat transport within the debris bed is primarily by conduction and relocation of molten materials, the representative value of thermal conductivity for each control volume is of primary importance. With the code improvements implemented for use with MELCOR, a representative thermal conductivity is calculated each timestep for each bed control volume, based upon the relative masses of each debris constituent phase within the control volume.

Figure 2.3 (three pages) provides plotted information showing the temperature dependencies of the thermal conductivities of Zircaloy, stainless-steel, boron carbide, and the oxides ZrO₂ and UO₂ [9]. Based upon this information and considering the temperature range of interest for the BWR lower plenum debris bed calculations, the arrays TCSOL(K) and TCLIQ(K) have been placed within subroutine BHED2. These arrays are used to

BH Package Reference Manual

provide values for the thermal conductivity of the solid phase (TCSOL) and liquid phase (TCLIQ) of each debris bed constituent, as listed in Table 2.3.

As indicated in footnote b of Table 2.3, the variations in the thermal conductivities of the solid-phase zirconium metal and the stainless-steel components (see Figure 2.3) with temperature are considered significant over the range of interest and are included in the setting of the representative thermal conductivity for each control volume.

The variation of the solid-phase thermal conductivity of zirconium metal as shown for zircaloy in Figure 2.3 is approximated within the lower plenum debris bed models as

$$TCSOL(1) = 7.511 + TF \times [0.02088 - TF \times (1.45E-05 - 7.668E-09 \times TF)]$$

whereas the thermal conductivity of the solid-phase stainless-steel components follows Figure 2.3 as

$$7.58 + 0.0189 \times TF \text{ for } TF < 1671 \text{ K}$$

and

$$610.94 - 0.34218 \times TF \text{ for } TF > 1671 \text{ K}$$

with a minimum value of 20.0 W/(m-K).

The thermal conductivities (solid and liquid) for the Ag-Cd-In alloy are taken from Reference [10]. Because of the low melting temperature (~1050 K), it is not considered necessary to represent the variation of thermal conductivity for the solid alloy. The thermal conductivity of the liquid is approximately constant with temperature over the range of interest.

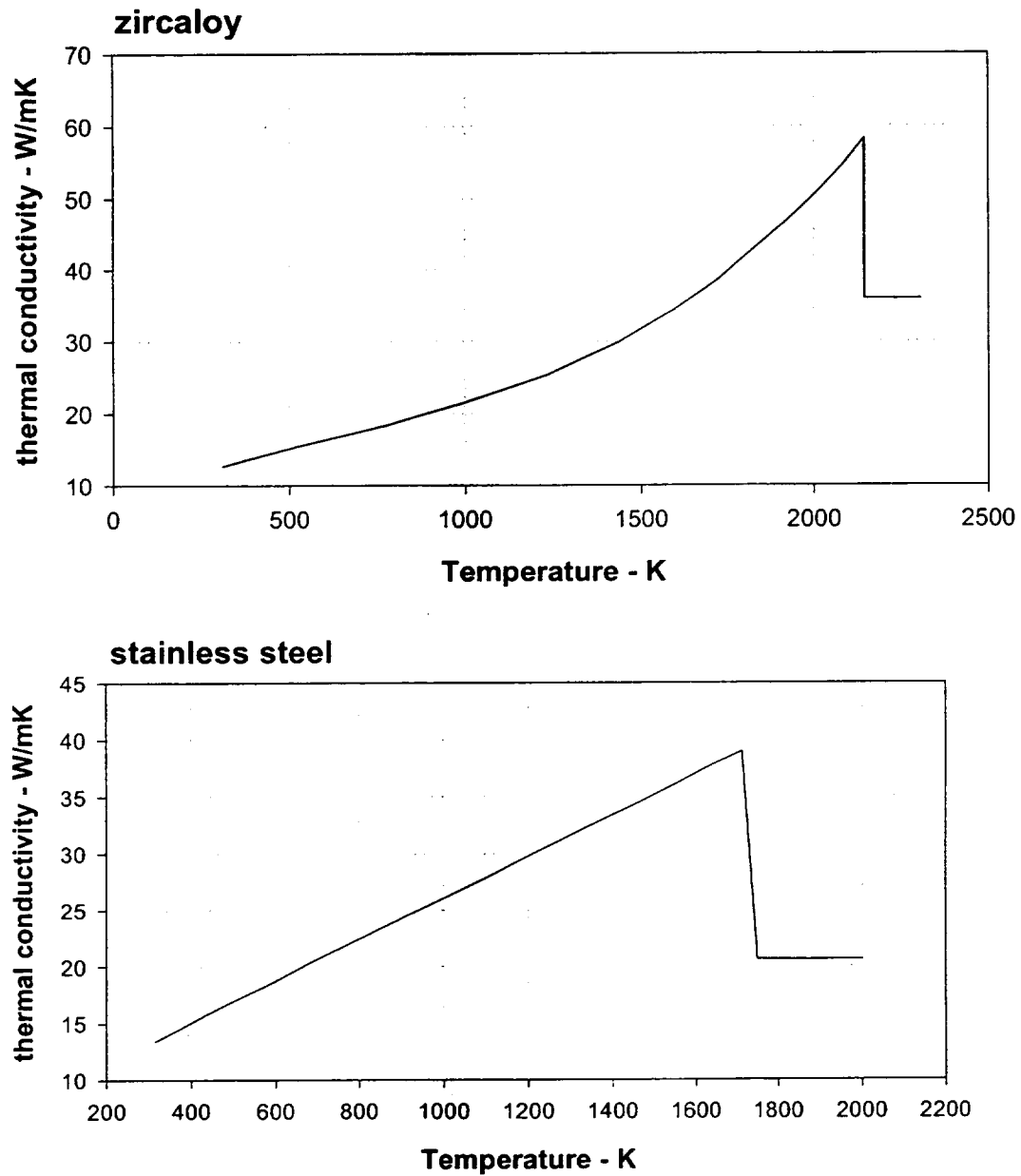


Figure 2.3 Material Thermal Conductivities Considered in Calculation of Debris Bed Control Volume Mass-Averaged Thermal Conductivity [9]

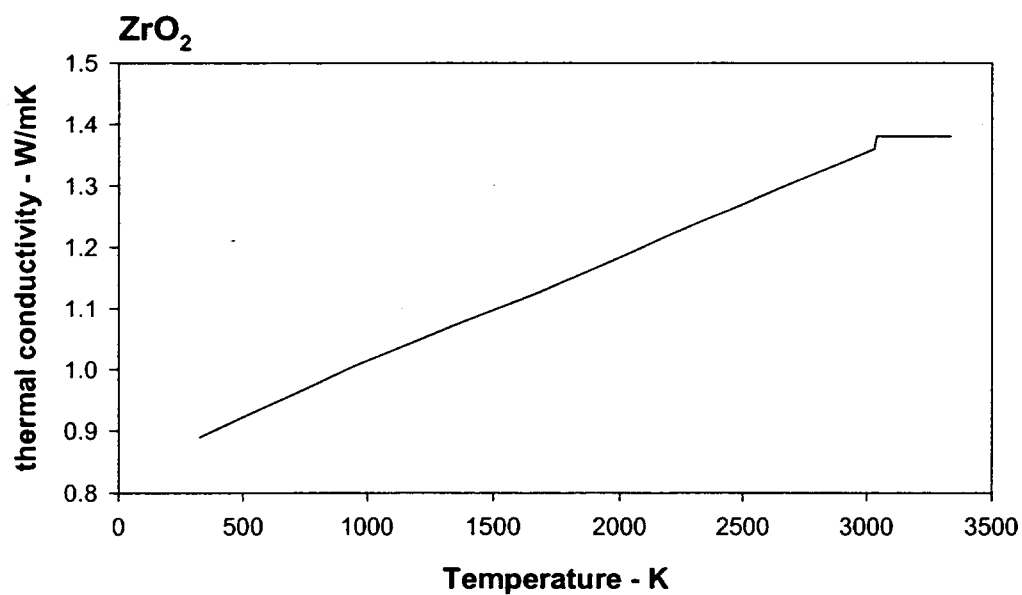
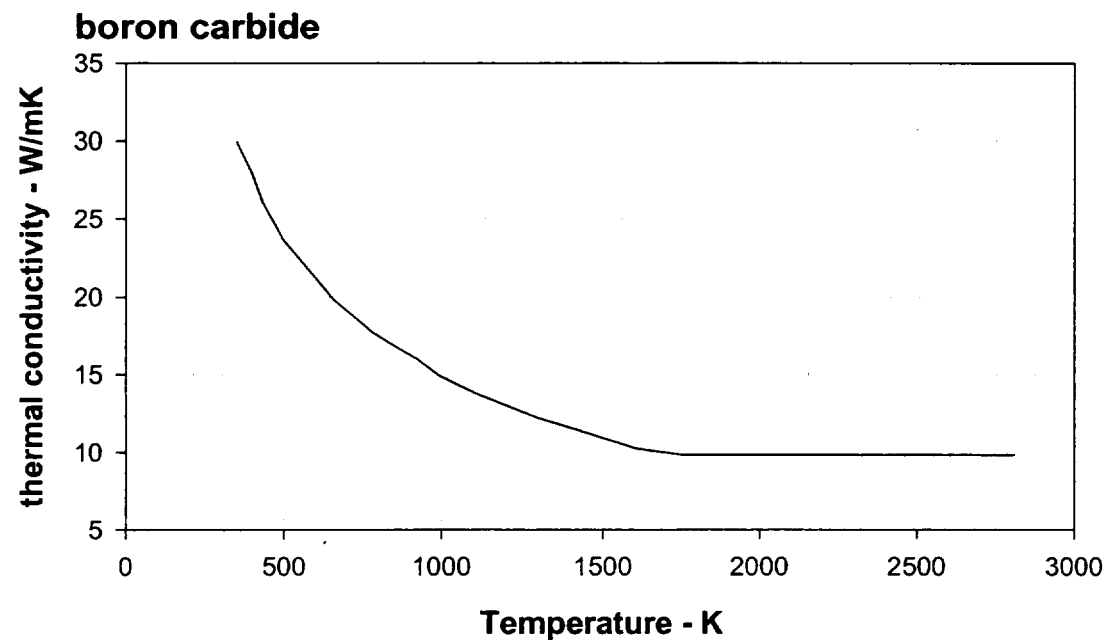


Figure 2.3 (continued)

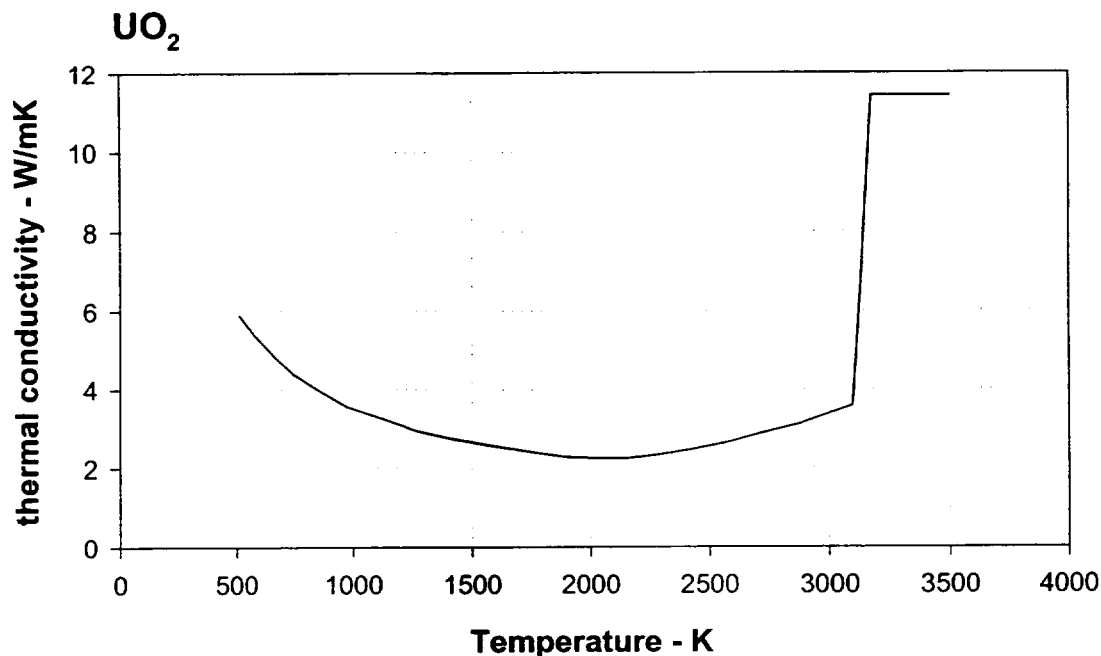


Figure 2.3 (continued)

The representative debris bed control volume thermal conductivities determined within subroutine BHED2 are stored within array CONDB(I,J). These values are adjusted to account for the effect of radiative heat transfer between the particles of the debris bed using the method described in Section 2.3.1 of Reference 11. (A single user-input particle diameter DPART [card BH0500] applies for all bed control volumes.) At low porosity, the thermal conductivity represents conduction through the solid and liquid phases of the debris. As the control volume porosity increases, the thermal conductivity increasingly represents particle-to-particle radiation in a steam atmosphere. Therefore, the effect of increasing voids is to lower the control volume representative thermal conductivity, even at high temperatures.

It should be noted, however, that control volume porosities greater than 0.50 are not normally predicted by the lower plenum debris bed model. This is because molten material relocating downward from the middle debris layer leads to adjustment of control volume dimensions (Section 4.3) or merging with the overlying layer three control volumes before such large porosities can develop. The models for control volume merging are discussed in Section 4.4.

Most lower plenum debris bed response calculations are performed with the assumption that bottom head penetration failures do occur as conditions warrant. Accordingly, the liquid fraction within any calculational control volume remains small since the liquid drains from the reactor vessel as it is formed. The model can be exercised, however, with the provision that penetration failures cannot occur, in which case the control volumes will

eventually consist primarily or even totally of liquid. Within the upper liquid regions of the debris bed, heat transport would be greatly enhanced by the buoyancy-driven circulation of molten liquids. While the model has no representation of this liquid circulation, the associated increase in heat transport is represented by increasing (by a factor of ten) the effective mass-averaged and phase-averaged thermal conductivity whenever the liquid mass within a control volume exceeds two-thirds of the total control volume mass.

Table 2.3 Array Elements for Material Thermal Conductivities

Material Index K	Material	TCSOL(K) ^a W/(m·K)	TCLIQ(K) ^a W/(m·K)
1	Zr	40.427 ^b	36.003
2	Fe	38.703 ^b	20.000
3	Cr	38.703 ^b	20.000
4	Ni	38.703 ^b	20.000
5	—	0.0	0.0
6	Ag	92.500	48.000
7	Cd-In	92.500	48.000
8	—	0.0	0.0
9	—	0.0	0.0
10	B ₄ C	9.969	9.751
11	ZrO ₂	1.277	1.402
12	FeO	1.558	1.662
13	Fe ₂ O ₃	0.0	0.0
14	Fe ₃ O ₄	1.558	1.662
15	Cr ₂ O ₃	1.558	1.662
16	NiO	1.558	1.662
17	B ₂ O ₃	1.558	1.662
18	UO ₂	3.001	11.506
19	—	0.0	0.0
20	—	0.0	0.0

^a The TCSOL and TCLIQ Arrays are provided via DATA statements in subroutine BHED2.

^b The TCSOL elements for Zr and the stainless-steel constituents are updated each timestep with temperature-dependent values (see text).

2.5 Properties of Alloy Constituents

Debris liquids will be formed within the bed control volumes according to the pure species or eutectic mixture definitions established by user input. The properties of the mixture are determined by mass-averaging of the properties of the individual pure species. For the

density, this is appropriate since experience dictates that the density of a mixture lies somewhere between the densities of the mixture components.

For a property such as thermal conductivity, however, measurements show that the actual value for an alloy is in general much less than the value obtained by mass-averaging the thermal conductivities of the individual constituents. For these properties, the user must choose between:

- a. setting the actual pure species' properties in which case the portion of the debris acting as a eutectic mixture will not have correct properties, or
- b. assigning the properties of the eutectic mixture to each of the pure species components. Here the mixture will be treated correctly, but any pure species left over after the mixture is formed within each bed control volume will not have correct properties.

This choice is necessary because code logic cannot distinguish (for the purpose of properties) between materials as pure species and materials as part of a eutectic mixture.

As explained in Sections 2.1 through 2.4, DATA statements in BH package subroutines follow option (a) for density and follow option (b) for specific heat and thermal conductivity.

3. Debris Heat Transfer and Oxidation

The energy balances for each debris control volume are initiated at the time of lower plenum dryout. Heat transfer by conduction is calculated for control volume-to-control volume and control volume-to-wall energy transfer. Additionally, radiation and convection from the surfaces of the upper debris layer control volumes to the vessel atmosphere and to intact structures above the debris bed are considered. Radiation to the shroud and axial conduction along the vessel wall causes boiloff of water remaining in the downcomer jet pump region. Also included in the control volume energy balances are the change-of-phase heat of fusion of pure species or eutectic mixtures as they melt or refreeze within the bed.

The energy balance for control volumes beneath the surface layer of the bed is described in Section 3.1. The additional heat transfer terms applicable to the control volumes that interface with the vessel atmosphere are discussed in Sections 3.2 and 3.3. These calculations are performed within subroutine BHHED2.

3.1 Heat Transfer Between Bed Control Volumes

The debris bed is considered to consist of a solid porous medium in the presence of liquid. The amount of liquid occupying the interstitial pores can vary from insignificant to

BH Package Reference Manual

overwhelming, in which case individual control volumes have become almost entirely or even completely liquid.

The radial heat transfer between control volumes in the same debris layer is represented in the energy balance as

$$AR_{CV} \frac{T_R - T_{CV}}{\frac{XR_{CV} - R_{CV}}{CON_{CV}} + \frac{R_R - XR_{CV}}{CON_R}} + AR_L \frac{T_L - T_{CV}}{\frac{XR_L - R_L}{CON_L} + \frac{R_{CV} - XR_L}{CON_{CV}}} \text{ Watts}$$

where

- AR = interface area AINFCR(I,J) at the right vertical boundary of the control volume, m²
- T = control volume temperature TMLPO(I,J), K
- XR = radius XRT(I,J) from the lower plenum centerline to the right vertical boundary of control volume (I,J), m
- R = radius RNODE(I,J) from the lower plenum centerline to the center of mass of control volume (I,J), m
- CON = representative thermal conductivity CONDB(I,J) for the debris within control volume (I,J), W/(m·K)

The subscripts identify the relative radial positions of the three control volumes as:

- CV = control volume for which the heat balance is being performed
- L = control volume to the left
- R = control volume to the right

Only the first radial heat transfer term is used for the centerline control volume in each debris layer; conversely, the outermost control volume uses only the second term.

Axial heat transfer for the middle (second) debris layer control volumes is represented in the heat balance as

$$AA_B \frac{T_B - T_{cv}}{\frac{YT_B - H_B}{CON_B} + \frac{H_{cv} - YT_B}{CON_{cv}}} + AA_{cv} \frac{T_U - T_{cv}}{\frac{YT_{cv} - H_{cv}}{CON_{cv}} + \frac{H_U - YT_{cv}}{CON_U}} \text{ Watts}$$

where

- AA = upper surface area AINFCA(I,J) of the control volume, m²
- YT = elevation YRT(I,J) of the upper surface of the control volume above vessel zero, m
- H = elevation HNODE(I,J) of the control volume center of mass above vessel zero, m

As before, the subscript CV identifies the control volume for which the heat balance is being performed. The other subscripts identify the relative axial positions of the adjacent control volumes as:

- B = the control volume below
- U = the overlying control volume

Layer three control volumes employ only the first axial heat transfer term while layer one control volumes use only the second term.

Each control volume heat balance incorporates central heat sources and sinks as follows:

- QDOT(I,J) = control volume decay power heat source (based upon amount of UO₂ present), Watts
- QPFGS(I,J) = heat sink to the gas mixture passing through the control volume (after penetration failure), Watts
- QPFMW(I,J) = metal-steam reaction heat source within control volume, Watts

BH Package Reference Manual

QMLDEB(J) = heat source to layer one control volumes (only) by molten liquid flow through penetration failures, Watts

The rationale for QPFGS(I,J) and QPFMW(I,J) is described in Section 3.4. The basis for QMLDEB(J) is described in Section 5.3. Any of these three control volume heat transfer rates can have negative values, for which sources become sinks and vice-versa.

All debris bed control volumes in layer one plus control volumes (2,5) and (3,5) abut the reactor vessel bottom head wall (Figure 1.10). For these control volumes, conduction into the adjacent wall is considered within the heat balance. This is accomplished by summing over the wall nodes adjacent to the control volume:

$$AH \frac{THD - T_{cv}}{\frac{LW}{CON} + \frac{LH}{2 \times BHAKCS}} \quad \text{Watts}$$

where

- AH = AHEAD(M), inner surface area of wall node M, m²
- THD = THDWO(1,M), temperature of the first (inner) segment of wall node M, K
- LW = XLW(I,J), radial distance from center of mass of control volume (I,J) perpendicular to the adjacent wall, m
- LH = XLHEAD(1,M), radial thickness of the inner segment of wall node M, m
- BHAKCS = function BHAKCS(THD), temperature-dependent conductivity of carbon steel, W/(m·K)

Provision is made to account for slippage of the debris downward past the wall nodes as the bed settles. Array elements HTW(M) are set to 0.0 for each wall node above the bed surface and to 1.0 for each wall node in contact with a debris bed control volume at the time of lower plenum dryout. Array elements HTW2(M) are also set to zero at this time. As the bed settles, the HTW(M) array elements are reset to zero if wall node M loses contact with its original adjacent debris bed control volume. Furthermore, the elements of the HTW2(M) array are reset from 0.0 to 1.0 as control volume (3,5) slides down and replaces control volume (2,5) as adjacent to wall node M. The calculated heat conduction rates to the wall are then multiplied by HTW(M) or HTW2(M) as appropriate to adjust for changes in the bed geometry.

3.2 Heat Transfer with the Vessel Atmosphere

Radiation and convection from the upper surface of the debris bed to the vessel atmosphere are considered by the lower plenum model. The general arrangement of the BWR reactor vessel lower plenum structures is shown in Figure 3.1. The entire debris bed would be contained within the portion of the lower plenum beneath the downcomer region baffle plate, see Figure 1.6. Individual surface temperatures are calculated for each of the five control volumes of the upper debris layer.

Before entering into a detailed description of the heat transfer calculations, it should be noted that the general concept of the "vessel atmosphere" differs for the periods before and after the third debris layer is established. As described in Sections 1.1.2 and 1.1.3, the second debris layer is initiated at the time of lower plenum dryout and continues to build until its temperature is sufficient to trigger the initiation of layer three.

During the period while layer two continues to build, the heat sink associated with the vessel atmosphere is considered to be dominated by the metallic mass of the remaining portions of the control rod guide tubes and other lower plenum structures above the current elevation of the debris bed surface. Accordingly, the temperature (TGRID2) of this stainless-steel mass is calculated within the BH package each timestep, based upon the heat transfer from the bed surface. The MELCOR interface routine BHRUN1 then provides a calculation of heat transfer between the control rod guide tubes and the lower plenum atmosphere, based upon the temperature TGRID2.

When debris bed layer three is established, however, all remaining lower plenum structural mass is considered to be subsumed within this layer. Therefore, from this time forward, the vessel atmosphere heat sink consists only of the lower plenum gases above the bed surface. The bed surface-to-atmosphere heat transfer rates established within the BH package are not applied within this package, but instead are passed back to MELCOR, where the current vessel atmosphere temperature is calculated each timestep.

3.2.1 Surface Heat Transfer Coefficients

The coefficients for heat transfer between the reactor vessel atmosphere and the debris bed surfaces or exposed segments of the bottom head wall are calculated within subroutine BHHED2 by means of calls to subroutines BHST2P and BHHIRST. These seven coefficients include the effects of both natural convection and radiation and are stored in the array HSURF(N). The seven surfaces represented are defined in the following table, where the control volume layer index NT is initially 2, then becomes 3 after the third debris bed layer is established.

BH Package Reference Manual

Table 3.1 Surfaces Considered for Heat Transfer with the Vessel Atmosphere

Surface N	Definition
1	Debris control volume (NT,1) upper surface
2	Debris control volume (NT,2) upper surface
3	Debris control volume (NT,3) upper surface
4	Debris control volume (NT,4) upper surface
5	Debris control volume (NT,5) upper surface
6	Inner segment of wall node 17
7	Exposed bottom head wall segments between the bed surface and the bottom of wall node 17

Wall node 17 is located just below the shroud baffle as shown on Figure 1.10. The surface temperatures are stored in the array TDBSUR(N) while the characteristic lengths (area-to-perimeter ratios) for each surface are stored in array CLS(N).

The calculation of the surface heat transfer coefficients is controlled by subroutine BHED2. For each surface N, the first step is to call subroutine BHST2P with the constituent masses of the lower plenum atmosphere, the atmosphere temperature TGXXXX, the vessel pressure PVSL, and the surface temperature. Table 3.2 indicates the information returned.

Table 3.2 Mixture Parameters Returned by subroutine BHST2P

Parameter	Definition	Mixture
CONDMR PRMR	Mixture thermal conductivity W/(m•K) Mixture Prandtl number	Constituent gases at PVSL and TDBSUR(N)
VISMB RHOMB	Mixture viscosity kg/(m•s) Mixture density kg/m ³	Constituent gases at PVSL and TGXXXX

Provision is made for consideration of a mixture of the constituent gases steam, hydrogen, carbon monoxide, carbon dioxide, and methane.

The next step is to calculate the natural convection heat transfer coefficient based upon the Grashof number

$$Gr = C_g \times \left(\frac{RHOMB}{VISMB} \right)^2 \times BETA \times [TS - TG] \times (CL)^3$$

where

Cg = acceleration of gravity, 9.81 m/s²

TS = surface temperature TDBSUR(N), K

TG = atmosphere temperature TGXXXX, K

$$\text{BETA} = \frac{1}{\left(\frac{\text{TS} + \text{TG}}{2}\right)} \text{ K}^{-1}$$

CL = characteristic length equal to twice the area-to-perimeter ratio CLS(N), m. For the annular bed surfaces, this is the outer radius minus the inner radius. For the exposed wall nodes, CL is the vertical nodal height

The natural convection coefficient is then

$$\text{HNC} = C_1 \times \text{CONDMR} \times \frac{[\text{GR} \times \text{PRMR}]^{C_2}}{\text{CL}} \text{ W/(m}^2 \cdot \text{K)}$$

where C_1 and C_2 are constants with values determined by the Grashof number as indicated in the following table.

While these C_1 values strictly apply only for an upward-facing horizontal surface, the differences for a vertical surface are slight and the same values are used. The C_2 values are identical [12].

Table 3.3 Values of C_1 and C_2 (Reference 12)

Constant	Value	
	GR x PRMR < 1.0 x 10 ⁸	GR x PRMR ≥ 1.0 x 10 ⁸
C_1	0.54	0.14
C_2	0.25	0.33

The heat transfer coefficient for radiation between the surface N and the atmosphere is now determined by means of a call to subroutine BHRST with the surface temperature TDBSUR(N), the atmosphere temperature TGXXXX, and the steam partial pressure PSV. The stainless-steel emissivity is calculated within BHRST as

$$\text{EMISSW} = 0.25617 + 0.000348 \times [\text{TDBSUR(N)} - 616.67]$$

based upon information provided in Reference 13. The absorptivity of steam ABSOR is obtained by a call to MELCOR Core (COR) package subroutine CORABS, where

BH Package Reference Manual

interpolation of tabular data taken from Reference 14 is performed based upon the surface temperature, the steam partial pressure and temperature, and the lower plenum beam length.

The radiative heat flux is calculated within subroutine BHRST by a parallel plane model

$$Q_{RADFX} = 5.6686 \times R \times \left[\left(\frac{TS}{100} \right)^4 - \left(\frac{TG}{100} \right)^4 \right] \text{ W/m}^2$$

where

$$R = \frac{1.0}{\frac{1.0}{EMISSW} + \frac{1.0}{ABSOR} - 1.0}$$

TS = surface temperature TDBSUR(N), K

TG = vessel atmosphere temperature TGXXXX, K

The radiation heat transfer coefficient is then

$$H_{RAD} = \frac{Q_{RADFX}}{TS - TG} \text{ W/(m}^2 \cdot \text{K)}$$

where the absolute value is taken.

Finally, the overall surface heat transfer coefficient is established within subroutine BHED2 as

$$H_{SURF}(N) = H_{NC} + H_{RAD} \text{ W/(m}^2 \cdot \text{K)}$$

for each of the seven surfaces.

3.2.2 Establishing the Debris Bed Surface Temperatures

Heat transfer from the upper debris layer to the vessel atmosphere is calculated based upon the temperature difference between each debris control volume and the vessel atmosphere. Then the control volume surface temperature TDBSUR(N) is calculated for use in determining the surface heat transfer coefficient in the manner explained in Section 3.2.1.

For each of the five upper layer control volumes, the rate of heat transfer to the vessel atmosphere is established within subroutine BHHED2 as

$$QTOGAS = AA_{cv} \frac{T_{cv} - T_G}{\frac{YT_{cv} - H_{cv}}{CON_{cv}} + \frac{1.0}{HS}} \quad \text{Watts}$$

where

- AA_{cv} = upper surface area AINFCA(NT,J) of the control volume, m^2
- NT = index of the upper debris layer, either 2 or 3
- J = index of control volume within layer NT, J = 1 to 5
- YT_{cv} = elevation YRT(NT,J) of the control volume upper surface, m
- H_{cv} = elevation HNODE(NT,J) of the control volume center of mass, m
- CON_{cv} = representative thermal conductivity CONDB(NT,J) for the control volume debris, $W/(m \cdot K)$
- HS = surface heat transfer coefficient HSURF(J), $W/(m^2 \cdot K)$

This heat transfer is considered in the control volume heat balance along with the conduction terms described in Section 3.1. The index NT is 2 until the third debris layer is established, when it becomes 3. It remains 3 unless and until the layer three and layer two control volumes within a radial zone are merged late in the calculation. It can occur that NT will be 3 in some radial zones and 2 in others.

The control volume surface temperature is based upon the heat transfer rate as follows:

$$TDBSUR(J) = \frac{QTOGAS}{AINFCA(NT,J) \times HSURF(J)} + TGXXXX \quad K$$

where J is the index of the control volume within debris layer NT.

3.2.3 Exposed Vessel Wall Nodes

As described in Section 1, the lower plenum debris bed and bottom head response model is initiated at the time of lower plenum dryout. At this time debris layer three does not exist

BH Package Reference Manual

and there will be three wall nodes exposed to the reactor vessel atmosphere between the bed surface and the bottom of the shroud baffle. With reference to Figure 1.11, these are wall nodes 15, 16, and 17; wall node 18 is adjacent to the water in the downcomer region. When the third layer is formed (the situation illustrated in Figure 1.11), then only node 17 will be exposed to the vessel atmosphere. However, the bed may settle later in the calculation causing control volume (3,5) to slide downward so that wall nodes 16 and 15 may again be exposed.

Heat transfer between the vessel atmosphere and any exposed vessel wall node is calculated within subroutine BHED2 as

$$AH \frac{TG - THD}{\frac{1.0}{HS} + \frac{LH}{2 \times BHAKCS}} \quad \text{Watts}$$

where

- AH = AHEAD(1,M), inner surface area of exposed wall node M, m²
- TG = vessel atmosphere temperature, K
- THD = THDWO(1,M), temperature of the inner segment of wall node M, K
- HS = HSURF(N), surface heat transfer coefficient for exposed portion of wall, W/(m²·K)
- N = 6 for wall node 17 or 7 for wall node 16 (and any exposed wall nodes below 16)
- LH = XLHEAD(1,M), radial thickness of inner segment of wall node M, m
- BHAKCS = function BHAKCS(THD), temperature-dependent conductivity of carbon steel, W/(m·K)

3.3 Radiation to the Lower Plenum Structures

After lower plenum dryout, direct radiation from the upper surfaces of the debris bed would not only heat the vessel atmosphere, but would also fall upon the core plate, the core shroud and downcomer region baffle plate, and the exposed portion of the bottom head wall. See Figure 3.1 and Figure 1.12 for the orientation of these structures.

ORNL-DWG 91M-2834AC ETD

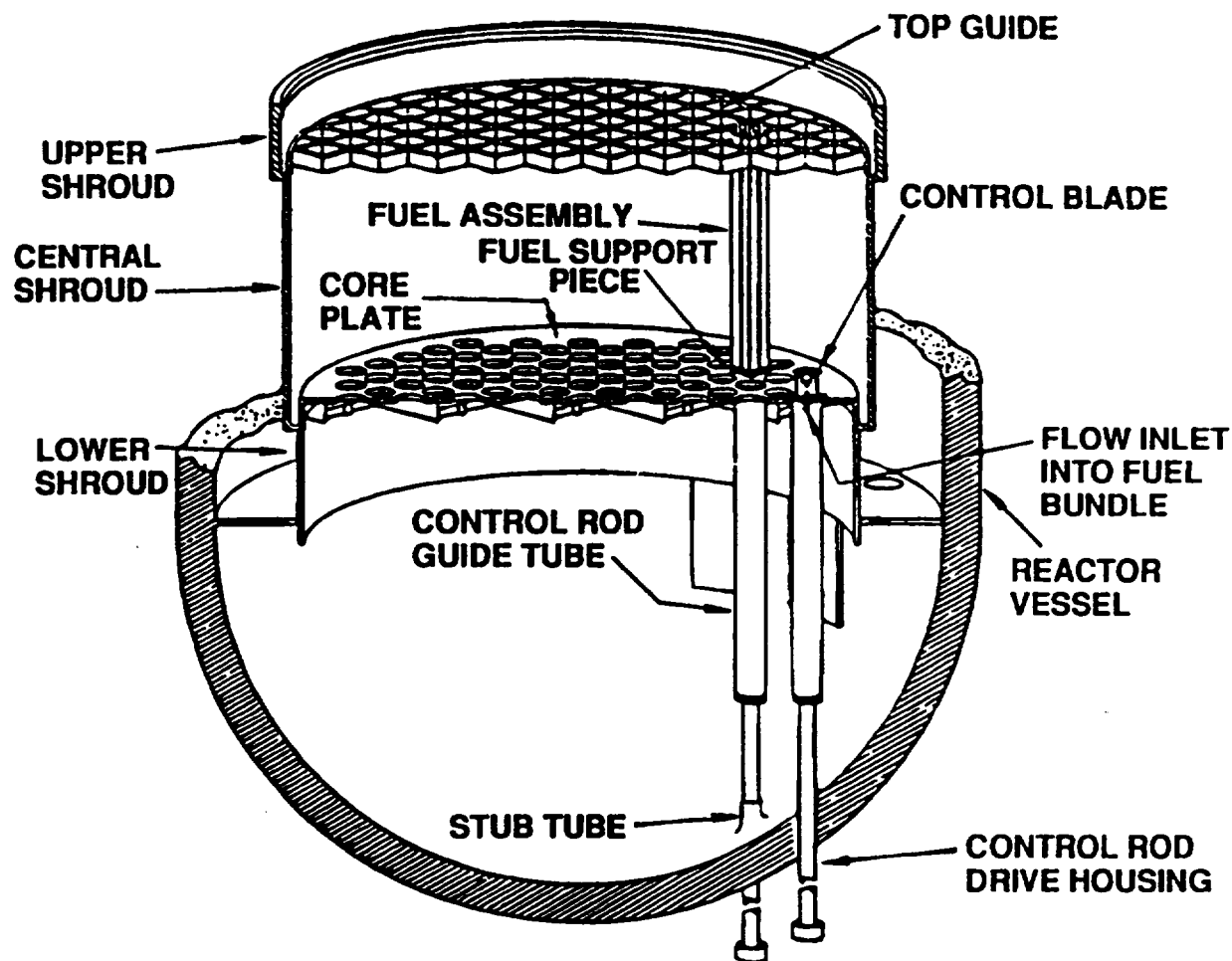


Figure 3.1 Arrangement of BWR Reactor Vessel Lower Plenum Structures

Heat transfer from the vessel atmosphere to the lower core shroud is calculated within the Heat Structures (HS) package of MELCOR. The temperature T_{MA}SJP of the water within the downcomer region is then provided each timestep to the BH package, where it is used as the heat sink temperature associated with convective heat transfer from the inner surface of the uppermost bottom head wall node NWALL.

Radiation from the debris bed surfaces to the exposed portion of the inner surface of the vessel wall is calculated within the BH package, as explained in Sections 3.3.1 and 3.3.2. Radiation from the debris surfaces to the core plate, the lower core shroud, and the downcomer region baffle plate is calculated within the COR package of MELCOR, and the radiation rates each timestep are passed to the BH package.

3.3.1 Heat Transfer Coefficients for Radiation to the Vessel Wall

The heat transfer coefficients for the direct radiation pathways from the debris bed surfaces to the exposed (i.e., not covered by debris) vessel wall nodes are calculated within subroutine BHHED2 and stored in the array HRADIT(N). The five heat transfer pathways represented are listed in the following table.

Table 3.4 Lower Plenum Debris-to-Wall Heat Transfer Pathways Calculated by the BH Package

Pathway No. N	From Upper Surface Debris Bed Control Volume	To
1	(NT,1)	Exposed vessel wall
2	(NT,2)	Exposed vessel wall
3	(NT,3)	Exposed vessel wall
4	(NT,4)	Exposed vessel wall
5	(NT,5)	Exposed vessel wall

As before, the control volume layer index NT indicates the bed layer (either 2 or 3) with which the uppermost control volume within a debris bed radial zone is associated.

The heat flux from each debris bed surface to the exposed portion of the vessel wall is based upon the direct radiation interchange (reflections are neglected). The calculation follows the method suggested in Section 13.6 of Reference 12

$$Q_{RADTW} = VF \times FACTR \times [(TS)^4 - (TEX)^4] \text{ W/m}^2$$

where

View Factor (VF) for radial zone	=	0.135	0.154	0.191	0.376	0.564
FACTR	=	constant = 3.40116E-8				
TS	=	bed surface temperature TDBSUR(N), K				
TEX	=	area-averaged temperature TDBSUR(6) of the exposed bottom head wall nodes, K.				

The view factors listed above are the default values based upon a fully developed (three-layer) debris bed within the lower plenum of a 251-inch (6.38 m) ID BWR reactor vessel such as installed at the Grand Gulf facility. These default values were calculated by the codes and techniques described in References 15 and 16. However, as explained in the BH Package Users' Guide (see entry VIEW2(LL,JJ) on input record BH18JJJK), these view factors as well as the view factors from the debris bed surfaces to the lower core shroud and to the core plate can be modified within the input deck. Once established,

however, radiation from the debris bed to the overlying structures is based on these view factors throughout the MELCOR calculation.

The constant FACTR is the product of the Stefan-Boltzman coefficient (5.6686E-8) and a radiation exchange conductance term taken to be 0.6 for the (gray) materials within the BWR lower plenum. (The conductance term is the product of the emissivities of the two surfaces involved in the radiation exchange, both assumed to be oxidized stainless-steel.) The reader should recognize that the bed surface temperatures used in the calculation of QRADTW are determined from the conditions of the lower plenum atmosphere as explained in Section 3.2.2.

Finally, based upon the individual values of QRADTW for N = 1 through N = 5,

$$HRADIT(N) = \frac{QRADTW}{[TS - TEX]} \quad W/(m^2 \cdot K)$$

are the heat transfer coefficients for direct radiation exchange between the exposed vessel wall nodes and debris bed radial zones 1 through 5, respectively. Radiation to the exposed wall surfaces from the three inner debris bed radial zones is neglected during the period while the control rod guide tubes remain intact since the associated views are considered to be blocked during this period.

3.3.2 Direct Radiation Exchange

For each of the five upper debris bed control volumes, radiative heat transfer based upon the bed surface temperatures TDBSUR(N) to the exposed portion of the vessel wall is calculated within the BH package. Radiation from these surfaces to the upper reactor vessel structures, however, is calculated within the COR package of MELCOR. The upper reactor vessel structures are comprised of the structural components of the lower core shroud, as established by HS package input, and the structural components of the core plate, as established by the COR package input. The calculated radiation heat transfer rates are passed to the BH package each timestep by means of the array QFMTOS, via the subroutine BHQSLU argument list. (See Section 8.2.1.)

The first dimension of array QFMTOS(N,NSW) is the index of the debris bed radial zone, N = 1,5. The second dimension is the index of the lower plenum structure receiving radiation from the bed surfaces as defined in the following table.

Table 3.5 Lower Plenum Structure Indices

Index NSW	Lower Plenum Structure
1	Exposed portion of vessel wall
2	Downcomer region baffle plate
3 through NSHDLP + 1	Cylindrical (vertical) sections of lower core shroud
NSHDLP + 2 through 1 + NSHDLP + NRAD	Core plate sections

As may be inferred from the information provided in this table, NSHDLP is the number of lower core shroud sections (including the downcomer baffle plate) while NRAD is the number of radial sections into which the core plate is divided. Both are determined by user input provided in record BH1800 (NSHDLP) and record COR00000 (NRAD).

The arrangement of the lower plenum upper structures for a typical calculation is shown in Figure 3.2. Here user input has divided the lower core shroud into two vertical sections (NSHDLP = 3) and the core plate into four sections (NRAD = 4). For this example arrangement, array QFMTOS would be dimensioned as QFMTOS(5,8).

For the exposed reactor vessel bottom head wall nodes, the heat transfer from each upper bed control volume as calculated in subroutine BHHED2 is

$$QFMTOS(J,1) = \sum AH \frac{T_{cv} - THD}{\frac{YT_{cv} - H_{cv}}{CON_{cv}} + \frac{1.0}{HR} + \frac{LH}{2 \times BHAKCS}} \quad \text{Watts}$$

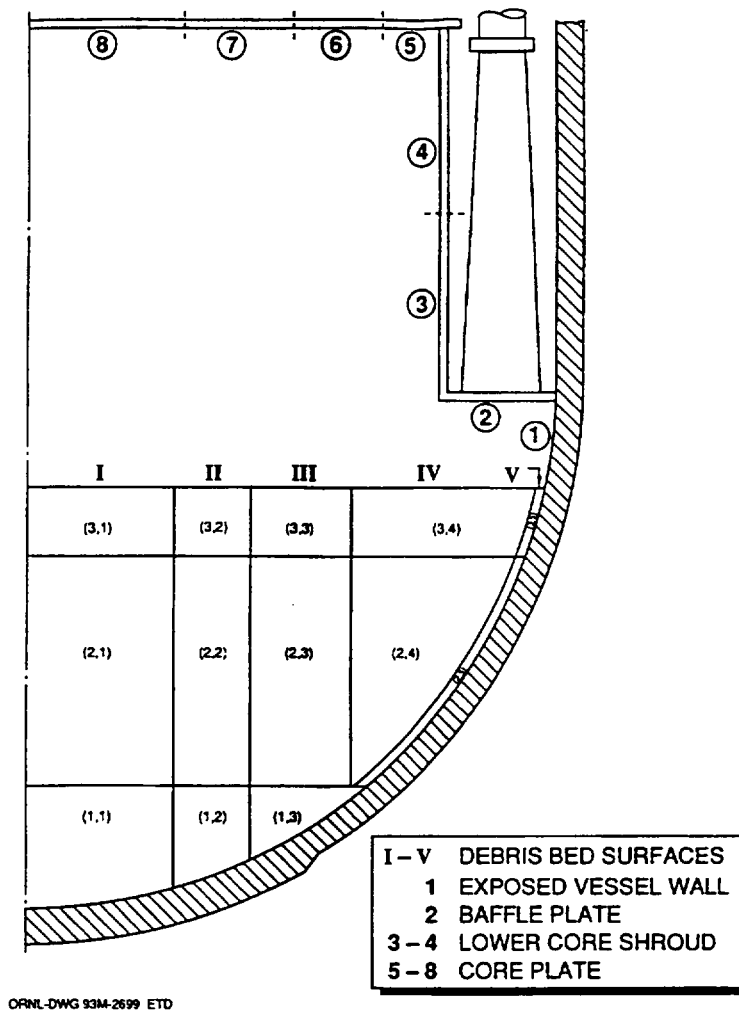


Figure 3.2 Typical Nodalization of the Upper Structures for the Radiative Heat Transfer Within the BWR Lower Plenum

BH Package Reference Manual

where the summation is taken over the exposed wall nodes and

J	= control volume index within layer NT, 1 to 5
NT	= upper debris layer index (2 or 3)
AH	= AHEAD(1,M), inner surface area of exposed wall node M, m ²
THD	= THDWO(1,M), temperature of the inner segment of exposed wall node M, K
YT _{cv}	= elevation YRT(NT,J) of control volume upper surface, m
H _{cv}	= elevation HNODE(NT,J) of control volume center of mass, m
CON _{cv}	= representative thermal conductivity CONDB(NT,J) for the control volume debris, W/(m·K)
HR	= direct radiation heat transfer coefficient HRADIT(J), W/(m ² ·K)
LH	= XLHEAD(1,M), radial thickness of the inner segment of wall node M, m
BHAKCS	= function BHAKCS(THD), temperature-dependent conductivity of carbon steel, W/(m·K)

It is important to note that although all radiation from bed control volume J to the exposed wall nodes is stored in the single array element QFMTOS(J,1), the radiation received by the individual exposed wall nodes is accounted for separately within the BH package. In other words, separate energy balances are performed for each individual wall node.

As described previously, elements QFMTOS(J,2) through QFMTOS(J,8) for the example arrangement shown in Figure 3.2 pertain to sections of the lower core shroud and the core plate and would be calculated within MELCOR. None of the surface radiation pathways are calculated for the central three control volumes of debris bed layer two during the period before layer three is established, because it is considered that the intact control rod guide tube structures would block the radiation pathways to the wall, shroud, and core plate. All calculated energy transfers from the debris bed surfaces to the exposed wall nodes and to the shroud and core plate are appropriately entered into the debris bed control volume heat balances and the vessel wall response calculations. Similarly, all radiative heat loads to the core plate and core shroud are passed into the COR and HS packages, where their effects are properly represented.

The upper debris bed surface radiation exchange calculations provide a reasonable representation of heat transfer with the core plate, the core shroud, the downcomer region baffle plate, and the exposed portion of the vessel wall. The thermal response of the lower

plenum debris bed is primarily determined by the decay heating, which is the dominant factor. Since the lower plenum debris bed would be large, its rate of temperature increase would be relatively slow with important events such as the melting of individual species or eutectic mixtures occurring over a period of hours.

The current version of the BH package permits the user to divide the representation of the core plate and the lower core shroud into several sections and to provide individual view factors from each debris bed radial zone to each section. As mentioned previously, however, the decay heat release dominates the events within the lower plenum debris bed. Although the integrated transfer of energy from the bed surface to the overlying structures is an important consideration to the overall calculation, the precise rate of energy transfer at any particular time is not.

3.3.3 After Downcomer Dryout

While water remains in the vessel downcomer region, heat transfer to this water from the uppermost bottom head wall node NWALL is modeled within the BH package (Section 1.2). After downcomer dryout, however, radiation heat transfer between the shroud and the uppermost wall node (number 18 in Figure 1.10) can become important.

With the downcomer region dry, the radiation heat transfer from the shroud to the uppermost wall node NWALL is calculated each timestep within the MELCOR-BH package interface and passed to the BH package as variable QRNWAL(1) (J) within the subroutine BHQSLU argument list. The calculation is based upon the lower shroud temperatures as determined by the MELCOR HS package and the temperature THDWO(1,NWALL) of the inner segment of wall node NWALL as determined within the BH package.

After downcomer dryout, radiation from the debris bed surfaces can elevate the temperature of the lower core shroud to the stainless-steel melting point; hence, consideration of the radiative exchange between the core shroud and the vessel wall is important. Within the BH package, the temperature of wall node NWALL is appropriately adjusted each timestep in response to the energy transfer represented by the variable QRNWAL(1).

3.3.4 Shroud Melting and Relocation

As the calculated bed surface temperatures increase, radiative energy exchange with the overlying structures causes the evaporation (or boiling) of the water trapped within the downcomer region. The shroud temperature remains approximately equal to the water temperature and therefore (while the reactor vessel remains depressurized) approximately constant. For calculations in which bottom head penetration failures are modeled, failure of the vessel wall (and release of the remaining debris from the lower plenum) will (in general) occur before the water in the downcomer region is exhausted.

BH Package Reference Manual

For calculations in which bottom head penetration failures are not represented, dryout of the vessel downcomer region will (in general) occur while the bottom head remains intact. The temperature of the lower core shroud will then increase, leading to a corresponding increase in the debris bed surface temperatures. Eventually, the shroud temperature will reach the steel melting temperature. All of these events are appropriately predicted to occur by the radiation exchange calculations.

The structural relocations associated with the shroud heatup and melting are calculated within the MELCOR-BH package interface for BWR applications. First, the entire shroud would move downward because the baffle plate (Figure 3.2) would lose strength at elevated temperature and could no longer support the weight.* For the calculation, this movement occurs whenever the predicted baffle plate temperature exceeds the user-input failure temperature TFAILS (BH1800). At this time, the baffle plate component masses are added to the upper debris layer via the AMCRPT array (Section 8.2.1). Also, to recognize that the relocated shroud would now interpose between the central portion of the debris bed and the vessel wall, the elements of the VIEW2 array representing the view factors between surfaces I, II, and III (Figure 3.2) and the exposed vessel wall are set to zero.

Radiation from the relocated shroud to the exposed wall nodes is calculated within the MELCOR-BH package interface and passed to the BH package via the QRNWAL array. Whereas QRNWAL(1) represents the radiation (J) from the shroud to wall node 18 for all timesteps after downcomer dryout, QRNWAL(2) and QRNWAL(3) remain zero until the time of baffle plate failure. Subsequently, these represent the radiation energy transfers from the relocated shroud to wall nodes 17 and 16, respectively. (See Figure 1.10 for the locations of the wall nodes.)

When the lower portion of the relocated shroud reached the melting temperature, a period of continuous melting would begin. As the lower shroud disintegrates, the liquid steel would be added to the upper layer of the debris bed and the upper shroud would move downward to take its place. These occurrences are modeled in the MELCOR-BH package interface with the liquid steel transferred to the BH package via the AMCRPT array.

More information concerning the shroud melting and relocation model is provided in Section 9.2.

3.4 Metal-Steam Reaction in the Debris Bed

Typically, the lower plenum debris bed includes large quantities of metals at elevated temperatures. If steam becomes available within the bed, then large amounts of energy

* The support columns (best shown on Figure 1.7) are immersed in the debris bed and would have failed shortly after lower plenum dryout.

can be released by metal oxidation. Steam would be generated within the bed if water is introduced to the lower plenum after debris bed dryout; models for the associated countercurrent flooding phenomena are discussed in Section 7. Steam can also exist within the bed as a result of bottom head penetration failures, which can be initiated as described in Section 5.

With failure of the reactor vessel pressure boundary by penetration failures, a leak path from the vessel to the drywell atmosphere would be created. Subsequently, the vessel gaseous content would blow down if the reactor vessel is at pressure or, if the vessel is depressurized, slowly leak out as the gas temperature increases and the water in the reactor vessel downcomer region surrounding the jet pumps is boiled away. The leak path for the steam generated from the water surrounding the jet pumps is up through the downcomer region, down through the core region, and out through the debris bed. Thus, the steam available in the vessel after the time of pressure boundary failure would pass through the debris and would react with the zirconium and stainless-steel during its passage.

The metal-steam reaction is calculated in subroutine BHMWDE for each debris bed control volume where boiling is occurring or through which steam is passing, provided that the local temperature exceeds 1100 K. The reaction rate as limited by solid state diffusion is calculated as:

$$X_{DTO} = \frac{\sqrt{X_o^2 + 2Ae^{\frac{-B}{T_{cv}}} \times DTM} - X_o}{DTM} \quad \text{m/s}, \quad (3.1)$$

where

A, B = reaction constants

DTM = timestep length, s

T_{cv} = control volume temperature TMLPO(I,J), K

I = layer index

J = radial zone index

X_o = thickness of oxide layer at beginning of timestep, m

This is the integrated form of the reaction rate equation [17,18]. It produces an average oxidation rate that is dependent upon the timestep length, being smaller for longer timesteps. This is appropriate for the concept that the oxide layer remains in place and builds up over the metallic surface. However, sloughing of the oxide layer after a specified

thickness has been attained can also be represented, as explained in the following discussion.

3.4.1 Oxidation of Zirconium

The oxide thickness X_o over the debris bed particles is permitted to increase over succeeding timesteps until the user-specified limit XOZRMX (BH0700) is reached. The Cathcart relation[19] is used for control volume temperatures T_{CV} less than or equal to 1853 K so that

$$\begin{aligned} A &= 3.730 \times 10^{-6} \text{ m}^2/\text{s} \\ B &= 20100.6 \text{ K} \end{aligned}$$

For control volume temperatures greater than 1853 K, the Baker-Just relation [20] is used for which

$$\begin{aligned} A &= 3.94 \times 10^{-5} \text{ m}^2/\text{s} \\ B &= 22900.0 \text{ K} \end{aligned}$$

The reaction rate as limited by gaseous diffusion is calculated for the debris bed particles by the Baker-Just relation [20]:

$$XDTO1 = 5.636 \times 10^{-10} \times \frac{\left(\frac{DFRAG}{2}\right) \times T_f^{0.68}}{\left(\frac{DFRAG}{2} - X_o\right)^2} \text{ m/s} \quad (3.2)$$

where

DFRAG = diameter of debris particles, m (Provided as DPART in BH package input [BH0500])

T_f = film temperature

$$= \frac{T_{CV} + \frac{T_{in} - T_{out}}{2}}{2} \text{ K}$$

T_{in} = temperature of steam entering control volume, K

T_{out} = temperature of steam leaving control volume, K

The reaction rate used for zirconium metal within the debris bed control volume is then

$$XDTO = \frac{\text{MIN}[XDTO, XDTO1]}{\text{SFCRDB}} \quad \text{m/s} \quad (3.3)$$

which is the minimum of the rates limited by solid state diffusion and gaseous diffusion divided by the user-input shape factor (BH0700).

The shape factor SFCRDB is intended to permit the user to adjust for the non-cylindrical geometry and decreased surface-to-volume ratio that may be associated with the debris particles in the lower plenum. In effect, the zirconium-steam reaction rate is calculated for the current conditions assuming cylindrical geometry and then divided by the shape factor. Since the actual representative geometry for the debris particles is unknown, this permits the user to parametrically investigate the effect of particle shape and other uncertainties that might contribute to reduction of the metal-steam reaction rate. It should be noted that use of a shape factor greater than one can also be employed as a means to reduce the zirconium-steam reaction rate to represent the effect of steam tunneling.

It is next necessary to apply the reaction rate XDTO over the surface area of zirconium metal. First, the total surface area of the debris particles is estimated as

$$\text{BDAREA} = \frac{V_{\text{cv}} \times 6.0 \times (1 - \text{PORB})}{\text{DFRAG}} \quad \text{m}^2 \quad (3.4)$$

where

$V_{\text{cv}} = \text{VLP(I,J)}$, total volume within control volume, m^3

$\text{PORB} = \text{PORB(I,J)}$, porosity of control volume debris

and the particles are represented as being either spherical or of cylindrical shape with length equal to diameter (typical of BWR fuel pellets).

Second, the fraction of the total debris surface area that is zirconium metal is taken to be the same as the volume fraction of zirconium within the debris:

$$\text{FZRNOD} = \frac{\text{ZRAVIL}}{\text{AMSUM(I,J)}} \times \frac{\text{RHOAVG}}{\text{RHOZR}} \quad (3.5)$$

where

$\text{RHOAVG} = \text{average debris density, kg/m}^3$

BH Package Reference Manual

RHOZR = zirconium density, kg/m^3

ZRAVIL = zirconium mass (solid + liquid) associated with debris particles, kg

AMSUM(I,J) = total mass within control volume, kg

The mass of zirconium metal considered eligible for oxidation (if sufficient steam is available) during a timestep is then

$$\text{DELZRO} = \text{XDTO} \times \text{BDAREA} \times \text{FZRNOD} \times \text{RHOZR} \times \text{DTM} \quad \text{kg} \quad (3.6)$$

It should be noted that DELZRO is actually independent of the value of RHOZR, since this quantity appears in the denominator of the expression for FZRNOD. The term RHOZR is included in the printed logic only to improve the clarity of the approach.

Finally, the power produced by the metal-steam reaction within the control volume is the minimum of

$$4.179013 \times 10^{10} \times \text{XDTO} \times \text{BDAREA} \times \text{FZRNOD} \quad \text{W} \quad (3.7)$$

and

$$1.6282 \times 10^7 \times \text{WSO} \quad \text{W}. \quad (3.8)$$

Here WSO is the rate (kg/s) at which the steam entering the upper surface of the control volume (if penetrations have failed) or being created within the control volume by boiling (if the lower plenum has been flooded) becomes available to the zirconium surfaces. (Oxidation of one m^3 of zirconium releases 4.18×10^{10} J, while 1.63×10^7 J are released per kg of steam reacted with zirconium.)

If the reaction rate is limited by the availability of steam, which is the usual case within the lower plenum debris bed, then the mass DELZRO reacted is reduced accordingly. At this point, it is important to note that whatever steam is available within a control volume must be divided between the zirconium metal and stainless-steel surfaces that are being oxidized. This is done by first calculating the steam demands for the zirconium and stainless-steel reactions separately, and then apportioning the available steam according to the relative magnitudes of the two demands.

3.4.2 Oxidation of Stainless-Steel

The option to represent stainless-steel oxidation whenever steam becomes available within the lower plenum debris bed is an important augmentation of the capabilities of MELCOR. Detailed information concerning the rationale for and the importance of representing stainless-steel oxidation is provided in Reference 17. While there are different metals

reacting with steam and different reaction rates, the code logic for oxidation of the stainless-steel components is analogous to the logic for zirconium oxidation. For example, a user-specified maximum oxide thickness XOSSMX is employed to limit the thickness of the oxide layer over the steel surfaces in the same manner as XOZRMX is employed for the zirconium oxide layer. The gaseous diffusion limitation (Equation (3.2)) is applied (with appropriate coefficients) to the steel oxidation rate under steam-lean and hydrogen-excess conditions.

From Reference 17, Table 3.6 provides the relative energy releases per unit metal mass reacted and per kilogram of steam consumed for the metals of interest, at the melting temperature of stainless-steel. For preparation of this table, stainless-steel (SS) is defined in the typical manner, as a mixture of 0.74 Fe, 0.18 Cr, and 0.08 Ni by weight. It should be noted that the oxidation of nickel is endothermic. As indicated, the overall energy release associated with the oxidation of one kg of stainless-steel is about one-sixth of the energy release accompanying the oxidation of the same mass of zirconium.

Table 3.6 Heats of Reaction at 1,700 K

Metal	kJ/kg Metal	kJ/kg Steam
Zr	6,425.7	16,282.0
Fe	500.5	1,165.0
Cr	3,506.6	6,753.5
Ni	-330.2	-1,080.0
SS	975.1	2,236.6

The stainless-steel oxidation reactions represented in this table occur under steam-rich conditions, with the products Fe_2O_3 , Cr_2O_3 , and NiO . Other reactions are expected to occur under steam-lean or hydrogen-excess conditions. The complete range of possibilities is addressed by the BH package code logic as explained in the following paragraphs.

3.4.2.1 Steam-Rich Conditions

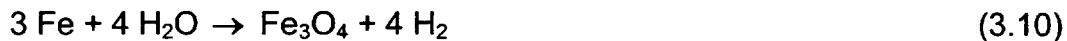
In accordance with Baker's criteria [18], stainless-steel oxidation under "steam-rich conditions" will occur whenever the steam-to-hydrogen partial pressure ratio in the surrounding atmosphere equals or exceeds

$$1122.475 \times e^{-\frac{4250.7}{T}} \quad (3.9)$$

which is a temperature-dependent quantity with T in Kelvin. In the actual coding, the partial pressure ratio is represented by the molar ratio. As an example, at 1,700 K the ratio of moles of steam to moles of hydrogen within a debris bed control volume atmosphere would have to exceed 92.1 in order for steam-rich conditions to prevail.

BH Package Reference Manual

The oxidation reactions under steam-rich conditions are



with an energy release of

$$[49031.16 + T \times (0.00655833 \times T - 28.20968)] \times \frac{2326.0}{40.0} \text{ J/kg steam} \quad (3.11)$$



with an energy release of

$$[102987 + T \times (0.00542125 \times T - 18.55925)] \times \frac{2326.0}{30.0} \text{ J/kg steam} \quad (3.13)$$

and



with an energy release of

$$-[522.34 + 2.4167 \times T] \times \frac{2326.0}{10.0} \text{ J/kg steam} \quad (3.15)$$

Example values of the energy releases for Fe, Cr, and Ni at 1,700 K are listed in Table 3.6. Also occurring under steam-rich conditions is the oxidation reaction



with an energy release of

$$[7948.74 + 0.2874 \times T] \times \frac{2326.0}{10.0} \text{ J/kg steam} \quad (3.17)$$

At 1,700 K, this reaction releases 1,959 kJ/kg steam reacted. As explained in Section 3.4.2.2, FeO is produced by the oxidation of iron under steam-lean conditions.

The steel oxidation rate for steam-rich calculations is determined by use of White's kinetics correlations [18] as follows. The linear portion of the solid state diffusion limitation is

$$0.362426 \times e^{-\left(\frac{22320.1}{T}\right)} \text{ m/s} \quad (3.18)$$

while the parabolic portion is determined utilizing Equation (3.1) with rate constants of

$$A = 13.02840 \text{ m}^2/\text{s}$$

$$B = 42428.0 \text{ K}$$

It is the minimum of these two rates that is applied for the steam-rich case. Continuing the set of examples for 1,700 K and assuming a timestep length of one second with a representative initial oxide layer thickness of 1×10^{-6} m, the calculated rates are

$$\text{linear: } 7.197 \times 10^{-7} \text{ m/s}$$

and

$$\text{parabolic: } 1.846 \times 10^{-5} \text{ m/s}$$

so that the linear rate would be used. Lower temperatures and larger oxidation layer thicknesses reduce the parabolic to linear rate ratio.

3.4.2.2 Steam-Lean Conditions

Again, following Baker's criteria [18], "steam-lean" conditions prevail whenever the steam-to-hydrogen partial pressure ratio is less than the lower boundary value (Equation (3.9) for the steam-rich regime, but equals or exceeds

$$3.137 \times e^{-\left(\frac{2858.0}{T}\right)} \quad (3.19)$$

which represents the upper boundary for the hydrogen-excess regime. Continuing the 1,700 K example, the steam-lean reaction correlations would be applied for ratios between 0.584 and 92.1.

Under steam-lean conditions, the iron reaction is



with an associated energy release of

$$[9294.8 - 3.2744 \times T] \times \frac{2326.0}{10.0} \text{ J/kg steam} \quad (3.21)$$

Thus, iron oxidized under steam-lean conditions follows a two-step pathway to becoming Fe_3O_4 , with the second step performed when (and if) steam-rich conditions are resumed. The associated total energy release at 1,700 K is indicated in Table 3.7.

Table 3.7 Heats of Reaction for FeO Two-Step Pathway

Metal		kJ/kg Fe	kJ/kg Steam
Fe	→ FeO	279.7	867.2
FeO	→ Fe_3O_4	210.6	1,959.0
Fe	→ Fe_3O_4	490.3	1,140.1

As expected, the total energy releases for the two-step pathway are very close to the energy releases for the direct pathway as listed in Table 3.6.

The only other oxidation reaction to occur under steam-lean conditions is the chromium reaction, which is the same as for steam-rich conditions and is represented by Equations (3.12) and (3.13). Specifically, neither nickel nor FeO is oxidized under steam-lean conditions.

The steel oxidation rate for steam-lean conditions is determined considering solid-state diffusion as predicted by the White correlations in the same manner as for steam-rich conditions, taking the minimum of the two rates according to Equations (3.18) and (3.1) with the rate constants listed in Section 3.4.2.1. In addition, weight is given to the oxidation rate as predicted by Baker's correlation for hydrogen excess conditions by utilizing Equation (3.1) with rate constants of:

$$A = 2.376 \times 10^{-5} \text{ m}^2/\text{s}$$

$$B = 25163.6 \text{ K}$$

and then averaging this rate with the White result. For example, at 1700 K, a timestep length of one second, and with an assumed initial oxide thickness of $1.0 \times 10^{-6} \text{ m}$, the minimum of the two White predictions is $7.197 \times 10^{-7} \text{ m/s}$ as explained in Section 3.4.2.1. The Baker correlation predicts a rate of $3.326 \times 10^{-6} \text{ m/s}$, so the average

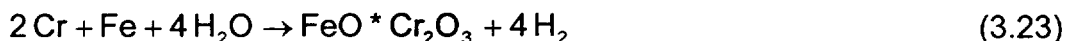
$$\frac{7.197 \times 10^{-7} + 3.326 \times 10^{-6}}{2.0} = 2.023 \times 10^{-6} \text{ m/s} \quad (3.22)$$

is taken to be the stainless-steel oxidation rate.

3.4.2.3 Hydrogen Excess

The appellation "hydrogen excess," according to Baker [18], applies to atmospheres for which the steam-to-hydrogen partial pressure ratio is less than the value given by Equation (3.19). As described in Section 3.4.2.2, hydrogen excess conditions exist at 1,700 K only for partial pressure ratios less than 0.584.

Oxidation under hydrogen excess occurs according to the reaction



where $\text{FeO} \cdot \text{Cr}_2\text{O}_3$ is a "spinel" compound. This reaction may be thought of as a simple addition of Equations (3.12) and (3.20), and the associated energy release is calculated (using Equations (3.13) and (3.21)) as if this were the case. There is a linkage, however, between the amounts of Fe and Cr reacted that does not exist under other than hydrogen excess conditions.

In practice, the stainless-steel reaction rate is calculated in the same manner as for the steam-lean case, and this is used to determine the amount of chromium to be reacted during a timestep. The amount of Fe to be included is then established based upon the relation that one mole of Fe is reacted for every two moles of Cr.

3.4.3 Treatment of Excess Liquids

With small amounts of liquid, it is reasonable to assume that the liquid is smeared over the surfaces of the debris bed particles from which the liquid is oozing. (The liquid is formed at the pure metal surface, then must pass through the overlying rough oxide layer to reach the surface, from which any excess would drip.) With larger amounts of liquid, some would remain as a smear over the particle surfaces, while some would pool in the lower portion of the control volume. The portion of the liquid that is pooled will have a much lower effective surface area for oxidation by the overlying steam.

Normally, the control volume debris includes a large proportion of solids, including the high-melting-temperature oxides ZrO_2 and UO_2 . Code logic represents the debris bed particles, of total diameter DFRAG (see Equations (3.2) and (3.4)), as having solid cores surrounded by an outer liquid layer of thickness not more than one-tenth of DFRAG, or one millimeter, whichever is smaller. Since the volume of the individual particles is proportional to the cube of the diameter, this means that for values of DFRAG less than 0.010 m (one cm), up to 48.8 percent of the total particle volume can be occupied by liquids. For larger values of DFRAG, the one-mm liquid layer thickness limitation takes effect. For example, if DFRAG is 3 cm, then the liquid layer can occupy no more than 18.7 percent of the total particle volume.

Excess liquids, that cannot be carried over the solid cores of the bed particles, are represented as pooled over the floor of the control volume with a total surface area exposed to steam equal to the volume/height ratio of the control volume. The surface area of the particles exposed to steam is reduced appropriately to recognize that some of the particles in the lower portion of the bed would be covered by the pooled liquids and, therefore, not available for oxidation.

3.4.4 User Controls

User controls of the lower plenum debris bed oxidation rates are provided in BH package input (BH0700). By setting of the input parameter IMWDEB, the user can specify no metal oxidation, zirconium oxidation only, steel oxidation only, or full oxidation (both zirconium and steel).

The user also specifies XOZRMX and XOSSMX, which are the maximum oxide thicknesses over the zirconium and steel metal surfaces, respectively. The code logic keeps track of the buildup of these oxide layers as oxidation progresses. When these limits are reached, the code provides that the excess oxides are shed. A representative value for these parameters is 1.0×10^{-6} m, which serves to maintain a conservatively high oxidation rate. If higher oxide layer thicknesses are specified, the reaction rates will be reduced, and the period during which oxidation occurs will be extended.

The shape factors SFCRDB and SFCRSS have the effect of limiting the zirconium and stainless-steel reaction rates during each timestep, but their use does not permanently exclude any of the zirconium or steel from reaction with steam. This can be done by use of the input parameters FZRMX1 and FSSMX1; the zirconium steam reaction within the lower plenum is terminated whenever the fraction FZRMX1 of the total zirconium metal mass that has been introduced to the lower plenum has been reacted. Similarly, steel oxidation is terminated whenever the fraction FSSMX1 of the total stainless-steel inventory that has been introduced to the lower plenum has been oxidized.

3.4.5 General Effects of Metals Oxidation

As explained in the introduction to this section, it is expected that a reactor vessel lower plenum debris bed would include large masses of zirconium and stainless-steel, particularly in BWRs. There is a clear potential for significant energy release within the bed by oxidation of these metals. The degree of accuracy to which oxidation rates can be estimated by application of the available experimentally derived correlations is limited, but it is important to recognize that separate and independent logic is employed within subroutine BHMWDE to correctly limit the extent of oxidation according to the availability of both metal surfaces and steam. In other words, the calculated rates for oxidation may be too fast or too slow, but there will be no violation of the conservation of mass or energy.

In general, the period of metal oxidation is relatively brief when compared to the typical time duration (3–4 hours) between water addition to a heated lower plenum debris bed and predicted gross bottom head failure by creep rupture. Thus, even if the calculated oxidation rates are an order of magnitude too high, the appropriate amount of energy is being released within the debris before the predicted bottom head failure.

The basic approach provided by the BH package logic is to employ the White and Baker correlations in such a manner as to calculate reasonable but conservative (i.e., on the high side) oxidation rates, while allowing the user, by means of code input, to adjust the calculated values so that parametric variation analyses can be performed. When oxidation occurs, it is assumed to first take place within the liquid layer overlying the particle surfaces.

The mass of liquid zirconium (or stainless-steel) within the control volume is reduced as necessary to adjust for the amount of metal oxidized and if this is insufficient, then the remaining mass of metal oxidized is subtracted from the solid zirconium (or stainless-steel components) present. The masses of liquid and solid zirconium oxide (or of the steel oxides) within the control volume are increased appropriately. (Oxidation of liquid metals produces liquid oxides while oxidation of solids produces solid oxides.) If liquid oxides are formed while the control volume temperature is below the liquid oxide freezing temperature, then a phase change for the oxides is carried out in another portion of the BH package (subroutine BHEUTF) during the same timestep.

The mass flow of steam leaving the control volume is equal to the entering flow plus any internal steam generation minus the steam consumption rate. The mass flow of hydrogen leaving the control volume is equal to the entering flow plus the hydrogen production equivalent to the steam consumption, which for zirconium is

$$\left(\frac{2.14594}{18.01534} \right) \times \text{DWSBO} \text{ kg/s} \quad (3.24)$$

where DWSBO is the steam consumption rate (kg/s). Analogous expressions are employed for the steam consumption rates associated with the steel components or the FeO, which are represented within the code logic by H2OFE, H2OCR, H2ONI, and H2OFEO, respectively.

The metal-water reaction energy release within a control volume is transferred to the debris. The gas mixture flowing through the control volume is assumed to exit at the control volume temperature and the appropriate amount of energy for this is transferred between the debris and the gas. If penetration failures have occurred, then the gas mixture leaving one control volume enters the next lower control volume or escapes from the vessel, as appropriate to the location of the control volume in the gas escape pathway.

4. Debris Melting and Relocation

This section describes the melting and relocation of pure species and eutectic mixtures within the debris bed. Information concerning the melting temperatures, molecular weights, and heats of fusion for the pure species is provided as user input (BH0200). Additional user input is required if the formation of eutectic mixtures is to be considered.

4.1 Material Relocation

Within the debris bed, molten material moves downward from one control volume to another as long as void space (free volume) remains within the lower control volume. Once the interstitial void in the underlying control volume is filled, the molten liquid can move horizontally within the bed as necessary to keep the liquid level approximately constant within a layer. An exception occurs in the case of the two outermost control volumes in layer two if penetration weld failure occurs at the wall. For control volumes (2,4) and (2,5), simultaneous movement downward to the void space in the (single) underlying control volume (1,3) and horizontally to exit the vessel through the failed penetration welds can occur.

In all cases, the rate of movement of molten material through the debris bed is controlled by a user-input time constant DTHEAD (BH0500), usually set at one minute. Thus, for example, if the calculational timestep for the lower plenum model is 0.2 minute (and with the one-minute time constant), 20% of the molten material within a control volume can move vertically downward each timestep. Horizontal movement of molten material proceeds at one-half the rate of vertical movement.

As liquid debris relocates from one control volume to another or escapes from the lower plenum, the free volume associated with the interstitial voids in the source control volume is increased. In the former case, the transfer of liquids within the bed is calculated by subroutine BHDBME. In the latter case, the escape of liquids from the lower plenum via penetration failures is calculated by subroutine BHDBMX.

In either case, the increase of free volume within the source control volume is

$$\sum_{K=1}^{20} \frac{MTRAN(K)}{RHOLIQ(K)} \quad m^3$$

where

MTRAN(K) = liquid mass of material K currently being transferred, kg

RHOLIQ(K) = density of liquid K, kg/m³

and the summation is over the 20 debris materials. (Several of the array elements available to represent the debris materials are currently vacant, however—see Table 2.1.)

If the liquid transfer is to another bed control volume, then the free volume of the receiver is decreased by an identical amount. Furthermore, the temperature of the receiver control volume is adjusted as necessary to compensate for the inflow of energy and liquid mixture mass. If the transfer causes cooling of the relocating liquid and heating of the receiver control volume, then logic within subroutine BHDBME freezes an appropriate portion of the higher-melting temperature constituents of the liquid mixture and checks for induced melting of a portion of the solid material originally present.

If, on the other hand, the liquid transfer causes cooling of the receiver control volume and heating of the transferred liquid, then the code logic checks for freezing of any of the liquid materials originally present (before the transfer).

One important effect of the downward relocation of molten material occurs relatively early in the debris bed response calculation. As discussed in Section 1.1, MELCOR normally predicts a large fraction of oxides to be included among the debris present within the BWR lower plenum at the time of bed dryout. Since the bottom bed layer comprises a representative sampling of this debris, the mass ratio of oxides to metals in the layer one control volumes can initially be quite high (typically in the vicinity of 0.60).

This large initial fraction of oxides, however, in turn produces a significant representative porosity for the solid debris of the bottom layer control volumes. As the temperature of the central region of the bed reaches the melting points of its constituent metals and metallic mixtures, liquid metals relocate downward to the bottom debris layer. This results in an early temperature increase for the bottom layer combined with elimination of the local free volume and significant reduction of the oxides-to-metals ratio. The large additional metallic heat sink provided by this early relocation then significantly delays the subsequent temperature increases within the bottom debris layer.

4.2 Formation of Eutectic Mixtures

As the temperature of the debris increases, the lower plenum model calculates the melting, migration, freezing, and remelting of the materials within the control volumes that represent the bed. Both melting of materials as pure species and melting of materials as constituents of eutectic mixtures are represented. The compositions of the eutectic mixtures to be considered (as many as ten) are specified by user input. As a guide toward the realistic formulation of this input, the eutectic mixtures formed and the associated melting temperatures determined in a recent small-scale experiment [21] to investigate the melting and relocation of BWR debris are listed in Table 4.1.

BH Package Reference Manual

Table 4.1 Eutectic Mixture Compositions Determined for the Lower Plenum Debris Bed

Eutectic Mixture	Mole Fractions	Melting Temperature	
		K	°F
Zr - SS ^a	0.100 - 0.900	1523	2282
Fe - Cr - Ni ^b	0.733 - 0.192 - 0.075	1700	2600
Zr - SS - UO ₂	0.367 - 0.605 - 0.028	1873	2912.
ZrO ₂ - UO ₂	0.868 - 0.132	2573	4172.

^a SS represents stainless-steel.

^b This is the stainless-steel eutectic mixture.

The information listed in Table 4.1 or other combinations of materials and melting temperatures to form eutectic mixtures is specified by means of input records BH0800, BH0900, and BH1000.

It is instructive to see how the melting temperatures of the eutectic mixtures described in Table 4.1 relate to the melting temperatures of the pure material species considered in a typical calculation. Table 4.2 provides the list of debris constituents represented in a recent example, in order of increasing melting temperature.

Table 4.2 Debris Constituents Considered in a Typical Calculation

Constituent	Melting Temperature (K)
FeO	1650
Mixture 1	1723
Mixture 2	1733
Fe ₃ O ₄	1839
Mixture 3	1873
Ni	1900
Fe	1900
Zr	2125
Cr	2144
NiO	2244
Cr ₂ O ₃	2572
Mixture 4	2573
B ₄ C	2728
B ₂ O ₃	2728
ZrO ₂	2978
UO ₂	3011

These constituents and melting temperatures are considered to provide a reasonable representation of the actual debris bed composition that would be formed in an unmitigated

BWR accident; these are the constituents that were represented when the calculations whose results are discussed in Section 6 were performed.

Within each bed control volume, the question of debris constituent melting is pursued in a stepwise fashion as the temperature increases. As the temperature reaches the melting point of a pure species, additional energy released within or transferred into the control volume is consumed in melting the remaining mass of the species. But when the control volume temperature reaches the melting point of a eutectic mixture, the question as to how much of the mixture can be formed from the locally available constituents must be answered before the amount of energy consumed in melting the mixture can be determined.

Eutectic mixtures are treated within the lower plenum debris bed model by subroutines BHEUTM, BHEUTF, and BHEUTK. The amount of the mixture that can be formed within a control volume given the current constituent masses is determined by BHEUTK. The energy transfers associated with heatup or cooldown past the eutectic melting point are determined by BHEUTM or BHEUTF, respectively. The operation of these subroutines is described in detail in the following paragraphs.

Subroutine BHEUTF is called on a control volume basis whenever the local temperature is decreasing. The purpose is to identify any pure species or eutectic mixture that should begin a phase transition from liquid to solid, to carry out the appropriate portion of this transition, and to determine the final control volume temperature. The major steps in this process are outlined below.

1. Each of the 20 pure material species that may be present within the debris (Table 2.1) is evaluated to establish how much of the liquid mass currently present within the control volume is tied up with eutectic mixtures that have freezing temperatures lower than the current control volume temperature. Any remaining liquid masses are identified as potential candidates for freezing and stored in the array AMINSP(20).
2. The second step is to establish the order in which pure species and eutectic mixtures (if any) are in line for freezing. This is done by evaluating each constituent liquid that is represented within array AMINSP(20) by a mass of at least 0.1 kg to determine which of these, if any, have freezing temperatures equal to or higher than the current control volume temperature. From this group, the constituent with the highest freezing temperature is first in line and the constituent with the freezing temperature closest to the current control volume temperature is identified as last in line for freezing.
3. Steps 3 through 7 are carried out for each constituent liquid present within the control volume that is in line for freezing. Beginning with the first (highest freezing point) constituent, the amount of energy that would be required to increase the current control volume temperature to the freezing point of the constituent is

$$\text{DELQ} = \text{AMSUM} \times \text{CPDEB} \times [\text{TMLTBH} - \text{TMLP}(\text{I}, \text{J})]$$

where

$\text{AMSUM}(\text{I}, \text{J})$ = total mass within the control volume, kg

$\text{CPDEB}(\text{I}, \text{J})$ = representative control volume specific heat, J/(kg • K)

TMLTBH = freezing temperature of the constituent liquid mass, K

$\text{TMLP}(\text{I}, \text{J})$ = control volume temperature, K

4. Subroutine BHEUTK is called to determine whether the available subcooled liquid is present as a pure species or as a member of a eutectic mixture. The number of moles of liquid available for freezing is determined in either case. If a eutectic mixture is involved, this includes the number of moles contributed by the other liquid material components. (Additional information concerning the operation of subroutine BHEUTK is provided at the end of this section.)
5. The energy that would be released by freezing all of the available subcooled liquid is

$$\text{DUFREZ} = \text{AMRX} \times \text{AMLF}$$

where

AMRX = moles of liquid available for freezing

AMLF = heat of fusion, J/mole

and the sum is taken over all of the component liquids if a eutectic mixture is involved.

6. The fraction of the available subcooled liquid to be frozen is then

$$\text{FRAC} = \frac{\text{DELQ}}{\text{DUFREZ}}$$

constrained to be not more than 1.0.

7. The control volume temperature increase associated with the freezing of the identified fraction of the available subcooled liquid is then calculated as

$$\frac{\text{FRAC} \times \text{DUFREZ}}{\text{AMSUM} \times \text{CPDEB}} \text{ K}$$

The cycle consisting of steps 3 through 7 is repeated in turn for each pure species or eutectic mixture in line for freezing until either the new control volume temperature exceeds the freezing temperature of the next constituent liquid in the queue or all of the constituents originally in the queue have been frozen.

Subroutine BHEUTM is called on a control volume basis whenever the local temperature is increasing, which is the normal situation after lower plenum debris bed dryout. The purpose is to identify any pure species or eutectic mixture that should begin a phase transition from solid to liquid, to carry out the appropriate portion of this transition, and to determine the final control volume temperature. The major steps carried out within subroutine BHEUTM are described below.

1. A search is conducted to identify any solid debris constituents within the control volume with melting temperatures below the current control volume temperature.
2. If any such solid superheated debris constituents exist, they are treated in order, starting from the available superheated solid with the lowest melting point.
3. Steps 3 through 7 are repeated for each of the superheated solids. The energy release that would be attained by lowering the current control volume temperature to the melting temperature of the superheated solid is:

$$\text{DUMELT} = \text{AMSUM} \times \text{CPDEB} \times [\text{TMLP} - \text{TMLTBH}]$$

where TMLTBH represents the melting temperature of the superheated solid.

4. Subroutine BHEUTK is called to determine whether the available superheated solid is present as a pure species or as a member of a eutectic mixture; the number of moles available for melting is established in either case. [If a eutectic mixture is involved, this includes the number of moles contributed by the other solid material components.]
5. The energy that would be required to melt all of the available superheated solid is:

$$\text{DUMELX} = \text{AMRX} \times \text{AMLF}$$

Where,

AMRX = moles of solid available for melting,

BH Package Reference Manual

AMLF = heat of fusion, J/mole

and the sum is taken over all of the component solids if a eutectic mixture is involved.

6. The fraction of the available superheated solid to be melted is:

$$\text{FRAC} = \frac{\text{DUMELT}}{\text{DUMELX}}$$

And is constrained to be not more than 1.0.

7. The reduction in control volume temperature associated with melting of the identified fraction of the available superheated solid is then

$$\frac{\text{FRAC} \times \text{DUMELX}}{\text{AMSUM} \times \text{CPDEB}} \text{ K.}$$

The cycle consisting of steps 3 through 7 is repeated in turn for each superheated pure species or eutectic mixture until either the new control volume temperature is below the melting temperature of the next solid in line or all of the solids originally identified as superheated have been melted.

As noted above, subroutines BHEUTF and BHEUTM both call subroutine BHEUTK to determine the nature of the debris constituent about to undergo a change of phase, which is termed the "key" constituent. The question is whether this key constituent is to be treated as a pure species or as the identifying component of a eutectic mixture; in the latter case, what are the other components of the mixture and how much of the mixture can be formed within the control volume?

Subroutine BHEUTK finds the number of moles of the key constituent as:

$$\text{DDMRX} = \frac{\text{AMSCV}}{\text{AMMLWT}} \text{ kg-moles}$$

Where,

AMSCV(KEY) = mass of the key constituent within the control volume, kg, and

AMMLWT(KEY) = molecular weight of the key constituent, kg/kg-mole.

For calls from subroutine BHEUTF, AMSCV is constrained to exclude any constituent liquids that are components of eutectic mixtures that have freezing temperatures lower than the current control volume temperature.

The total number of moles to undergo phase change is then:

$$\text{AMTOT} = \frac{\text{DDMRX}}{\text{FRNKEY}} \text{ kg-moles}$$

where FRNKEY is the mole fraction of the key constituent within its associated eutectic mixture and is set to 1.0 for a pure species. If AMTOT is equal to DDMRX, then the key constituent is to be treated as a pure species and the call to subroutine BHEUTK is returned.

If AMTOT is greater than DDMRX, however, then the key constituent is the identifying component of a eutectic mixture and the other components must now be identified. To do this, subroutine BHEUTK makes use of the two series identified in Table 4.3.

The material series at the left of Table 4.3 is derived from user input and is the same as has been discussed previously. The constituent series at the right of Table 4.3 is derived from the material series (neglecting the vacant slots) plus the list of eutectic mixtures to be considered. That both series as listed on Table 4.3 have 20 members is a matter of coincidence. This occurs because the four vacant slots (8, 9, 19, 20) of the material series are exactly counterbalanced by the four eutectic mixtures considered in this calculation. Since as many as ten eutectic mixtures can be specified, the constituent species can have up to 30 members (if all 20 slots in the material species were utilized). On the other hand, since only 16 members of the material species are currently represented, the number (NSPECS) of constituent series members can be as few as 16, if no eutectic mixtures are specified.

It should be noted that the members of the constituent series are arranged in order of ascending melting temperatures, which are indicated in Table 4.2. (Although slots are reserved in the material series for C, B, U, and Fe_2O_3 , current BH package logic does not actually produce any of these materials within the lower plenum debris bed and hence, for simplicity, they have been omitted from Table 4.2.)

Returning to the discussion of the method by which subroutine BHEUTK identifies the materials to undergo phase change, the key constituent is identified within subroutines BHEUTF or BHEUTM as a member of the constituent series. As an example, suppose that the control volume temperature has just increased above 1839 K; then any Fe_3O_4 within the control volume would be identified within subroutine BHEUTM as a superheated solid (Table 4.2). The index of the key constituent would be 6 (Table 4.3). The index within the material series would be 14, which is stored in the NEUKEY(30) array as

BH Package Reference Manual

element NEUKEY(6). Since FRNKEY(6) has a value of 1.0, subroutine BHEUTK identifies the debris constituent about to undergo melting as the pure species Fe_3O_4 .

Table 4.3 Constituent Series Employed by Subroutine BHEUTK with Example of Use of Cross-Reference Index for a Pure Species

Material Series Elements 1 through 20		Constituent Series Elements 1 through NSPECS	Mixture Key Component
1. Zr		1. U	
2. Fe		2. FeO	
3. Cr		3. Mixture 1	Fe
4. Ni		4. Fe_2O_3	
5. C		5. Mixture 2	Cr
6. B	KEY	6. Fe_3O_4	
7. U		7. Mixture 3	Zr
8. —		8. Ni	
9. —		9. Fe	
10. B_4C		10. Zr	
11. ZrO_2		11. Cr	
12. FeO		12. NiO	
13. Fe_2O_3		13. B	
NEUKEY(KEY) 14. Fe_3O_4		14. Cr_2O_3	
15. Cr_2O_3		15. Mixture 4	ZrO_2
16. NiO		16. B_4C	
17. B_2O_3		17. B_2O_3	
18. UO_2		18. ZrO_2	
19. —		19. UO_2	
20. —		20. C	

As an example involving a eutectic mixture, suppose that the control volume temperature has just increased above 1873 K, which is the melting temperature of the third eutectic mixture (Table 4.1 and Table 4.2). As indicated in Table 4.4, the key (identifying) component of this mixture, which occupies position 7 in the constituent series, is Zr, which occupies position 1 in the material series. (The key components for each mixture are assigned by user input.) The mole fraction FRNKEY(7) of Zr within mixture 3 is 0.300 (Table 4.1). Therefore, subroutine BHEUTK provides a first estimate for the maximum number of moles of mixture 3 that could be formed within the control volume of:

$$\text{AMTOT} = \frac{\text{DDMRX}(1)}{0.300} \text{ kg-moles}$$

where $DDMRX(1)$ is the number of moles of Zr locally available.

The other components of the eutectic mixture are identified through use of the array $NEU(K,KEY)$, whose elements have a value of 1 if the material with index K in the material series is a component of the mixture with index KEY in the constituent series. As indicated in Table 4.4, KEY has a value of 7 for the third eutectic mixture and the elements $NEU(K,7)$ have values of 1 for $K=1$ (Zr), $K=2$ (Fe), $K=3$ (Cr), $K=4$ (Ni), and $K=18$ (UO_2).

If any mixture component has a mass of less than 0.1 kg within the control volume, then logic within subroutine BHEUTK concludes that the eutectic mixture cannot be formed and the call is returned indicating that no mixture is available for melting. If, on the other hand, sufficient quantities of each component are present within the control volume, then subroutine BHEUTK employs the array

$$XNEU(K,KEY)$$

to determine if the maximum number of moles $AMTOT$ (based upon the amount of the key [identifying] component) can be formed.

The elements of array $XNEU(K,KEY)$ represent the mole fractions of each material K within mixture KEY of the constituent series. The amount of material K required to form the maximum possible amount of mixture is:

$$XNEU(K,KEY) \times AMTOT \text{ kg-moles.}$$

If each component K has at least this many moles locally available, then $AMTOT$ moles of mixture can be formed and the call is returned. If any component has fewer than the required number of moles available, however, then the maximum possible amount of mixture that can be formed within the control volume must be recalculated, based upon the most limiting of the components.

Logic within subroutine BHEUTK identifies the most limiting component by calculating the ratio of moles available to moles required for each material for which $NEU(K,KEY)$ is equal to 1. The component K with the smallest value of this ratio is most limiting. A new value for the number of moles $AMTOT$ of mixture that can be formed is then established by dividing the locally available number of moles of the limiting component by the mole fraction $XNEU(K,KEY)$ of this component within the mixture. Finally, subroutine BHEUTK returns the array

$$AMRX(20) \text{ kg-moles}$$

BH Package Reference Manual

whose elements represent the number of moles of the materials (in the material series) that would be included in the key mixture if the maximum possible amount were formed within the control volume. The actual amount that is formed and melted (or frozen) depends upon the available energy and is determined within subroutine BHEUTM (or BHEUTF), as previously described.

Table 4.4 Constituent Series Employed by Subroutine BHEUTK with Example of Use of Cross-Reference Index for a Eutectic Mixture

Material Series Elements 1 through 20		Constituent Series Elements 1 through NSPECS	Mixture Key Component
NEU(1,7)=1	1. Zr	1. U	
NEU(2,7)=1	2. Fe	2. FeO	
NEU(3,7)=1	3. Cr	3. Mixture 1	Fe
NEU(4,7)=1	4. Ni	4. Fe ₂ O ₃	
	5. C	5. Mixture 2	Cr
	6. B	6. Fe ₃ O ₄	
	7. U	7. Mixture 3	Zr KEY
	8. —	8. Ni	
	9. —	9. Fe	
	10. B ₄ C	10. Zr	
	11. ZrO ₂	11. Cr	
	12. FeO	12. NiO	
	13. Fe ₂ O ₃	13. B	
	14. Fe ₃ O ₄	14. Cr ₂ O ₃	
	15. Cr ₂ O ₃	15. Mixture 4	ZrO ₂
	16. NiO	16. B ₄ C	
	17. B ₂ O ₃	17. B ₂ O ₃	
NEU(18,7)=1	18. UO ₂	18. ZrO ₂	
	19. —	19. UO ₂	
	20. —	20. C	

4.3 Adjustment of Control Volume Dimensions

As individual constituent pure species or material mixtures within the debris bed melt and relocate downward, provision is made to reconfigure the dimensions of the source control volumes in recognition of the shrinking mass. This is accomplished by means of calls to subroutine BHDCHA, which adjusts the control volume interface radii, bottom and surface heights, location of center of mass, and heat transfer lengths.

Within subroutine BHDCHA, bed control volumes are selected for redimensioning if the internal free volume has increased by one or more percent since the dimensions were last set, or if more than one-third of the current control volume mass is in the liquid phase. The first step in the redimensioning process is to set the new total volume.

$$VLP(I,J) = \frac{AMSUM}{RHODB \times (1.0 - PORB)} \text{ m}^3$$

Where,

I = layer index,

J = radial zone index,

AMSUM(I,J) = total control volume mass, kg

RHODB(I,J) = representative density, kg/m³ and,

PORB(I,J) = representative porosity.

The representative porosity and density for each control volume are calculated each timestep in subroutine BHED2, as explained in Sections 2.1 and 2.2.

Based upon the new total volume, the new free volume is

$$FVLP(I,J) = PORB(I,J) \times VLP(I,J) \text{ m}^3$$

It is important to recognize that the porosity represents the fraction of the total volume that is occupied by neither solid nor liquid debris. Thus, the porosity can be zero for control volumes in which some solid material remains, if the interstitial regions between the solid particles is filled with liquid.

The next step in the redimensioning process is to establish the new locations of the boundary points defining the control volume cross-sections as shown in Figure 1.9. These locations are set in the cylindrical coordinate system as explained in Table 4.5.

Table 4.5 Cylindrical Coordinates of Boundary Points for Debris Bed Control Volume (I,J)

Coordinates	Definition
XLT(I,J) YLT(I,J)	radial distance to left upper corner elevation of left upper corner
XRT(I,J) YRT(I,J)	radial distance to right upper corner elevation of right upper corner

BH Package Reference Manual

Coordinates	Definition
XRB(I,J) YRB(I,J)	radial distance to right lower corner elevation of right lower corner
XLB(I,J) YLB(I,J)	radial distance to left bottom corner elevation of left bottom corner

The radial distances cited in Table 4.5 are measured from the lower plenum centerline. The elevations are measured from vessel zero.

Not all of the coordinates listed in Table 4.5 are involved in the redimensioning process for each bed control volume. For example, XLB(I,1) and XLT(I,1) (for the center radial zone) are always zero. In general, XLB(I,J) will equal XLT(I,J) for all control volumes in radial zones one through four while XRB(I,J) will equal XRT(I,J) in the central three radial zones.

If a bottom layer control volume is redimensioned, then both overlying control volumes (in the middle and upper debris layers) will automatically be redimensioned also. Similarly, if a middle layer control volume is redimensioned, then the dimensions of the overlying layer three control volume (if it exists) will also be adjusted. In this manner, tight contact is maintained between the vertically aligned bed control volumes.

After the debris bed control volume dimensions have been revised as appropriate, logic within subroutine BHDCHA calculates the new vertical thickness and sets the new vertical length of the right boundary of each (interior) control volume as:

$$HLAYER(I,J) = YLT(I,J) - YLB(I,J) \text{ m}$$

and

$$HINFC(I,J) = YRT(I,J) - YRB(I,J) \text{ m}$$

respectively. Other geometric parameters affecting conduction heat transfer that are recalculated within BHDCHA at this time are defined in Table 4.6.

Table 4.6 Heat Transfer Geometric Parameters Recalculated in BHDCHA Whenever the Debris Bed Is Reconfigured

Parameter	Definition	Units
HNODE(I,J)	Elevation of control volume center of mass	m
RNODE(I,J)	Radial distance from lower plenum centerline to control volume center of mass	m
AINFCR(I,J)	Interface area for radial heat transfer at the outer vertical boundary of the control volume	m ²
XLW(I,J)	Distance from control volume center of mass to inner surface of vessel wall (only for control volumes that abut the wall)	m
XLR2(3)	Distance from center of mass of control volume (2,4) to control volume boundary along path between centers of control volumes (2,4) and (2,5)	m
XLR2(4)	Distance from center of mass of control volume (2,5) to control volume boundary along path between centers of control volumes (2,4) and (2,5)	m
XLR3(3)	Distance from center of mass of control volume (3,4) to control volume boundary along path between centers of control volumes (3,4) and (3,5)	m
XLR3(4)	Distance from center of mass of control volume (3,5) to control volume boundary along path between centers of control volumes (3,4) and (3,5)	m

As the central portion of the debris bed settles, the upper surface of one control volume may sink beneath the lower surface of an adjacent control volume. Whenever this happens, the appropriate element of the array HTR(I,J) is shifted from a value of 1.0 to 0.0. The elements of this array in effect serve as on-off gates for conduction from control volume (I,J) to control volume (I,J+1) within each bed layer. In this manner, they fulfill the same purpose for conduction within the bed as do the elements of array HTW (discussed in Section 3.1) for conduction from the bed to the bottom head wall.

4.4 Merging of Bed Control Volumes

Code logic provides for merging of two lower plenum debris bed control volumes within the same radial zone whenever continued representation of the local bed region as a three-layered or two-layered structure would not be realistic. Merging can occur only for control volumes vertically aligned; it does not encompass joining of two control volumes within the same debris layer.

4.4.1 Merging Criteria

The checking of current bed conditions to determine whether or not merging of any two control volumes should occur is carried out each timestep within subroutine BHHED2. The criteria considered are as follows:

1. Any bed control volume is flagged for merging if:
 - a. its current mass is less than 20% of the debris mass within its boundaries at the time that the third debris layer was established or
 - b. more than 44% of the solid mass within the control volume has been ablated.
2. In addition, any of the three layer one control volumes are flagged for merging if bottom head penetration failures are considered and
 - a. their current mass is less than 10% of the overlying layer two control volume mass, or
 - b. their volume has been reduced to the point that the right-hand corner of the (descending) overlying layer two control volume has come into contact with the bottom head wall .
3. Additional special criteria are applied to flag layer two control volumes for merging if the overlying layer three control volume exists and
 - a. more than 66.7% of the layer two control volume is in the liquid phase, or
 - b. if the right adjacent layer three control volume does not exist, or
 - c. if the current elevation of the layer two control volume upper surface is less than the elevation of the right adjacent layer one control volume upper surface.

All of these criteria have been developed as results of experience, gained by a process of exercising the lower plenum debris bed and bottom head response models over a series of BWR accident sequences, with and without bottom head penetration failures. As before, the goal is to maintain a realistic representation of the bed configuration as materials melt and relocate.

Each criterion has its own rationale. For example, criterion 1(b) above is necessary for calculations for which bottom head penetration failures are considered and significant ablation of the bottom layer debris is predicted to occur. [See Section 5.3 for a description of this process, which is largely controlled by user-input.] This protection is necessary because code logic does not increase available free volume in response to material ablation. Consequently, control volume settling is not predicted and a situation can

develop in which vertical "worm-holes" have enlarged around the original penetration locations within the debris while the original elevation of the control volume surface is maintained.

The solution provided by criterion 1(b) is based upon the assumption that it is reasonable to expect collapse of the standing debris whenever the "worm-hole" volume exceeds 80% of the volume currently occupied by solid debris. Stated another way, this is equivalent to ablation of 44.4% of the material initially within the control volume.

4.4.2 Merging Process

Once the code logic in subroutine BHHED2 has selected a debris bed control volume for merging, the actual merging process is accomplished by means of a call to subroutine BHMERG. If the selected control volume has a counterpart in an overlying debris layer, then the merging is accomplished from above. Otherwise, the selected control volume merges with its counterpart below.

The temperature of the new control volume is established as the mass-averaged temperature of its two constituent sources. If this is less than the previous temperature of the control volume in this location, subroutine BHEUTF is called to check for and, as necessary, compensate for sudden freezing of pure material species or mixtures. If, on the other hand, the merging has caused the representative control volume temperature to increase, then subroutine BHEUTM is called to adjust, as necessary, for material melting.

The porosity of the new control volume is established as the volume-averaged porosity of its two constituent sources. Finally, its free volume and surface elevation are determined by a call to subroutine BHDCHA, which also provides boundary dimensions for the new control volume in a manner similar to that described in Section 4.3.

5. Failure of the Bottom Head

The Bottom Head (BH) package will consider penetration failures if the user specifies that bottom head penetrations exist. This is done by setting non-zero values for the array NPIPES via input record BH1100. The bottom head failure models will then recognize two different modes of reactor vessel bottom head penetration failure. The first involves creep rupture of the welds holding the instrument tubes and the control rod drive mechanism assemblies within the reactor vessel and is described in Section 5.1. The second, described in Section 5.2, involves direct melting of the instrument guide tubes within the interior of the debris bed. (It is assumed that ex-vessel tube failure will follow the entry of molten debris into the tube.)

As explained in the User's Guide, array elements NPIPES(1) through NPIPES(3) represent the numbers of instrument guide tubes passing through the central, middle, and outermost

BH Package Reference Manual

control volumes of debris bed layer one, respectively. These numbers are employed to determine the regional material ablation rates after instrument guide tube failures have been predicted and a flow of molten liquids through the tube locations has been initiated. The models for debris and wall ablation are described in Section 5.3. If, however, it is desired that penetration failures not be considered in the calculation, then NPIPES(1) through NPIPES(3) should each be set to zero and all debris liquids will be retained within the lower plenum until creep rupture of the bottom head itself is predicted. The models for bottom head creep rupture are described in Section 5.4.

5.1 Penetration Welds

As described in Section 1, many penetration welds are located at or near the inner surface of the lower portion of the vessel bottom head (see Figure 1.7 and Figure 1.8). The BH package recognizes the potential for failure of these welds over the region represented by wall nodes one through nine (see Figure 1.10). For the lowest wall node adjacent to the middle debris layer (wall node nine), these welds are modeled to fail when the temperature of control volume (2,5) (a narrow strip of debris [input parameter THKCRS] adjacent to the wall) satisfies creep rupture criteria (input parameters THK6 and THK60, provided via input record BH0600). Within the bottom debris layer (wall nodes one through eight), the welds will fail whenever the average of the temperature of the inner wall segment and the temperature of the adjacent debris control volume exceeds the creep rupture criteria. The failure time for these Inconel-stainless-steel welds is established as follows.

For each timestep while the penetration welds remain intact, a remaining time before failure is established within subroutine BHHED2 for wall nodes one through nine as:

$$DTFAIL = e^{ATF \times T_{WELD} + BTF} \text{ seconds}$$

where

$$ATF = \frac{A \log(3600) - A \log(360)}{THK60 - THK6} K^{-1},$$

$$BTF = A \log(3600) - ATF \times THK60,$$

$$THK6 = \text{temperature for creep rupture in six minutes, K,}$$

$$THK60 = \text{temperature for creep rupture in 60 minutes, K,}$$

$$T_{WELD} = \text{current temperature at the weld as described in the previous paragraph, K.}$$

As indicated, ATF and BTF are constants based upon user input; their values are established within MELCOR at the time of lower plenum dryout prior to the first call to BH package subroutine BHQSLU.

Based upon the individual values of DTFAIL, a local weld failure time is then associated with each wall node adjacent to the bottom debris layer (wall nodes one through eight) and with the lowest wall node adjacent to the middle debris layer (wall node nine) in the array:

$$\text{TIMFAL}(I) = \text{ATIME} + \text{DTFAIL seconds}$$

where I is the wall node index and ATIME is the current problem calculation time (seconds).

The predicted bottom head penetration weld creep rupture failure times stored in array TIMFAL are never allowed to increase, once set. (They can, of course, decrease as temperatures ascend.) Whenever the current problem time ATIME exceeds a previously-set weld failure time, penetration weld failure is assumed to occur at that wall node and a special output message is written (Section 6.5). Note that the user should adjust the input values of THK6 and THK60 as necessary to conform with the expected reactor vessel pressure at the time that high debris bed temperatures would begin to challenge the weld integrity.

When weld failure is predicted to occur, gas blowdown from the reactor vessel to the drywell is permitted through a user-defined break area intended to represent several failed penetrations. Thus, the predicted gas blowdown (Section 5.5) is rapid. It is important, however, to recognize that **the rate of transfer of molten debris from the reactor vessel to the drywell floor is not determined by the size of this opening.** Rather, molten material is transferred from control volume to control volume within the lower plenum debris bed and from the control volumes adjacent to the vessel wall to the drywell floor in accordance with the input time constant DTHEAD (input record BH0500). In actuality, use of realistic values of DTHEAD will always produce the result that the rate of material transfer from the lower plenum to the drywell is determined by the rate of material melting.

Penetration weld failures can occur only as the initial failure mode within a debris layer. If instrument tube failures (discussed in the following section) have previously occurred within a layer, subsequent weld failures are not considered. Furthermore, if release of debris liquids from the lower plenum is initiated by means of penetration weld failure and instrument tube failures occur subsequently, then liquid release at the penetration welds is terminated and release through the instrument tubes is initiated.

5.2 Instrument Guide Tubes

The second mode of reactor vessel bottom head penetration failure recognized by the BWR lower plenum debris bed models involves the establishment of a leakage pathway through the reactor vessel wall by means of the instrument guide tubes. (Failure of the tubes ex-vessel is assumed to occur as a consequence of the entry of molten debris.) Such a pathway will be established within the middle layer control volumes whenever three conditions are met. First, the debris bed control volume temperatures within the middle layer must exceed the melting temperature of the (stainless-steel) guide tubes; second, sufficient molten material must have been relocated into the underlying bottom debris layer control volume to reduce its free volume to no more than 10% of the total volume; third, molten material must be available in the middle layer to flow into the guide tubes. Instrument guide tube failures are normally predicted to occur in more than one middle layer control volume during the period of a calculation. This is an important consideration, since liquid debris materials must move within the bed (based upon input time constant DTHEAD) to the location where the penetration failure has occurred in order to be released.

Instrument guide tube failure can also occur within any of the bottom layer control volumes, if the local temperature exceeds the stainless-steel melting temperature. Once this occurs, debris liquids are released equally from all three bottom layer control volumes, regardless of the location of the initial bottom layer penetration failure (weld or instrument guide tube).

The opening associated with the instrument tubes for the purpose of gas blowdown is the same as used for the case of penetration weld failure. The flow of molten material from the reactor vessel through the instrument guide tube locations (input parameter NPIPES) is augmented by ablation of the surrounding debris of the bottom layer and of the bottom head itself, as described in the following section.

5.3 Ablation Induced by Flow of Molten Material

As previously discussed, failure of the instrument housing guide tubes within the middle debris layer provides a path for molten materials in the vicinity to pour through the bottom debris layer and the reactor vessel bottom head wall. The lower plenum debris bed and bottom head response model considers the potential for this flowing liquid to ablate the material surrounding the original instrument housing guide tube locations in both the bottom debris layer and in the vessel wall.

The user-input parameters (BH1100) employed by the model that are most important in determining the calculated reactor vessel wall temperatures are listed in the following table.

Table 5.1 User-Input Parameters Affecting the Vessel Wall Temperature Calculation

	Parameter	Representative Value	
DPIPES	Inner diameter of instrument guide tubes	0.0457 m	(0.150 ft)
HPIPES	Coefficient for heat transfer between molten material flowing through the instrument tube locations in the bottom debris layer and the surrounding metallic debris and bottom head wall	$1022.1 \frac{\text{W}}{\text{m}^2 \text{K}}$	$\left(180 \frac{\text{BTU}}{\text{hr ft}^2 \text{F}}\right)$
NPIPES(3)	Number of instrument guide tubes through debris bed lower layer control volumes (1,1), (1,2), and (1,3)	19, 19, 20	
TABLAT	Ablation temperature for solid material in bottom debris layer	1756 K	(2700°F)
THKCRS	Thickness of the debris node adjacent to the vessel wall	5.08 cm	(0.167 ft)

As described in Sections 5.1 and 5.2, movement of the molten material through the bed to the instrument housing guide tubes is controlled by input time constant DTHEAD. The augmentation of this flow by ablation of the surrounding metallic material of the bottom layer and the vessel bottom head is controlled by input parameters HPIPES and TABLAT. Heat transfer from the melting (ablating) surfaces surrounding the flowing debris to the interior of the remaining solid portions of the bottom layer or wall nodes is calculated by the model.

5.3.1 Ablation of the Wall

The ablation of the reactor vessel bottom head wall is calculated in subroutine BHDBMX. The procedure is based upon information provided in References 22 and 23 and basically follows the methodology originally developed by Pilch and Tarbell.

As explained previously, if instrument guide tube (or penetration weld) failures are predicted to occur in any one of the three control volumes of the bottom debris layer, then they are assumed to also occur (simultaneously) in the other two. The calculation considers each bottom layer control volume separately, based upon the local quantity of liquid available for release and the number of penetrations passing through the control volume.

BH Package Reference Manual

The uppermost wall node adjacent to each bottom layer control volume is taken to be representative. With reference to Figure 1.10, these are wall node three for control volume (1,1); wall node five for control volume (1,2); and wall node eight for control volume (1,3).

Calculations are then performed for each of the three wall segments that make up wall nodes 3, 5, and 8 (see Figure 1.11).

The temperature of the liquid entering the penetration pathways through the bottom head wall is taken to be the temperature of the source control volume. The temperature of the inner surfaces of the penetration pathways within the wall are taken to be the melting temperature of carbon steel (1811 K [2800 °F]). As long as the temperature of the flowing liquid exceeds this temperature, then heat is transferred from the liquid to the wall. Some of this energy is further transferred into the interior of the wall segment, increasing its average temperature; the remainder of this energy is consumed in ablation of the wall at the inner surface of the penetration.

Material ablated from the wall is added to the flowing liquid, increasing its mass and lowering its temperature. Thus, the temperature decreases as the liquid passes through the three wall segments. If the temperature of the flow falls below the carbon steel melting temperature, then heat transfer with the wall in the remaining wall segment(s) is not calculated and the flowing liquid enters the drywell at this temperature.

For each bottom layer control volume, calculation of the ablation of the adjacent vessel wall proceeds as follows.

1. The liquid mass entering the wall during the timestep is:

$$\text{SUMIJ} = \sum_{K=1}^{20} \text{AMLP}(K) \times \text{DTR} \text{ kg}$$

where,

$\text{AMLP}(1,J,K,2)$ = mass of the liquid phase of material K within the control volume, kg

J = index of the control volume within layer one

K = index of material in the material series (Table 4.3), and

DTR is the ratio of the current timestep length to the user-input time constant DTHEAD (provided via Input Record BH0500). The initial temperature of the liquid mixture (as it enters the wall) is taken to be the representative temperature of the source control volume.

2. The liquid mass per instrument guide tube is:

$$\text{SUMLIN} = \frac{\text{SUMLJ}}{\text{APIPES}} \text{ kg}$$

where APIPES is simply the floating point value of NPIPES(J).

3. Steps 3 through 9 are carried out for each of the three wall segments of the representative (uppermost) adjacent wall node. The inner surface area of the cylindrical penetration pathways is

$$\text{AREAD} = \pi \times \text{DABWHL} \times \text{XLHEAD} \text{ m}^2$$

where

DABWHL(J,M) = diameter of penetrations in segment M, m

M = index of wall segment,

XLHEAD(M,N) = radial thickness of segment M within wall node N, m and

N = index of representative wall node.

DABWHL(J,M) is initially set to DPIPES (Table 5.1) but, as indicated in step 7 below, its value can increase during the calculation. Use of XLHEAD to determine AREAD is not strictly correct, since the instrument guide tube passage through the wall is in the vertical, not radial direction. However, the instrument tubes pass through only the lower portion of the vessel wall so the associated error is small.

4. The heat transferred to the inner surface of the cylindrical penetration opening is QLD, taken as the minimum of:

$$\text{AREAD} \times \text{HPIPES} \times (\text{TLLIQ} - \text{AMCS}) \times \text{DTM J}$$

and

$$\text{SUMLIN} \times \text{CPLIQ} \times (\text{TLLIQ} - \text{AMCS}) \text{ J '}$$

where the second quantity serves as a check that no more energy will be transferred than would cause the liquid temperature to decrease to the carbon-steel melting temperature. Terms used in these expressions that have not previously been defined are:

HPIPES = user-input heat transfer coefficient (Table 5.1), $\text{W}/(\text{m}^2 \cdot \text{K})$

BH Package Reference Manual

TLLIQ	= temperature of the flowing liquid as it enters wall segment M, K
AMCS	= carbon steel melting temperature, K
DTM	= length of BH package timestep, s and
CPLIQ	= mass-averaged specific heat of the flowing liquid, J/(kg · K) .

5. The heat transferred from the cylindrical penetration inner surface to the wall segment is:

$$QMLD = AREAD \times \frac{AMCS - THDWO}{\left(\frac{0.0509}{BHAKCS} \right)} \times DTM \text{ J}$$

where

THDWO(M,N)= temperature of the wall segment at the beginning of the timestep, K and

BHAKCS = function BHAKCS(THDWO) for temperature-dependent conductivity of carbon steel, W/(m · K) .

The constant in the denominator of this equation reflects an approximation that the average distance between the inner surface of the penetration and the wall segment center-of-mass is 0.0509 m (two inches).

6. The energy per unit volume required to bring this wall segment to the melting temperature and to melt it is:

$$QMELT = RHOCS \times [AMLAMF + BHPCPS \times (AMCS - THDWO)] \text{ J/m}^3$$

Where,

RHOCS = carbon steel density, kg/m³

AMLAMF(2) = iron heat of fusion, J/kg and,

BHPCPS = function BHPCPS(THDWO) for temperature-dependent specific heat of carbon steel, J/(kg · K) .

The volume that will be ablated from the inner surface of the penetration within this wall segment this timestep is then:

$$\text{DELV} = \frac{\text{QLD} - \text{QMLD}}{\text{QMELT}} \text{ m}^3$$

where the numerator is the portion of the energy transfer from the flowing liquid to the wall that is retained for surface melting.

7. The ablation enlarges the penetration diameter so that:

$$\text{DABWHL}_N = \sqrt{\text{DABWHL}_O^2 + \left(\frac{4.0}{\pi}\right) \frac{\text{DELV}}{\text{XLHEAD}}} \text{ m}$$

where the subscripts N and O represent the new and old values, respectively. The mass of wall surface ablated within the wall segment is:

$$\text{AWMELT} = \text{DELV} \times \text{RHOCS} \text{ kg}$$

8. The temperature of the flowing liquid is reduced in passing through the wall segment by the heat transfer to the wall so that

$$\text{TLLIQ}_N = \text{TLLIQ}_O - \frac{\text{QLD}}{\text{SUMLIN} \times \text{CPDEB}} \text{ K}$$

This temperature is further reduced by the infusion of liquid carbon steel from the ablated wall. Allowing for this,

$$\text{TLLIQ}_N = \frac{\text{SUMLIN} \times \text{TLLIQ}_N + \text{AWMELT} \times \text{AMCS}}{\text{SUMLIN} + \text{AWMELT}} \text{ K}$$

is used as the entrance temperature for the liquid flowing into the next wall segment.

9. The mass entering the next wall segment (or, for segment three, escaping into the drywell) is then

$$\text{SUMLIN}_N = \text{SUMLIN}_O + \text{AWMELT} \text{ kg.}$$

The representative temperature of the liquid release to the drywell during the timestep is the mass-averaged temperature of the release from all of the bottom layer control volumes.

BH Package Reference Manual

Predicted penetration weld failures in wall node nine (the lowest of the wall nodes adjacent to control volume (2,5)) provide a direct release pathway for liquid materials in control volumes (2,3), (2,4), and (2,5). (Inclusion of control volume (2,3) in the direct release pathway is necessary because control volumes (2,4) and (2,5) are normally at lower temperatures so that liquid moving laterally from (2,3) would freeze before becoming eligible for release in a two-step pathway.) The associated flows will produce the same effects of wall segment heatup and surface ablation described above for the bottom layer control volumes.

Once instrument tube failure occurs in the middle debris layer, the liquid release point is shifted away from the wall, which introduces the effects of prior interaction with and ablation of the debris surrounding the instrument guide tube locations in the bottom debris layer. As described in the following section, this will alter the characteristics of the flow before the liquid reaches the inner wall surface.

5.3.2 Ablation of the Bottom Debris Layer

As explained in the previous section, liquids generated within the middle debris layer can flow through the bottom debris layer if local (middle layer) instrument guide tube failures have been predicted to occur. Within the bottom debris layer, the flowing liquid would quickly ablate the surrounding stainless-steel tubes, then begin to ablate the surrounding debris.

Calculation of debris ablation within the bottom bed layer is more complicated than the calculation of vessel wall ablation because several solid materials are involved and the length of the release pathway is not constant. The structural foundation for the calculation is set in subroutine BHEDN at the time of lower plenum dryout, when the bottom and middle debris layers are first established.

Since each of the three bottom layer control volumes is shaped by the curvature of the vessel bottom head, the average lengths of the instrument guide tube pathways through these control volumes are different. For control volumes (1,1) and (1,2), this average length is:

$$YHMEAN = \frac{YLT(1,J) - YLB(1,J) + YRT(1,J) - YRB(1,J)}{2.0} \text{ m}$$

whereas for control volume (1,3) the right corners coincide (see Figure 1.9) and the instrument guide tubes pass through the central portion so

$$YHMEAN = YLT(1,J) - YLB(1,J) \text{ m.}$$

As defined in Table 4.5, the terms on the right side of these expressions represent the elevations of the control volume boundary points above vessel zero.

The representative (average) instrument guide tubes for each bottom layer control volume are then divided into not more than ten axial segments, each at least three inches in length. The number of axial segments in each control volume is stored in the array

$$\text{NABHOL}(J)$$

where J is the control volume index (1, 2, or 3) within the bottom layer. The initial segment lengths within each control volume are stored in the array

$$\text{HABHOL}(J,M) = \frac{\text{YHMEAN}}{\text{NABHOL}(J)} m$$

where M is the segment index. As established within subroutine BHHEDN, all segment lengths within a given control volume are equal. The initial diameters of all instrument tube segments in all control volumes are equal and are stored in the array

$$\text{DABHOL}(J,M) = \text{DPIPES } m.$$

DPIPES is the user-input value for the inner diameter of the instrument guide tubes as defined in Table 5.1 and input on record (BH1100).

As in the case of the vessel wall, the ablation calculations for the bottom debris layer are carried out within subroutine BHDBMX.

1. The liquid mass entering the bottom layer control volume during the timestep is:

$$\text{SUML} = \sum_{K=1}^{20} \text{AML P}(K) \times \text{DTR } \text{kg}$$

Where,

$\text{AML P}(2,J,K,2)$ = liquid mass within the overlying layer two control volume(s), kg

K = material index (Table 4.3) and

DTR = ratio of timestep length to liquid relocation time constant DTHEAD (Input Record BH0500).

BH Package Reference Manual

The initial temperature of the liquid mixture (as it enters the bottom layer control volume) is taken to be the representative temperature of the source (layer two) control volume. However, since the combined drainage from bed control volumes (2,3), (2,4), and (2,5) enters bottom layer control volume (1,3), the entering temperature of the combined flows to this control volume is the flow-averaged temperature of its three source control volumes.

2. The liquid mass per instrument guide tube is:

$$\text{SUMLIN} = \frac{\text{SUML}}{\text{APIPES}} \text{ kg}$$

where APIPES is the number of instrument guide tubes passing through the bottom layer control volume.

3. Steps 3 through 10 are carried out for each of the NABHOL(J) axial segments of the representative instrument tube passing through bottom layer control volume (1,J). The inner surface area of each representative cylindrical instrument guide tube pathway is:

$$\text{AREAD} = \pi \times \text{DABHOL} \times \text{HABHOL} \text{ m}^2$$

where independent values of DABHOL and HABHOL are stored for each axial segment of each control volume, as explained above.

4. The heat transferred to the inner surface of the cylindrical instrument guide tube pathways is QLD, taken as the minimum of:

$$\text{AREAD} \times \text{HPIPES} \times (\text{TLLIQ} - \text{TABLAT}) \times \text{DTM}$$

and

$$\text{SUMLIN} \times \text{CPLIQ} \times (\text{TLLIQ} - \text{TABLAT}) \text{ J}$$

The second quantity serves as a check that no more energy will be transferred from the liquid than would cause its temperature to decrease to the user-input debris ablation temperature TABLAT. See Table 5.1 for representative values of TABLAT and the heat transfer coefficient HPIPES. The other terms used in these expressions that have not been previously defined in this section are:

TLLIQ = temperature of the flowing liquid as it enters the bottom layer control volume, K

DTM = length of BH package timestep, s, and

CPLIQ = mass-averaged specific heat of the flowing liquid, J/(kg · K).

5. The heat transferred from the inner surface of the representative instrument guide tube pathway to the surrounding control volume debris is

$$QMLD = AREAD \frac{TABLAT - TMLPO}{\left(\frac{0.0509}{CONDB} \right)} \times DTM$$

where

TMLPO(1,J) = control volume temperature at the beginning of the timestep, K, and

CONDB(1,J) = thermal conductivity of the control volume debris, W/(m · K).

The representative thermal conductivity for the debris within each bed control volume is determined each timestep within subroutine BHHED2. The constant in the denominator of this equation reflects an approximation that the average distance from the inner surface of each instrument guide tube pathway to the center-of-mass of the associated control volume debris is 0.0509 m (two inches).

6. The heat per unit volume required to bring the debris associated with the representative instrument tube to the melting temperature and to melt it is:

$$QMELT = RHODB \times [HFMN + CPDEB \times (TABLAT - TMLPO)] J/m^3$$

where,

RHODB(1,J) = representative density of control volume debris, kg/m³

HFMN = mass-averaged heat of fusion for control volume materials, J/kg

CPDEB(1,J) = mass-averaged specific heat of control volume debris, J/(kg · K).

7. The volume of instrument guide tube pathway inner surface that will be (radially) ablated this timestep is:

$$DELV = \frac{QLD - QMLD}{QMELT} m^3$$

where the numerator is the portion of the energy transfer from the flowing liquid to the surrounding debris that is retained for surface melting.

BH Package Reference Manual

8. The ablation enlarges the flow area associated with the representative instrument guide tube so that:

$$DABHOL_N = \sqrt{DABHOL_O^2 + \left(\frac{4.0}{\pi}\right) \frac{DELV}{HABHOL}} \text{ m}$$

is the new (end-of-timestep) diameter for this pathway. The mass of debris ablated from this axial segment of the bottom layer control volume during this timestep is

$$AMELT = DELV \times RHODB \text{ kg.}$$

9. The temperature of the liquid passing downward through the axial segment is reduced by the heat transfer to the surrounding debris so that

$$TLLIQ_N = TLLIQ_O - \frac{QLD}{SUMLIN \times CPLIQ} \text{ K.}$$

The temperature of the flow is also reduced by the infusion of the liquid debris ablated from the instrument guide tube pathway inner surface so that

$$TLLIQ_{NN} = \frac{SUMLIN \times TLLIQ_N + AMELT \times TABLAT}{SUMLIN + AMELT} \text{ K}$$

is used as the entrance temperature for the liquid flowing into the next axial segment of the control volume.

10. The mass entering the next axial segment (or, for the last axial segment, entering the vessel wall) is then

$$SUMLIN_N = SUMLIN_O + AMELT \text{ kg.}$$

The total debris mass ablated from bottom layer control volume (1,J) during the timestep is

$$AMMELT = APIPES \times \sum_{M=1}^{NABHOL(J)} AMELT(M) \text{ kg}$$

which is appropriately subtracted from the remaining mass.

The total heat transfer from the ablating instrument guide tube pathway surfaces to the surrounding debris is

$$QMLDEB(J) = \frac{APIPES}{DTM} \times \sum_{M=1}^{NABHOL(J)} QMLD(M) \text{ J/s}$$

where DTM is the timestep length (seconds). This is the heat source to the layer one control volumes by molten liquid flow through penetration failures that is utilized in the control volume heat balance, as described in Section 3.1.

Since the moving liquid would cool as it flowed through the bottom layer debris, the calculated ablation is greatest in the first axial segment and decreases as the flow continues through the layer. Thus, the ablating surface comes to resemble the sloping shape of a funnel. Ablation of the material in the bottom layer reduces the debris mass retained within the control volume(s) through which the molten material is flowing. As described in Section 4.4.1, provision is made to merge the bottom layer control volume if the enlarged (worm-hole) volume around the instrument guide tubes exceeds 80% of the volume currently occupied by solid debris. Once a bottom layer control volume has been merged, the instrument guide tube pathways are considered to be destroyed and ablation ceases. (Ablation of the bottom head wall continues.)

5.4 Creep Rupture of the Vessel Wall

All liquid and solid debris remaining within the reactor vessel lower plenum is immediately transferred to the containment drywell whenever structural failure of the wall is predicted to occur.

As described in Section 1.2, each vessel bottom head wall node is divided into three radial segments. The criterion for bottom head creep rupture is satisfied for any wall node beneath the skirt attachment if the current problem time exceeds the local failure time, which is established each timestep within the code in the following manner.

1. The wall tensile stress is determined by the weight of the debris in the lower plenum and the differential pressure DP (Pa) between the reactor vessel and the drywell:

$$WTENS = \frac{9.80 \times DEBMAS + \pi(RXIDX)^2 \times DP}{ACSW \times 10^6} \text{ MPa}$$

Where,

BH Package Reference Manual

DEBMAS = mass of bottom head debris plus mass of vessel wall and pendant assemblies beneath this wall node, kg

RXIDX = vessel inner radius, m, and

ACSW = cross-sectional area of vessel wall based upon local wall thickness including effect of any local wall melting, m².

2. The local Larson-Miller parameter, ALMP is then determined from the wall tensile stress as

$$31.11 - 0.9880 \times (WTENS - 2.0) \quad \text{when } WTENS < 5.0,$$

or

$$28.06 - 0.3221 \times (WTENS - 5.5) \quad \text{when } 5.0 \leq WTENS < 20.0,$$

or

$$22.83 - 0.0955 \times (WTENS - 30.0) \quad \text{when } WTENS \geq 20.0.$$

This approximate solution for the Larson-Miller parameter is based upon the results of the recent (1991) series of carbon steel creep rupture tests [24] performed at Idaho National Engineering Laboratory (INEL) for the SA533B1 carbon steel of the BWR reactor vessel. These experiments extend the range of available data into the very low wall tensile stress regime, which is applicable to the depressurized BWR reactor vessel.

The potential for failure by creep rupture is applicable only to the wall nodes beneath the skirt attachment because the nodes above the attachment point would not be in tension with the reactor vessel depressurized. The wall tensile stress imposed by the dead weight of the core and structural debris and the bottom head itself is typically about 1.9 MPa beneath the skirt attachment. Thus, the first expression given above for the Larson-Miller parameter is used for the depressurized BWR accident sequences.

3. For each timestep while the bottom head remains intact, a remaining time before failure is established for each wall node beneath the vessel skirt as:

$$TF = e^{BWF - AWF \times TAVCR} \text{ seconds}$$

where

$$AWF = \frac{A\text{LOG}(3600) - A\text{LOG}(360)}{TF6 - TF60} K^{-1}$$

$$BWF = A\text{LOG}(3600) + AWF \times TF60,$$

$$TF6 = 52.6316 \times ALMP \text{ K},$$

$$TF60 = 50.0 \times ALMP \text{ K},$$

ALMP = Larson-Miller parameter, determined in step 2, and,

TAVCR = current average wall node temperature, K

The variables TF6 and TF60 are the temperatures for creep rupture of carbon steel in six minutes and sixty minutes, respectively, as determined by the current value of the Larson-Miller parameter. It is easy to show by substitution of variables (for carbon steel) that BWF has a constant value equal to 51.9378.

4. The local creep rupture failure time is established for each wall node beneath the skirt attachment by adding the time-to-failure established in step 3 to the current problem calculation time ATIME (s). These predicted failure times are stored in the array TCRPHD (I) where I is the wall node index.

The predicted bottom head wall node creep rupture failure times stored in array TCRPHD can decrease as local temperatures ascend, but are never permitted to increase. Whenever the current problem time ATIME exceeds a previously set nodal failure time, creep rupture failure of the bottom head is assumed to occur and a special output message is written (Section 6.5). As mentioned previously, all liquid and solid debris within the lower plenum is immediately transferred to the drywell. However, since the status of the remaining wall nodes (carbon steel that has not previously been ablated) is unknown, no logic has been added to include the remaining wall nodes with the debris.

After bottom head creep rupture, the lower plenum debris bed model responds to calls from MELCOR simply by reclassifying the entering debris (from the core region) as released debris (to the drywell). No debris bed calculations are performed; the transfers between storage arrays are made, and the call is returned.

5.5 Gas Blowdown from Vessel

The mass flow rate through failed penetrations is determined within the MELCOR interface by the equation for orifice flow:

BH Package Reference Manual

$$W = C A \sqrt{2 \times \rho \times DP} \text{ kg/s}$$

where,

C = 0.583

A = user-defined break size (m²) (See Input Record BH1900, entry 3 for IABCFN.),

ρ = density of lower plenum atmosphere after heating to the average temperature of the debris bed layer in which the failure occurs (kg/m³), and,

DP = differential pressure between the vessel and the drywell (Pa).

The FL package routine FLCOK is then called to limit the flow to no more than that at the velocity of sound at the user-input break area, taken to be the minimum section of the orifice.

6. Examples of Calculated Results

Two pages of printed output are generated within subroutine BHHED2 at the completion of each user-specified printout interval for the Bottom Head (BH) package. A portion of the first output page is dedicated to the presentation of certain calculated results in a pictorial display. It is the purpose of this section to provide an explanation of the information contained in this display as well as the additional information printed in tabular format. This is facilitated by means of discussion of the printed results for an example calculation, which was performed (1992) to investigate the short-term station blackout accident sequence based upon the Peach Bottom plant configuration. At the time of lower plenum dryout, the BH package calculation was initiated for debris bed layers one and two; the third (uppermost) debris layer had not yet been formed.

6.1 Initial Debris Bed Configuration

The pictorial display of the initial configuration of the lower plenum debris bed immediately after dryout is reproduced as Figure 6.1. The left-hand portion of this figure represents the thirteen debris bed control volumes, which are numbered and shown to scale in Figure 1.9. However, since the outermost control volumes (2,5) and (3,5) are relatively small, they are shown on an expanded scale at the center of Figure 6.1. As mentioned previously, none of the layer three control volumes have yet been formed.

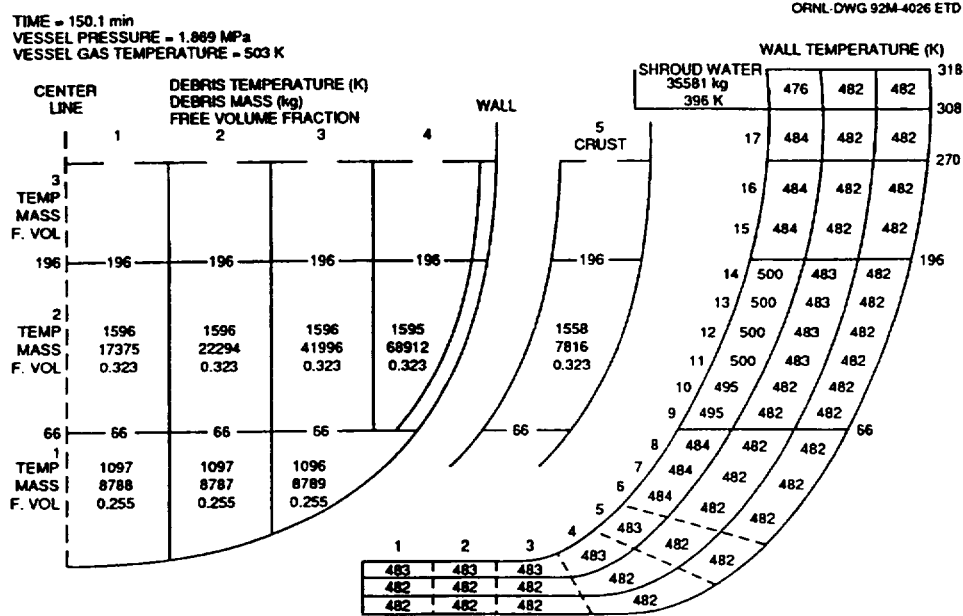


Figure 6.1 Initial Configuration of the Lower Plenum Debris Bed and the Initial Bottom Head Wall Temperatures

For each debris bed control volume, the current temperature (K), total mass of debris (kg), and embedded free volume (fraction of total volume) are listed on Figure 6.1. (The individual material masses contained within the bed layers of the initial configuration are provided in Table 6.1.) Since all of the initial control volume temperatures are below the melting temperatures of the first eutectic mixture (Table 4.1) and the first debris constituent (Table 4.2), all of the bed materials are entirely solid at this time.

Immediately above the outline of each control volume in Figure 6.1 is indicated the local height above vessel zero of the control volume upper surface, in centimeters. In this initial bed configuration, the upper surface heights of all control volumes within a layer are equal (196 centimeters for layer two, for example). As the calculation proceeds, however, the debris constituents will melt and relocate downward, causing the bed to settle. The basic pictorial representation of the bed structure will remain the same as shown in Figure 6.1 while the current local control volume heights (which will change during the calculation) will be indicated numerically. The heights indicated to the left of the vertical dashed center line will, however, always represent the initial bed layer heights.

The right-hand portion of Figure 6.1 represents the reactor vessel bottom head wall. (The wall nodalization and the division of each node into three radial segments has been described in Section 1.2 and illustrated in Figure 1.10 and Figure 1.11). Wall nodes 1 through 17 are numbered along the inner wall surface in Figure 6.1. Within the wall, temperatures are indicated for each wall segment. Along the outer wall surface are indicated the heights above vessel zero (cm) of the inner wall termini of the dividing lines

BH Package Reference Manual

between the 8 wall nodes originally adjacent to debris layer one, the 6 nodes adjacent to debris layer two, the two nodes adjacent to debris layer three, the single node (17) between the upper bed surface and the bottom of the shroud baffle, and the single node (18) adjacent to the lower portion of the downcomer region. While the wall node locations will never change, the debris control volumes adjacent to the wall can settle downward. For example, bed control volume (3,5) might be adjacent to wall node 14 late in the calculation instead of control volume (2,5) as in the original configuration shown in Figure 6.1.

Table 6.1 Material Masses (kg) Included in the Initial Setup of the Debris Bed Layers for Peach Bottom Short-Term Station Blackout

Material	Layer 1	Layer 2	Total
Zr	3414.	24453.	27867.
Fe	5593.	17528.	23121.
Cr	1360.	4264.	5624.
Ni	605.	1895.	2500.
B ₄ C	50.	356.	406.
ZrO ₂	423.	3032.	3455.
FeO	32.	231.	263.
Cr ₂ O ₃	9.	64.	73.
NiO	4.	25.	29.
UO ₂	<u>14874.</u>	<u>106545.</u>	<u>121419.</u>
Totals	26364.	158393.	184757.

Finally, Figure 6.1 also provides information as to the mass and temperature of the water remaining in the downcomer region between the core shroud and the vessel wall. This information is listed under the heading "SHROUD WATER" adjacent to the inner surface of the uppermost wall node. As indicated, the initial mass (35581 kg) is significant. The source of this water and the effect that the water has upon the debris bed response calculation have been discussed in Section 1.2.

6.2 Formation of the Third Debris Layer

The example MELCOR calculation proceeds after lower plenum dryout with an average timestep length of about 11 seconds. By timestep 19 of the example calculation, the predicted temperatures at the central portion of the debris bed have increased to the point where melting of the FeO constituent can begin. (Melting temperatures of the debris constituents are listed in Table 4.2.) As explained in Section 1.1.4, the predicted presence of material liquids within the bed triggers the initial setup of debris layer three. Figure 6.2 illustrates the printed output at timestep 20, including the initial configuration of the upper layer.

The individual debris constituent masses within each bed layer at the time that layer three is established are listed in Table 6.2. As indicated, layer three is initially comprised entirely of stainless-steel components, which are derived from the portion of the lower plenum structures (represented by input record series BH04LL) previously considered to be suspended above the surface of debris bed layer two.

As indicated in Figure 6.2, layer three is initially small and relatively cold, extending to a height of 231 cm above vessel zero. This is sufficient to cover wall node 15, but the inner surface of wall node 16 remains exposed. As the calculation proceeds, additional solid material relocating downward from the core region is added to the upper surface of layer three as will be described in Section 6.3. (Relocating liquids will be added to the layer three interstitial voids.)

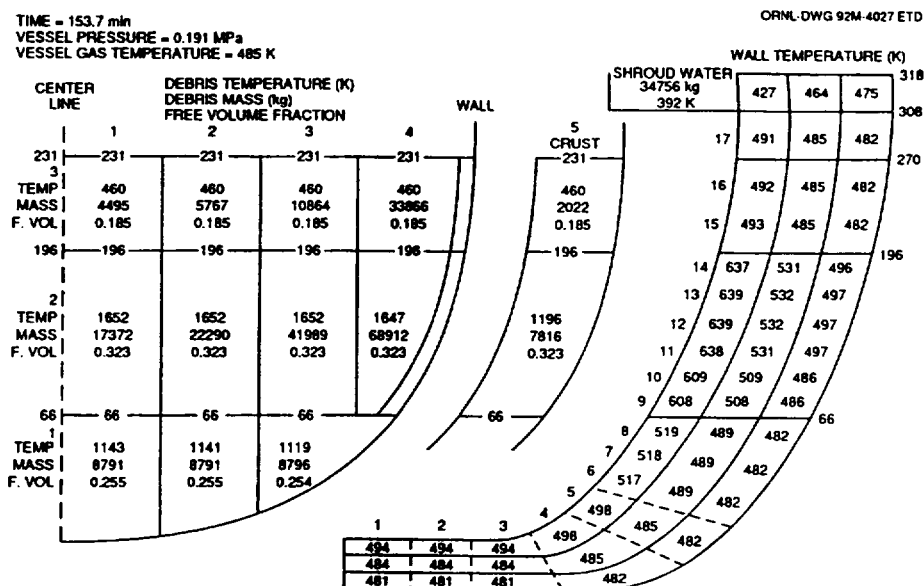


Figure 6.2 Lower Plenum Debris Bed and Vessel Wall Response for the Example Calculation at the Time that Debris Layer Three Is Established

It should be noted that the total debris mass listed in Table 6.2 for layer one has increased slightly (15 kg) over that listed for layer one in Table 6.1, whereas the total mass associated with layer two has decreased accordingly; this small shift is caused by the downward relocation of some of the liquid FeO from layer two into layer one.

The radial temperature profile across the vessel wall is significantly developed by timestep 20 after lower plenum dryout, as may be seen by comparing the wall temperatures shown in Figure 6.1 and Figure 6.2. The temperature of control volume (2,5) has decreased as heat has been transferred to the wall. About 825 kg of water has evaporated from the downcomer region during the intervening period of about 3.7 minutes.

BH Package Reference Manual

As time proceeds, the effects of material relocations play an increasingly important role in determining the predicted results for the example calculation. Specifically, metallic liquids forming within bed layer two relocate into the interstitial voids among the solid particles of layer one, while the composition of layer three is dramatically altered and the size of this layer is increased by the downward relocation of metals and oxides from the core region.

The reader is cautioned that the results described here are intended only to demonstrate the operation of the BH package; no conclusions with respect to accident progression at Peach Bottom should be derived from these examples of code printed output.

Table 6.2 Material Masses (kg) at the Initial Setup of Debris Bed Layer Three for Peach Bottom Short-Term Station Blackout

Material	Layer 1	Layer 2	Layer 3	Total
Zr	3414.	24453.	0.	27867.
Fe	5593.	17528.	42190.	65311.
Cr	1360.	4264.	10263.	15887.
Ni	605.	1895.	4561.	7061.
B ₄ C	50.	356.	0.	406.
ZrO ₂	423.	3032.	0.	3455.
FeO	47.	216.	0.	263.
Cr ₂ O ₃	9.	64.	0.	73.
NiO	4.	25.	0.	29.
UO ₂	<u>14874.</u>	<u>106545.</u>	<u>0.</u>	<u>121419.</u>
Totals	26379.	158378.	57014.	241771.

6.3 Lower Plenum and Bottom Head Response

With all three bed layers represented, the calculated lower plenum debris bed and reactor vessel bottom head response will be described for the case without penetration failures at time 196 minutes and at time 533 minutes, which is just prior to bottom head creep rupture. The initial debris bed configuration just after the time of lower plenum dryout (150.1 minutes after the inception of the accident) has been provided in Figure 6.1 and described in Section 6.1. The bed configuration at the time (153.7 minutes) that the third debris layer is established is described in Section 6.2.

The calculated situation at time 196 minutes is reproduced in Figure 6.3. No free volume remains in the layer one control volumes since molten materials relocating from layer two have filled the previously existing interstitial region voids. The increased masses and temperatures of the layer one control volumes also reflect the effects of these material relocations. However, since the layer one temperatures are well below the melting temperature (1723 K) of the first eutectic mixture, almost all of the relocating liquids have

solidified within layer one. (A small amount of FeO within control volume (1,1) is in the liquid phase at this time.)

Large amounts of molten debris materials exist at this time within layer two. As indicated, the temperatures of the central four control volumes of this layer exceed the melting temperatures of the first three eutectic mixtures (Table 4.1). The height of the central region of layer two has been reduced and much of the previously existing free volume within this layer has disappeared as the interstitial pores filled with liquid. The temperature of the thin crust control volume (2,5) is close to the temperature of the wall. The mass within this control volume has increased since debris bed dryout and the free volume has disappeared as liquid materials from the adjacent control volume (2,4) relocated laterally and solidified.

All of the debris in layer three remains in the solid phase at this time. The layer three mass has increased considerably, however, as materials have continued to relocate downward from the core region. The effects of this relocation can be seen by comparing the layer masses listed in Table 6.3 with those listed for layer three in Table 6.2.

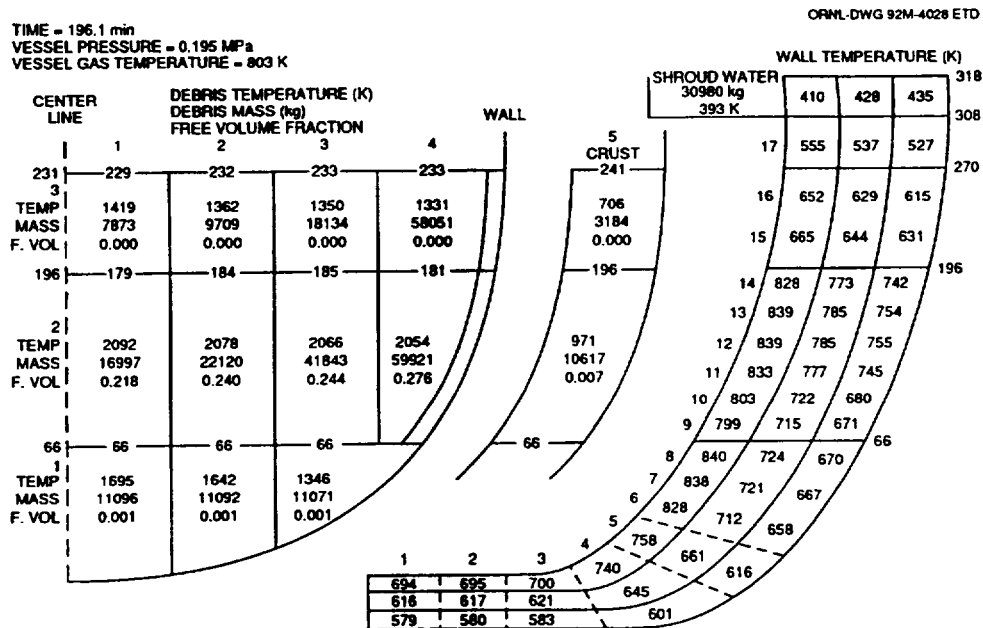


Figure 6.3 Lower Plenum Debris Bed and Vessel Wall Response at Time 196 Minutes after Scram for the Example Calculation

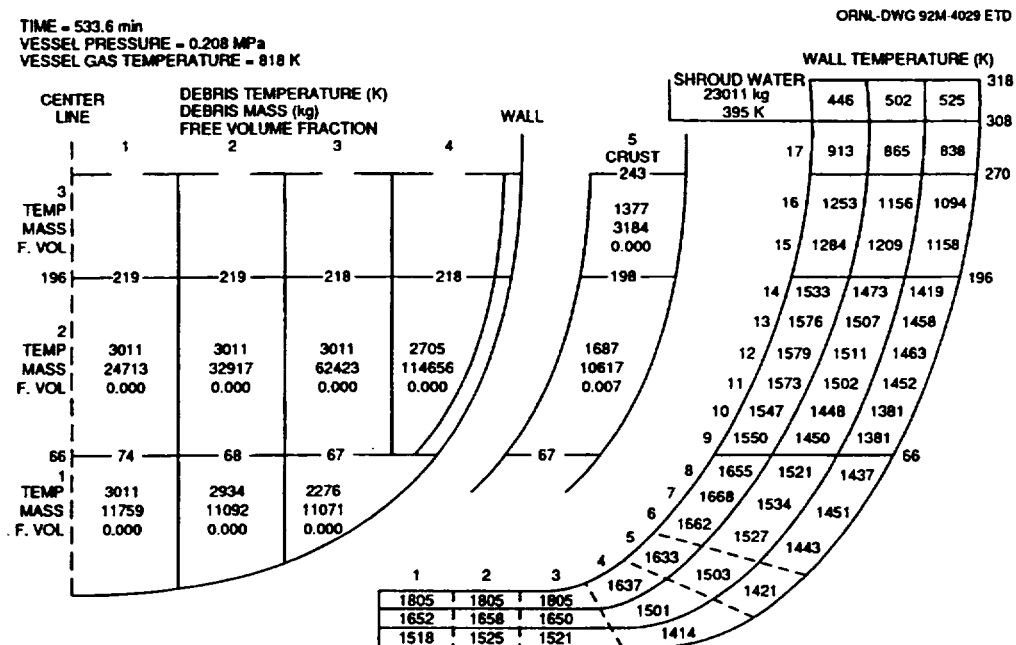
While the size of debris layer three has increased, however, the elevations of the lower boundaries of the control volumes within the central region have been reduced as the layer two control volumes collapsed beneath them. While the net result of mass additions from above and a sinking floor has been that the elevations of the upper surfaces of the central

BH Package Reference Manual

control volumes are about the same as shown in Figure 6.2, the elevation of the upper surface of crust control volume (3,5) is 10 cm higher than that shown in Figure 6.2.

While the vessel wall temperatures have increased, they have not reached threatening values. About 3,776 kg of water have evaporated from the downcomer region since debris bed layer three was established. The water temperature will not vary significantly during the calculation since it is for all practical purposes the saturation temperature corresponding to the vessel pressure and the vessel is maintained depressurized.

Moving ahead about 5-1/2 hours to time 533 minutes, the calculated situation is reproduced in Figure 6.4. Without the escape pathways that would be provided by bottom head penetration failures, all liquid debris has remained within the lower plenum and a molten pool has formed in the central region of the bed. As layer two became predominantly liquid, the solid-phase layer three control volumes (3,1) through (3,4) merged with their layer two counterparts. The pool temperature at time 533 minutes is that of liquid UO_2 (Table 4.2), so the only remaining solid in control volumes (2,1) through (2,3) and (1,1) is uranium dioxide, which is undergoing a phase transformation. The situation depicted is just before bottom head creep rupture.



temperature of this node is 1518 K, a level at which carbon steel creep rupture would be anticipated (with the reactor vessel depressurized).

Second, it should be noted that slightly more than 23,000 kg of water are predicted to remain in the downcomer region at this time. Previously, this water has played an important role during the calculation as a vessel heat sink in removing heat from the upper vessel wall and, more importantly, in cooling the vessel shroud. For calculations in which this water is predicted to become exhausted, the upward radiation from the top of the debris bed will cause the shroud temperature to increase to the steel melting point; prior to dryout, this radiation is primarily consumed in evaporating water from the downcomer region.

For calculations in which downcomer dryout is predicted to occur, the shroud water mass is indicated as 0.0 kg after dryout and the temperature of the lower shroud is displayed. This continues until the time that shroud melting is predicted to begin. Subsequently, the title "SHROUD WATER" is replaced by the message "MELTED MASS = " and the cumulative mass of the shroud that has melted since the time of downcomer dryout is printed. (This includes consideration of the entire shroud; hence, melting may be indicated even though the temperature of the lower shroud has not reached the melting point.)

Table 6.3 Material Masses Included in Debris Bed

Material	Mass (kg)
Zr	17674.
Fe	51672.
Cr	12569.
Ni	5586.
B ₄ C	264.
ZrO ₂	4702.
FeO	3241.
Cr ₂ O ₃	896.
NiO	347.
UO ₂	0.
Total	96951.

6.4 The Case with Penetration Failures

If the user permits penetration failures to occur in the calculation (by parameter NPIPES on input record BH1100), then failure of the bottom head structural boundary is accelerated. As described in Section 5.3.1, molten material flowing through the penetration assemblies ablates the wall. The calculated situation just before wall failure for a case in which penetration failures were represented is reproduced in Figure 6.5. This case is identical to that discussed in Sections 6.1 through 6.4 except that penetration failures are allowed. The initial penetration failure is predicted to occur at time 160.6 minutes. Accordingly, Figure 6.1 and Figure 6.2 apply to this case as well.

BH Package Reference Manual

The first thing to note with respect to Figure 6.5 is that no temperatures are shown for the inner surface (first) segments of wall nodes 1 through 5. This occurs because the bottom head wall response model has predicted that these wall segments no longer exist; they have been ablated away.

Second, it should be noted that the central portion of the debris bed has collapsed to the extent that the remaining solid debris approaches the shape of the confining (hemispherical) walls. At this point, about 122,000 kg of mostly metallic debris has been predicted to be released to the drywell while about 170,000 kg of mostly oxidic debris is predicted to remain in the lower plenum debris bed.

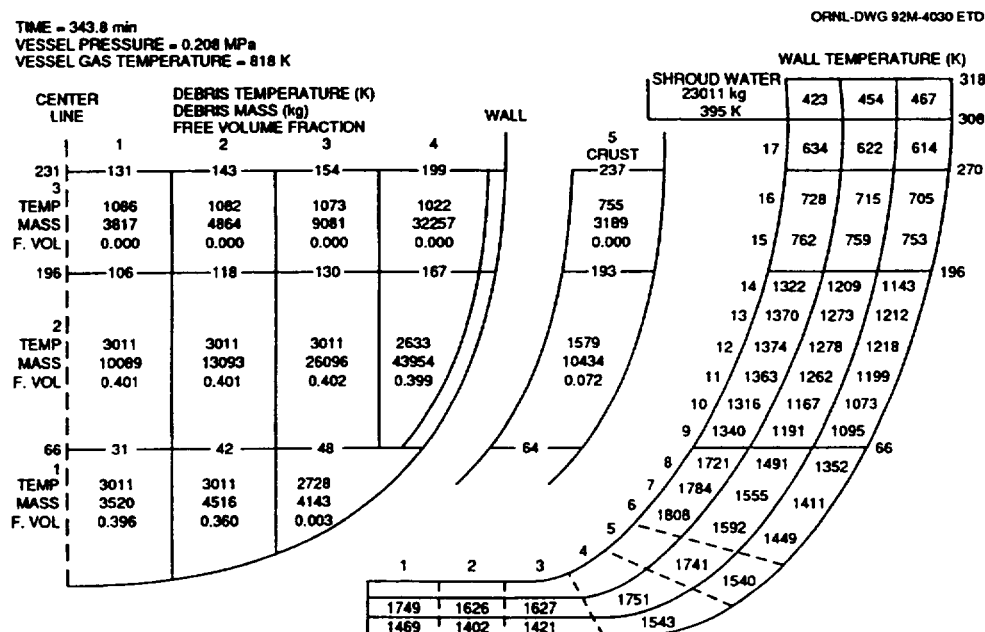


Figure 6.5 Results for a Case with Penetration Failures

Evidence of a downward slippage of the outer two control volumes of bed layers two and three is also provided. The current elevation of the upper surface of control volume (3,4), which is 199 cm, is only slightly higher than the original elevation (196 cm) of the lower surface of this control volume. The slippage of the outer crust control volumes (2,5) and (3,5) has been much less, only about three cm for control volume (2,5).

As indicated Figure 6.5, the central three control volumes of layer two and layer one control volumes (1,1) and (1,2) have a representative temperature equivalent to the UO₂ melting temperature. Because of the prior release of lower-melting materials to the drywell, each of these control volumes comprise at this time only solid UO₂ particles plus a relatively small amount of transient UO₂ liquid. These control volumes would continue to shrink as

mass was lost if the calculation proceeded; however, as previously mentioned, predicted gross failure of the bottom head wall is imminent.

Finally, with reference to Figure 6.5, it is worth noting that a large amount of water remains in the downcomer region. It is typical of calculations in which bottom head penetration failures are represented to find that downcomer dryout does not occur before gross failure of the bottom head wall is predicted.

6.5 Tabulated Output

On the same first output page and immediately beneath the pictorial representations described in Sections 6.1 through 6.4 is printed certain specific information (not shown) concerning the calculated debris bed response. Six information entries provide both current timestep values and cumulative totals for items such as heat transfer to vessel heat sinks or hydrogen generation. The seventh entry addresses the fraction of metal oxidation. Each of these entries is explained below, followed by a discussion of the tabulated output printed on the second page.

The nature of the first two entries depends upon whether or not the third debris layer has been established. Before the third debris layer is established, the lower plenum atmosphere above the bed surface is considered to be dominated by the presence of the control rod guide tube heat sinks as represented by the VPS array entered via Input Record BH04II. The first two items of printed output are:

Temperature of CR guide tubes (above debris) = _____ K

Heat transfer from guide tubes to vessel atmosphere and wall:

This timestep = _____ Joule Total since bottom head dryout = _____ Joule

In effect, code logic recognizes that the mass of the lower plenum atmosphere is insignificant compared to the mass of the control rod guide tubes (and other lower plenum structures above the surface of the debris bed) and that the atmosphere-to-guide tube heat transfer area is large. Heat transfers from the debris bed surfaces are calculated based upon the assumed presence of an atmosphere comprised of the actual lower plenum gases with a temperature equivalent to the temperature of the control rod guide tubes. The intermediate steps of a calculation of an increase in the atmosphere temperature and the concomitant heat transfer from the atmosphere to the control rod guide tubes are considered unnecessary and are omitted. The calculated energy transfers are applied directly to the control rod guide tube mass and a new guide tube temperature is calculated.

Once the third debris bed layer is established, however, all lower plenum structures above the surface of debris layer two are assumed to be subsumed into this layer. Now the code logic recognizes the existence of both the core shroud and an independently-modeled

BH Package Reference Manual

lower plenum atmosphere above the bed surface; the first two routinely printed entries are now:

Net heat transfer to vessel heat sinks (after third bed layer is established):
This timestep = ____ Joule Total since layer 3 established = ____ Joule

Net heat transfer to vessel atmosphere (after third bed layer is established):
This timestep = ____ Joule Total since layer 3 established = ____ Joule

Thus, without the overwhelming presence of the control rod guide tubes, heat transfers from the bed surfaces to the core shroud and to the vessel atmosphere are calculated separately.

Specifically, the first entry now represents the net heat transfer to the core plate and the lower core shroud (including the baffle plate) from the debris bed upper surfaces and to the downcomer region water from the uppermost bottom head wall node NWALL. After downcomer dryout, this entry represents the net heat transfer to the core plate and lower core shroud plus the radiant heat transfer to the lower core shroud from the uppermost bottom head wall node.

The second entry now represents the net heat transfer to the lower plenum atmosphere from:

1. the debris bed upper surfaces and
2. the exposed bottom head wall nodes.

The sum of these two entries now provides a record of the net energy transfer from the debris bed and bottom head wall to the reactor vessel atmosphere, the lower core shroud (including the baffle plate), and the core plate after lower plenum dryout and the establishment of debris bed layer three.

The third item of printed output

Decay heat in debris in vessel lower plenum:
This timestep = ____ Joule Total since bottom head dryout = ____ Joule

simply records the energy release by decay heating within the reactor vessel lower plenum. (Energy released within debris that has escaped to the containment drywell is not included.)

The final three items of printed output reflect the effects of the metal-steam reaction within the debris bed. These are:

Metal/steam reaction energy in debris:
This timestep = ____ Joule Total since bottom head dryout = ____ Joule

Hydrogen generated in lower plenum debris bed:

This timestep = _____ kg Total since bottom head dryout = _____ kg

Fraction of zirconium (below core plate) reacted = _____

Metal-steam reaction within the lower plenum debris bed is of course zero unless water is introduced to the bed or until bottom head penetration failures occur, providing an escape pathway for steam to pass through the bed. The last item, however, is based upon the current ratio of zirconium within the oxide to total zirconium within the lower plenum (or released to the drywell) and, therefore, represents the effects of metal oxidation that occurred in the core region as well. It appears at the bottom of the first printed output page only after the third debris layer has been established.

The second page of printed output provides a "Material Breakdown of Debris" in tabular format. An example of these output tables as generated for a typical calculation is illustrated in Table 6.4. (The numbers shown are typical, but are not intended to relate directly to any other example results cited in this text.)

As indicated, the upper set of tables relates to the materials currently present within the lower plenum debris bed and provides a breakdown according to the distribution of these materials among the bottom (1), middle (2), and upper (3) debris layers. This distribution is further subdivided for each material in each layer so as to specify the individual masses of the solid and liquid components.

BH Package Reference Manual

Table 6.4 Example Showing Format of Second Page of Printed Output

*****Material Breakdown of Debris*****

Debris masses in vessel bottom head (kg):

Material	Layer No. 1		Layer No. 2		Layer No. 3		***** All Layers *****	
	State		State		State		State	
	Solid	Liquid	Solid	Liquid	Solid	Liquid	Solid	Liquid
Zr	5351.5	0.0	16175.8	241.5	14743.8	0.0	36271.1	241.5
Fe	8569.1	0.0	1728.5	165.4	52356.6	0.0	62654.2	165.4
Cr	2153.9	0.0	290.0	0.0	12735.4	0.0	15179.3	0.0
Ni	477.2	0.0	160.9	306.6	5660.2	0.0	6298.3	306.6
B ₄ C	57.3	0.0	459.5	0.0	184.2	0.0	701.0	0.0
ZrO ₂	400.8	0.0	3287.3	0.0	6674.4	0.0	10362.5	0.0
FeO	248.0	0.0	11.5	0.0	3258.7	0.0	3518.2	0.0
Cr ₂ O ₃	8.0	0.0	63.9	0.0	900.5	0.0	972.4	0.0
NiO	3.1	0.0	24.7	0.0	348.5	0.0	376.3	0.0
UO ₂	14090.7	0.0	111582.3	238.3	0.0	0.0	125673.0	238.3
Totals	31359.6	0.0	133784.4	951.8	96862.3	0.0	262006.3	951.8

Debris masses ex-vessel:

Material	This Timestep	Total Released
Zr	49.4	7354.1
Fe	33.8	13090.3
Cr	0.2	3285.2
Ni	62.2	1601.6
ZrO ₂	0.0	0.6
FeO	0.0	0.5
UO ₂	49.5	1229.6
Total	195.1	26561.9

Temperature 1871.0 K

Decay heat in ex-vessel debris = 0.196534E+06 Watt

The list of materials at the left side of the upper set of tables will include only the materials actually present within the debris bed. Late in the calculation, if all of the stainless-steel components have been released from the lower plenum, then Fe, Cr, and Ni will disappear from this list.

A relevance criterion for the materials to be listed is also applied to the lower portion of Table 6.4. Here the list includes only those materials for which some portion (at least 0.1 kg) has escaped from the reactor vessel. It should be obvious that the number of materials listed in this category will increase as the calculation progresses. For example, Table 6.4 indicates that B₄C is currently present within the lower plenum debris bed, but none has yet (melted and) escaped from the reactor vessel. When it does, the list of materials at the lower portion of Table 6.4 will become longer by the addition of B₄C.

For each material, both the mass released from the reactor vessel during the current timestep and the cumulative mass released since the beginning of the BH package calculation are displayed. The listed temperature is the mixed-mean temperature of the release during the current timestep. The indicated decay heat is the power associated with the cumulative UO₂ release.

It should be noted that the information displayed in the lower portion of Table 6.4 will only be printed after some material release from the reactor vessel has occurred. Therefore, for calculations in which penetration failures are not modeled, no information will be printed in this location until the time that gross failure of the bottom head wall is predicted. At that time, all lower plenum debris will be transferred to the containment drywell during one timestep, and the BH package calculation will be terminated. Should this occur, logic within subroutine BHED2 ensures that this one-time transfer will be recorded (printed) in the format demonstrated in Table 6.4.

As a final note, it should be recognized that only liquid materials are predicted to escape from the reactor vessel via bottom head penetration failures. The only occasion during the calculation when both solid and liquid materials escape the reactor vessel simultaneously is at the time of gross reactor vessel bottom head failure.

6.6 Special Messages

Special printed output is provided to record the occurrence of important individual events at the time they occur. These messages are printed at the end of and on the same page as the tabular output from the previous regularly scheduled status update.

As described in Section 3.4, the user can limit the extent of the calculated metal-steam reaction in the lower plenum debris bed by setting the input parameter FZRMX1 (BH0700) to a fraction less than one. If this is done, the message

Bottom head Zr oxidation stopped _____ kg reacted

is printed at the time that the permissible fraction of the initial zirconium inventory has been reacted. This message indicates the mass of zirconium that has been oxidized within the lower plenum since the inception of the BH package calculation. Code logic precludes the calculation of any additional oxidation after the appearance of this message.

If bottom head penetrations are represented, then creep rupture of a penetration weld at the wall as described in Section 5.1 is reported by the message

*P. weld temperature in layer no. _____ exceeds _____ K at time = _____
Release of debris liquids from layer _____ begins*

where the index of the debris layer will be indicated as 1 (bottom layer) or 2 (middle layer).

Failure of the instrument guide tubes in the manner described in Section 5.3 (melt overflow from the middle or bottom debris layer) is reported by the message

BH Package Reference Manual

*Inst. tube fails in layer no. _____, control volume _____
(temp. = _____ K) at time = _____*

where the layer index will be 1 or 2 and the indicated temperature is that of the control volume where the failure is predicted to occur.

Gross failure of the bottom head wall can occur either by ablation (discussed in Section 5.3) or creep rupture (Section 5.4). If an entire wall node is ablated away, then the printed message is

*Lower head ablated in wall node _____ at time = _____
All remaining lower plenum debris transferred to the drywell*

If the wall fails by creep rupture, then the message is similar:

*Lower head creep rupture in wall node _____ at time = _____
All remaining lower plenum debris transferred to the drywell*

As indicated, the concept is that all remaining debris is released from the vessel at the time of gross wall failure.

7. Models for Water in the Lower Plenum

The models described in this chapter enable the calculation of bed response if the BWR lower plenum is flooded at the time of transition to the BH package or reflooded after debris bed dryout. The present version has removed the requirement for lower plenum dryout before transition to the BH models. As a result the models that are described here for the case where water is reintroduced after dryout and transition to BH are applied also to the case in which water is present at the time of transition to BH. For conventional BWR (CBWR) applications, the late-phase introduction of water into the lower plenum might occur as a direct consequence of restoration of electrical power after a prolonged station blackout, whereas the early presence of water can occur simple due to the relocation of sufficient core debris into the lower plenum prior to dryout. For the Simplified Boiling Water Reactor (SBWR) design, failure of the short-term cooling mode of the Gravity Driven Cooling System (GDCS), followed later by operation of the long-term cooling mode, could result in late flooding of a badly degraded core.

It should also be noted that in addition to removing the requirement for lower plenum dryout as a criterion for transition to the BH models, the ownership of hydro-materials has been removed from the BH package in the current version. This means that BH cannot subsume water from the CVH package or inject water directly into the BH package. The hydro-materials inventories and thermodynamic conditions (i.e. lower plenum pool mass and temperature) are imposed upon BH by the CVH package. Although the BH package performs dry-out calculations that involve steaming rates, the BH package no longer

produces steam, rather it passes the total energy transferred from the debris to the pool back to the CVH package and the CVH package calculates the rate of steam production. The same is true regarding the interface between BH and the lower plenum atmosphere. The BH package does not transfer steam into the lower plenum atmosphere. The only exception to this is that H_2 , CO, and CO_2 produced in interactions of core debris with pool water are added to the CVH lower plenum atmosphere along with their associated enthalpies.

In order to cool the inner regions of a debris bed, water must be able to enter the bed, which means that the debris must contain voided regions to serve as water passages. The porosity is defined as the ratio of the voided volume of a region to the total volume of the region. In general, the porosity of a particle bed depends upon the shape of the particles and the manner in which they are fitted together but not upon the size of the particles. For example, the porosity of a bed of uniform solid cubes is zero whereas a bed of uniform spheres can have a porosity ranging from 0.259 for a rhombohedral configuration to 0.476 for a cubic configuration. For debris produced during an actual accident, the bed composition would be nonuniform* [25, 26] so that the local porosities would be expected to vary radially and axially over a range extending from a low of about 0.10 to values as high as 0.60.

Thus the effects of water introduced over the surfaces of a dry debris bed depend upon the bed porosity; all other boundary conditions are of secondary importance. Yet determination of porosity would require knowledge of particle size distributions, shapes, and weight fractions as well as the local bed configuration. Since these are not known, the best that can be done for purposes of analysis is to vary the assumed porosity over a reasonable range of values. Stated another way, a parametric analysis can be performed to determine the effectiveness of water cooling over a range of potential bed porosities. With the new models described in this chapter, the set of calculations required for the parametric analysis can be performed with MELCOR by use of the BH package. Section 2.12 of the BH Package Users' Guide describes the special control functions that may be used for the introduction of water over the lower plenum debris bed.

Subroutine BHBWET permits calculation of heat transfer by convection and radiation to water overlying the bed and by boiling to water within the bed. Subroutine BHBWET calculates the depth of water over the debris bed (Section 7.1), the dryout heat flux for the bed radial zones (Section 7.2), hydrogen generation within the bed (Section 7.3), and the heat transfer at the bed surfaces (Section 7.4) and exposed reactor vessel inner wall surfaces (Section 7.5). The total heat transfer to the lower plenum water is returned to MELCOR (CVH). The time-dependent mass of water in the lower plenum, its temperature,

* For the distribution of debris produced during the TMI accident, see Section 3.7 of Reference 25. For a description of the homogeneous particulate debris that formed from previously molten material, see Reference 26.

BH Package Reference Manual

and the steam generated are calculated by the CVH package from the heat load provided by the BH package. Hydrogen generated as a result of water addition to the lower plenum debris is added to the vessel atmosphere.

Special provisions are necessary if water is predicted to exist within the lower plenum after penetration failures have occurred. The code logic utilized for this case is discussed in Section 7.6. Late debris pours from the core region would interact with any water overlying the debris bed, and the methodology employed for calculating these effects is described in Section 7.7. The special printed output associated with the effects of water in the lower plenum is demonstrated in Section 7.8.

7.1 Water Depths

Subroutine BHBWET includes provision for calculation of water height within the reactor vessel lower plenum and the individual water depths over the upper surface of each bed radial zone. The logic applies also to cases in which a limited amount of water becomes available late in the accident sequence so that the central (sunken) portion of the bed is covered while the outer radial zones remain dry.

The following time-dependent variables reflect the amount of water in the lower plenum and the configuration of the bed surface.

AMASLP = mass of water in lower plenum, kg

TMASLP = temperature of lower plenum water, K

YLT = YLT(I,J), height of control volume surface above vessel zero, m

I,J = indices of bed layer (I=1,3) and radial zone (J=1,5)

IT = IT(J), flag indicating the upper layer index for each radial zone

IVLP = IVLP(J), flag changing value from 1 to 0 to indicate that a bed control volume no longer exists

Bed control volumes cease to exist whenever their internal debris masses and energies are merged with those of another control volume, as described in Section 4.4. It should be noted that IVLP(1,4) and IVLP(1,5) are zero from the beginning of the calculation since these bed control volumes are never formed (see Figure 1.9).

The time-dependent variables that are calculated in subroutine BHBWET to describe the water depths are

YLIQ = height of water surface above vessel zero, m

HWAT = HWAT(J), depth of water above the surface of radial zone J, m, and

IWET = IWET(J), flag changing value from 0 to 1 to indicate that water covers the surface of a bed radial zone.

Table 7.1 indicates typical values of the IT and IVLP arrays late in a calculation with penetration failures.

Table 7.1 Typical Values of the IT and IVLP Arrays after Bed Settling and Control Volume Merging

Array	Radial Zone				
	1	2	3	4	5
IT(J)	2	2	2	3	3
IVLP(3,J)	0	0	0	1	1
IVLP(2,J)	1	1	1	1	1
IVLP(1,J)	1	1	1	0	0

The IWET array elements are used within subroutine BHHED2 to determine whether heat transfer from each bed surface should be to atmosphere (IWET = 0) or to an overlying water pool (IWET = 1). As the central portion of the bed sinks, some radial zones may be dry while others are covered with water. It should also be recognized that after merging occurs, the bed surface may be comprised of layer two control volumes in the central region and layer three control volumes near the wall (as in the bed configuration represented by Table 7.1).

The height of the lower plenum water surface is used to determine which of the exposed reactor vessel wall nodes (those above the debris surface) are subject to water cooling. (Wall node indices are indicated in Figure 1.10.) The sixth and seventh elements of the IWET(7) array are used as flags changing value from 0 to 1 to indicate that the inner surfaces of the exposed bottom head wall nodes are covered by water:

IWET(6) = Flag for wall node 17 and

IWET(7) = Flag for wall nodes 9 through 16.

Surface heat transfer coefficients for natural convection and radiation to the lower plenum atmosphere are calculated (as described in Section 3.2.1) only for wall nodes not covered by water. Specifically, HSURF(6) for wall node 17 is calculated only if IWET(6) = 0, and HSURF(7) for wall nodes 16 and below is calculated only if IWET(7) = 0. (See Table 3.1.)

For water-covered wall nodes, individual surface-to-water heat transfer coefficients are calculated based upon the local surface temperature and nodal characteristic length. An exposed wall node is considered to be covered by water if:

$$YLIQ > \frac{YLTW(M) + YLTW(M - 1)}{2.0}$$

Where,

M = wall node index, and

YLTW = height of upper boundary of inner nodal surface above vessel above, m.

Heat transfer at the inner surface of water-covered exposed wall nodes might be either by nucleate or film boiling, depending upon the temperature differential between the surface and the water.

7.2 Dryout Heat Flux

If the water initially introduced over the bed surface is subcooled, condensation of the steam within the bed would rapidly draw water into the upper debris voids. This initial water entry would quickly be evaporated, however, and countercurrent flows of upward-flowing steam and downward-flowing water would soon be established.[27] As explained in Reference 28, the extent of water penetration is not uniform over the bed cross-section but rather takes the form of water channels between scattered pockets of bypassed hot, dry debris. However,

“the average quench rate of the bed can be predicted reasonably well based on the assumption that the supply of water to the bed is controlled by the hydrodynamics of countercurrent two-phase flow.... The prediction can be made using a one-dimensional model without considering the water penetration pattern.” [28]

Stated another way, the bed quench rate and steam generation are flow-limited rather than particle-water heat transfer limited. Thus, the dryout heat flux (the power per unit area removed at the bed surface) establishes the average rate of bed quenching.

The preeminence of the dryout heat flux in determining the heat removal from a debris bed by water cooling is also evident from the information provided in Reference 29, where experimental results again demonstrate that:

“the mechanism that limits the bed cooling rate in both transient quench and steady state dryout is two-phase countercurrent bed hydrodynamics.”

and

“the steady-state models provide reasonable characterization of the transient bed quench steam generation rate.” [29]

Thus, importantly, it is not necessary to attempt to calculate the details of the water penetration process.

7.2.1 Calculation

The dryout heat flux is calculated within subroutine BHBWET by the method of Lipinski [30]. Its magnitude decreases rapidly as the bed porosity decreases; hence, the efficacy of the water will depend upon the state of the bed at the time that the water is introduced. (After lower plenum dryout, melting and relocation of lower-melting temperature materials progressively reduce the porosity in the lower portions of the bed.)

For each water-covered bed radial zone, the dryout heat flux is determined for each control volume as

$$DFLX(I,J) = QT \times \left[\sqrt{1.0 + \left(\frac{QT}{2 \times QL} \right)^2} - \frac{QT}{2 \times QL} \right] \frac{\text{Watts}}{\text{m}^2}$$

where

$$QT = QT1 \times \sqrt{\frac{\varepsilon^3}{1 - \varepsilon}},$$

$$\varepsilon = \text{PORB}(I,J), \text{ control volume porosity,}$$

$$QT1 = HLV \times \sqrt{\frac{\rho_s \times \rho_l \times (\rho_l - \rho_s) \times G \times DFRAG}{F6}},$$

$$HLV = \text{heat of vaporization for water, J/kg}$$

$$\rho_s = \text{steam density, kg/m}^3$$

$$\rho_l = \text{liquid density, kg/m}^3$$

$$G = \text{acceleration of gravity, m/s}^2$$

$$DFRAG = \text{particle diameter, m (provided as DPART in BH package input [BH0500])}$$

$$F6 = 1.75 \times (\rho_s^{1/6} + \rho_l^{1/6})^6,$$

$$QL = QL1 \times \frac{\varepsilon^3}{[1.0 - \varepsilon]^2},$$

BH Package Reference Manual

$$QL1 = HLV \times \frac{\rho_l - \rho_s \times G \times DFRAG^2}{F4},$$

$$F4 = 150 \times (VKS^{1/4} + VKL^{1/4})^4,$$

VKS = steam viscosity m²/s and,

VKL = water viscosity m²/s.

Property values together with calculated intermediate terms and final results for an example calculation are shown in Table 7.2.

Table 7.2 Example Results for the Dryout Heat Flux Calculation

Parameter	Value	Source
DFRAG	0.01 ^a m	Geometric Quantities (Given) Property Values for Vessel Pressure of 0.186 MPa
ε	0.2088 ^b	
ρ_s	1.037 kg/m ³	
ρ_l	945.011 kg/m ³	
HLV	2208.85 x 10 ³ J/kg	
VKS	1.2353 x 10 ⁻⁵ m ² /s	
VKL	2.5564 x 10 ⁻⁷ m ² /s	
F6	8795.3 kg/m ³	Calculated Quantities
QT1	7096.5 W/m ²	
F4	0.00671 m ² /s	
QL1	305.0 x 10 ⁶ W/m ²	
QT	758.9 x 10 ³ W/m ²	
QL	4434.1 x 10 ³ W/m ²	Final Result ^{c-e}
DFLX	696.73 x 10 ³ W/m ²	

^a The particle diameter DFRAG for this example is representative of the size of a UO₂ fuel pellet.

^b The control volume porosity ε has been lowered from its initial value because molten material from elsewhere in the bed has previously relocated into the volume.

^c Reducing the particle diameter to 0.001 m while holding all else constant in this example decreases the calculated value of DFLX to 42.95 x 10³ W/m².

^d Use of a particle diameter of 0.001 m combined with a bed porosity of 0.40 while holding all else constant produces a calculated DFLX of 389.29 x 10³ W/m².

^e In general, the dryout heat flux increases with both particle diameter and bed porosity. Curves illustrating these trends are provided in Section 6.5 of Reference 25.

7.2.2 Application to Bed Radial Zones

Given the dryout heat flux DFLX, the maximum power that can be removed through the upper surface area AINFCA of bed control volume (I,J) is:

$$QSUR(I,J) = AINFCA(I,J) \times DFLX(I,J) \text{ W.}$$

This is the maximum power that can be removed from the control volume by means of boiling heat transfer; that is, through the mechanism of saturated water flowing in (downward) and saturated steam flowing out (upward). For this maximum power to be attained, the upward flow of steam at the control volume surface must not be impeded.

Since the lower plenum debris bed is normally arranged in three layers, it is necessary to consider the effect of the overlying debris in blocking the escape of steam from the middle and lower layer control volume surfaces. At the same time, the effects of steam entering the middle and upper layer control volumes from below must be considered. Accordingly, the effectiveness of water cooling within each of the three stacked control volumes must be calculated separately.

For the upper control volume,

$$QWET(3,J) = QSUR(3,J) - QSUR(2,J) \text{ W}$$

is the internal boiling power based upon the dryout heat flux limitation at the control volume surface and the maximum power inflow from the middle control volume. Based upon this relation, the calculated boiling power within the upper control volume will be severely curtailed if the calculated value of QSUR(2,J) is large. This is not realistic, however, since the downward-flowing water enters the upper control volume first. In recognition of this, the calculated value of QWET(3,J) is adjusted, if necessary, to be no less than 80% of QSUR(3,J).

It will be shown below how the final value of QWET(3,J) is applied in the determination of the cooling effectiveness in the central control volume. First, however, it is necessary to consider the potential for reduction in the calculated value of QWET(3,J) as the debris temperature TMLPO(3,J) approaches the saturation temperature TSAT. As the bed loses superheat, it becomes necessary to consider the local decay power QDOT(3,J), which will become the dominant source of energy for transfer to water. The approach is described in the following Table 7.3, which is applicable to any bed control volume (I,J) and addresses four possibilities.

BH Package Reference Manual

Table 7.3 Effect of Debris Temperature Upon Boiling Power

Debris Temperature (K) TMLPO(I,J)	Maximum Boiling Power (W) QWET(I,J)
$\leq \text{TSAT}$	0.0
$\text{TSAT} \leq \text{TMLPO} \leq \text{TSAT}+2.0$	QDOT
$\text{TSAT}+2.0 < \text{TMLPO} < \text{TSAT}+10.0$	$\text{QDOT} + [\text{QWET} - \text{QDOT}] \times \left(\frac{\text{TMLPO} - \text{TSAT}}{10.0} \right)$
$\geq \text{TSAT}+10.0$	No change

As indicated in Table 7.3, the calculated value of QWET(3,J) will not be reduced as long as the local debris temperature exceeds the saturation temperature by at least 10 K. This is in line with the reasoning that the local water boiling serves only to remove a portion of the debris superheat; therefore, there is no need to address the decay power separately when calculating the boiling power.*

For debris temperatures between 2 K and 10 K greater than saturation temperature, the adjusted value of QWET(3,J) will vary linearly between the decay power QDOT(3,J) and the original value of QWET(3,J), which was derived (as described in the previous paragraphs) solely by consideration of the local countercurrent two-phase flow limitation. In other words, the original value of QWET(3,J) is based upon an assumption that the boiling rate is not limited by the particle-to-water heat transfer mechanism. The purpose of the logic described here is to accomplish a smooth transition from the countercurrent flow limiting condition to the heat transfer rate limitation, where the debris is quenched and only the decay power is transmitted to the water, while continuing to produce steam.

The effect of this logic is that once the control volume debris is quenched at constant pressure, the heat transfer rate will be controlled so that the debris temperature will be maintained within 2 K of the saturation temperature while the decay power is removed by boiling. In the actual case, however, the vessel pressure will not be constant and the constraints described in Table 7.3 will cause the calculated boiling power to vary in a manner such that the control volume debris temperature follows the saturation temperature.

With the upper control volume boiling power QWET(3,J) known, the middle layer situation can be established. First, the power QTOP2 that can be removed by steam passage through the upper surface of the middle layer control volume is limited to the minimum of

* The decay power is of course considered in the overall control volume energy balance, which is performed in subroutine BHED2. As part of this energy balance, QDOT(I,J) is added and QWET(I,J) is subtracted.

$$QSUR(3,J) - QWET(3,J) ,$$

and

$$QSUR(2,J) .$$

The first of these quantities is the portion of the power transfer capacity through the surface of the upper control volume that is not required to transmit the boiling power generated within the upper control volume itself. The second is the maximum power that can be removed through the surface of the middle control volume, based upon the debris properties within the volume.

It is now necessary to consider the effect of any steam entering the middle control volume from the bottom control volume in limiting the local boiling power:

$$QWET(2,J) = QTOP2 - QSUR(1,J) \text{ W}$$

However, similar to the reasoning employed in the case of the upper control volume, this calculated value for $QWET(2,J)$ is adjusted, if necessary, to be no less than 80% of $QTOP2$.

The logic described in Table 7.3 to cause the local boiling power to approach the decay power as the local debris temperature approaches the saturation temperature is also applied, as appropriate, as a final adjustment to $QWET(2,J)$.

For the bottom control volume, the power $QWET(1,J)$ removed by boiling is the amount that can be removed by steam passage through the upper surface. It is limited to the minimum of :

$$QSUR(3,J) - QWET(3,J) - QWET(2,J) ,$$

and

$$QSUR(1,J) .$$

The first comparative quantity is the remaining power transfer capability through the surface of the upper control volume. The second is the power that could be removed by steam flow through the surface of the bottom control volume, if there were no overlying debris.

BH Package Reference Manual

The logic described in Table 7.3, which comes into play to further limit QWET(1,J) if the local debris temperature TMLPO(1,J) is within 10 K of the saturation temperature, is also applied to the lower control volume.

The calculations described in this section for the upper, middle, and bottom control volumes are applied sequentially to each of the five radial zones of the lower plenum debris bed. Special provisions (described by COMMENT statements in subroutine BHBWET) are employed for radial zones four and five to recognize that control volume (1,3) constitutes the bottom control volume for these radial zones as well as for radial zone three. (See Figure 1.9.)

For a superheated debris bed comprised of three-mm particles unencumbered by local porosity restrictions and with ample water available, the power QSUR(3,J) that can be removed from radial zone J by means of steam flow through the upper bed surface will be taken 80% from control volume (3,J), 16% from control volume (2,J), and 4% from control volume (1,J). Once the upper layer is quenched, the local decay power will be removed by boiling and the remaining capacity through the bed upper surface will be taken 80% from control volume (2,J) and 20% from control volume (1,J).

The way that the QSUR(3,J) power should be allocated among the upper, middle, and lower control volumes of a bed radial zone has been demonstrated experimentally to be a function of the particle size. The 80%-16%-4% allocation cited in the previous paragraph has been used in this discussion for illustrative purposes, but within subroutine BHBWET applies only to cases for which the user-input particle diameter DPART (BH0500) is equal to 3.0 mm.

The experimental evidence demonstrates that the quench front for large particles (greater than three mm) is two-dimensional in that fingers of liquid penetrate through the entire bed producing local quenching but leaving stable surrounding dry regions which act as steam escape pathways. These dry regions subsequently become quenched from the bottom up as the accumulating water pool rises from the bottom of the bed. To approximate the effect of size for large particles, the portion of QSUR(3,J) that is allocated to the upper control volume is determined by a linear relation within subroutine BHBWET; this allocation ranges from 80% for three-mm particles through 56% for particles with diameters of 20.0 mm. (For the case of 20-mm particles, the overall allocation will be 56%-25%-19% for the upper, middle, and bottom control volumes, respectively. Forty-mm particles would have an allocation of 27%-20%-53%.)

As the bed particle size becomes smaller, the experimental observations are that the quench front tends to become one-dimensional and to progress uniformly downward. In subroutine BHBWET, this behavior is approximated by having the portion of QSUR(3,J) that is allocated to the upper control volume increase linearly from 80% for particles of 3.0 mm diameter to 96% for particles of 0.50 mm diameter (or less). The allocation to the upper control volume is not allowed to reach 100% because of the original existence of the control rod guide tubes and instrument tubes within the debris. Although the stainless-steel

of these guide tubes is assumed to be assimilated into the debris, it is reasonable to expect that axial columns of locally reduced porosity would exist within the original locations of these tubes; the effect of this for small particle beds can best be approximated by ensuring that at least a small portion of any introduced water will be represented to reach the bottom of the bed.

7.2.3 Limited Water Availability

Should evaporation of all of the water existing within the lower plenum at the beginning of a calculational timestep prove insufficient to consume the sum of the calculated QWET(I,J) boiling powers across the bed control volumes during the timestep, then the QWET(I,J) quantities must be reduced. This is accomplished for each radial zone and individually for each control volume within each radial zone as follows:

$$QWET(I,J) = QWET(I,J) \times \frac{QZNE}{SQWT} W$$

where

QZNE = HWAT x AINFCA x RHOL x HLV, J

HWAT = HWAT(J), depth of water above the control volume surface, m

AINFCA = AINFCA (IT(J), J), surface area of upper control volume, m²

IT = IT(J), flag indicating the upper layer index for each radial zone

SQWT = [QWET(1,J) + QWET(2,J) + QWET(3,J)] x DTM, and

DTM = timestep length, s.

It is readily evident that QZNE represents the energy required to evaporate all of the water overlying the radial zone. The quantity SQWT represents the energy release by the boiling powers calculated for the radial zone during the timestep based upon the bed configuration and current water/steam properties.

7.2.4 Experimental Evidence for Oxidic Debris Bed Quenching

The logic made operational within subroutine BHBWET as described in Sections 7.2.1 through 7.2.3 is based upon the experimental results discussed in References 25–30. In general, the experiments cited were performed with metallic particles of spherical shape. It is intended, however, that subroutine BHBWET will be applied to consideration of the effects of water in cooling the hypothetical debris beds that might form in a BWR lower

plenum under accident conditions. These beds would be comprised of both metallic and oxidic particles, of various sizes, and various shapes. This section provides a brief discussion of the available experimental results concerning the introduction of water into nonuniform oxidic debris.

The Degraded Core Coolability (DCC) series of experiments was conducted at Sandia National Laboratories during 1983–1985 for the purpose of determining the coolability of fission-heated UO_2 rubble beds in water. Experiments DCC-1 and DCC-2 examined the coolability of 0.5 m (1.64 ft) deep homogeneous beds comprised of small- and medium-sized (respectively) UO_2 particulates and are described in Reference 31. The DCC-3 experiment addressed a stratified bed (small particles overlying large particles) and is described in Reference 32.

References 31 and 32 provide a wealth of information concerning the effects of particle size, size distributions, and stratification. Most important to the purpose here, however, is that the experimental results they describe support application of the Lipinski dryout heat flux calculational methodology to internally heated oxidic debris. This point can best be demonstrated by quoting from the CONCLUSIONS section of Reference 32:

"The DCC experimental series has provided a data base for debris coolability in which prototypic materials are used and prototypic pressures are realized.... The dryout behavior of beds composed of prototypic materials appears to be consistent with that observed in out-of-pile experiments using simulant [sic] materials at low pressures.

The behavior of debris beds at this point is reasonably well understood. Several analytical models, among them the Lipinski model, do a reasonable job of predicting dryout heat fluxes. The obvious problem is in determining the proper debris bed configuration for LWR reactor accidents. In particular, more information is needed on the particle size distribution, void fraction, bed depth, and degree of stratification (if it occurs). Given this information, reasonably accurate predictions can be made about the coolability of a prototypic debris bed...."

The DCC series test results also demonstrate the same dependence of quench behavior upon particle size that was observed in the previous tests with metals and which is described in the last two paragraphs of Section 7.2.2. Since similar results are observed for tests with pure metal particles and for tests with pure oxide particles, some degree of confidence is obtained for application of the dryout and quenching models to BWR lower plenum debris, which would be comprised of a mixture of oxides and metals.

Recent tests at Argonne National Laboratory [33] have demonstrated the quenching of high-temperature (3000 K) liquid pours of 60% UO_2 , 16% ZrO_2 , and 24% stainless-steel entering water at atmospheric pressure. In all cases, quenched beds were formed with some oxidation of the stainless-steel, but never a steam explosion.

Nevertheless, neither the DCC series, the recent Argonne pours, nor any of the other debris bed experiments have included zirconium metal within their superheated beds and, therefore, the consequences of hydrogen generation after water entry have not been assessed experimentally. The next section describes the models within subroutine BHBWET that are employed to represent the effects of internal hydrogen generation upon the bed internal flows.

7.3 Effects of Hydrogen Generation

Water entry to superheated debris bed control volumes will produce steam at rates corresponding to the boiling powers calculated as described in Section 7.2. The way that the countercurrent flow limitation restricts the amount of bed cooling that can be provided by lower plenum flooding is described there. That discussion, however, is based solely upon the available experimental evidence and, following the experiments, neglects the effects of hydrogen generation within the bed. It is now necessary to consider the hydrogen generation that would occur as a consequence of the availability of this steam to the metal surfaces within each control volume.

The calculation of hydrogen generation is described in Section 7.3.1. The effectiveness of rising steam and hydrogen in blocking the downward entry of water (the momentum flux) is expected to be, based upon physical principles, the same as the blocking effect of steam alone at the dryout point. As described in Section 4.1.5 of Reference 34, given the steam flow in the absence of hydrogen generation, an estimate of the steam flow with hydrogen generation can be based upon an application of the Wallis flooding correlation. [35] The way that this is accomplished within subroutine BHBWET is described in Section 7.3.2.

7.3.1 Metal-Steam Reaction Rate

With water introduced into the lower plenum debris bed, steam is first generated by contact with hot particles, then metal-steam reaction calculations predict the associated hydrogen generation. The steam generation rate for a bed control volume is:

$$WSO = \frac{QWET(I,J)}{HLV} \text{ kg/s}$$

Where,

$QWET(I,J)$ = local boiling power, W and

HLV = heat of vaporization, J/kg.

BH Package Reference Manual

The amount of hydrogen generated is obtained by means of a call to subroutine BHMWDE with the arguments WSO and a steam temperature equivalent to the saturation temperature. The calculational process that occurs within this subroutine is described in Section 3.4.

Subroutine BHMWDE returns the rate of hydrogen generation WHO (kg/s), the hydrogen temperature TOUT (K), and the metal-steam reaction energy release rate QMWDB (W). In addition, the magnitude of the variable WSO is reduced correspondingly; subsequent to the call, it represents the effective steam generation rate after the steam consumption associated with hydrogen generation has been subtracted.

The metal-steam reaction energy release rate for each control volume is stored in the array

$$QPFMW(I,J) = QMWDB \ W,$$

and is included as a positive term in the control volume energy balance carried out each timestep within subroutine BHHED2. The local hydrogen generation is stored in the array

$$WHS(I,J) = WHO \text{ kg/s.}$$

Here I is the debris bed layer index and J is the index of the radial zone.

The energy associated with any remaining steam is added to the overlying water pool together with the energy required to cool the hydrogen gas to the saturation temperature. For each control volume, the associated energy release rates are:

$$WSO \times HLV + WHS(I,J) \times CPH \times (TOUT - TSAT) \ W,$$

where CPH is the specific heat of the hydrogen gas and TSAT is the saturation temperature corresponding to the current reactor vessel pressure. The sum of these energy release rates over all control volumes is QH2LPW (W).

Within subroutine BHHED2, the quantity:

$$QLPWAT = (QTOLPW + QH2LPW) \times DTM \ J$$

represents the total heat transfer to the water during a timestep of length DTM. (Here QTOLPW is the energy transfer rate by nucleate or film boiling at the bed surface, obtained as described in Section 7.4.) The quantity QLPWAT (J) is returned to the MELCOR interface, where it is applied each timestep as an energy addition to the lower plenum water pool.

The total gas generation during the timestep is:

$$H2LPW = \sum WHS(I,J) \times DTM \text{ kg,}$$

and this hydrogen mass is added to the vessel atmosphere at temperature TSAT. The corresponding amount of water

$$H2LPW \times \frac{18.01534}{2.01594} \text{ kg}$$

is subtracted from the mass of the lower plenum water pool.

7.3.2 Effect on Dryout Heat Flux

The rate at which water can enter the upper surface of a debris control volume under dryout conditions will be increased if the countercurrent flow consists of a mixture of hydrogen and steam instead of steam alone. As explained in Section 4.1.5 of Reference 34,

$$WSWH = \sqrt{\frac{RHOG \times (RHOL - RHOG)}{RHOSLS}} \times WSNH - WHST \text{ kg/s}$$

where,

WSWH = steam escape with hydrogen, kg/s

WSNH = steam escape without hydrogen, kg/s

WHST = hydrogen generation rate, kg/s

$$RHOG = \frac{WSWH + WHST}{\frac{WSWH}{RHOS} + \frac{WHST}{RHOH}}, \text{ average density, kg/m}^3$$

RHOS = steam density, kg/m³

RHOH = hydrogen density, kg/m³

RHOSLS = RHOS x (RHOL - RHOS), kg/m³, and

RHOL = water density, kg/m³.

BH Package Reference Manual

In practice, an iterative procedure is applied to determine WSWH since the average density RHOG depends upon its value.

Once the reduced steam flow is known, then the maximum power that can be removed from a control volume by boiling is redefined as:

$$QSUR(I,J) = \left(WSWH + \frac{18.01534}{2.01594} \times WHST \right) \times HLV \ W .$$

It is then this increased value of QSUR that is used to determine the boiling power QWET for each control volume as described in Section 7.2.2.

7.4 Heat Transfer at the Bed Surface

Radiation from the upper surfaces of water-covered debris bed radial zones to the upper vessel structures and to the vessel atmosphere is terminated at the time that water is introduced to the vessel lower plenum. Representation of convective heat transfer to the overlying pool begins for each covered zone at the time that the local radiation calculation is terminated.

Heat transfer to the overlying pool can be by film boiling for large surface-to-water temperature differences or by nucleate boiling at lower temperature differentials. The critical heat flux is the maximum power per unit area that can be maintained over a surface by nucleate boiling.

7.4.1 Critical Heat Flux

The critical heat flux is calculated by application of Equation 2.110 of Section 2.6.4.2 of the MELCOR HS Package Reference Manual. (This is the Zuber relation given as Equation (2-4.27) of Reference 36, with modification of the leading coefficient.) However, rather than solve this equation each timestep, and recognizing that the critical heat flux is a function only of vessel pressure, a set of empirical fits has been implemented within subroutine BHED2. These empirical relations are listed in Table 7.4.

Table 7.4 Empirical Fits for the Critical Heat Flux

Reactor Vessel Pressure Range (Pa)	Critical Heat Flux (W/m ²)
PVSL < 551581.	$9.748 \times 10^5 + 5.79321 \times \text{PVSL} - 4.1095 \times 10^{-6} \times (\text{PVSL})^2$
$551581. \leq \text{PVSL} < 827371.$	$2.04 \times 10^6 + 1.59542 \times \text{PVSL}$
$827371. \leq \text{PVSL} < 4136854.$	$2.044 \times 10^6 + 1.93848 \times \text{PVSL} - 4.552 \times 10^{-7} \times (\text{PVSL})^2 + 4.10 \times 10^{-14} \times (\text{PVSL})^3$
$\text{PVSL} \geq 4136854.$	$4.85 \times 10^6 + 0.07977 \times \text{PVSL}$

To provide a feel for the numbers, it may be observed that the critical heat flux is 2.26 MW/m² at 0.276 MPa (40 psia) and is 3.96 MW/m² at 1.379 MPa (200 psia). If the reactor vessel were to remain fully pressurized, the critical heat flux would be 5.40 MW/m² at 6.895 MPa (1000 psia).

In practice, the critical heat flux is calculated each timestep in subroutine BHED2 and then used to determine the corresponding surface temperature TCRIT for each water-covered surface as follows:

$$\text{TCRIT} = \text{TREC} + \frac{\text{QCRIT}}{\text{HSF}} \text{ K}$$

where,

TREC = water temperature, K

QCRIT = critical heat flux, W/m² and,

HSF = heat transfer coefficient for nucleate boiling, W(m² · K).

If the actual surface temperature TDBSUR is higher than TCRIT, then the surface is too hot to maintain nucleate boiling. In this case, the film boiling heat transfer coefficient is used to determine the surface-to-water heat transfer rate.

7.4.2 Film Boiling Coefficient

The film boiling heat transfer coefficient is calculated by application of the modified Bromley correlation listed as Equation 2.112 in Section 2.6.4.4 of the HS Package Reference Manual. (See also Reference [36] with respect to the discussion of Equation (2-4.35).) In subroutine BHBWET:

$$HFILM = 0.943 \times (TRM1 \times TRM2)^{1/4} + FACTR \times [(TDBSUR)^4 - (TSAT)^4] / TDIF$$

W/(m² · K), where the second term represents the effect of radiation across the film and,

$$TRM1 = \frac{\rho_s \times (\rho_l - \rho_s) \times G \times (CONDV)^3}{VISV},$$

CONDV = vapor thermal conductivity W/(m² · K),

VISV = vapor dynamic viscosity kg/(m · s),

$$TRM2 = \frac{HLV + 1/2 \times TDIF \times SPHEAT}{TDIF \times CL}$$

HLV = heat of vaporization for water, J/kg,

TDIF = TDBSUR – TSAT, K,

SPHEAT = vapor heat capacity, J/(kg · K),

CL = characteristic length equal to twice the area-to-perimeter ratio CLS(N), m. For the annular bed surfaces, this is the outer radius minus the inner radius. For the exposed wall nodes, CL is the vertical nodal height, and

FACTR = 0.60 x Stefan-Boltzman coefficient = 3.40116 x 10⁻⁸.

It should be noted that the terms CONDV and VISV are evaluated at the average of the surface and saturation temperatures whereas SPHEAT is evaluated at the saturation temperature.

7.4.3 Nucleate Boiling Coefficient

The Rohsenow correlation for nucleate boiling has been implemented within subroutine BHHED2 for calculations of the heat transfer coefficient for surfaces where the local temperature TDBSUR is below the value required to induce film boiling. This correlation is expressed as Equation 2.108 of the HS Package Reference Manual and is discussed in Section 2.6.4.1 of that manual and in Section 2–4 of Reference [36].

Rather than solve the Rohsenow correlation directly for each surface each timestep, the nucleate boiling heat transfer coefficients are calculated in subroutine BHHED2 of the BH package as:

$$HSF = CNB \times (TDBSUR - TREC)^2 \quad W/m^2 \cdot K.$$

The factor CNB depends only upon vessel pressure and is determined once each timestep as indicated in Table 7.5.

Table 7.5 Empirical Fits for the Nucleate Boiling Calculation

Reactor Vessel Pressure Range (Pa)	Factor CNB $W/(m^2 \cdot K^3)$
PVSL < 551581.	$24.84 + 6.207 \times 10^{-4} \times PVSL$
$551581. \leq PVSL < 827371.$	$215.71 + 2.794 \times 10^{-4} \times PVSL$
$827371. \leq PVSL < 4136854.$	$420.07 + 3.229 \times 10^{-5} \times PVSL$
$PVSL \geq 4136854.$	$301.96 + 6.084 \times 10^{-5} \times PVSL$

It should be noted that the pressure intervals expressed on the left side of Table 7.5 are the same as those listed in Table 7.4, which simplifies the coding required to implement these empirical fits.

As a practical demonstration of the BH package surface heat transfer algorithms for water-covered surfaces, Table 7.6 lists results for a case with the reactor vessel at atmosphere pressure.

Table 7.6 Surface Heat Transfer Parameters and Calculated Results

Parameter		Value
Vessel pressure	PVSL	101353. Pa
Saturation temperature	TSAT	373.15 K
Critical heat flux	QCRIT	$1.52 \times 10^6 \quad W/(m^2 \cdot K)$
Nucleate boiling factor	CNB	$87.74 \quad W/(m^2 \cdot K^3)$
Critical temperature	TCRIT	399.03 K
Assumed surface temperature	TDBSUR	399.03 K
Nucleate boiling coefficient	HSF	$58766. \quad W/(m^2 \cdot K)$
Characteristic length	CL	.8572 m
Film boiling coefficient	HFILM	$165.5 \quad W/(m^2 \cdot K)$

Here the characteristic length of 0.8572 m corresponds to the actual value for the surface of the debris bed central radial zone in the example calculation. The nucleate boiling and film boiling heat transfer coefficients are evaluated at the transition point, since the local bed surface temperature is assumed to be equal to the critical temperature for this example. The large difference between the nucleate boiling and film boiling heat transfer coefficients at the transition point is evident.

BH Package Reference Manual

Table 7.7 provides an example of how the film boiling and nucleate boiling coefficients are predicted to change as the debris surface temperature decreases through the transition point. These example results, which pertain to the upper control volume (3,1) of the central debris bed radial zone, are taken from an actual MELCOR calculation. Water was introduced into the lower plenum at BH package timestep 209, when the surface temperature of the central zone was 904 K. BH package timestep 325 begins 9.67 min (580 s) later, when the central zone surface temperature has decreased to 416 K through the combined mechanisms of internal boiling and surface cooling (also by boiling).

A standard length of five seconds was used for each of the timesteps represented in Table 7.7. Film boiling occurs during BH package timesteps 325 and 326 (the nucleate boiling heat transfer coefficients are shaded to indicate that they are not used). The transition to nucleate boiling occurs during BH package timestep 327, when the calculated surface temperature TDBSUR falls below the critical temperature for the first time. Subsequent to BH package timestep 327, the surface temperature decreases much more rapidly because of the much greater surface heat transfer coefficients (here the shading over the film boiling heat transfer coefficients indicates that they are not used).

Table 7.7 Example Results for Water Cooling of the Central Radial Zone

Parameter		Timestep				
		325	326	327	328	329
PVSL	Pa	188111.	188131.	188114.	188146.	188151.
TSAT	K	390.67	390.67	390.67	390.67	390.67
QCRIT	W/(m ² ·K)	1919173.	1919259.	1919186.	1919323.	1919341.
TCRIT	K	411.15	412.96	414.95	487.37	761.89
TDBSUR	K	416.39	415.33	414.29	402.51	396.72
TDIF	K	25.72	24.66	23.63	11.84	6.04
HSF	W/(m ² ·K)	93676.3	86113.5	79042.5	19849.9	5170.4
HFILM	W/(m ² ·K)	196.4	198.4	200.0	233.9	*
QTOGAS	W	10699.7	10331.9	11801.8	11322.6	10812.6

*HFILM is not calculated for values of TDIF less than 10 K.

The last entry QTOGAS in Table 7.7 is the heat transfer rate (W) from the upper control volume (3,1) to the overlying water during the timestep. It is calculated in the same manner as the heat transfer to the lower plenum atmosphere for the dry case, as described in Section 3.2.2, except that HSF or HFILM is used in lieu of HSURF. The value of QTOGAS does not increase radically during the transition from film to nucleate boiling because the majority of the resistance to heat transfer lies not at the debris surface but rather along the conduction pathway through the upper half of the debris control volume.

Finally, it is important to appreciate the relative magnitudes of the internal boiling and surface heat transfer contributions to debris cooling in the upper bed. During the period

covered by Table 7.7, the temperature at the center of the upper control volume in the central radial zone is predicted to decrease from 537 K to 514 K while the internal boiling power increases slightly, from 1.842 MW to 1.856 MW. Thus the internal boiling power is about 185 times the surface heat transfer rate and continues to be significant long after the surface temperature has closely approached the saturation temperature.

7.5 Heat Transfer at Exposed Wall Nodes

Exposed reactor vessel bottom head wall nodes are by definition those not covered by debris. With reference to Figure 1.10, wall node 17 is the only exposed node at the time that debris bed layer three is formed. Wall nodes 16, 15, and lower may, however, become exposed as the debris volume shrinks by the effects of internal melting and downward material relocation and, for cases with consideration of penetration failures, by the release of materials into the drywell. The criterion for a wall node to be exposed is that there is no adjacent debris extending above the lower nodal boundary.

If the water level YLIQ within the lower plenum becomes sufficiently high that the exposed wall nodes become covered by water, then their internal surface areas will undergo heat transfer by either nucleate or film boiling. In either case, the appropriate heat transfer coefficient is determined in the same manner as for the debris bed radial zones, as described in Section 7.4. The criterion for an exposed wall node to be considered to be water-covered is that YLIQ is greater than the height of the middle of the node.

7.6 The Case of Lower Plenum Water with Penetration Failures

For the case with water in the lower plenum after bottom head penetration failures have occurred, countercurrent flow would not limit the introduction of water into the upper bed control volumes. Rather, the steam (and any hydrogen) produced within the bed would escape from the bottom of the vessel via the failed penetration assemblies. The absence of a countercurrent flow limitation in the presence of a lower gas escape pathway has been observed experimentally as described in Reference 28.

This section describes the special provisions within subroutine BHBWET for application to calculations for which the existence of failed bottom head penetration assemblies is combined with the presence of water overlying the debris bed. The prediction of water flow into the upper bed surface is explained in Section 7.6.1. The calculations of steam and hydrogen generation are discussed in Sections 7.6.2 and 7.6.3, respectively. The gases reaching the bottom of the bed are released into the drywell with exit conditions determined as described in Section 7.6.4.

7.6.1 Water Flow

The water flow into the bed surface (without countercurrent flow limitation) is assumed to be equal to the rate at which steam can escape (via the failed penetrations) from the bottom of the reactor vessel. Although hydrogen would be mixed with the steam in the actual case and the water flow would be unsteady for some period after initial introduction, this approach is considered to yield a reasonable approximation to the actual flow.

The water flow WLTOBD into the bed surface is calculated in subroutine BHBWET as:

$$ABRK \times CBRK \times \sqrt{2.0 \times RHOS \times [DP + YLIQ \times RHOL \times G]} \text{ kg/s}$$

where,

- ABRK = penetration flow area, m²
- CBRK = orifice coefficient (= 0.583),
- RHOS = steam density, kg/m³
- DP = reactor vessel-to-drywell pressure differential, Pa
- YLIQ = height of liquid within the vessel, m
- RHOL = water density, kg/m³ and,
- G = the acceleration of gravity, m/s².

The value of ABRK is the same user-defined break area as is used for gas flow through failed penetrations in the absence of water (Section 5.5). The actual flow area that would be associated with failed instrument guide tubes under accident conditions is of course unknown. A value of 0.010 m² would be representative of the opening provided by several failed guide tubes.

It should be noted that the calculated flow into the bed will increase with reactor vessel pressure and with the height of water within the vessel. As an example, predicted water flow into the bed surface is 2.35 kg/s for an initial reactor vessel pressure of 188000 Pa (27.3 psia), a break area of 0.010 m², a differential pressure DP of 54,000 Pa (7.8 psi), and a water height YLIQ of 2.70 m (8.8 ft).

The overall water flow WLTOBD is apportioned among the upper bed control volumes according to their relative free volumes (or porosities).^{*} Furthermore, the overall water flow exiting the upper control volumes is reapportioned among the middle bed control volumes according to the relative porosities there, and the same reapportionment of flow occurs for flow exiting the middle control volumes and entering the bottom control volumes. Stated another way, the flow is modeled to follow the larger-porosity pathways (the paths of least resistance) to the bottom of the bed.

If there is no free volume within the set of upper radial zone control volumes then the flow is considered to be blocked and no water enters the bed. Similarly, if there is no free volume within the set of middle (or lower) bed control volumes, then the flow is considered to be blocked at the middle (or lower) level.

The same apportionment of flow occurs for any steam or hydrogen generated within the bed control volumes. As described in the next section, steam generation occurs within any control volume with a debris temperature greater than TSAT for which water is predicted to enter. Hydrogen generation is discussed in Section 7.6.3.

7.6.2 Steam Generation

Since the dryout heat flux concept is not applicable to debris bed control volumes for which the water and steam flow are in the same (downward) direction, it is necessary in this case to make a straightforward estimate of the particle-to-water heat transfer rate. This is accomplished in subroutine BHBWET by means of an assumption that the debris particles constitute a set of uniform spheres. Then, the heat transfer coefficient appropriate for the overall surface area of these spheres is determined in a manner identical to that described in Section 7.4.3. (As appropriate to the exiting conditions, either nucleate or film boiling is represented to occur over the collective surface area of the spheres.)

The total particle surface area within a control volume is:

$$PSA = (VLP - FLP) \times \frac{6.0}{DFRAG} \text{ m}^2$$

where

$$VLP = VLP(I,J), \text{ total local volume, m}^3$$

^{*} The fraction of the total flow that enters each upper control volume is the local free volume divided by the sum of the free volumes for all upper control volumes.

BH Package Reference Manual

FVLP = FVLP(I,J), local free volume, m³ and,

DFRAG = particle diameter, m.

It should be noted that the quantity 6.0/DFRAG represents not only the surface-to-volume ratio of a sphere, but also the surface-to-volume ratio for a cylinder with height equal to diameter (typical of BWR fuel pellets).

The boiling power QWET(I,J) based upon particle heat transfer within a debris bed control volume is then:

$$PSA \times \frac{TMLPO - TSAT}{\frac{0.1127 \times DFRAG}{CONDB} + \frac{1.0}{HS}} W$$

where,

TMLPO = TMLPO(I,J), local debris temperature, K

CONDB = CONDB(I,J), local debris thermal conductivity, W/(m-K)

HS = local surface heat transfer coefficient, W/(m²-K).

The use of the factor 0.1127 in the denominator of this expression derives from a recognition that TMLPO does not represent the temperature at the center of the particles, but rather represents the volume-averaged temperature of the particles. Thus, the effective heat transfer length of conduction through the debris is less than the particle radius.

The local boiling power QWET(I,J) is constrained to be not more than the power necessary to evaporate all of the water entering the control volume. Any water not evaporated is considered to enter the underlying set of bed control volumes or if appropriate, to exit the vessel.

7.6.3 Hydrogen Generation

As downward-flowing water is increasingly converted to steam while passing through the bed control volumes, the steam becomes available to drive the metal-steam reactions that produce hydrogen. Within each bed control volume, the local steam availability WSO (kg/s) is the combination of steam entering from above plus the local steam generation.

Subroutine BHMWDE is called with the arguments WSO and the average steam temperature within the control volume. (The calculational process within this subroutine

is described in Section 3.4.) The rate of hydrogen generation WHO (kg/s), the hydrogen temperature TOUT (K), and the metal-steam reaction energy release rate QMWDB (W) are returned. In addition, the steam availability WSO is reduced appropriately. Subsequent to the call, WSO represents the effective steam generation rate after the steam consumption associated with hydrogen generation has been subtracted.

The metal-steam reaction energy release rate is stored in the array:

$$QPFMW(I,J) = QMWDB \ W.$$

and is included as a positive term in the bed control volume energy balance carried out each timestep in subroutine BHHED2. The local hydrogen generation is stored in the array:

$$WHS(I,J) = WHO \text{ kg/s.}$$

Here I is the debris bed layer index and J is the index of the radial zone.

As the remaining steam flows downward through the bed, its temperature follows the local debris temperature. The associated transfer rate of energy from the debris to the flowing steam within each control volume is:

$$QPFGS(I,J) = WSO \times SPHEAT \times (TMLPO - TSTMA) \ W$$

where,

SPHEAT = steam specific heat, J/(kg-K)

TSTMA = average temperature of steam entering or generated within the control volume, K.

The term QPFGS(I,J) is entered as a negative term in the control volume energy balances carried out within subroutine BHHED2.

7.6.4 Exit Conditions

For the case with penetration failures, water flows downward into the surface of the debris bed. Within the bed control volumes some (or all) of this water is converted to steam. During the period while local debris temperatures remain high and zirconium metal remains present, some (or all) of the steam is converted to hydrogen. Therefore, the fluid release

BH Package Reference Manual

from the reactor vessel lower plenum to the drywell is comprised of liquid water plus a mixture of hydrogen and steam.

Depending upon bed conditions, any of these three fluids may not exist at the vessel exit. In general, all water will be evaporated and all steam will be consumed in reactions with zirconium during the initial period after water is introduced so that only hydrogen will enter the drywell. Later, when bed temperatures are reduced and much of the original zirconium has been consumed, a mixture of steam and hydrogen will be predicted to enter the drywell. Still later, when the bed has cooled so that the calculated hydrogen generation is insignificant, a mixture of water and steam will exit the vessel. Finally, when the bed is quenched, the steam generation will be limited to that necessary to remove decay heat and all excess water will enter the drywell.

Any water entering the drywell is assumed to exit the vessel at the saturation temperature corresponding to the vessel pressure. For the steam-hydrogen mixture, the average temperature is

$$\frac{MSTM \times CPS \times TSTM + MHYD \times CPH \times THYD}{MSTM \times CPS + MHYD \times CPH} \text{ K}$$

where

MSTM, MHYD = mass flows of steam and hydrogen, kg/s

CPS, CPH = specific heats of steam and hydrogen, J/(kg-K) and,

TSM, THYD = steam and hydrogen gas temperatures at the bottom of the bed, K.

Within the MELCOR-BH package interface, the water is added to the pool overlying the drywell floor, whereas the steam and hydrogen are added to the drywell atmosphere.

7.7 Interaction of Water with Late Debris Pours

As explained in Section 1.1.4, the third (upper) debris layer is formed when the bed temperature increases after lower plenum dryout. Subsequently, any material relocating downward from the core region as predicted by MELCOR is added to the upper debris bed control volumes throughout the period of the BH package calculation. In general, these predicted late (after lower plenum dryout) debris pours occur intermittently and vary in both material composition and quantity. If water has been reintroduced into the lower plenum and overlies the bed surface, then these late material pours will interact with this water to produce steam and (if zirconium is present) hydrogen above the bed surface. Models for this debris-water interaction are provided in subroutines BHBWET and BHED2.

Recently-obtained information concerning the jet breakup length and fragmentation of corium melt streams in water is provided by Reference 33. Based upon that information, a uniform diameter of 0.005 m is assigned to the (spherical) particles of the swarm formed after jet breakup. Heat transfer is assumed to be by film boiling over the total particle surface area as defined by the pour constituent masses and densities. The film boiling heat transfer coefficient HFLMPR is determined within subroutine BHBWET by the method described in Section 7.4.2 (but using the pour temperature TPOUR in lieu of TDBSUR).

Again following Reference 33, the jet breakup length over each of the bed radial zones is taken to be equal to 12 jet diameters. The actual diameters of the various flow passages through the core plate are, of course, unknown. A representative value of 0.0254 m (one inch) for the jet diameters is employed in subroutine BHBWET.

The duration DTMPR (s) of the transit of the particle swarm through water for each bed radial zone is obtained by subtracting the jet breakup length from the local water depth and dividing by the assumed fall speed of 1.0 m/s.[†] A first estimate of the energy transfer QPRCV to water is then obtained by applying the film boiling heat transfer coefficient HFLMPR over the total particle surface area for this duration. This estimate will then be reduced if it exceeds the energy transfer corresponding to the permissible quench fraction for the pour, which (following Reference 33) varies linearly from 0.35 for saturated water to 0.72 for water subcooled by 40 K or more.

The predicted steam production during the pour is equal to the calculated energy transfer divided by the energy per kilogram required to bring the lower plenum water to saturation temperature and for evaporation.* The fraction of this steam that is produced in the vicinity of zirconium is assumed equal to the volume fraction of zirconium within the pour. One-third (STMREA [kg]) of this local steam generation is assumed to be available to drive the metal-steam reaction.

The first estimate for metal-steam reaction energy release during the pour is:

$$QPRMW = 1.6282 \times 10^7 \times STMREA \text{ J}$$

where the constant term is the energy release (J) associated with the consumption of one kilogram of steam in the reaction with zirconium. This estimate will then be reduced if the corresponding metal oxidation fraction exceeds that observed in the experiments of

[†] A minimum value of 0.01 s is imposed for DTMPR for applications in which the jet breakup length exceeds the local water depth.

* Appropriate constraints (applied for each bed radial zone) ensure that the predicted local steam generation cannot exceed the locally available water mass.

BH Package Reference Manual

Reference 33. The metal oxidation limit as imposed in subroutine BHBWET decreases from 0.34 for saturated water to 0.02 for water subcooled 40 K or more.

The hydrogen production during the pour is:

$$H2DRP = \frac{2.01594}{18.01534} \times STMREA \text{ kg}$$

which originates at the debris temperature. The energy required to cool this gas to the water saturation temperature is:

$$QH2CL = H2DRP \times (HHYDP - HHYDW) \text{ J}$$

where HHYDP and HHYDW are the specific enthalpies of hydrogen at the pour temperature and the water temperature, respectively.

The debris-to-water heat transfer plus the hydrogen cooling energy transfer are additive terms in the lower plenum water energy balance carried out within the MELCOR interface. (All of the metal-steam reaction energy release is assumed to remain with the falling debris.)

The amount of zirconium consumed is calculated in subroutine BHED2 as:

$$WZRR = RHOZR \times \frac{QPRMW}{4.179013 \times 10^{10}} \text{ kg}$$

where the constant term in the denominator is the energy release (J) associated with oxidation of one cubic meter of zirconium. The associated production of ZrO_2 is:

$$WZRO2C = \frac{123.219}{91.22} \times WZRR \text{ kg.}$$

The appropriate subtraction of zirconium metal and addition of zirconium dioxide is made to correct the debris inventories for the upper control volume of each radial zone that receives the pour.

It is important to recognize, for a given mass of lower plenum water, that the water depth will vary over the bed radial zones, especially for cases with debris loss through penetration failures so that the bed surface has a cupped shape (see, for example, Figure 6.5). This means that the debris-water interaction will occur over a longer period of time in the central radial zones. Consequently, if zirconium is present in the pour, the central zone upper

control volumes will exhibit a higher temperature than the peripheral zones after the pour. The converse is true if the pour does not include zirconium, since the cooling effect of the water will dominate.

7.8 Special Printed Output

The message

Water level in lower plenum = _____ cm

is printed each timestep when water is present. When appropriate, this message will appear at the upper center of the standard pictorial display of the BH package output, examples of which are shown in Figure 6.1 through Figure 6.5. The printed value is YLIQ, as defined in Section 7.1, but converted to centimeters for compatibility with the other heights listed on the pictorial display.

The tabulated output for standard BH package calculations (without water in the lower plenum) is discussed in Section 6.5. Here the special printed output obtained only when water is present is described.

With water in the lower plenum, the message

and to pool = _____ Joule Total to overlying water pool = _____ Joule

reports the debris and exposed wall node surface heat transfer during the timestep while the message

plus boiling = _____ Joule Total to boiling within debris = _____ Joule

reports the energy transfer associated with the internal boiling. These two special messages are listed consecutively and immediately follow the standard message

*Net heat transfer to vessel atmosphere (after third bed layer is established):
This timestep = _____ Joule Total since layer 3 established = _____ Joule,*

which appears in the dry case. Some bed surface-to-atmosphere heat transfer can occur with water in the lower plenum if the height of the water surface is insufficient to cover all of the debris.

8. Package Organization

This section describes the basic organization of the Lower Plenum Debris Bed (BH) package and the exchange of information across the interface of this package with MELCOR.

8.1 Arrangement of Subroutines and Commons

The Bottom Head (BH) package comprises 33 subroutines and 19 commons for the internal exchange of information. The package subroutines are listed in Table 8.1, together with cross-reference information defining the exchange of calls among them. For example, subroutine BHAXCO (second table entry) is called by subroutine BHHED2 and calls subroutine BHAKCS (which, as the table earlier reveals, is also called by three other subroutines).

A brief description of the purpose that each subroutine fulfills in the overall BH package calculation is provided in Table 8.2. As indicated, the primary interface with MELCOR occurs within two package subroutines, BHQSLU and BHPENF. Calls are made to MELCOR Core (COR) package subroutines CORABS and CORPOL.

A cross-reference of subroutines and commons is provided in Table 8.3 and Table 8.4. Not all of the package subroutines depend upon common statements for information transfer. Those that do are listed in the first column of Table 8.3 with their included commons listed in the second column. The obverse of this matrix is provided in Table 8.4, where each of the 15 package internal commons is listed in the first column and the subroutines that include each Common are listed in the second column.

As indicated in Table 8.4, commons /BHBWLV/, /BHCHAR/, /BHCHED/, /BHDBML/, /BHDMXX/, /BHHABL/, /BHHDIN/, /BHHEDM/, /BHHEDK/, /BHLPXX/, /BHPROP/, /BHVER/, and /BHVLVX/ also extend into MELCOR. This is for the purpose of loading the appropriate user-input information described in the BH Package User's Guide and for convenience in the provision of restart capability.

Included among the commons listed in Table 8.4 are five special-purpose commons identified as /BHRSS1/ through /BHRSS5/, which are intended primarily for the transmission of restart information between MELCOR and BH package subroutines BHQSLU, BHHED2, BHHEDN, BHMWDE, and BHDBME, respectively. These special-purpose commons are listed, opposite to their parent subroutines, in the right column of Table 8.3. (Commons /BHRSS1/ through /BHRSS4/ are also used to convey internal information for mass/energy balance purposes as indicated in Table 8.4.)

Table 8.1 BH Package Subroutine Organization

Subroutine	Calls	Is Called By
BHAKCS		BHAXCO BHDBMX BHHED2 BHLPLN
BHAXCO	BHAKCS	BHHED2

BH Package Reference Manual

Subroutine	Calls	Is Called By
BHBWET	BHMWDE BHTHTH BHTHTS	BHHED2
BHCPCS	BHLPOL	BHDBMX BHHED2 BHHEDN BHLPLN
BHDBME	BHDPOL BHEUTF BHEUTM BHMENT	BHHED2
BHDBMX	BHAKCS BHCPCS BHLPOL BHMENT	BHHED2
BHDCHA	BHFALS	BHHED2 BHMERG
BHDPOL		BHDBME
BHEUTF	BHEUTK	BHDBME BHHED2 BHMERG
BHEUTK		BHEUTF BHEUTM
BHEUTM	BHEUTK	BHDBME BHHED2 BHMERG
BHFALS	BHVLPL BHVOLL	BHDCHA BHHEDN
BHFPST		BHHED2

BH Package Reference Manual

Subroutine	Calls	Is Called By
BHHED2	BHAKCS BHAXCO BHBWET BHCPCS BHDBME BHDBMX BHDCHA BHEUTF BHEUTM BHFPST BHLPOL BHHEDN BHHRST BHLPLN BHMENT BHMERG BHPAGE BHST2P BHTHTS	BHQSLU
BHHEDN	BHFALS BHCPCS BHLPOL BHMENT	BHHED2
BHHRST	CORABS	BHHED2
BHLPLN	BHAKCS BHCPCS	BHHED2
BHLPOL		BHCPCS BHDBMX BHHED2 BHHEDN
BHMENT		BHDBME BHDBMX BHHED2 BHHEDN BHMWDE BHQSLU
BHMERG	BHDCHA BHEUTF BHEUTM	BHHED2
BHMWDE		BHBWET BHMENT BHPENF

Subroutine	Calls	Is Called By
BHPAGE		BHHED2
BHPENF	BHMWDE BHST3P	MELCOR
BHQSLU	BHHED2 BHMENT	MELCOR
BHST2P	BHTCH4 BHTHTH BHTHTS BHHTPO BHHTP2	BHHED2
BHST3P	BHTCH4 BHTHTH BHTHTS BHHTPO BHHTP2	BHPENF
BHTCH4	CORPOL MELCOR	BHST2P BHST3P
BHTHTH	CORPOL	BHBWET BHST2P BHST3P
BHTHTS	CORPOL	BHBWET BHHED2 BHST2P BHST3P
BHHTP2	CORPOL	BHST2P BHST3P
BHHTPO	CORPOL MELCOR	BHST2P BHST3P
BHVLPL		BHFALS
BHVOLL		BHFALS

Table 8.2 Purpose of BH Package Subroutines

Subroutine	Purpose
BHAKCS	Function for temperature-dependent thermal conductivity of carbon steel.
BHAXCO	Calculates axial conduction in the reactor vessel bottom head wall.
BHBWET	Calculates the water height above each bed radial zone and the dryout heat flux for each debris control volume; used only for calculations in which the lower plenum is reflooded after initiation of the BH package.
BHCPCS	Function subprogram for temperature-dependent specific heat of carbon steel.

BH Package Reference Manual

Subroutine	Purpose
BHDBME	Controls melting, relocation, and freezing of materials within the lower plenum debris bed.
BHDBMX	Calculates liquid release from lower plenum via failed penetrations and associated material ablation along escape pathway.
BHDCHA	Adjusts control volume dimensions in response to material relocations and recalculates heat transfer lengths.
BHDPOL	Linear interpolator used by the BHDBME subroutine.
BHEUTF	Controls freezing of liquid material within each control volume.
BHEUTK	Determines the control volume debris constituents to be included in the melting or freezing processes.
BHEUTM	Calculates melting of solid materials within each control volume.
BHFALS	Utility solver for finding roots by the method of regula falsi.
BHFPST	Initializes fission product inventories in the BH debris bed control volumes; partitions fission products relocating from the core region into the appropriate BH debris bed control volumes.
BHHED2	Main program for the BH package; calculates energy balances and heat transfers within the lower plenum debris bed and generates printed output.
BHHEDN	Establishes lower plenum debris bed layers one and two at time of lower plenum dryout and initiates layer three upon temperature flag; establishes nodal structure for the bottom head wall.
BHHRST	Calculates wall-to-steam radiation heat transfer coefficients for debris bed surfaces, exposed portions of the vessel wall, and the lower core shroud.
BHLPLN	Calculates reactor vessel bottom head structural heatup and melting.
BHLPOL	Linear interpolator.
BHMENT	Returns the material enthalpies and material average specific heats.
BHMERG	Calculates the merging process for vertically aligned bed control volumes.
BHMWDE	Calculates the zirconium-steam reaction within debris bed control volumes after bottom head penetration failure and for cases without penetration failure if water enters the lower plenum after bed dryout.
BHPAGE	Prints output page header.
BHPENF	Package entry point after bottom head penetration failures occur; calculates gas blowdown rate and heat transfer between flowing gas and lower plenum debris.
BHQSLU	Package entry point throughout calculation. Performs conversion of units and loads materials relocated from core region into appropriate arrays.
BHST2P	Determines the thermophysical properties of a flowing gas stream comprised of steam, hydrogen, carbon monoxide, carbon dioxide, and methane.

Subroutine	Purpose
BHST3P	Given the temperature, pressure, and composition of a mixture of steam, hydrogen, carbon monoxide, carbon dioxide, and methane, returns the gas specific enthalpies and weight fractions, plus the mixture specific heat.
BHTHTH	Thermodynamic and transport properties of hydrogen.
BHTHTS	Thermodynamic and transport properties of steam.
BHTTPO	Thermodynamic and transport properties of carbon monoxide.
BHTTP2	Thermodynamic and transport properties of carbon dioxide.
BHTCH4	Thermodynamic and transport properties of methane.
BHVLPL	Function subprogram primarily used by BHFALS when called by BHDCHA. Calculates total volume versus height for control volumes whose outer boundaries reflect the bottom head curvature.
BHVOLL	Function subprogram primarily used by BHFALS when called by BHHEDN. Calculates total volume versus cylindrical radius to right vertical boundary for the bottom layer control volumes (1,1) and (1,2).

Table 8.3 Cross-Reference Index of Subroutines and Commons

Subroutine	Commons
BHBWET	/BHCHED/ /BHDBML/ /BHDMXX/ /BHHABL/ /BHHDIN/ /BHPROP/
BHDBME	/BHDBML/ /BHDMXX/ /BHHED3/ /BHRSS5/ /BHVLVX/
BHDBMX	/BHDBML/ /BHDMXX/ /BHHABL/ /BHHDIN/ /BHHEDM/
BHDCHA	/BHDBML/ /BHDMXX/ /BHHABL/ /BHLPXX/ /BHVLVX/

BH Package Reference Manual

Subroutine	Commons
BHEUTF	/BHDBML/ /BHHED3/ /BHHEDM/ /BHHEDK/
BHEUTK	/BHDBML/ /BHHED3/ /BHHEDM/
BHEUTM	/BHDBML/ /BHHED3/ /BHHEDM/ /BHHEDK/
BHFALS	/BHLPPX/
BHFPST	/BHDBML/ /BHHEDM/ /BHRSS3/ /BHRSS1/
BHHED2	/BHCHAR/ /BHCHED/ /BHDBML/ /BHDMXX/ /BHHABL/ /BHHDIN/ /BHHEDM/ /BHLPPX/ /BHPROP/ /BHRSS2/ /BHRSS4/ /BHVLVX/
BHHEDN	/BHBWLX/ /BHCHED/ /BHDBML/ /BHDMXX/ /BHHABL/ /BHHDIN/ /BHHEDM/ /BHLPPX/ /BHRSS3/ /BHVLVX/
BHMERG	/BHDBML/
BHMWDE	/BHCHED/ /BHDBML/ /BHRSS4/

BH Package Reference Manual

Subroutine	Commons
BHPAGE	/BHVER/
BHPENF	/BHDBML/ /BHDMMX/ /BHPROP/
BHQSLU	/BHHEDM/ /BHRSS1/ /BHRSS2/
BHVLPL	/BHDBML/ /BHDMMX/ /BHVLVX/
BHVOLL	/BHLPXX/

Table 8.4 Cross-reference Index of Commons and Subroutines

Commons	Subroutine
/BHBWLX/	BHHEDN MELCOR
/BHCHAR/	BHHED2 MELCOR
/BHCHED/	BHBWET BHHEDN BHHED2 BHMWDE MELCOR
/BHDBML/	BHBWET BHDBME BHDBMX BHDCHA BHEUTF BHEUTK BHEUTM BHFPST BHHEDN BHHED2 BHMERG BHMWDE BHPENF BHVLPL MELCOR

BH Package Reference Manual

Commons	Subroutine
/BHDMXX/	BHBWET BHDBME BHDBMX BHDCHA BHHEDN BHHED2 BHPENF BHVLP MELCOR
/BHHABL/	BHBWET BHDBMX BHDCHA BHHEDN BHHED2 MELCOR
/BHHDIN/	BHBWET BHDBMX BHHEDN BHHED2 MELCOR
/BHHED3/	BHDBME BHEUTF BHEUTK BHEUTM
/BHHEDK/	BHEUTF BHEUTM MELCOR
/BHHEDM/	BHDBMX BHEUTF BHEUTK BHEUTM BHFPST BHHEDN BHHED2 BHQSLU MELCOR
/BHLPPX/	BHDCHA BHFALS BHHEDN BHHED2 BHVOLL MELCOR

Commons	Subroutine
/BHPROP/	BHBWET BHHED2 BHPENF MELCOR
/BHRSS1/	BHFPST BHQSLU MELCOR
/BHRSS2/	BHHED2 BHQSLU MELCOR
/BHRSS3/	BHFPST BHHEDN MELCOR
/BHRSS4/	BHHED2 BHMWDE MELCOR
/BHRSS5/	BHDBME MELCOR
/BHVER/	BHPAGE MELCOR
/BHVLVX/	BHDBME BHDCHA BHHEDN BHHED2 BHVLP MELCOR

8.2 Information Exchange with MELCOR

The BH package is initiated whenever sufficient solid debris has accumulated within the lower plenum. Subsequently, calls from MELCOR to subroutine BHQSLU are made each timestep, sending and receiving information pertaining to the calculated debris bed response. If reactor vessel bottom head penetration failures are predicted to occur, then calls from MELCOR to subroutine BHPENF also exchange pertinent information from that time forward. It is the purpose of this section to provide a detailed description of these information transfers.

8.2.1 Calls to BHQSLU

The argument list for the call from MELCOR to subroutine BHQSLU provides the following information needed to drive the lower plenum debris bed and bottom head response

BH Package Reference Manual

calculation. (These driver items are listed in the same order that they appear as call arguments).

1. DFRAG (DPART) is the debris bed representative particle diameter (m). It is specified in BH package input (card BH0500) and is used in the calculations of effective thermal conductivity for the bed control volumes (Section 2.4), the metal-steam reactions (Section 3.4), and the interactions of water with the debris (Sections 7.2 and 7.6).
2. AMASJP is the mass of water (kg) surrounding the jet pumps in the downcomer region of the reactor vessel. While water remains, it is an important lower plenum heat sink (Section 3.3) and source of steam for the metal-water reaction in the bed control volumes (after bottom head penetration failure).
3. TMAJSP is the temperature (K) of the downcomer region water pool and is the receiver temperature (Section 3.3) for convective heat transfer from the uppermost bottom head wall node to this water. After dryout of the downcomer annulus, TMAJSP is the temperature of the lower shroud wall and is used within the BH package only in the printed output.
4. PVSL is the reactor vessel pressure (Pa). It is used in the calculation of wall-to-steam heat transfer coefficients (Section 3.3.1).
5. DKDROP (DECAYP) is the current decay power (Watts) associated with the cumulative UO_2 that has escaped from the lower plenum to the drywell.
6. TDB is the temperature (K) of the debris relocated from the core region this timestep. If no debris is relocated, this temperature will not be used.
7. NSTEP (ICYCLO + 1) is the index of the BH package timestep, used only for the printed output. NSTEP is initiated as 1 at the time of transition to BH.
8. CH_4 is the mass (kg) of methane in the lower plenum atmosphere.
9. CO is the mass (kg) of carbon monoxide in the lower plenum atmosphere.
10. CO_2 is the mass (kg) of carbon dioxide in the lower plenum atmosphere.
11. HYD is the mass (kg) of hydrogen in the lower plenum atmosphere.
12. PSV is the partial pressure of steam (Pa) in the lower plenum atmosphere. It is used in the calculation of wall-to-steam heat transfer coefficients (Section 3.3.1).
13. STM is the mass (kg) of steam in the lower plenum atmosphere.

14. TGX is the temperature (K) of the lower plenum atmosphere. It is the receiver temperature for wall-to-atmosphere heat transfer (Section 3.2).
15. DP1 (DP) is the differential pressure (Pa) between the lower plenum atmosphere and the containment drywell. It is used to determine the gas flow through the debris bed if penetration failures occur; otherwise, it is used in the calculations for gross failure of the bottom head wall by creep rupture (Section 5.4).
16. TSHWAL is the initial temperature (K) of the vessel wall node adjacent to the lower downcomer region (node 18 as shown in Figure 1.10). It is set within MELCOR to the saturation temperature corresponding to the pressure within the lower plenum CVH control volume.
17. DELSMT (SSCM) is an array DELSMT(2) that transmits information concerning the initial status of the lower plenum structural steel. The first array element DELSMT(1) is the structural steel mass (kg) that melted and entered the debris, but is solid at the debris temperature when the BH package is first called. DELSMT(2) is the mass of structural steel that has melted and remains in the liquid phase.
18. QGDATM is the current heat transfer rate (W) from the control rod guide tubes to the lower plenum atmosphere, calculated within MELCOR. It is used only during the period before debris bed layer 3 is established.
19. TGRID2 is the initial temperature (K) of the lower plenum stainless-steel structure mass that has never melted. After the initial setup of the lower plenum debris bed, this temperature is calculated within the BH package and returned to MELCOR.
20. THEAD is the initial temperature (K) of the vessel bottom head wall nodes beneath the shroud. It is used only to establish the initial temperatures of the wall segments (Section 1.2).
21. AMCRPT is an array AMCRPT (20, 2) that transmits information concerning the debris constituent masses (kg) that are relocating from the core region to the lower plenum this timestep. The first array counter (1 to 20) indicates the material species (Table 4.3) while the second counter (1 or 2) identifies the phase (solid or liquid).
22. ATIM1 (TIME) is the MELCOR problem time (s) at the beginning of the current BH package timestep. It is used only for the printed package output.
23. DTM (DT) is the timestep (s) to be used for the BH calculation. Since the BH package is called for each MELCOR timestep, this is the same as the MELCOR timestep. It is worth noting, however, that the relatively slow progression of events within the lower plenum debris bed would justify the use of a much larger timestep.

BH Package Reference Manual

24. DTPNTB (DTPNPR) is the time interval (s) to elapse between BH package printed outputs.
25. NOUT is the output device to be used for printing the BH package output.
26. IRTYP indicates the type of reactor under consideration. Normal BH package calculations proceed for IRTYP = 0, which indicates a conventional BWR. IRTYP=1 indicates a PWR and IRTYP = 2 indicates the SBWR.
27. CRLSMS is the mass (kg) of lower plenum structural steel that has been released from the BWR lower plenum into the drywell as predicted by MELCOR at the time the BH package is initiated. It is used only in the initial setup of the debris bed control volumes. The sum CRLSMS + DELSMT(1) + DELSMT(2) is the total structural mass that ever melted before lower plenum dryout.
28. QCNWAL is the heat (J) conducted into the uppermost bottom head wall node NWALL from the overlying (cylindrical) portion of the vessel wall this timestep.
29. QRNWAL is an array containing the energies (J) radiated from the core shroud to uncovered portions (if any) of the bottom head wall this timestep. QRNWAL(1) is the radiation to node NWALL (node 18); QRNWAL(2) is the radiation to node 17; and QRNWAL(3) is the radiation to node 16.
30. NRAD is the number of radial rings representing the core plate within the COR package. These rings are recognized within the BH package as heat sinks for radiation from the debris bed surfaces.
31. NSHDLP is the number of core shroud and downcomer region baffle plate structures below the core plate. These structures are recognized as heat sinks for radiation from the surfaces of the lower plenum debris bed.
32. VIEW2 is an array VIEW2(5, 1 + NSHDLP + NRAD) that transmits the view factors between the debris bed surfaces and the exposed wall nodes, the baffle plate and lower shroud structures, and the core plate structures. Only the view factors to the exposed wall are used within the BH package. (See Section 3.3.1.)
33. QFMTOS is an array QFMTOS(5, 1 + NSHDLP + NRAD) that transmits the current heat transfer rates (W) for radiation from debris bed surfaces 1 through 5 to lower plenum structures 1 through (1 + NSHDLP + NRAD). The heat transfer rates between the bed surfaces and the exposed portions of the vessel wall are set within the BH package; all others are set within MELCOR.
34. AMASLP is the mass (kg) of water in the reactor vessel lower plenum. Calculations within subroutine BHBWET of the BH package predict the interactions of this water

with the wetted portions of the debris bed surface and any wetted reactor vessel wall nodes above the bed surface.

35. TMASLP is the temperature (K) of the lower plenum water mass AMASLP. It is calculated each timestep within MELCOR.
36. XMSHDT is the total shroud mass (kg) that has melted and been relocated into the lower plenum debris bed after the time of downcomer dryout. It is used within the BH package solely for the purpose of printed output. (The associated liquid stainless-steel components are added to the bed upper layer by means of array AMCRPT [item 21 above].)
37. CVDH is an array CVDH (3,5) that provides the decay heat (Watts) within each of the bed control volumes this timestep.
38. ABRK is the user-defined total flow area (m^2) of failed penetrations; set by evaluation of a user-prescribed control function; used to calculate gas flow into the dry debris bed (Section 5.5) or water flow into the debris bed (Section 7.6.1).
39. NMCLSX is the maximum number of fission product classes allowed by the RN package (currently equal to 20).
40. NUMCLS is the actual number of fission product classes employed by the MELCOR user.
41. NNCAV is the maximum of one and the actual number of CAV package cavities represented by the MELCOR user.
42. XFPMOV is an array XFPMOV(NUMCLS) that represents the mass (kg) of each fission product class that is added to the BH debris bed each system cycle from the core region.
43. XMBH is an array XMBH(NCRMAT) of COR package material masses (kg) that have ever been relocated into the BH debris bed from the core region.
44. FPMBH is an array FPMBH(NUMCLS) that represents the mass (kg) of each fission product class that has ever been relocated from the core region into the BH debris bed.
45. IDRYO is the beginning of cycle value of the BH package lower plenum dryout flag used to initialize BH package operation(0-water remains ==>no BH operation,1-water exhausted ==> BH may commence if sufficient solid debris exists in the lower plenum).

As explained previously, the items listed above are established within MELCOR and transmitted each timestep to the BH package. These calls to subroutine BHQSLU also

BH Package Reference Manual

return information calculated within the BH package for use within MELCOR. Before proceeding to a discussion of these items of returned information, however, it is necessary to clarify some points with respect to the calls to BHQSLU at the time of initial setup of the debris bed control volumes.

At the time that sufficient solid debris has accumulated, MELCOR calls subroutine BHQSLU twice. (This is the only time that a double call [two calls for one timestep] is made.) Most of the items in these two call argument lists are identical. The differences lie in item 21 (AMCRPT) above.

The purpose of this double call is to permit MELCOR to differentiate between the initial compositions of the debris to be included within the bottom and middle debris layers. The bottom debris layer will be comprised of the material identified by the AMCRPT array in the first call; any overflow (as determined by the H1MAX parameter [Input Record BH0500]) will be used to initiate the second layer. The remainder of the initial volume of the second layer will then be filled with the additional material relocated to the lower plenum by the AMCRPT array during the second call to subroutine BHQSLU.

Items of calculated information returned from the BH package to MELCOR via subroutine BHQSLU include the following (listed in order of appearance in the argument list):

1. QTOWA1 (QTOWAT) is the net energy (Joules) transferred to the water in the vessel downcomer region during the BH package timestep. (After downcomer dryout, QTOWA1 is merely set to zero.)
2. IFAIL is a flag indicating the status of the debris bed and bottom head wall; see item 5 below.
3. IFAIL1 is a flag reset from 0 to 1 in subroutine BHED2 to indicate that penetration failures (either weld or instrument guide tube) have occurred within the bottom debris layer.
4. QDBGA1 (QDBGAS) is the upward energy transfer (Joules) from the bed surface during the BH package timestep; see the following item.
5. QVATW1 (QVATWL) is the energy transfer (Joules) from the lower plenum atmosphere to the vessel structures. The heat transfer pathways depend upon the value of IFAIL in the following manner.
 - a. IFAIL = 0: debris bed layer three does not exist; QDBGAS represents heat transfer from the upper surfaces of the layer two control volumes to the lower plenum structures and QVATWL represents heat transfer from the lower plenum structures to the exposed portions of the vessel wall.

- b. IFAIL = 1: debris bed layer three has been established and the lower plenum structures have been subsumed within the debris. QDBGAS represents heat transfer from the bed surfaces to the lower plenum atmosphere. QVATWL represents heat transfer from the lower plenum atmosphere to the exposed regions of the bottom head wall. The net heat transfer to the lower plenum atmosphere is QDBGAS-QVATWL (Joules).
 - c. IFAIL = 2: penetration or instrument tube failures have occurred.
 - d. IFAIL = 3: bottom head creep rupture; all remaining debris transferred to drywell; BH package calculations terminated.
6. QRVDWL is an array QRVDWL (20) that returns the calculated energy transfer (Joules) from the outer surface of each reactor vessel bottom head wall node to the drywell atmosphere or water pool (for the case of drywell flooding) this timestep. The heat transfer coefficient and sink temperature used for the calculation at the external surface of each bottom head wall node are calculated within the MELCOR interface and are stored in array HTCT in Common BHCHED.
7. AMLOS is an array AMLOS (20,2) that returns information concerning the debris constituent masses (kg) that have escaped from the lower plenum and entered the pedestal region of the drywell during this timestep. The first array counter identifies the material species (Table 2.1) while the second counter (1 or 2) identifies the phase (solid or liquid).
- Liquid transfers (only) are permitted from the vessel lower plenum to the drywell pedestal region while the bottom head wall remains intact. At the time of gross bottom head failure by creep rupture or ablation, all remaining lower plenum debris (solid and liquid) is transferred to the drywell and the BH package calculations are terminated.
8. TLLOS is the mixed-mean temperature (K) of the materials escaping from the lower plenum this timestep.
9. The array TDBSUR (7) contains the current surface temperatures (K) for the surfaces considered for heat transfer with the lower plenum atmosphere (see Section 3.2.1).
10. The elements of the array IWET(7) are reset from 0 to 1 to indicate that the associated surfaces are covered by water:
- IWET(1–5) for the debris bed radial zones
 - IWET(6) for bottom head wall node 17

BH Package Reference Manual

IWET(7) for wall nodes below node 17

The bed-to-shroud radiation calculations normally carried out within the MELCOR-BH package interface are not performed for bed radial zones for which the IWET flag is set to 1.

11. QLPWAT is the total energy transfer (J) this timestep from the debris bed radial zones and the exposed vessel wall nodes to the mass AMASLP of lower plenum water. QLPWAT includes both energy transfer by internal boiling within the bed and the contribution of nucleate or film boiling at the bed or wall surface.
12. H2LPW is the hydrogen (kg) generated by water interacting with the lower plenum debris bed this timestep (see Section 7.3.1).
13. The array UTRAN (4,5,4,5) reports the movement of UO_2 (kg) into the lower plenum debris bed from the core region. These UO_2 additions are defined by elements UTRAN (ITO,JTO,4,1) where ITO and JTO identify the bed layer and radial zone indices receiving the pour. The magnitudes of the UO_2 relocations are used to define the partitioning of fission products as they accompany UO_2 relocation from the core. Elements UTRAN (ITO,JTO,IFROM,JFROM) for IFROM = 4 and JFROM = 1 are currently unused.
14. XMSBHN is an array XMSBHN(NMCLSX = 20, NUMAXL = 3, NUMRAD = 5) that identifies the fission product class inventories (kg) in each of the debris bed control volumes. Fission products are moved between control volumes in the same proportions as UO_2 inventories are relocated.
15. BMSCAV is an array BMSCAV(NUMCLS,NNCAV) that identifies the fission product class masses (kg) ejected to the drywell each system cycle subsequent to either penetration or bottom head failure.
16. XFPMXV is an array XFPMXV(NUMCLS) that represents the cumulative fission product class masses (kg) ejected to the drywell subsequent to either penetration or bottom head failure.
17. BHFBPM is an array BHFBPM(NUMCLS) that represents the current total fission product class inventories (kg) extant in the entire BH debris bed.
18. XMLY3 is the mass of UO_2 (kg) that may be temporarily withheld (due to geometric constraints) from debris bed representation until debris bed layer three is formed.
19. XFPLY3 is an array XFPLY3(NUMCLS) of fission product class masses (kg) associated with XMLY3.

BH Package Reference Manual

Several items in the BHQSLU argument list are included simply to facilitate the restart capability for the BH package. In the order of their listing, these are:

1. WHBK2 is the mass (kg) of hydrogen leaving the debris bed (via penetration failures) this timestep.
2. WHBKI is the mass (kg) of hydrogen entering the debris bed from the lower plenum atmosphere this timestep.
3. The array AOVRP (20) contains the area-to-perimeter ratios (m) of the bottom head wall nodes.
4. The array CLS (7) contains the characteristic lengths (m) for the surfaces considered for heat transfer with the lower plenum atmosphere (see Section 3.2.1).
5. The array CPDEB (3,5) contains the representative specific heats (J/(kg·K)) for the lower plenum debris nodes.
6. The array CSAWAL (3,20) contains the cross-sectional area (m²) for the bottom head wall segments.
7. The array XLWALL (3,20) contains the lengths (m) along (not across) the wall for the bottom head wall segments.
8. The array RELOCM (20,2) contains the solid (K,1) and liquid (K,2) masses (kg) for each considered material (K = 1,20) that enters the lower plenum after the initial setup of debris layer 3. After these material masses are added to the debris bed, the array elements are reset to zero.
9. RELOCP is the specific heat (J/(kg·K)) associated with material entering the lower plenum after debris bed layer 3 has been established.
10. RELOQ is the energy (J) associated with material entering the lower plenum after debris bed layer 3 has been established.
11. The array THDW (3,20) contains the current temperatures (K) for the bottom head wall segments.

In general, these eleven time-dependent quantities and arrays are initially set to zero within MELCOR and then reset as appropriate within the BH package during the period of the calculation.

8.2.2 Calls to BHPENF

The BH package subroutine BHPENF is called after bottom head penetration failure is predicted to occur (IFAIL = 2). The argument list provides the following information in this order:

1. PVSL is the reactor vessel pressure (Pa), used to determine the mixture properties of the reactor vessel atmosphere. (PVSL is also present in the subroutine BHQSLU argument list.)
2. IFAIL is a flag indicating the status of the debris bed and bottom head wall (also present in the subroutine BHQSLU argument list). It is set within the BH package during the call to subroutine BHQSLU as described in Section 8.2.1. Within subroutine BHPENF, it is used only to flag the time of bottom head creep rupture after which the calculations associated with gas flow and metal water reaction within the debris bed are bypassed.
3. IFAIL1 is a flag indicating whether or not a penetration failure has occurred within debris layer one (also present in the subroutine BHQSLU argument list).
4. DFRAG (DPART) is the representative diameter (m) for the bottom head debris bed particles (also present in the subroutine BHQSLU argument list).
5. STM is the mass (kg) of steam in the lower plenum atmosphere (also present in the subroutine BHQSLU argument list).
6. HYD is the mass (kg) of hydrogen in the lower plenum atmosphere (also present in the subroutine BHQSLU argument list).
7. CO is the mass (kg) of carbon monoxide in the lower plenum atmosphere (also present in the subroutine BHQSLU argument list).
8. CO₂ is the mass (kg) of carbon dioxide in the lower plenum atmosphere (also present in the subroutine BHQSLU argument list).
9. CH₄ is the mass (kg) of methane in the lower plenum atmosphere (also present in the subroutine BHQSLU argument list).
10. TGX is the temperature (K) of the lower plenum atmosphere and is used as the temperature of the gas flow entering the upper surface of the debris bed. (TGX is also present in the subroutine BHQSLU argument list.)
11. DP1 (DP) is the differential pressure (Pa) between the lower plenum atmosphere and the containment drywell. Within the MELCOR interface, positive values of DP are used to calculate the gas flow through the debris bed. If DP as set by MELCOR

is zero or negative, then debris bed gas flow is set to zero. (DP is also present in the subroutine BHQSLU argument list.)

12. DTM (DT) is the timestep (s) used for the BH package calculation. (DTM is also present in the subroutine BHQSLU argument list.)
13. WGBRK is the mass flow (kg/s) from the vessel atmosphere to the drywell via bottom head penetration failures. It is calculated within the MELCOR interface.

Items of calculated information returned from the BH package to MELCOR via the subroutine BHPENF argument list include the following:

1. WGII is an array WGII (5) containing the individual masses (kg) of the gases entering the upper surface of the debris bed during the BH package timestep. The five gases, in the order that they are stored within the array, are steam, hydrogen, carbon monoxide, carbon dioxide, and methane.
2. WGOO is an array WGOO (5) containing the individual masses (kg) of the gases exiting the debris bed and entering the drywell atmosphere during the BH package timestep. The five gases are stored in array WGOO (5) in the same order as they are stored in array WGII (5).
3. TGBOUT is the temperature (K) of the gas mixture exiting the debris bed and entering the drywell during the BH package timestep.
4. WATRL is the mass of water (kg) exiting the debris bed and entering the drywell during the BH package timestep.

8.2.3 Special Requirements for MELCOR Input

A few special measures are required for use of the BH package with MELCOR. Before describing these measures, however, it is important to note that all of the coding associated with the BH package and the BH package-MELCOR interface can be easily isolated. This permits code checkout by the MELCOR development staff at Sandia National Laboratories of their local code modifications without interference from coding changes associated with the BH package. It also permits users to easily obtain and compare results for cases calculated with and without use of the models of the BH package [37].

It is necessary to specify either "PWR," "BWR," or "SBWR" on Input Record COR00002 as explained in Section 2.1 of the BH Package Users' Guide. This permits access to the coding associated with the BH package and the BH package-MELCOR interface.

Another measure that must be taken when the BH package is to be used is to provide representation of the gas exchange between the reactor vessel lower plenum and the

BH Package Reference Manual

containment after gross failure of the vessel bottom head. As explained in Section 3 of the BH Package Users' Guide, this is done by means of an FL package flow path whose area fraction is specified by the BH package control function variable BH-FFLAG and which provides for continued calculation of the bottom head/containment gas flow after gross bottom head failure. (Prior to gross failure of the bottom head, gas flow through the failed penetrations is calculated within the BH/MELCOR interface routines using FL package-type models. See the discussion in Section 5.5 and the description of BH input parameter IABCFN [Input Record BH1900] in Section 2.12 of the BH Package Users' Guide.)

In addition to changes to the interface with the FL package, a modification has been made to allow the BH package to more fully interface with the HS package. This is achieved by use of a control function to represent an internal volumetric power source within an HS structure. In order to mimic conduction up the wall from BH package lower plenum wall node 18 to the lowest "active" reactor vessel wall heat structure (Figure 1.11), the user must include a control function (MELCOR Input Record HSCCCCC300) to identify an internal power source, using the BH control function variable BH-COND-POW as one of the arguments to the control function.

Finally, the user must construct the COR package input in a manner that permits reactor vessel lower plenum dryout to be predicted by the MELCOR debris quenching model. In effect, the user must override the default COR package input variables including sensitivity coefficients (SC) that affect the debris quenching calculation. These are identified in Table 8.5.

The values listed in the second column of Table 8.5 have been successfully employed at Oak Ridge to produce lower plenum dryout. Although the debris quenching models are parametric (i.e., simple and allowing the user to control the major characteristics), the suggested values in column two of Table 8.5 are considered to be realistic. Other combinations to produce a prediction of lower plenum dryout are possible. It has been found most important, however, to slow the rate of debris fall through the water-covered lower plenum structures (parameter VFALL) and to increase the penetration failure temperature TPFALL as well as to decrease the heat transfer from the debris to the wall and to the penetrations. (Otherwise, the COR package will unrealistically predict underwater failure of the penetration assemblies or bottom head prior to lower plenum dryout.) Note however, that the 1.8.5 version no longer requires lower plenum dryout for transition to BH. Therefore, it is no longer important to assure that the COR package can calculate dryout of the lower plenum control volume in order to guarantee transition to BH.

Table 8.5 The User Must Override MELCOR Default COR Package Input to Permit Lower Plenum Dryout

Variable	BH Package Calculation Example	MELCOR Default	MELCOR Input Location
VFALL (m/s)	0.1	5.0	COR00012
HDBH20 (W/m ² •K)	750.0	—	COR00012
PPFAIL (Pa)	2.2x10 ⁷	2.0x10 ⁷	COR00012
DHYDP (m)	0.01	—	CORIJJ04
TSPRS (s)	360.0	3.0	SC1020(1)
TSPRM (s)	60.0	1.0	SC1020(2)
Minimum Lipinski Porosity	0.4	0.15	SC1244(3)
HDBPN (W/m ² •K)	10.0	1000.0	COR00009
HDBLH (W/m ² •K)	10.0	1000.0	COR00009
TPFAIL (K)	1700.0	1273.15	COR00009

8.2.4 Deactivating the BH Package

Having prepared working MELGEN/MELCOR input decks and utilizing the BH package to perform debris/bottom head analyses as described in Section 8.2.3, the user can, if desired, perform subsequent MELCOR calculations without employing the BH package by making only minor modifications to the previously-prepared MELGEN/MELCOR input decks. First, the BH package will not be active within MELCOR if the BH0000 input record does not exist. BH0000 can be effectively removed by inserting a comment character '*' in front of the line. All remaining BH package input records will be ignored and will be identified as never having been read at the end of the MELGEN output listing. The BH package portion of the overall MELCOR data base will not be allocated and all calls of the BH package executive level routines will be bypassed.

A second required modification is that the flow path representing vessel failure, the FL flow path utilizing the BH package control function variable BH-FFLAG, must be either removed or modified as necessary to refer to a similar variable in the COR package.

The third required modification for deactivation of the BH package is the removal of the internal volumetric power source via the BH control function BH-COND-POW. This can be accomplished by changing the control function input from

CFAAAjj 1.0 0.0 BH-COND-POW

to

CFAAAjj 0.0 0.0 TIME * Will always produce a value of 0.0.

BH Package Reference Manual

If the user decides not to use the BH package, then the original COR package algorithms will be employed throughout the calculation. Thus, after dryout of the lower plenum water pool (as produced by the default data of Table 8.5), the debris/bottom head calculation will continue to be calculated by the COR package. Therefore, the user must ensure that all COR package input is appropriate. Examples include TPFAIL, HDBPN, and HDBLH on Input Record COR00009 and input associated with the CORLHDii and CORPENnn input records.

9. The MELCOR Interface

The MELCOR-BH package interface is comprised of special logic passing information to and from the BH package when it is active. In several instances, preexisting subroutines have been modified as appropriate for BH package requirements. In others, entirely new subroutines have been added. In all cases, logic necessary for the BH package is bypassed if the MELCOR user chooses not to execute the BH package.

The organization of the MELCOR interface is described in Section 9.1. Section 9.2 describes the interface model development required to represent the behavior of the core boundary not previously represented in MELCOR. An introduction is provided in Section 9.2.1. Section 9.2.2 describes modifications to the HS and COR packages necessary to model core boundary melting prior to downcomer dryout and core boundary failure. (Note: activation of this model is independent of the BH package.) Section 9.2.3 describes a model calculating radiative heat transfer from the surfaces of the BH lower plenum debris bed to the overlying structures of the COR and HS packages. Section 9.2.4 describes new models developed to continue the core boundary heatup, melting, and melt mass relocation after the lower plenum portion of the core boundary has failed.

Debris relocations from the BH package to the CAV package are described in Section 9.3. Section 9.4 describes fission product release calculations performed for the BH package debris bed.

Section 9.5 provides a brief discussion of modifications to the EXEC package that now support auditing of the BH package energy balance.

9.1 Interface Organization

Several of the subroutines that are employed by the MELCOR-BH package interface are listed in Table 9.1 together with a brief statement of the purpose of each. These routines have either been created anew or modified as necessary for interfacing with the other packages of MELCOR. Several standard interface routines such as HSECOM and CVHMDT, which are associated with the HS and CVH packages, respectively, are also employed.

Table 9.1 Purpose of BH Package Interface Subroutines

Subroutine	Purpose
CAVDOP	Driver routine for passing debris relocations into CAV from TP Package. For BH applications (and fuel dispersal interaction [FDI] inactive), the LIQSL2 option flag and special TSOL and TLIQ values are passed to routine CCCPEN.
CCCPEN	Calculates debris enthalpy as function of TLLOS; latent heat modification made if the argument list contains the IOPT=-1 option flag, and TSOL and TLIQ are appropriately defined.
CCCFND	Determines pure species' melting temperature and latent heat of melting; provides information necessary to determine pure species' enthalpy at TLLOS.
BHORB8	Reformats BH package debris relocations from vessel into form acceptable to the TP package; solids and liquids processed separately.
BHRUN3	Passes debris relocation information from BH to TP by calling routine TPIN separately for debris solids and liquids.
BHRAD2	Calculates debris-to-overlying surface radiation model. Called by CORRNB; calls CORRDG; accumulates QFMTOS(I,J) over the various COR package subcycles as heat loads (J); QFMTOS(I,J) converted back to Watts in BH routine BHRUN1 prior to calling BHQSLU.
BHRAD3	Calculates debris-to-core boundary radiation (QFMTOS array) after the lower portion of the core boundary has failed and the remaining structures of the core have collapsed and relocated into the lower plenum debris bed; called by BHRUN0.
BHRAD4	Calculates core boundary-to-vessel wall radiation (QRAD1 array) after the boundary has failed; called by BHRUN0.
BHRAD5	Calculates gas-to-core boundary radiation (QRGAS array) for inner and outer surfaces of the core boundary after the baffle plate has failed; called by BHRUN0.
BHRNG4	Calculates VIEW1(1,1) for the lowermost core boundary segment to the exposed vessel wall after the core boundary has failed; called by BHRUN0.
BHPAC1	Performs heatup, melting, and upper core boundary relocations as the lower core boundary melts and moves into the lower plenum debris bed after boundary failure; called by BHRUN0.
BHSHSL	Initialization routine for the failed core boundary heatup, melting, and mass relocation model; called by BHRUN0.
BHCNV	Calculates convective heat transfer (QCNV array) from the inner and outer surfaces of the failed core boundary; called by BHRUN0.

9.2 MELCOR Core Boundary Modeling Enhancements

9.2.1 Introduction

The core shroud of a large (251 in. diameter) BWR is a massive structure surrounding the core and extends from the baffle plate at the bottom of the downcomer annulus to the upper dome at the top of the upper plenum. Its mass is on the order of 60000 kg and is a significant fraction of the mass of steel associated with the core and lower plenum structures. Typically the core shroud constitutes the radial boundary structures of the

various axial segments of the COR package and the upper axial boundary structure for each COR package radial ring. In addition, the core shroud is heated directly by the core structures (including particulate debris) and fluid on its inner surface but is cooled by radiation to the vessel wall and by convection to the relatively cool fluid in the downcomer annulus. The downcomer fluid is cool for much of the period of a MELCOR calculation because of the slow boiloff of the water pool trapped in the downcomer region surrounding the jet pumps.

However, if the downcomer water inventory is completely boiled dry or the shroud experiences direct radiative heating by debris lying on the core plate above the water level in the downcomer annulus, the core shroud may become partially molten with attendant steel relocation into either the core region or into the lower plenum region. Simple extension of COR package input to include the shroud as another OS component in a separate radial ring bypass region was judged unacceptable as the COR package performs OS component convective heat transfer with a single fluid region (not with two, as would be required to model the hot core-side fluid and the cold downcomer-side fluid).

For the PWR, the core boundary typically consists of a core baffle structure separating the core and core bypass region. This structure is thin (.0254 m) with a total mass of 1900 kg and the dry portions above the adjacent liquid levels are also expected to heat rapidly during the degraded core phase of a PWR accident.

Therefore, the purpose of this section is to describe the modeling enhancements implemented to perform core boundary heatup and melt relocation during the various periods of a MELCOR calculation. In some cases, new routines have been developed and included with the BH package. In others, existing routines have been modified in the HS and COR packages.

9.2.2 Core Boundary Model Prior to Lower Plenum Dryout

The HS package degassing model has been modified to calculate BWR and PWR core boundary melting. Stainless-steel (SS) has been added as a valid degassible material and inputs to the model consist of the melting temperature range and the latent heat of melting. Because stainless-steel is not a hydrodynamic material treated in the CVH package, the normal disposition of molten steel mass degassing from a core boundary structure is directed into the degraded core mass relocation logic of the COR package where its disposition as particulate debris within the vessel is calculated. The allowance of stainless-steel as a degassible material is restricted to calculations employing the COR package, not the BH package. If COR is not employed, the stainless-steel degassing option is simply ignored.

Briefly, the modifications of the COR package accounting for molten steel addition consisted of adding an element (LVHSST) to the array VOLU to represent the volume of unmelted mass of any HS package heat structure associated with a given core cell IA, IR,

where IA is the axial segment index and IR is the radial ring index. Thus, VOLU(LVHSST, IA, IR) represents the volume of unmelted HS boundary structure material, and for the core boundary segments, only the outer radial ring (IR=NRAD) entries have non-zero values. In essence, this entry in the VOLU array serves as a pseudo-component of the COR package with the entries 1 to KCMP being the fuel, cladding, canister not by blade, canister by blade, control blade, and particulate debris. KCMP is thus 6 and, therefore, LVHSST is 7. Likewise, the COR cell total volume entry, LVTOT, of VOLU was also modified to include this HS structure volume. Because the mass relocation logic within the COR package depends on the availability of free volume into which particulate debris may relocate, the logic calculating the fluid and free volume (LVFLU and LVFRE) entries of the VOLU array has also been modified to consider the remaining material volume of this pseudo core component for each IA, IR.

The HS package calculates the mass melted for each system cycle for each core boundary segment that degasses (input records beginning with HSDG) steel. The molten mass for each structure is saved in array XMLTSS and passed to the COR package. The COR package then enters the molten masses stored in the XMLTSS array as particulate debris into the outermost ring core cell at the corresponding axial COR segment.

Because the BWR shroud extends well above the core and may also be subject to heating and melting, degassing steel structures may also lie above the core. The modified COR package logic accepts molten steel originating from these structures and identifies it as originating from the uppermost axial segment of the outermost ring of the core. These above-core structures are not represented as pseudo-components of the core and thus their volumes are not represented in the VOLU(LVHSST, NAXL, NRAD) entry. As such, molten steel is added as an external source and the associated virtual volume changes within the CVH volumes due to melting are explicitly represented.

Melting/"degassing" of the core boundary is calculated until the cumulative mass melted (XMLCSS) for each boundary segment is within a user-specified amount (C4205) from the initial mass (HTCICE). The C4205 quantity is specified as an HS package sensitivity coefficient and has a current default value of 10 kg. When the difference in cumulative molten mass and HTCICE for each segment reaches C4205, the heat structure is deactivated and all thermal interactions of the core boundary segment with the COR package are discontinued.

9.2.3 Core Boundary Model After Lower Plenum Dryout

After arrival of sufficient core debris, the BH package is functional, and the core boundary modeling (as described above) continues to be exercised for portions of the core at and above the core plate. It also operates for core boundary segments below the core plate but any molten steel produced is transferred directly into the BH package lower plenum debris bed via the AMCRPT array loaded in BH routine BHRUN1. During periods when

BH Package Reference Manual

the lower plenum is dry, the core boundary structures overlying the debris bed are exposed to intense radiative heating from the lower plenum debris bed.

A BH package model has been developed to evaluate this radiative heat transfer and the various inputs required for it are described in the BH Package Users' Manual for the BH18 series of input records. COR package routines CORDBD, CORRN1, and CORRN3 have been modified to execute this BH package model. The overlying structures are identified in user input and for the BWR consist of the baffle plate at the bottom of the downcomer, the segments of the core shroud below the core plate, and the radial segments of the core plate. For the PWR, the overlying structures are the portions of the core baffle lying below the core plate and the rings of the core plate.

The radiation model is evaluated in the COR package because the COR package is called before the BH and HS packages and because of the desire to incorporate the associated radiative heat loads within the appropriate packages all on the same system cycle. If the model were evaluated in either the BH or HS packages, then a system cycle offset would be necessary in incorporating the radiative heat loads into the energy balances performed for the affected portions of the core plate in the COR package.

The lower plenum debris-to-structure radiation model is executed with a call of routine BHRAD2 from CORRN3 on all subcycles of the COR package. The call of BHRAD2 is conditioned on MONBH = 1 and IDRY = 1. The radiative heat loads calculated by BHRAD2 are evaluated using beginning-of-cycle database information from the BH and HS packages. End-of-subcycle database information is used from the COR package.

The radiative heat loads calculated each subcycle are passed to routines CORRN1 and CORRN3, which are also called each COR subcycle. CORRN1 has been modified to update the energy balance of the core plate at axial level NTLP with the calculated radiative heat loads if the BH package is active (MONBH = 1) and if IDRY = 1. CORRN3 has been modified to call HSECOM to pass the radiative heat loads for the affected core boundary surfaces to the appropriate structures of the HS package.

The calculated radiative heat transfers (J) from the debris bed surface to the overlying structures are accumulated over the various subcycles of the system cycle and are stored in the QFMTOS(I,J) array. (Radiative heat transfer from the debris bed surface to the exposed vessel wall above the debris QFMTOS(I,1) is calculated within BHHED2 as described in Sections 3.3.1 and 3.3.2.) At the end of COR package subcycling across a system cycle, routine BHRUN1 converts the accumulated heat loads from Joules back to Watts by dividing by the system cycle length. The QFMTOS(I,J) array is then passed to the BH package routine BHQSLU where the various transfers from debris surface I are summed over surfaces J, where J is the overlying structure surface index. The net radiative debris surface heat loss is incorporated into the appropriate debris bed upper layer control volume energy balance.

9.2.4 Core Boundary Model After Lower Core Shroud Failure

As mentioned previously, the fluid in the BWR downcomer annulus is relatively cool due to steaming produced during the boiloff of the water pool trapped around the jet pumps. Thus most of the core shroud tends to remain relatively cool and intact for much of the MELCOR calculation. The boiling rate increases when the lower core shroud is subjected to the intense radiative heating from the dry lower plenum debris bed. However, once the annulus water inventory is depleted, the temperatures of the lower portions of the core shroud and the baffle plate rapidly increase.

It is expected that the baffle plate will reach a temperature where it can no longer support the weight of the core shroud and any remaining core structures supported by the intact core plate. It is postulated that the baffle plate would fail at high temperature and would result in the relocation downward of the entire length of remaining intact core shroud onto the lower plenum debris bed. Because the core plate would relocate when the baffle plate fails, it is also postulated that the remaining core structures and core debris supported by the core plate would also relocate into the lower plenum.

A new model is required to model this BWR behavior because the HS package cannot represent the gross movements of the upper shroud downward toward the debris bed after lower portions have melted.

The purpose of this section is to describe the model that has been developed for the BH package to represent the continued heating of the BWR core shroud (after downcomer dryout and failure of the baffle plate), melting of the lower core shroud, relocation of the molten steel into the debris bed, and gross movement of the upper shroud downward after lower portions have completely melted and relocated. This interface description is an extension of the discussion provided in Section 3.3 and the reader is urged to read that section prior to reading the material here.

This model is active only for BWR calculations.

9.2.4.1 Initiation Characteristics and Model Description

Logic has been developed to track the average baffle plate temperature throughout the period when the BH package is operating. (The baffle plate is shown in Figure 3.2 as Surface 2, is the upper structure closest to the debris, is subjected to the most intense radiative heating after downcomer dryout, and is the structure most likely to thermally fail.) The baffle plate temperature tracking logic exists in routine BHRUN0 and calculates the volume-averaged temperature each cycle, which is compared to the user-specified failure temperature TFALS (see BH1800 input record in the BH Package Users' Guide). Once the average temperature meets or exceeds TFALS and the downcomer annulus has boiled dry, the model flag IFLGSN is changed from 0 to 1 indicating that the shroud has failed. At this point, the model is initialized and HS package modeling of the core shroud is discontinued.

BH Package Reference Manual

Model initialization is performed in routine BSHSL where individual segments of the lower shroud are modeled separately while the entire mass of the upper shroud is represented as a single section. Arrays initialized include steel mass (XMSLHS), specific energy (XESLHS), temperature (TSLHS), volume (VLSLHS), and surface area (ARSLHS) for each shroud section modeled. Information required to initialize these arrays is taken from the HS package for those structures identified by user input as representing the entire length of the core shroud (see array IHSOF2 on Input Record BH181KK). Having initialized the model, the HS package structures representing the shroud are deactivated via calls of IHSOFF in routine BHRUN3. Because the baffle plate has failed, its mass, temperature, and melt fraction are loaded into the shroud material transfer variables XMSHD, XTSHD, and XFSHD, respectively. This mass and energy information is passed to BHRUN1 where it is reformatted and added to the debris bed through the normal COR-to-BH package material relocation array AMCRPT.

After the baffle plate has failed and relocated into the bed, no support remains for the core shroud or for the core components remaining above the core plate. Therefore, Core (COR) package routine CORSLU has been modified to collapse the remaining portions of the core into the lower plenum at baffle plate failure. Since any remaining portion of the core plate is also collapsed into the lower plenum at this time, the upper bed surface has a clear view of the entire inner surface of the core shroud. This fact permits the continued use of the debris-to-overlying structures view factors that are utilized prior to core shroud failure (see array VIEW2 on Input Record BH18JJKK).

The view factor array VIEW2 is defined with respect to the surfaces shown in Figure 3.2:

VIEW2(I,J) = view factor between the upper debris surface index I ($1 \leq I \leq 5$) and the overlying surface J [$1 \leq J \leq (1 + \text{NSHDLP} + \text{NRAD})$],

NSHDLP = number of baffle plate and lower core shroud HS package structures,

NRAD = number of core plate radial sections (COR package radial rings).

Therefore, the total number of overlying structures prior to core shroud failure is:

$$1 + \text{NSHDLP} + \text{NRAD}.$$

The number of debris bed upper control volume surfaces is 5.

After shroud failure, the view factors corresponding to the core plate radial sections for each debris surface are lumped together to form the new view factor from the surface to the entire length of the core shroud previously above the core plate. This view factor lumping is performed in BSHSL for each upper layer debris control volume I and may be represented as:

$$\text{VIEW2}(I, 1 + \text{NSHDLP} + 1) = \sum_J \text{VIEW2}(I, 1 + \text{NSHDLP} + J)$$

$1 \leq J \leq \text{NRAD}$, e.g., summed over all core plate rings

The portions of the lower shroud identified via the ISHDLP array on Input Record BH18JJ continue to provide a convenient nodalization scheme representing the lower core shroud after baffle failure. Lumping of lower segments of the shroud (as described above for the upper shroud) is not appropriate as these shroud portions are closest to the debris bed and are more apt to melt due to the intense radiative heating. Thus the VIEW2 view factor information between the debris and the lower shroud sections (shown in Figure 3.2) is retained after baffle plate failure even though the entire shroud is assumed to have moved downward and come to rest on the debris bed. This is acceptable due to the uncertainties caused by the changing debris bed configuration as the porous bed melts and collapses upon itself and the unknown extent to which the shroud would sink into the bed.

Because the core shroud has relocated downward, the view between the central bed surface and the exposed reactor vessel wall (above the debris) is blocked by the intervening shroud. Thus the elements of VIEW2 corresponding to the exposed wall are zeroed for debris surfaces I, II, and III. Likewise the view factors corresponding to the lowermost portion of the core shroud, e.g., Surface 3 in Figure 3.2, are correspondingly enhanced. That is, for debris surfaces $I = 1, 2$, and 3 :

$$\text{VIEW2}(I, 3) = \text{VIEW2}(I, 3) + \text{VIEW2}(I, 1), \text{ and}$$

$$\text{VIEW2}(I, 1) = 0.0.$$

Zeroing the view factors from the interior debris bed surfaces to the exposed vessel wall eliminates radiative heat transfer from these surfaces to the exposed vessel wall as described in Section 3.3.1. Debris surfaces IV and V continue to radiate directly to the exposed wall with the appropriate (unmodified) VIEW2 factors.

Finally, since the baffle plate has failed and relocated into the debris bed and because the entire core shroud has moved downward to rest upon the bed surface, the elements of VIEW2 corresponding to the lowermost portion of the core shroud are enhanced by the baffle view factors, which are then zeroed. Therefore, for debris surfaces $I = 1$ through 5 :

$$\text{VIEW2}(I, 3) = \text{VIEW2}(I, 3) + \text{VIEW2}(I, 2), \text{ and}$$

$$\text{VIEW2}(I, 2) = 0.0.$$

It should be clear from the preceding discussion that there are $\text{NSHDLP} + 1$ segments defined for the failed core shroud. The lower NSHDLP segments correspond to those defined prior to shroud failure, while the uppermost segment corresponds initially to a lumped representation of the intact shroud at and above the core plate. It should also be

BH Package Reference Manual

clear that the segment represented by the baffle plate is a dummy segment as the baffle plate no longer exists after shroud failure.

Radiation heat transfer from the outer surfaces of the failed core shroud segments to the reactor vessel wall is important and is calculated in routine BHRAD4. It is also important to note that these exchanges cannot be calculated by the HS package structure-to-structure radiation model as the pertinent shroud structures are deactivated at the time of shroud failure. The number of surfaces considered in BHRAD4 are $NSHDLP + 1 + NVWALL$ of which the first $NSHDLP$ are associated with the active portions of the failed shroud while the last $1 + NVWALL$ surfaces correspond to the vessel wall.

Of the wall surfaces, $NVWALL$ correspond to the HS package structures identified on Input Records BH1400 and BH142JJ with the remaining wall surface comprised of the exposed vessel wall above the debris bed as represented by the BH package wall model. The HS package wall structures are stored in array $IHSBH(K)$ where $(NSHDLP + 2) \cdot K \cdot (NSHDLP + 1 + NVWALL)$. (The first $NSHDLP + 1$ entries of $IHSBH$ are not defined via input but correspond to the $NSHDLP$ active segments of the failed shroud and the exposed wall above the BH debris bed.) The shroud and wall surfaces are stored in the order of increasing elevation from the bottom of the vessel.

View factors used in BHRAD4 are stored in array $VIEW1$ and are referenced by $VIEW1(I,J)$ where $1 \leq I \leq NSHDLP$ and $1 \leq J \leq (1 + NVWALL)$. Definitions of these view factors are as follows:

$VIEW1(1,1)$ = lowermost core shroud segment to exposed reactor vessel wall above the debris. This view factor is calculated in BHRNG4 (using formula 28 from Appendix C of Reference 38),

$VIEW1(I,1) = 0.0$ for $I > 1$,

$VIEW1(1,J) = 0.0$ for $J > 1$,

$VIEW1(I,1) = 1.0/NVWALL$ for $I > 1$ and $J > 1$.

This is in recognition that the view factor between the core shroud and the vessel wall is unity; the view factor is simply divided among the number of HS package structures the user has defined for the vessel wall above the lower head.

It should also be noted from the definitions above, that $VIEW1(1,J)=0.0$ for $J > 1$. For this to be realistic, the view factor $VIEW1(1,1)$ must be large and therefore requires that the lowermost core shroud section be sufficiently long. A warning message is printed from routine BHRUN0 whenever the calculated $VIEW1(1,1)$ from routine BHRNG4 is less than 0.5. Since the user inputs the geometry of this lowermost section in the original HS package input to MELCOR, the message suggests that the user increase the length of this

section so that the view factor is enhanced. (A length of 1.3 m should be sufficient to avoid this condition for typical 251-inch ID reactor vessel BWR geometry.)

As described above, the geometry represented in the shroud heatup, melting, and relocation model is the same as that shown in Figure 3.2 with the exceptions that the entire shroud has moved downward to rest upon the debris bed, the core region structures no longer exist, and the upper core shroud above the core plate location is represented as a single mass. Thus, five debris bed surfaces are represented as are NSHDLP + 1 core shroud surfaces (with the first being a dummy surface). A total of 1+NSHDLP+1 surfaces overlying the debris bed are represented, the first being the exposed wall above the debris followed by NSHDLP+1 core shroud surfaces.

9.2.4.2 Shroud Heat and Mass Balance

The heat and mass balances for the relocated core shroud are performed in routine BHPAC1 after the various heat loads are calculated for a given timestep and passed into BHPAC1. (The heat loads are calculated within various subroutines indicated below and the reader should directly examine the FORTRAN [and local comment statements] if more information is desired.) The net energy added for each section of the failed core shroud is as follows:

$$\text{DENET} = (\text{QFMTOS} - (\text{QCNV}(1) + \text{QCNV}(2))) \times \text{DT} + \text{QRAD1}(2) + \text{QRGAS}(1) + \text{QRGAS}(2),$$

where,

DENET = net energy (J) added to core shroud structure over the system cycle,

QFMTOS = sum of the radiative powers (W) from all debris bed surfaces to core shroud structure; QFMTOS is determined in BHRAD3,

QCNV(1) = convective power (W) from shroud inner surface; calculated in BHCNV,

QCNV(2) = convective power (W) from shroud outer surface; calculated in BHCNV,

DT = system cycle timestep (s),

QRAD1(2) = radiative heat load to the outer surface (J) due to radiative exchange with the vessel wall; calculated in BHRAD4,

QRGAS(1) = radiative heat load (J) to inner shroud surface due to gas/shroud radiation; calculated in BHRAD5, and

BH Package Reference Manual

QRGAS(2) = radiative heat load (J) to outer shroud surface due to gas/shroud radiation; calculated in BHRAD5.

The DENET variable is passed along with the shroud segment specific energy XE (J/kg) and mass XM (kg) to COR package routine CORUV1. Returned from CORUV1 are updated values of specific energy XE and the equilibrated temperature XT. The variables XE, XM, and XT are local working variables within BHPAC1 and are initialized to beginning-of-timestep values of the database variables XESLHS, XMSLHS, and TSLHS.

Melting is next considered if XE is greater than COR package variable EMLT(SS), e.g., the specific energy of solid stainless-steel at its melting temperature. If no melting has occurred, then:

$XESLHS = XE,$

$TSLHS = XT,$

XMSHD = cumulative shroud steel mass melted over the cycle(kg) from all segments of the shroud; initialized to 0.0 at beginning of cycle, and

XESHD = enthalpy associated with XMSHD above (J).

If melting is indicated, the melted fraction FRACM is determined by routine BHFMLT, which interpolates with XE between EMLT and EMLT+ELHF, where ELHF is the steel latent heat of melting. The melt mass XMLT for the shroud segment is:

$XMLT = XMSLHS \times FRACM,$

and the segment mass is decreased by this amount:

$XMSLHS = XMSLHS - XMLT.$

If the updated XMSLHS is zero, then all of the structure is melted and XESLHS, TSLHS, VLSLHS, and ARSLHS are all zeroed. (VLSLHS and ARSLHS are the volume and surface area of the structure.) If XMSLHS remains greater than zero, then the energy, temperature, and volume are set as follows:

$XESLHS = EMLT,$

$TSLHS = TMLT,$

$VLSLHS = XMSLHS / RHOM,$ and

where RHOM is the COR package steel density and TMLT is the steel melting temperature. In addition, if the shroud segment corresponds to the portion above the core plate, then the area (ARSLHS) is reduced to reflect the higher temperatures (compared to

the average) near the bottom of this long structure. This contrasts with the lower shroud structures for which no modification is made to the segment surface areas. The lower portions of the shroud are assumed to melt radially outward from the inner surface and not from the bottom upward.

If melting is indicated from the energy balance, then the accumulation variables XMSHD and XESHD are incremented for the melt mass and energy. Having looped through all of the 1 + NSHDLP shroud structures in the manner described above, the total mass and energy of molten steel from the entire shroud is stored in XMSHD and XESHD. Routine CORUV1 is called again to determine the mass-averaged temperature XTSHD of this molten steel, and the melt fraction XFSHD is determined by a call to BHFMLT. The variables XMSHD, XTSHD, and XFSHD are then passed into routine BHRUN1, which reformats them into the normal interface AMCRPT mass array and debris pour temperature TDB as described in Section 8.2. Also updated in routine BHRUN1 is the XMSHDT variable, which represents the cumulative shroud mass that has melted and relocated directly into the lower plenum debris bed after the time of downcomer and lower plenum dryout.

9.2.4.3 Gross Shroud Relocations

An outcome of the heat and mass balance procedure described in Section 9.2.2 is that the lower segments of the core shroud may become empty. Whenever this occurs, a procedure developed in the last portion of routine BHPAC1 acts to relocate shroud mass and energy from upper portions of the shroud into the (vacant) lower segment locations. This is done to represent the gross settling of the shroud as lower portions are consumed by the lower plenum debris bed.

The magnitude of gross shroud movement is such that the original mass within the empty lower shroud segment is completely restored. The algorithm searches upward from the empty segment through the remaining shroud sections until sufficient mass is identified. This searching process may extend over several segments as the upper shroud mass may have become reduced due to local melting. Since the temperature and therefore the specific energy of each of these segments may differ, the energy associated with the mass taken from each is accumulated so that a total energy associated with the required mass is identified. Likewise, the mass and energy of each of the overlying structures is reduced as they are processed in the searching procedure.

Once sufficient mass has been identified to restore the empty shroud segment, then the restored segments temperature is determined by a call of CORUV1 using the mass and the total energy from the upper segments. Having restored the empty shroud segment, the procedure proceeds to the next higher shroud segment and the process is repeated until the last segment corresponding to the shroud section above the core plate (1+NSHDLP) has been processed.

9.3 Interface Modifications for Debris Relocations from the Vessel to Containment

The capability of CAVDOP, CCCPEN, and CCCFND routines of MELCOR 1.8.4 have been extended to appropriately represent the energy state of eutectic materials entering the CAV package via the Transport Process (TP) package. The following paragraphs describe the MELCOR 1.8.4 BH-to-CAV debris transfer process.

The BH package provides the amounts of liquid and solid released from the reactor vessel to the containment each timestep for each material as elements of the AMLOS array; the associated average release temperature is TLLOS. Both pure species and eutectic mixtures are considered to exist within the lower plenum debris bed. When materials melt as constituents of eutectic mixtures, they can be released from the reactor vessel at temperatures below their pure species' melting temperatures. (The pure species considered within the BH package are listed in Table 4.3 and the formation of eutectic mixtures is described in Section 4.2). Formatting of the debris releases into a form acceptable to the TP package is performed in BHORB8 separately for the solid and liquid debris ejections. Loading of these relocations into TP is performed in BHRUN3 near the end of BH processing for a given system cycle by calling routine TPIN twice (one parcel each for the liquids and solids). The temperature associated with the parcels are loaded as TLLOS for the solids and -TLLOS for the liquids.

For the interface between the TP and CAV packages, enthalpies are determined by performing two sets of calculations corresponding directly to the solid and liquid entries of the AMLOS array for each parcel at the release temperature TLLOS.

If the debris parcel corresponds to the solid debris portion of AMLOS ($T = TLLOS$), then pure species' debris energies are evaluated initially at TLLOS in routine CCCPEN called by CAVDOP. In addition, if TLLOS is greater than the melting temperature of each species present in the solid debris pour (solids occur only during the single cycle following the gross failure of the bottom head) then the pure species' latent heat of fusion is removed so that the enthalpy returned to routine CAVDOP contains no latent heat. (That the latent heat is to be removed from the BH-originated debris is identified by special flags passed in the CCCPEN argument list.)

If the debris parcel corresponds to the liquid debris portion of AMLOS ($T = -TLLOS$), then the pure species' debris energies are evaluated initially at TLLOS again in routine CCCPEN called by CAVDOP. In addition, if TLLOS is less than the melting temperature of each species present in the liquid pour, then the pure species' latent heat of fusion is added so that the enthalpy returned to CAVDOP reflects the addition of latent heat. Again, special flags are passed to routine CCCPEN to identify that the debris is liquid and that it originates from the BH package.

The actual mapping employed by the BH-to-CAV material transfers is indicated in Table 9.2. The materials are first mapped into an intermediate material array (BMEJ) for the TP package from the BH package (via routines BHORB8, BHRUN3, and TPIN) and then into

the CAV metal and oxide mass arrays (via routine CAVDOP). The procedure followed in this mapping is analogous to that employed by the COR package. Note that materials B_4C , B_2O_3 , Ag, and InCd are not mapped into CAV and are, therefore, not represented in the CORCON calculation. This is necessary because of the lack of representation of reactor poisons in the CAV material database and, again, is analogous to the procedure adopted for material releases originating within the COR package. Finally, BH material index 14 (Fe_3O_4) is mapped into CAV material 3 (FeO) due to lack of CAV representation of Fe_3O_4 .

Table 9.2 BH to CAV Material Mapping

BH Index	—TO—	CAV Index
1 Zr		46 Zr
2 Fe		43 Fe
3 Cr		44 Cr
4 Ni		45 Ni
5 blank		--
6 Ag		--
7 CdIn		--
8 blank		--
9 blank		--
10 B_4C		--
11 ZrO_2		21 ZrO_2
12 FeO		3 FeO
13 blank		--
14 Fe_3O_4		3 FeO
15 Cr_2O_3		22 Cr_2O_3
16 NiO		23 NiO
17 B_2O_3		--
18 UO_2		20 UO_2
19 blank		--
20 blank		--

It is important to note that the procedure for treating material liquids/solids in the AMLOS array does not necessarily imply full melting/freezing of each of the species at the release temperature TLLOS as represented in the CAV package. The energy states as represented within the BH package for the liquid/solid materials leaving the reactor vessel are preserved in the CAV package. These energy states will be reflected by the CAV package (and introduced into CORCON) as partially-liquid mixtures of pure species at individual temperatures different from the single-release temperature TLLOS.

In summary, the material masses released by the BH package are loaded via two calls to the TP routine TPIN, one each for the solids and liquids. The enthalpies of the solids to be added to the CAV package debris bed are calculated as a function of temperature TLLOS and reduced by the latent heat if TLLOS is greater than the pure species' melting

temperature. The enthalpies for the liquids, however, are those for the pure species at TLLOS enhanced by the latent heat if TLLOS is less than the pure species' melting temperature.

9.4 Fission Product Release from the BH Package Debris Bed

An approach analogous to that employed for fission product release determinations within the COR package has been implemented. The initial radioactive fission product mass totals are provided (by default) by the Decay Heat (DCH) package and are grouped (typically) into 15 separate classes. (The BWR fission product inventories and the associated decay powers stored in DCH were determined by an ORIGEN calculation for a large BWR.)

The initial fission product inventories associated with the BH package debris are identified from COR package array XMSCOR for materials in COR cells below the core plate at the time of BH package initiation. These initial fission product inventories are then redistributed among the control volumes of the BH package debris bed in routine BHFPST (subject to the existence of UO_2 in the control volume). These control volume inventories are then modified each system cycle to account for

1. additions from the core,
2. releases due to volatilization,
3. gross transfers due to UO_2 relocations from control volume to control volume within the debris bed, and
4. transfers due to UO_2 relocations from the vessel to the drywell.

The new fission product release model is based on the release modeling of the COR package and includes the CORSOR and CORSOR-M models both with and without the surface area-to-volume ratio option. The primary input to the release models is the debris temperatures for each of the 13 control volumes of the BH package debris bed. Because of the uncertainty in determining the surface area-to-volume ratio for a two-phase mixture of solid/molten debris, the surface area-to-volume ratio is simply set to $6/D$ where D is the diameter of debris particles used throughout the BH package and is input via BH package Input Record BH0500. Because the surface area-to-volume ratio is important to release modeling, the user may vary the calculated release rates by modifying the surface area-to-volume ratio base defined by RN package sensitivity coefficient 7104 (default value of 422.5 m^{-1}).

The fractional release for each RN class is calculated each system cycle for each BH debris bed control volume within routine BHRLS after the major portion of the physics advancement for BH is performed for the system cycle. These fractional releases are then

multiplied by the existing class inventories to determine the released class masses. The released class mass is summed over all the control volumes of the debris bed and stored in the XMRCOR array, which is then passed into the RN package where partitioning into either aerosols or vapors is performed. Releases of both radioactive and non-radioactive materials are calculated.

The releases are directed to the atmosphere of the lower plenum CVH volume. No modification of RN package routines was necessary as the XMRCOR array already processes fission product releases from the COR package. An Input Record BHRN10K, Section 2.13 of the BH Package Users' Guide, has been developed to specify the mapping employed between the 20 pure species materials of the BH package and the various classes of the RN package. Defaults are provided based on analogy with the mapping employed by the COR package.

An important feature of the fission product release model is the ability to track fission product relocations into, within, and from the debris bed. An array UTRAN has been defined (Section 8.2.1) such that the disposition of relocating UO_2 mass (sum of solid and liquid) from the core region into the lower plenum debris control volumes is stored for each system cycle. Routine BHFPST is called by BHED2 to perform an equivalent redistribution of relocating core fission products. Fission product relocations are also represented within the debris bed as UO_2 moves between control volumes. Routines BHDBME and BHMERG have been modified to perform these intrabed relocations. Finally, routines BHDBMX and BHED2 have been modified to track UO_2 relocations from the lower plenum to the drywell after bottom head failure. Once again, fission product relocations of the same relative magnitudes as UO_2 relocations are calculated to leave the lower plenum and enter the drywell. The total fission product class inventories entering the drywell each timestep are stored in the BMSCAV array.

Routine BHRUN2 was added to update the RN package fission product inventory array XMSCOR to account for fission product relocations from the lower plenum to the drywell. Fission products extant in all COR package cells below the core plate are coalesced into the particulate debris component storage bin for the innermost radial ring in the lowermost axial segment, e.g., XMSCOR (NCMATA, IDP = 6, CELL = 1, 1...NUMCLS). The inventories in this storage location are then decreased in BHRUN2 to account for relocations to the drywell so that the RN package mass accounting logic can accurately determine the location of all fission products. BHRUN2 also performs mass checks on each fission product class to ensure that the sum of the inventories stored in the XMSBHN array for all debris bed control volumes matches the inventories stored in both the debris bed global XMSCOR and BHFP array.

The previously described updating of the fission product inventories is performed prior to the calculation of the CORSOR releases. The control volume class inventories stored in the XMSBHN array are updated based on the CORSOR releases and the resulting inventories are saved in the data base for consideration during the next timestep.

9.5 Interface Modifications for the MELCOR Energy Balances

Modifications have been made to implement auditing of the BH energy balance into the EXEC package. Routines modified include MEGDB2, MEGZGE, MEXDBM, MEXRN1, MXXDBE, MXXPBD, and MXXRIO. In addition to installing the BH package energy balance audit, changes have been made to several of the COR and HS package routines to restore the energy balance audits for those packages for MELCOR calculations employing the BH package.

For the interested reader, a detailed discussion of the energy balance modifications can be found in Section 11.4.

10. Application to the SBWR

The capabilities of the BH package include accident calculations based upon the Simplified Boiling Water Reactor (SBWR) design [39]. The basic arguments for formation of a quenched lower plenum debris bed under accident conditions are enhanced for the SBWR design. In comparison to a conventional BWR of similar reactor vessel size, the SBWR has the same mass of water in the lower plenum but a reduced core size and a reduced core power density.

Since calculations based upon the SBWR design necessarily involve the use of proprietary information, special subroutines have been prepared for use with the BH package for this purpose. The role of these five special subroutines is identified in Table 10.1.

Table 10.1 BH Package Subroutine Equivalents for Application to Conventional BWRs and to the SBWR

Conventional BWR	SBWR
BHDCHA	BHSBCI
BHHED2	BHSBDI
BHHEDN	BHSBNI
BHVLPL	BHSBVV
BHVOLL	BHSBVP

Arrangements are made within subroutines BHQSLU, BHFALS, and BHMERG to call either the conventional BWR or the SBWR subroutines listed in this table depending upon the value of user-input parameter IRTYP.

The five special subroutines listed on the right side of Table 10.1 are withheld from the general release of the BH package. In their place for the general release are dummy subroutines that simply provide a program STOP if called. Upon the application of a user that is authorized access to the SBWR proprietary information and with the approval of the

NRC sponsors of the development of these special subroutines, the proprietary versions can be provided.

In addition to acquiring the SBWR-specific routines identified in Table 10.1 above, it is necessary for the user to specify the character string "SBWR" on COR Input Record COR00002. Most remaining input required for BH application to the SBWR is described in the BH Package Users' Guide. However, users authorized to perform BH package calculations for the SBWR should consult the BH package authors for special guidance.

11. Mass and Energy Balances

This Chapter describes the automatic mass and energy balances for the BH package. Information was previously provided in the tabulated package output (described in Section 6.5) as necessary to accommodate a hand-calculated energy balance whenever desired by the code user. Items provided for this purpose (both for the current timestep and cumulative for the calculation to date) include net heat transfer to the vessel heat sinks, net heat transfer to the vessel atmosphere, the decay heat release within the debris bed, and the metal/steam reaction energy release within the bed. The current masses within each control volume and the current control volume temperatures are also provided each timestep, as is information from which the mass ablated from the vessel wall can be determined. Finally, the current timestep and cumulative values of the debris masses released ex-vessel can also be employed in an overall hand-calculated mass and energy balance.

This provision of information to support hand-calculated mass and energy balances proved adequate for use at ORNL in support of code development activities. A crude energy balance calculation could be completed with about two hours' effort, whereas a careful balance involving individual consideration of all debris constituents required about one day. Peer reviewers, however, consistently cited the need for an automatic energy balance for the benefit and convenience of the code users.

As implemented, the automatic mass and energy accounting with respect to the BH package is comprised of three parts: the debris mass balance, the bottom head wall energy balance, and the debris bed energy balance. Each of these is described in the following sections of this Chapter.

11.1 Debris Mass Balance

The lower plenum debris bed mass balance within the BH package is carried out separately for each of the elements of the material series listed in the second column of Table 2.1. The mass error is calculated for each species each timestep as:

BH Package Reference Manual

$$WDIFF(K) = WLPNOW(K) - [WLPINT(K) + WLPADD(K) - TAMLOS(K)]$$

where,

WLPNOW(K) = mass of element K currently within the lower plenum, kg

WLPINT(K) = mass of element K originally within the lower plenum, kg

WLPADD(K) = cumulative transfer of material K into the lower plenum from the core region, kg, and

TAMLOS(K) = cumulative release of material K from the lower plenum to the drywell, kg.

The array element WLPADD(2) also contains the mass of Fe (iron) added to the bed if melting of the inner surface of the carbon steel wall (treated as pure iron) occurs.

If ablation of the vessel bottom head wall is predicted to occur during the calculation (as described in Section 5.3.1), then the entry of the ablated iron into the pouring debris liquids is accounted for by the adjustment:

$$WDIFF(2) = WDIFF(2) - WABLAT$$

where WABLAT is the total ablated mass. This is necessary because the array TAMLOS contains all of the material released from the vessel into the drywell, including any contribution by wall ablation. This adjustment compensates for the presence of the mass WABLAT within the element TAMLOS(2).

To evaluate the significance of the overall mass balance error, the terms:

$$WDIFT = \sum WDIFF(K)$$

and,

$$TMASS = \sum [WLPINT(K) + WLPADD(K)]$$

are evaluated. The effect of consumption of metals and production of oxides by the metal-steam reactions upon the overall mass balance is addressed by the following logic:

$$WDIFT = WDIFT - TZRREA$$

where TZRREA is the total mass gained by the oxidation of zirconium and stainless-steel.

The percent mass error is:

$$\text{PMEER} = 100 \times \frac{\text{WDIFT}}{\text{TMASS}}.$$

The cumulative debris bed mass error WDIFT and its expression as a percentage of the total mass originally within or subsequently added to the lower plenum are then printed each timestep (after the first) for which a set of BH package output is specified (by user input). The printed message, which appears at the end of the second page of output (see Table 6.4), is

*Sum of individual mass errors = (WDIFT) kg or (PMEER) %
of total initial plus added lower plenum mass.*

The calculated difference WDIFT between the debris mass in the lower plenum at any time and the sum of the initial mass (at the beginning of the calculation) plus the added mass minus the removed mass remains less than 0.005% throughout a typical CBWR or SBWR calculation.

11.2 Wall Energy Balance

For energy balance purposes, the bottom head wall is treated as a separate entity. The terms treated in the bottom head wall energy balance are illustrated in Figure 11.1 and have the following definitions:

EHDINT = initial wall stored energy (based on the wall temperature as predicted by MELCOR at the time of BH transition), J

EWLOS = energy associated with wall mass that has melted and run into the debris bed, J

QCNWLT = energy conducted into the uppermost bottom head wall node NWALL (node 18 on Figure 1.10) from the upper vessel wall, J

QDBTW = energy conducted from the debris bed into the adjacent wall, J

QDWNT = energy radiated from the bed surface to the exposed portion of the vessel wall, J

QGWT = energy transfer from lower plenum atmosphere (or water pool) to the exposed vessel wall, J

BH Package Reference Manual

QJPWT = energy transfer from the fluid (gas or water) in the downcomer (jet pump) region to the uppermost bottom head wall node NWALL, J

QMWALT = energy transfer from the debris liquid flow through failed penetrations to the vessel wall, J

QSTWT = radiation from the shroud to the inner surface of the vessel wall (after downcomer dryout), J, and

TQRVDW = energy transfer from the outer surface of the bottom head wall to the drywell atmosphere, J.

The combination $WABLAT \times HLFE$ shown on Figure 11.1 represents the energy carried away by the ablation of wall material; HLFE is the enthalpy of liquid iron.

The current bottom head wall energy balance error is calculated as follows:

$$EWDIFF = EWNOW - EHDINT - (TENWIN - EWLOS - WABLAT \times HLFE - TQRVDW)$$

where

EWNOW = total energy (J) currently stored within the bottom head wall nodes,

TENWIN = $QCNWLT + QDBTW + QDWNT + QGWT + QJPWT + QMWALT + QSTWT$
which is the total energy (J) transferred into the bottom head wall since the beginning of the calculation.

The energy addition terms that constitute TENWIN are as defined above.

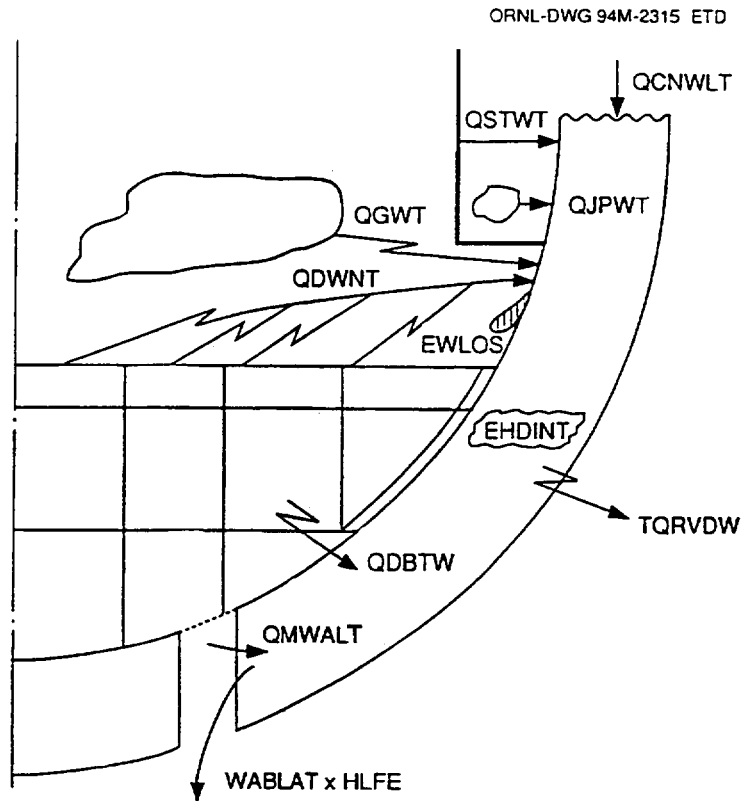


Figure 11.1 Energy Transfers Considered in the Energy Balance for the BWR Vessel Bottom Head Wall

A special feature of the bottom head wall calculation has required some special handling in the wall energy balance. As explained in Section 1.2, the portion of the bottom head wall above the debris bed surface is simply divided into three equal nodes during the period before debris bed layer three is formed. The final detailed calculation of the configuration of the upper wall is then performed just once, during the timestep in which the third debris layer is established. Accordingly, special logic has been provided to redefine the initial wall stored energy EHDINT during this single timestep as necessary to address the energy differences associated with the configuration changes.

The wall energy error is:

$$\text{PWEERR} = 100 \times \frac{\text{EWDIFF}}{\text{EHDINT} + \text{TENWIN}} \%$$

and the message:

BH Package Reference Manual

$$\text{Current bottom head energy error} = (EWDIFF) \text{ J or } (PWEERR) \% \\ \text{of total initial plus added wall energy}$$

is printed each timestep (after the first) for which a set of BH package output is specified.

The calculated energy difference (current – initial – added + removed) for the bottom head wall nodes remains less than 0.25% throughout a typical CBWR or SBWR calculation, including periods while the upper wall is melting or the lower wall is being extensively ablated.

11.3 Bed Energy Balance

By far the most difficult and demanding of the overall mass and energy balances that evaluate the internal accounting of the BH package is the debris bed energy balance. Similar to the case for the bed mass balance described in Section 11.1, the lower plenum debris bed energy balance within the BH package is carried out separately for each of the elements of the material series listed in the second column of Table 2.1. The energy error is calculated within subroutine BHED2 for each species each timestep as:

$$EDIFF(K) = ELPNOW(K) - [ELPINT(K) + ELPADD(K) - EAMLOS(K)]$$

where,

ELPNOW(K) = Energy associated with mass of material K currently within the lower plenum, J

ELPINT(K) = Energy associated with mass of material K originally within the lower plenum, J

ELPADD(K) = Cumulative addition of energy associated with material K into the lower plenum from the core region, J, and

EAMLOS(K) = Integrated energy removal associated with the release of material K from the lower plenum debris bed via penetration failure pathways, J.

The array element ELPADD(2) also includes the energy associated with any Fe (iron) added to the bed if melting of the inner surface of the carbon steel wall (treated as pure iron) is predicted to occur.

The elements of the EAMLOS array, which are loaded in subroutine BHDBMX, primarily represent the energies associated with the debris liquids that enter the penetration failure pathways from the control volumes located within bed layers one or two. Here the released energy added to the EAMLOS (K) element is the released mass of material K

times the enthalpy of the liquid at the control volume temperature. However, the EAMLOS array elements are also used to represent the energies associated with debris ablation within the layer one control volumes.

As explained in Section 5.3.2, liquids generated within layer two and flowing through layer one on their way out of the vessel can ablate the surrounding layer one debris. When this occurs, the energies of the ablated materials are added to the corresponding elements of the EAMLOS array as the energies of the respective liquids at the user-input debris ablation temperature TABLAT. The energy QLDTOT that is transferred from the flowing liquid into the surrounding layer one debris is considered in the energy balance as explained in the next paragraph. A portion of this energy causes the material ablation; the remainder simply serves to increase the layer one temperature (see Section 5.3.2).

To evaluate the significance of the overall energy balance error, the terms:

$$\begin{aligned} \text{EDIFT} = & \sum \text{EDIFF}(K) - \text{TDHDB} - \text{TMWDB} - \text{QLDTOT} - \text{TZRCE} \\ & + \text{QDBTW} + \text{QDWNT} + \text{TQDBGS} + \text{QGWT} \\ & + \text{TQUP} + \text{QPFGST} + \text{TQGRID} + \text{TQWET} \\ & + \text{TQTLPW} \end{aligned}$$

and

$$\text{TENRG} \sum [\text{ELPINT}(K) + \text{ELPADD}(K)]$$

are evaluated. The terms used in the calculation of EDIFT that have not been defined in Section 11.2 are:

QLDTOT = integrated energy transfer to layer one debris from liquids originating in layer two and passing through layer one via penetration failure pathways, J

QPFGST = integrated energy transfer from debris to gases traversing the bed after penetration failures, J

TDHDB = integrated decay heat release within the bed, J

TMWDB = integrated energy release by metal-steam reaction, J

TQDBGS = portion of the energy transfer from the bed surfaces to the vessel atmosphere that is retained by the atmosphere (not transferred from the atmosphere to the wall), J

BH Package Reference Manual

TQGRID = integrated energy transfer from control rod guide tubes to vessel atmosphere and exposed wall surfaces before layer three is formed, J

TQUP = integrated energy transfer from bed surfaces upward to the lower shroud and to the core plate, J

TQWET = energy transfer from debris to water within the bed control volumes, J

TQTLPW = energy transfer from bed surfaces to water overlying the bed, J, and

TZRCE = integrated internal energy addition by conversion of metals to oxides.

The sum of the terms TQDBGS + QGWT is the total energy transfer from the debris bed surfaces to the vessel atmosphere.

The error associated with the current debris bed energy imbalance is:

$$PEERR = 100 \times \frac{EDIFT}{TENRG + TDHDB + TMWDB} \%.$$

The cumulative debris bed energy error EDIFT and its expression as a percentage of the total energy originally within or subsequently added to the lower plenum are then printed each timestep (after the first) for which a set of BH package output is specified (by user input). The printed message appears immediately following the end of the second page of output, an example of which is shown as Table 6.4. The message is:

*Sum of energy error values = (EDIFT) J or (PEERR) %
of total initial plus added bed energies.*

The calculated difference EDIFT between the total debris energy in the lower plenum at any time and the sum of the initial total energy (at the beginning of the calculation) plus the added energy minus the removed energy does not exceed about one-fifth of one percent during a typical CBWR or SBWR calculation employing five-second timesteps.

This bed energy error, which is very small at the beginning of a calculation but increases steadily as the calculation proceeds is typical of explicit solution schemes, when applied to cases characterized by increasing control volume temperature for which temperature-dependent specific heats are employed. Briefly, the control volume temperature increases during each timestep so that the representative specific heat at the end of the timestep is slightly higher than that at the beginning of the timestep. However, the begin-timestep specific heat is used throughout the timestep. The consequence is very small for any single timestep, but over hundreds of timesteps the effect becomes noticeable in the form

of a non-physical apparent creation of energy. Use of smaller timesteps will alleviate the effect.*

There are many other consequences of the use of timestep-constant specific heats than illustrated by this simple example. In the lower plenum debris bed calculation we have solids melting, liquids freezing, interchange of liquids among bed control volumes, and control volume merging as significant energy exchange events. For each of these, use of the begin-timestep specific heat instead of a timestep-average value plays a role in establishing the current magnitude of the overall energy balance error. Whenever one of these events causes a control volume temperature to decrease during a timestep, the cumulative error is reduced. (For a calculation in which the control volume temperature increases were exactly offset by subsequent temperature decreases, the timestep-constant specific heat error would be eliminated; however, BWR lower plenum debris bed calculations generally involve steadily increasing control volume temperatures.)

The current end-of-calculation overall bed energy excess of no more than one-fifth of one percent is considered acceptable and practical. Stated another way, the effort that would be required for implementation of an implicit solution scheme or a predictor-corrector process and the additional CPU time that would be required for each calculation are considered to be neither justified nor practical in view of the numerous uncertainties involved in these accident calculations.

11.4 Energy Balances External to the BH Package

11.4.1 Purpose

The discussions provided in Sections 11.2 and 11.3 describe the auditing algorithms developed to monitor the energy balances performed for the BH package debris bed and the BH package bottom head wall. These internal BH package audits are printed with the BH package output; they are not included for printing at the beginning of each MELCOR edit. This section discusses the provisions for external MELCOR audits of the BH package energy balance and for audits of other packages when the BH package is operational. Previously, the necessary information required to automate and print out the BH package energy balance was not available. In addition, the audits performed for the COR, HS, and RN1 packages indicated apparent serious imbalances in the energy tracking algorithm.

The inaccuracies in the energy audits arose due to several causes and include: no recognition of debris mass and energy relocation from the COR package to the BH

* On the other hand, use of smaller timesteps will increase the total number of calculations and hence will increase the roundoff error. The net effect upon the overall energy balance error must be determined by trial.

BH Package Reference Manual

package, no representation of radiative exchanges between the BH debris bed surface and the COR package core plate structures (Section 9.2.3), no representation of the mass and energy moving from the HS package into the COR package due to shroud melting (Section 3.3.1 of the Core (COR) Package Reference Manual); inaccurate accounting of deactivated HS energy; and no relocation of the RN1 package inventories deposited on the surfaces of deactivated heat structures.

The purpose of this section is to describe the modifications made to restore the energy audits of the affected packages and to install the global auditing procedure for the BH package. The following sections describe in order the modifications made to the COR, HS, BH, and EXEC packages to incorporate and restore the global energy balance auditing.

11.4.2 COR Package

The COR package has been modified so that accurate tracking of mass, energy, and volume are performed internally to COR during all periods of a MELCOR calculation when the BH package is to be used. The internal auditing of these quantities is performed in subroutine CORBAL and warning messages are printed if the calculated relative errors in tracking these quantities are greater than 0.00005 (= 0.005%). The following sections describe the volume balance modifications and the mass and energy balance modifications.

11.4.2.1 COR Volume Balance Modifications

To restore the volume balance, a new variable VLTBHI added to Common CORINI now represents the total volume modeled by the COR package below the core plate (i.e., axial segment NTLP). VLTBHI includes the initial fluid volume, the initial material volume occupied by COR components, and the initial volume occupied by the core shroud. This variable is defined via MELGEN processing initially in routine CORPS2 and is updated in CORPS3 to include the shroud volume. In equation form, VLTBHI is defined by summing the following terms over all lower plenum axial segments IA (<NTLP) and all radial rings IR:

$$\begin{aligned} \text{VLTBHI} = & [\text{XMFU}(1, \text{IA}, \text{IR}) + \text{XMDP}(\text{LUO2}, \text{IA}, \text{IR})] / \text{RHOM}(\text{LUO2}) \\ & + \text{XMFU}(2, \text{IA}, \text{IR}) / \text{RHOM}(\text{LHT}) \\ & + [\text{XMCL}(1, \text{IA}, \text{IR}) + \text{XMCN}(1, \text{IA}, \text{IR}) + \text{XMCB}(1, \text{IA}, \text{IR}) \\ & + \text{XMSS}(4, \text{IA}, \text{IR}) + \text{XMDP}(\text{LZR}, \text{IA}, \text{IR})] / \text{RHOM}(\text{LZR}) \\ & + [\text{XMCL}(2, \text{IA}, \text{IR}) + \text{XMCN}(2, \text{IA}, \text{IR}) + \text{XMCN}(3, \text{IA}, \text{IR}) \\ & + \text{XMCB}(2, \text{IA}, \text{IR}) + \text{XMCB}(3, \text{IA}, \text{IR}) + \text{XMSS}(5, \text{IA}, \text{IR}) \end{aligned}$$

$$\begin{aligned}
& + \text{XMDP}(\text{LZRO2}, \text{IA}, \text{IR}) / \text{RHOM}(\text{LZRO2}) \\
& + [\text{XMSS}(1, \text{IA}, \text{IR}) + \text{XMDP}(\text{LSS}, \text{IA}, \text{IR})] / \text{RHOM}(\text{LSS}) \\
& + [\text{XMSS}(2, \text{IA}, \text{IR}) + \text{XMDP}(\text{LSSOX}, \text{IA}, \text{IR})] / \text{RHOM}(\text{LSSOX}) \\
& + [\text{XMSS}(3, \text{IA}, \text{IR}) + \text{XMDP}(\text{LCRP}, \text{IA}, \text{IR})] / \text{RHOM}(\text{LCRP}) \\
& + [\text{XMCL}(3, \text{IA}, \text{IR}) + \text{XMDP}(\text{LINC}, \text{IA}, \text{IR})] / \text{RHOM}(\text{LINC}) \\
& + \text{sum over materials IM and components IC of} \\
& \quad \text{XMDC}(\text{IM}, \text{IC}, \text{IA}, \text{IR}) / \text{RHOM}(\text{IM}) \\
& + \text{VOLU}(\text{LVFLU}, \text{IA}, \text{IR}) \\
& + \text{VOLU}(\text{LVHSST}, \text{IA}, \text{IR}).
\end{aligned}$$

The first eight line groupings represent the initial material volumes of the intact and particulate debris components, the ninth line is the initial material volume of any conglomerate debris on the COR components in the lower plenum, the 10th line is the initial fluid volume associated with all lower plenum COR cells, and the 11th line is the material volume of the core shroud structure. (The reader should note that the total number of axial segments in the reactor vessel modeled by COR is NAXL while the total number of radial rings modeled is NRAD.)

Most entries in this equation over the given range ($\text{IA} < \text{NTLP}$ and $\text{IR} \cdot \text{NRAD}$) are zero initially except line groupings 5, 10, and the $\text{IR} \cdot \text{NRAD}$ entries of line 11. Variable VOLTOI has the identical definition as VLTBHI above but is summed over all axial segments ($\text{IA} \cdot \text{NAXL}$) and radial rings ($\text{IR} \cdot \text{NRAD}$) represented by the user. Thus VLTBHI represents the part of the total vessel volume VOLTOI that is modeled by the COR package below the core plate (NTLP) prior to BH initiation, but that is no longer modeled by the COR Package after BH initiation.

Two volume discrepancy checks are performed in routine CORBAL, which is called by routine CORRN4 at the end of each COR timestep. The first volume discrepancy variable VOLERR is defined during the period of BH operation as:

$$\text{VOLERR} = \text{VOLTO} - (\text{VOLTOI} - \text{VLTBHI})$$

where VOLTO is defined in the same manner as VLTBHI above but differs in the range of IA for which the summation is performed; i.e., all axial segments IA at and above the core plate (NTLP). Thus VOLTO is the dynamic value of the active core volume. The difference VOLTOI- VLTBHI represents the precise core volume that should be modeled by COR during BH operation.

BH Package Reference Manual

The second volume discrepancy is stored in variable VOLER2 and during the period of BH operation is defined as:

$$\text{VOLER2} = \text{VOLTO} - \text{VOLCOR} - \text{VOLFL}$$

Where,

VOLCOR	= sum over all components IC, all axial segments IA at and above the core plate (NTLP), and all radial rings IR of VOLU (IC,IA,IR)+VOLY (IC,IA,IR)+VOLU (LVHSST,IA,IR),
VOLU(IC,IA,IR)	= material volume of component IC in cell IA,IR,
VOLY(IC,IA,IR)	= conglomerate debris volume on component IC in cell IA,IR,
VOLU(LVHSST,IA,IR)	= core shroud structure volume in cell IA,IR, and
VOLFL	= sum of the core cell fluid volume VOLU (LVFLU,IA,IR) over all segments IA at and above the core plate NTLP and over all rings IR.

It should be clear that each of these checks is dynamic and independent, and provides a measure of COR volume tracking performance when recast into relative terms. The relative volume error is defined in CORBAL as:

$$\text{VERREL} = \text{MAX} (\text{ABS} (\text{VOLERR}/\text{VOLINI}), \text{ABS} (\text{VOLER2}/\text{VOLINI}))$$

where VOLINI is the active core volume modeled by COR and is either VOLTOI when BH is not operating or VOLTOI-VLTBHI when BH is operating.

It is VERREL that is compared to 0.00005 in order to determine whether to print the warning message associated with volume checking. In all testing performed with these modifications, the condition is not violated and no messages are produced.

11.4.2.2 COR Mass and Energy Balance Modifications

To accurately track the mass and energy transfers involved with the exchanges between the HS and COR packages and between the COR and BH packages, the number of entries in the mass and energy balance arrays of the COR package have been increased. The dimension of the DXMTOT mass balance array was increased from NMMAT + 2 to NMMAT + 4 in order to store the cumulative mass of molten steel (element NMMAT + 3) added to the COR package by the degassing model of the HS package and to store the cumulative mass of all COR materials transferred from the COR package to the BH

package (element NMMAT + 4). The variable NMMAT is the total number of materials tracked by the CVH package.

Likewise, terms have been added to the COR energy balance EBAL array to track energy transfers between HS and COR and between COR and BH. The added EBAL terms are:

EBAL(13) = ETOHST: cumulative energy (J) of molten steel added to HS from COR; negative since steel is actually passed to COR from the HS shroud melting model

EBAL(14) = ETOBHT: cumulative energy (J) of debris transferred from COR to BH; always positive

EBAL(15) = ERBHT: cumulative energy (J) radiated to the BH debris bed surface from the core plate component summed across all rings; normally negative since energy is radiated from the debris surface to the core plate

EBAL(16) = EIGNOR: cumulative energy (J) of non-core structures previously considered by the COR package but not passed to any other package; this energy is no longer considered by COR except through the EIGNOR term used in the global energy balance. The energy composing this term is the penetration and bottom head wall energy at the time the BH package is initiated.

With the above additions, the energy and mass errors of the COR package are defined in routine CORBAL as:

$$\begin{aligned} \text{EERROR} = & \text{ECORT} - \text{ECORTI} \\ & - (\text{EFPDT} + \text{EMWRT} + \text{ECHST} - \text{ECNVT} - \text{EBNDT} - \text{ECAVT} \\ & - \text{ETOHST} - \text{ETOBHT} - \text{ERBHT} - \text{EIGNOR}) \end{aligned}$$

$$\begin{aligned} \text{XMERRR} = & \text{XMTOT}(\text{LUO2}) + \text{XMTOT}(\text{LZR}) + \text{XMTOT}(\text{LZRO2}) + \text{XMTOT}(\text{LSS}) \\ & + \text{XMTOT}(\text{LSSOX}) + \text{XMTOT}(\text{LCRP}) + \text{XMTOT}(\text{LHT}) \\ & + \text{XMTOT}(\text{LINC}) + \text{DXMTOT}(\text{KH2}) + \text{DXMTOT}(\text{KH2OVA}) \\ & + \text{DXMTOT}(\text{KCO}) + \text{DXMTOT}(\text{NMMAT} + 1) + \text{DXMTOT}(\text{NMMAT} + 2) \\ & + \text{DXMTOT}(\text{NMMAT} + 3) + \text{DXMTOT}(\text{NMMAT} + 4) - \text{XMTOTI} \end{aligned}$$

The ECORT and XMTOT terms are the total energy and species masses of the active portion of the core modeled by the COR package at the time CORBAL is called. As with the volume balances described in Section 11.4.2.1, the axial and radial extent over which the summations are performed depends on whether the BH package is operating. The remaining terms in the mass and energy error equations denote cumulative transfers (i.e., DXMTOT or EBAL) to or from the COR package. ECORTI and XMTOTI are the total

BH Package Reference Manual

energy and mass of materials modeled by the COR package at the beginning of the MELCOR calculation.

The magnitudes of the relative errors are used to decide when the energy or mass error is large enough to force a warning message to be printed by CORBAL. The relative errors are defined as:

$$EERREL = EERROR / (ECORT + ETOBHT - ECORTI), \text{ and}$$

$$XMEREL = ABS (XMERRR/XMTOTI).$$

As mentioned previously, if either of these relative errors exceeds 0.00005 (= 0.005%), then the applicable warning message is printed from CORBAL. In all testing performed using these modifications, the limits are not exceeded.

To provide the user a means of assessing the magnitudes of the new DXMTOT and EBAL terms, additional printouts have been added to the COR package edits and additional plot variables have been added to the plot file. The added printed information is self-explanatory and the new plot variables are as follows:

COR-MCTOHS-TOT	:	total mass of steel (kg) added to HS by COR; negative
COR-ECTOHS-TOT	:	total enthalpy (J) added to HS by COR; negative
COR-MCTOBH-TOT	:	total mass (kg) added to BH by COR
COR-ECTOBH-TOT	:	total debris enthalpy (J) added to BH by COR
COR-RCTOBH-TOT	:	total energy (J) radiated to BH by the COR core plate; normally negative

Two plot variables have been added to plot the COR package relative energy error defined in different ways. These are:

COR-REL-ENGY-ERR:	EERROR/EXXX, energy error versus current energy
COR-REL-ENGY-ERM:	EERROR/ (EXXX + ETOBH + ETOCAV), energy error versus the sum of the current COR energy plus energy added to BH and CAV packages

where $EXXX = ECORT - [EBAL(7) + EBAL(8)]$ and $EBAL(7)$ and $EBAL(8)$ are cumulative energy balance terms involving changes in composition due to the effects of oxidation. The term EXXX in the COR package output represents the current energy extant in the COR package even though the $EBAL(7)$ and $EBAL(8)$ terms are energy exchanges that accumulate over time.

11.4.2.3 Coupling of COR Energy Balance Modifications to the Executive Level (EXEC) Energy Balance Audit

Coupling of the new energy balance terms to the COR energy balance reported at the beginning of the MELCOR edit is performed in routine CORR6. CORR6 is executed only after all subcycling is completed for a given system cycle. The terms EPCOR, ETCOR, and ECCOR are defined in CORR6 and are stored in common block CORGEB for subsequent communication to the executive level routines performing the global energy balance audit for all of the packages of MELCOR. The EPCOR, ETCOR, and ECCOR variables are defined as follows:

EPCOR = current energy in the COR package (J); EXXX from Section 11.4.2.2

ETCOR = net energy transferred to the COR package over the given cycle (J); i.e., the energy transferred to the COR package minus the energy transferred from the COR package

ECCOR = energy created within the COR package over the given cycle (J)

Of these, only the ETCOR variable has been modified. It is now defined as

ETCOR = EBALN(2)-EBALO(2)

– (EBALN(4) – EBALO(4)) – (EBALN(5) – EBALO(5))

– (EBALN(13) – EBALO(13)) – (EBALN(14) – EBALO(14))

– (EBALN(15) – EBALO(15)) – (EBALN(16) – EBALO(16))

– (EBALN(6) – EBALO(6)) – (EBALN(7) – EBALO(7))

where EBALO and EBALN are the beginning and end of system cycle values of the EBAL array.

The executive level routine MEXRN1 defines ENOW, SETRN, and SECRN for the COR package as:

ENOW = EPCOR

SETRN = SETRN + ETCOR

SECRT = SECRT + ECCOR

so that SETRN and SECRT are time integrations of the transfer and creation energy terms. ENOW, SETRN, and SECRT are actually executive level arrays stored in common MXXGEB and are dimensioned such that one non-zero entry exists for each active package.

BH Package Reference Manual

No modifications were made to the logic of the EXEC routines processing the COR energy balance. However, it should be noted that the EXEC package routine MXXDBE defines the relative error for each package in the following manner:

$$\text{EERR} = \text{ENOW} - \text{ESTART} - \text{SETRN} - \text{SECR}$$

$$\text{EREL} = \text{EERR} / \text{ENOW} \text{ (for ENOW not equal zero)}$$

For the COR package, ENOW is EPCOR and similar terms are used for other packages. The ESTART term is the value of ENOW at the beginning of a MELCOR calculation.

If a package such as COR, HS, or BH loses energy, its relative error will increase assuming no corresponding reductions in the absolute error. This increase arises because the absolute energy error term is calculated from the current energy and the summations of energy transfers over time. As a result, the absolute energy error depends on the state of the package calculation throughout all previous periods and represents cumulative error. To define the relative energy error using only the current energy in the denominator is overly stringent and is misleading. It has been recommended (through a DIR) that the relative energy error be defined such that the denominator consists not only of the current energy of the package but also all energy that has ever left the package. In this way, the denominator would represent all of the energy that has passed into or through the package and both the numerator and the denominator would reflect the cumulative effects of the entire calculation.

11.4.3 HS Package

Two modifications have been performed for the HS package routines to restore the energy balances for both the HS package and the RN Package. The first modification simply corrects an error in the formulation of one of the terms used in the energy balance audit for the HS package. In this effort, several of the EXEC Package routines were altered as discussed in Section 11.4.5.

The second modification addresses correction of the RN Package energy balance by relocating deposited RN1 class inventories at the time of heat structure deactivation. Previously, these RN inventories were no longer tracked by the RN Package auditing process once a heat structure became deactivated. This resulted in both a deterioration in the RN Package relative energy error printed at the beginning of a MELCOR edit and an internal RN Package warning message printed from routine RN1RN6.

Section 11.4.3.1 discusses the correction to the HS energy audit while Section 11.4.3.2 discusses the relocation and disposition of the deposited radionuclide inventories on deactivated heat structures.

11.4.3.1 Correction of the HS Energy Balance Audit

HS Package routine HSRUN3 defines the terms EPHS, ETHS, and ECHS, which are stored in common block HSGEB similar to the CORGEB common discussed in Section 11.4.3.2. These terms are processed in MEXRN1 for the HS package in exactly the same fashion as the analogous terms for the COR package and are therefore used in the energy balance audit performed in MXXDBE for the HS package.

An error in the updating of the ETHS term associated with deactivation of heat structures was discovered and corrected in conjunction with this effort. At the position within routine HSRUN3 where this term is updated, the HSDGAS routine has been called and all deactivations of heat structures over the timestep due to the complete melting of a structure (as modeled by the HS degassing model) have been completed. In addition, since the HS package is called subsequent to the BH package, any deactivations of heat structures over the cycle due to initiation of the BH package (or the failed shroud model) have also been completed. Therefore, all possible occurrences of heat structure deactivation over a given cycle have been identified at the point within HSRUN3 that the ETHS variable is updated.

ETHS is defined such that it represents the net energy addition to the active heat structures of the HS package. The error occurred when the energy of the deactivated structure was erroneously added to the ETHS term. Since the absolute energy error is defined via subtracting the cumulative energy transfer (SETRN) term from the current energy (ENOW) term (see definition of the EERR variable in Section 11.4.3.2), the effect of adding the deactivated structure energy to the transfer term resulted in a strong negative biasing in the absolute energy error. Two simple fixes might have been to either add the deactivated structure energy to the EPHS term or to subtract the structure energy from the ETHS term. Either of these would have algebraically corrected the error.

These simple solutions were not pursued because the deactivated structure energy is not modeled by HS and does not fit either the definition of energy present as implied in the EPHS term or the definition of the energy transferred to or from active structures. Once a structure is deactivated, its energy is no longer part of the active HS package processing.

To remedy the difficulty, a new HS database variable EFFHS was defined to represent the cumulative energy of all structures that are deactivated. This variable is time dependent and is allocated in both the old and the new portions of the HS database. EFFHS is updated in HSRUN3 and includes the energies of structures deactivated via

1. initiation of BH,
2. complete melting of structures (such as the core shroud), or
3. initiation of the BH package model of the failed core shroud.

EFFHS is used to define another new variable EFHS stored in common block HSGB which is communicated to the EXEC package to perform the global energy balance for the HS package and is described in Section 11.4.5.

11.4.3.2 Relocations of RN Package Class Inventories Deposited on Deactivated Heat Structures

Modifications have been made to identify and relocate deposited radionuclide class inventories from the surfaces of heat structures that are deactivated during the course of a MELCOR calculation. Previously, these deposited RN inventories were unaccounted for in the RN1 energy balance audit and led to imbalances. Their presence on deactivated structure surfaces also led to the following message produced from routine RN1RN6: "PROBLEM WITH DECAY HEAT SPLIT AT TIME =". The difficulty was most noticeable for MELCOR calculations employing the BH Package, wherein core shroud melting led to deactivation of heat structures on which non-negligible inventories of RN class masses had been deposited. The modifications discussed in this Section eliminate the occurrence of this message and restore the RN1 energy edit.

The transfer of fission products from deactivated heat structures is facilitated by a call to HS Package routine HSOFF, which is responsible for deactivating a single heat structure. (The working level routine performing the actual calculations is HSOFFC while two executive level routines (HSOFFB and HSOFF) exist in the call chain ahead of HSOFFC.) A new array XFP has been added to the argument list of HSOFFC along with previously existing arrays ADEPN, VDEPN, RADEPN, RVDEPN, all of which are defined below:

XFP(ISIDE,ITYPE,ICLS) class masses (kg) deposited on the deactivated structure where:

ICLS - class index of RN classes

ISIDE - index which indicates the side of the heat structure bearing the RN inventories (1 = left, 2 = right)

ITYPE - index which indicates both type and form of the deposited RN inventories; (1 = radioactive elemental mass in the deposited aerosol, 2 = radioactive elemental mass in the deposited vapor, 3 = total compound form of radioactive and non-radioactive class masses in the deposited aerosol, 4 = total compound form of radioactive and non-radioactive class masses in the deposited vapor)

XFP(ISIDE,ITYPE,ICLS) class masses (kg) deposited on the deactivated structure where:

ADEPN(ICLS,ISUR)	total (radioactive plus non-radioactive) compound form of RN class masses (kg) in the aerosols deposited on heat structure surface ISUR
VDEPN(ICLS,ISUR)	total (radioactive plus non-radioactive) compound form of RN class masses (kg) in the vapors deposited on heat structure surface ISUR
RADEPN(ICLS,ISUR)	radioactive elemental form of RN class masses (kg) in the aerosols deposited on heat structure surface ISUR
RVDEPN (ICLS,ISUR)	radioactive elemental form of RN class masses (kg) in the vapors deposited on heat structure surface ISUR

Once the XFP array has been set within HSOFFC, the appropriate entries of ADEPN, VDEPN, RADEPN, and RVDEPN arrays are zeroed. The XFP array is then transmitted back to the package that requests the deactivation of the heat structure and the radioactive and non-radioactive RN inventories are reallocated to new hosts. It is the zeroing of the deposited aerosol and vapor arrays and the subsequent reassigning of the RN inventories that restores the RN energy balance and eliminates the warning message.

In addition to identifying and zeroing the RN deposition arrays for deactivated heat structures, additional special processing has been added for RN class masses defined by the user beyond the default classes. As an example, users often define the Csl class as class 16 and define the formation of Csl via RN input from releases of the default classes of Cs (class 2) and I_2 (class 4) from fuel. The RN Package then transports the constructed Csl and deposits some of the Csl onto heat structures as class 16 inventory. When these heat structures deactivate, there is some small (usually less than 1 kg) inventory of this class on the structure that must be reallocated.

A simple solution is to add the class 16 masses back to the identified hosts (see below) as class 16 materials. However, because the fission product release models (CORSOR and CORSOR-M) of the COR and BH packages are based on the default (1 through 15) class definitions, once the Csl is returned to a host, it may not be revolatilized regardless of the thermal conditions of the host.

Rather than returning the Csl to the host as Csl, an alternative has been developed such that the associated class 16 masses may be re-released from the hosts for subsequent transport through the reactor system. This is done by de-constructing the deposited Csl into the donor default classes (Cs class 2, and I_2 class 4) and incrementing the class 2 and 4 deposited inventories so that mass conservation is maintained while zeroing the class 16 deposited inventory. In this way, the deposited Csl radioactive elemental mass is

BH Package Reference Manual

added to the hosts as materials in the default classes. Because the hosts are usually hot, the returned Cs and I₂ can be re-released to form Csl, which the RN package can then transport throughout the reactor system as Csl.

The deconstruction of deposited user-defined class inventories (such as Csl) and the incrementing of the donor class inventories (such as Cs and I₂) deposited on a structure is performed in a new routine RN1CLS. RN1CLS is called by HSOFFC immediately prior to the determination of the XFP array.

11.4.3.2.1 Deactivation of Heat Structures by the BH Package

For the BH Package, there are two instances when heat structures must be deactivated. The first occurs at the beginning of the BH calculation when HS modeling of portions of the bottom head structure is no longer required. The radioactive elemental inventories of each class (aerosol and vapor) deposited on the left hand (inner) side of the deactivated heat structure are added to the XMSCOR array prior to setting up the BH debris bed inventories for each bed control volume. The non-radioactive compound form of the deposited aerosol and vapor for each class is added to the AER1GN array for the lower plenum control volume atmosphere. The inventories (radioactive and non-radioactive, compound and elemental) on the right hand (outer) side of these structures are added either to the CVH pool (arrays AER1LN, RDA1LN, VAP1LN, RDV1LN) or atmosphere (AER1GN, RDA1GN) depending on the wetted fraction of the outer surface. For wetted fractions meeting or exceeding 0.5, the pool inventories are updated while for fractions less than 0.5, the atmosphere inventories are updated. For all CVH atmosphere relocations, the inventories are loaded into the largest bin (NUMSEC) for each class.

The second instance within BH requiring the deactivation of heat structures arises when the BH package failed shroud model is activated. This reallocation is performed in BHRUN3 immediately upon core shroud failure. In this reallocation of the deposited radioactive elemental RN inventories, both the inner and outer surface class masses associated with the structures identified by the IHSOF2 array are added directly to the BH debris bed inventories (XMSBHN). The deactivated structure inventories are proportioned among all of the BH debris bed control volumes based on the preexisting fission product inventory in each volume. For instance, if a debris node contained twenty-five percent of the mass of a particular RN class, then that control volume would receive twenty-five percent of that radioactive (elemental) class mass from the deactivated heat structures. The compound forms of the non-radioactive deposited class masses are placed into the largest aerosol bin (NUMSEC) of the AER1GN array for the adjacent inner and outer control volume atmospheres.

If the failed shroud model activates after gross failure of the BH bottom head, then the RN class inventories deposited on each side of the deactivated core shroud structure are added to the corresponding adjacent CVH volume atmosphere inventory (AER1GN and RDA1GN). The left and right hand side CVH volumes for a given heat structure are

identified via user input; but for BWR core shroud heat structures, the CVH volumes should correspond to the outer COR ring interstitial CVH volume and the downcomer CVH volume. Both the deposited aerosols and the deposited vapors are added directly to the atmosphere aerosol inventory in the largest aerosol size bin (NUMSEC).

11.4.3.2.2 Deactivation of Heat Structures by the HS Package

Besides the BH Package, two routines in the HS package also call the HSOFF chain to deactivate heat structures. The first routine, HSRUN3, calls HSOFF for deactivation of heat structures representing ice beds after they have completely melted. For this call, the RN inventories should have been previously removed by a call to routine RN1HSR; however, for completeness, logic was added to move any class mass, radioactive or non-radioactive, elemental or compound, from the deactivated heat structure surfaces to the adjoining CVH pool volumes.

The second HS package routine calling HSOFF is HSDGAS. This routine calls HSOFF once the temperatures in all regions of a degassing heat structure (including steel structures) have exceeded the upper boundary of the user-defined melting temperature range or if the heat structure has completely melted.

The core shroud structures are normally radial boundary structures of the COR package identified via user input. As a result, the fission products (radioactive elemental RN class masses) deposited on the deactivated structures are assumed to relocate onto COR components within the outermost ring core cell in the axial segment for which the core shroud structure is the radial boundary structure.

The sequence in which the COR components in the cell are selected as the host for the relocated fission products is particulate debris, steel structure, channel box by control blade, channel box not by control blade, cladding, and fuel. If the cell does not contain any fission products, the next lower core cell in the outer ring is chosen. The selection criterion is repeated until a core cell is found that contains fission products or until the limiting lowermost axial segment is encountered. For deactivated heat structures that are boundaries above the core, the starting axial segment examined for extant fission product inventories is NAXL, while the starting radial ring index is that of the radial ring for which the deactivated structure is the axial boundary.

For each radial ring, the searching process extends to the bottom of the reactor vessel if the BH package is not operating or extends to and includes the core plate (axial segment NTLP) if BH is operating. Upon reaching the core plate with an operating BH package and not finding a suitable COR cell host, the reallocation procedure then distributes the deposited radioactive elemental RN class masses into the BH debris bed (if extant) as described in Section 11.4.3.2.1 for the failed shroud model.

If no suitable host can be found in a given radial ring for the deposited radioactive elemental RN inventories, then the searching procedure selects the next inner radial ring

BH Package Reference Manual

and begins the search again at the originating axial segment. If no hosts can be found after processing all radial rings, then the deposited radioactive elemental RN (aerosol and vapors) inventories are added to the adjacent CVH volume atmosphere array RDA1GN in the largest aerosol bin, NUMSEC.

The non-radioactive compound form of aerosols and vapors deposited on the surfaces of the deactivated core shroud are reallocated to the adjacent CVH volume atmosphere aerosol array AER1GN regardless of the disposition of the radioactive elemental inventories. Again, the largest bin size is chosen for disposition of each class.

11.4.4 Implementation of the BH Package Global Energy Balance

This section describes the modifications made to the BH Package to allow communication of energy balance information to the EXEC package. It is emphasized that the global energy balance auditing performed in EXEC is distinct from the internal BH package debris bed and wall energy balances described in Sections 11.2 and 11.3.

To include the BH package in the global energy balance auditing performed in the EXEC package, a new array BHEBAL was defined similar in purpose to the EBAL array discussed earlier for the COR package. This is a double precision array for short word computers and consists of 12 elements. The definitions of the elements of this array are as follows:

1. initial energy in the BH debris bed and BH wall models; redefined when debris layer 3 is formed; (J)
2. current energy in the debris bed and wall models of BH; (J)
3. net cumulative energy transfer to the debris and wall models of BH; positive if added to models; (J)
4. cumulative energy created by chemical oxidation within the debris bed model of BH; positive if added to the bed; (J)
5. current energy in BH water pool model; (J)
6. net cumulative energy added to BH pool model; (J)
7. current energy in the BH failed core shroud model; (J)
8. net cumulative energy added to the BH failed shroud model; (J)
9. cumulative energy of water added to the BH pool model; (J)

10. cumulative energy lost from the debris bed/wall models that does not enter the BH pool model or the BH failed shroud model; this is the sum of the appropriate negative terms of item 3; (J)
11. cumulative energy lost from the BH pool model; sum of the negative terms of item 6 above; (J)
12. cumulative energy lost from the BH failed shroud model that does not enter the debris/wall model or the BH pool model; sum of the appropriate negative terms composing item 8; (J)

Note that some of the negative energy transfers considered in item 3 above are included in items 6 and 8 as positive and cancel when considering the BH package as a whole. It should also be noted that items 10, 11, and 12 are used only in the determination of the relative energy error of the BH package.

As is the case with other packages in MELCOR, a global energy balance common block (BHGEb) exists for use in the global energy balance. The normal energy balance variables EPBH, ETBH, and ECBH are included in BHGEb. In addition, BHGEb has been modified to include two new variables ESBH and EOBH. All of these variables are defined in BHRUN4 after the BH package physics processing has been completed for a given system cycle. They are defined below in terms of the begin (BHEBLO) and end (BHEBLN) step BHEBAL array elements:

energy at the start of the BH calculation

$$ESBH = BHEBLN(1)$$

energy currently in BH

$$EPBH = BHEBLN(2) + BHEBLN(5) + BHEBLN(7)$$

net energy added to BH this cycle

$$\begin{aligned} ETBH &= BHEBLN(3) - BHEBLO(3) \\ &+ BHEBLN(6) - BHEBLO(6) \\ &+ BHEBLN(8) - BHEBLO(8) \end{aligned}$$

net energy created in BH this cycle

$$\begin{aligned} ECBH &= BHEBLN(4) - BHEBLO(4) \\ &+ BHEBLN(9) - BHEBLO(9) \end{aligned}$$

total energy transferred from BH this cycle

BH Package Reference Manual

$$\begin{aligned} \text{EOBH} &= \text{BHEBLN}(10) - \text{BHEBLO}(10) \\ &\quad + \text{BHEBLN}(11) - \text{BHEBLO}(11) \\ &\quad + \text{BHEBLN}(12) - \text{BHEBLO}(12) \end{aligned}$$

An energy balance check is performed in BHRUN4 to assess the current global energy balance for BH by evaluating the relative energy error. A warning message is printed for the first ten cycles that the absolute value of the relative energy error exceeds 0.01 (= 1%). To implement such a check, the current absolute energy error is first set as follows:

$$\begin{aligned} \text{ENGERR} &= \text{EPBH} \\ &\quad - [\text{BHEBLN}(1) + \text{BHEBLN}(3) + \text{BHEBLN}(6) + \\ &\quad \text{BHEBLN}(8) + \text{BHEBLN}(4) + \text{BHEBLN}(9)] \end{aligned}$$

The relative error is defined as:

$$\text{RELERR} = \text{ENGERR} / [\text{EPBH} + \text{BHEBLN}(10) + \text{BHEBLN}(11) + \text{BHEBLN}(12)]$$

The reader should note that the denominator in this definition of relative error represents the total energy that has ever existed in the BH package and that this is consistent with the relative energy error definition recommended for extension to all MELCOR packages as proposed in Section 11.4.2.3.

11.4.5 EXEC Package

Information presented in Sections 11.4.3.1 and 11.4.4 describes the addition of variables to the HS and BH Package global energy balance commons HSGEB and BHGEB. This section describes how the new variables in these commons are used by the EXEC package in the global energy balance auditing performed in MXXDBE and are printed at the beginning of a MELCOR edit for each of the active MELCOR Packages. EXEC Package routines are prefixed by the letters MEG, MEX, or MXX, and indicate execution within MELGEN, MELCOR, or combined MELGEN/MELCOR processing.

Routine MEXRN1 was modified to add the cumulative energy of all deactivated heat structures EFHS stored in common HSGEB to the ENOW term. As a result, the subsequent determination of the HS Package absolute energy error in routine MXXDBE is corrected for the deactivation of heat structures. In addition, the relative energy error calculated and printed for HS by routine MXXDBE is based on a ENOW term in the denominator that is closer to the definition of relative energy error as recommended in Section 11.4.2.3.

To implement the BH Package energy balance audit, the MXXGEB common block was modified by adding an additional array SETOT whose entries (one for each active package) explicitly store the cumulative energy transferred away from the package. The

need and rationale for such information was explained in Section 11.4.2.3 concerning the recommended definition of the relative energy error as calculated by routine MXXDBE. Since only the BH Package currently identifies this cumulative energy out term, all entries in the SETOT array corresponding to packages other than BH have zero values.

Routine MXXRN1 has been modified to set the ESTART term for the BH Package each system cycle. ESTART is used in the determination of the absolute energy error for BH, is set to ESBH, and requires redefinition when BH Package debris bed layer 3 is formed. MXXRN1 has also been modified to increment the SETOT for the BH Package with EOBH, i.e., the energy transferred away from BH during the cycle.

Routine MXXDBE has been modified such that the relative energy error determined for the BH package (and only the BH package) is defined as follows:

$$EERR = ENOW - ESTART - SETRN - SECTR$$

$$EREL = EERR / [ENOW + SETOT]$$

Routine MXXDBE has also been modified to add the ESTART energy for the BH Package to the global (sum over all packages) transfer term EGTRAN. This revision was necessary because the BH Package starting energy cannot be included in the global starting energy term (EGSTAR) since the BH Package energy is undefined at the beginning of the MELCOR calculation.

12. PWR Applications

Modifications to the BH Package implemented subsequent to the release of MELCOR 1.8.3 extend the capability of this package so that it can now be applied for PWR accident calculations. Because of major differences in the internal structures beneath the core and the lack of a lower core shroud and jet pump downcomer region with baffle plate for the PWR reactor vessels, a dedicated subroutine has been created to perform the PWR lower plenum calculations. There is also a special subroutine for Simplified Boiling Water Reactor (SBWR) calculations. Table 12.1 indicates the role of each of the three reactor type-specific lower plenum subroutines.

BH Package Reference Manual

Table 12.1 BH Package Subroutine Equivalents for Lower Plenum Response Calculations

	BWR	PWR	SBWR*
IRTYPE	0	1	2
Subroutine	BHHED2	BHPWRH	BHSBDI

Arrangement is made within subroutine BHQSLU to call either the BWR, the PWR, or the SBWR version of the lower plenum subroutine depending upon the user-input parameter IRTYP (Input Record COR00002).

12.1 PWR Materials

For PWR applications, it is necessary to calculate the effects of the silver-indium-cadmium control rod materials that would be present in the lower plenum debris bed. As indicated in Chapter 2, these materials are now represented by entries for "Ag" and "CdIn" in the properties arrays for density, specific heat, and thermal conductivity. It is also necessary to specify a molecular weight, a melting temperature, and a heat of fusion for these two "pure species" as elements 6 and 7 of the BH package input arrays AMMLWT(K), AMTMEL(K), and AMLAMF(K). (See BH Package Users' Guide Section 2.1 Input Record BH02JJ.)

In order to permit the eutectic liquid mixture Ag-CdIn to be formed within the debris bed control volumes, the characteristics of this mixture must be specified in the BH package input. This is accomplished as described in the BH Package Users' Guide Section 2.3, "Eutectic Mixtures."

Some PWR reactor vessel internal structures incorporate a large amount of Inconel, which is formed of the same materials as stainless-steel, but in different relative proportions. As an example, Table 12.2 indicates the mass fractions for stainless-steel and for the Inconel alloy used in the Three Mile Island PWR reactor vessel.

Table 12.2 Component Mass Fractions for Stainless-steel and the TMI-2 Inconel

Component	Fe	Cr	Ni	Other
Stainless-steel	0.740	0.180	0.080	—
Inconel	0.195	0.190	0.530	0.085

Since the "Other" components (Cb-Ta, Mo, Ti, Al) of the TMI-2 Inconel are not represented in the BH Package properties' tables, the Inconel composition would in practice be entered as 0.213 Fe, 0.208 Cr, and 0.579 Ni, which sum to 1.00.

* See Table 10.1 for other special SBWR-specific subroutines.

If both stainless-steel and Inconel contribute to the initial accumulation of solid debris in a bed control volume and if both the stainless-steel and the Inconel eutectics are represented in code input, then Inconel liquid will form first as the temperature increases. (The Inconel melting temperature [1670 K] is lower than the 1700 K melting temperature of stainless-steel.) This melting process will continue until all available free nickel has been exhausted, leaving excess iron and chromium, which will then behave as pure species. It is important to recognize that little, if any, liquid stainless-steel would be predicted to be formed as a result of slow (decay heating-induced) temperature increases during the calculation.

12.2 Special Logic

For cases in which MELCOR predicts sufficient core debris in the lower plenum during a PWR accident calculation, the BH Package can be applied to calculate the thermal response of the lower plenum debris bed, the heatup of the reactor vessel bottom head, and the release of core and structural materials from the reactor vessel to the containment in much the same manner as for a BWR calculation. The differences in code logic as applied to the PWR are described in this section. Special guidance with respect to the preparation of BH package input for PWR applications is provided in Section 12.3.

The major difference in code logic for the PWR arises because there is no lower shroud, baffle plate, or water-filled jet pump region within the PWR reactor vessel lower plenum. As indicated in Figure 1.11, wall node 18 must be treated separately for the BWR because it is located above the baffle plate. For the PWR, however, there is no baffle plate so that wall node 18 can be (and is) treated in the same manner as wall node 17. Specifically, wall node 18 is exposed to radiative heat transfer from the debris bed surfaces and to convection and radiation from the lower plenum atmosphere.

For the calculation of the surface heat transfer coefficients (discussed in Section 3.2.1), surface 6 for the PWR is comprised of the inner segments of both wall nodes 17 and 18 instead of just wall node 17, as for the BWR. (See Table 3.1.) Also for the PWR, heat transfer from the lower plenum atmosphere to the exposed wall nodes is calculated in the manner described in Section 3.2.3 for node 18 as well as for node 17.

With reference to Figure 3.2, structures 2, 3, and 4 do not exist for the PWR. Instead, structure 1, which represents the exposed wall, includes both wall nodes 17 and 18.

The discussion of Section 3.3.3, which pertains to heat transfer between the downcomer (jet pump) region water or shroud wall (if the downcomer is dry) and wall node 18 does not apply to the PWR. As explained previously, wall node 18 for the PWR reactor vessel is subject to radiative heat exchange with the debris bed surfaces in exactly the same manner as wall node 17.

Other differences in code logic for the PWR derive from the lack of control rod guide tube penetrations in the vessel bottom head and the finding that instrument guide tube failures are much less likely to occur in PWRs for the reasons (thicker tube wall, smaller internal tube diameter) reported in Reference 24. If the user chooses to include PWR instrument tube failures in a calculation, however, the logic described in Chapter 5 will apply except that penetration weld failures are considered only for the wall nodes (one through eight) adjacent to the bottom debris layer. (For the BWR, penetration weld failure is also possible at wall node 9, which is adjacent to the lower portion of the middle debris layer.)

The printed output for the PWR calculations is almost identical to that for the BWR, as shown in Figure 6.1 through 6.4, except that the representation of the shroud wall and downcomer region is removed. In its place, the index for wall node 18 is listed.

Finally, references to "CR guide tubes" in the printed messages described in Section 6.5 are replaced by references to "steel structures" for the PWR. (These are the steel structures beneath the core support plate such as the lower grid forging and the flow distributor, which are subsumed into the surrounding debris for the PWR in the same manner that the control rod guide tubes are subsumed into the lower plenum debris for the BWR.)

12.3 Guidance for Package Input

The BH Package input format was originally developed for the purpose of inserting information necessary to support BWR accident calculations. The definition of the input parameters is provided in the BH Package Users' Guide. However, with the capability of the BH Package extended to include PWR accident applications, it is necessary to provide additional guidance for some of these parameters, when used for this purpose. These parameters and the associated guidance are listed in the following table. (DRXID is the diameter of the hemispherical bottom head.)

Table 12.3 Guidance for Use of Certain BH Package Input Parameters for PWR Applications

Parameter	Input Record	Comment
HBSB	BH0100	Although there is no shroud baffle for PWRs, the bottom of wall node 18 will still be set at height HBSB. For PWRs, however, the input card value for HBSB is ignored, and a value equivalent to $DRXID/2.0 - 0.076$ m is assigned by the input processor. Thus wall node 18 has a length of 0.076 m (three inches).

Parameter	Input Record	Comment
VCORE	BH03II	Sufficient entries (at least 20) should be used to adequately define the free volume versus height relationship for the lower plenum considering the presence of structures (array VPS) and the effects of bottom head curvature. The VSHRD entries should all be 0.0.
VPS	BH04II	The VPS entries should represent the combined volumes of structural steel and Inconel in the lower plenum.
HD1D2	BH0500	For PWRs with uniform bottom head wall thickness, set HD1D2 to any height greater than HCYL (Input Record BH0700).
HSKIRT	BH0600	Height above vessel zero of the skirt attachment for PWRs that have a support skirt. For PWRs without a support skirt, set HSKIRT to any value greater than HCYL (Input Record BH0700).
HCYL RCYL	BH0700	Set both HCYL and RCYL to DRXID/2.0 for PWR applications.

Because of the relatively small Inconel masses included among the large stainless-steel structures in the PWR lower plenum, it is not considered necessary to require special input to describe the volume-versus-height configuration of the Inconel. Rather, as indicated in Table 12.3, it is expected that the mass of the intact lower plenum Inconel structures will be simply added to the stainless-steel mass whose distribution is represented by the VPS array. (The large amounts of Inconel relocating into the lower plenum from the core region will, however, be treated separately from the stainless-steel if the user defines an Inconel eutectic, as discussed in Section 12.1.)

13. References

1. L. J. Ott, "Advanced Severe Accident Response Models for BWR Application," Nuclear Engineering and Design, 115, pp. 289-303 (1989).
2. L. J. Ott, "Advanced Severe Accident Response Models for BWR Application," presented at the Fifteenth Water Reactor Safety Information Meeting, National Bureau of Standards, Gaithersburg, MD (October 29, 1987).
3. S. A. Hodge and L. J. Ott, Boiling Water Reactor Severe Accident Response (BWRSAR) Code Description and Assessment, Letter Report to Dr. Thomas J. Walker, Division of Systems Research, RES, USNRC, (February 1, 1989).
4. S. A. Hodge, C. R. Hyman, and L. J. Ott, "BWR Lower Plenum Debris Bed Models for MELCOR," presented at the Nineteenth Water Reactor Safety Information Meeting, Bethesda, MD (October 28, 1991).
5. G. E. Mueller and A. Sozer, Thermal-Hydraulic and Characteristic Models for Packed Debris Beds, NUREG/CR-4689 (ORNL/TM-10117), Oak Ridge National Laboratory (December 1986).
6. The BWR Owners' Group Emergency Procedure Guidelines, Revision 4 (March 1987).
7. S. A. Hodge et al., Identification and Assessment of BWR In-Vessel Severe Accident Mitigation Strategies, USNRC Report, NUREG/CR-5869 (ORNL/TM-12080), Martin Marietta Energy Systems, Inc., Oak Ridge National Laboratory (October 1992).
8. S. A. Hodge and W. J. McAfee, "Thermal Shock Considerations for External Flooding of a BWR Reactor Vessel," letter report (ORNL/NRC/LTR-92/23) to Dr. James T. Han, Reactor and Plant Systems Branch, Division of Systems Research, RES, USNRC (September 30, 1992).
9. D. L. Hagrman, "Materials Properties Models for Severe Core Damage Analysis," informal report (EGG-CDD-5801), Idaho National Engineering Laboratory (May 1982).
10. C. M. Allison, et al., SCDAP/RELAP5/Mod3 (8X) Code Manual Volume IV: MATPRO—A Library of Materials Properties for Light-Water-Reactor Accident Analysis, NUREG/CR-6150, EGG-2720, Volume 4, November 1993.
11. S. S. Dosanjh, Melt Progression, Oxidation, and Natural Convection in a Severely Damaged Reactor Core, NUREG/CR-5316, SAND88-3476, Sandia National Laboratories, Albuquerque, NM (February 1990).

12. W. H. Giedt, Principles of Engineering Heat Transfer, p. 217, D. van Nostrand Company, Inc., Princeton, NJ (1964).
13. L. J. Ott, "FRS Surface Emisivity," Thermal-Hydraulic Test Facility Bundle 3 In-Core Instrumentation and Operating History, NUREG/CR-2609 (ORNL/NUREG-75) Equation 8.6) pp. 72-79 (1982).
14. C. B. Ludwig and C. C. Ferris, "Prediction of Total Emissivity of Nitrogen-Broadened and Self-Broadened Hot Water Vapor," Journal of Quantitative Spectroscopy and Radiative Transfer, 7, pp. 7-26 (1982).
15. J. K. Lovin et al., User's Manual for RAVFAC, a Radiation View Factor Digital Computer Program, LMSC/HREC D148620-A, Lockheed Missiles and Space Co., Inc., Huntsville Research and Engineering Center (August 1973).
16. E. F. Puccinelli, "View Factor Computer Program (Program VIEW) User's Manual," Goddard Space Flight Center, X-324-73-272 (July 1973).
17. S. A. Hodge, "Oxidation of Steel Within the BH Package Lower Plenum Debris Bed," letter report (ORNL/NRC/LTR-96/38) to Mr. R. B. Foulds, Accident Evaluation Branch, Division of Systems Research, RES, USNRC (January 1997).
18. L. Baker, Jr., An Assessment of Existing Data on Zirconium Oxidation Under Hypothetical Accident Conditions in Light Water Reactors, ANL/LWR/SAF 83-3, Argonne National Laboratory (1983).
19. J. V. Cathcart, "Quarterly Progress Report on the Zirconium Metal-Water Oxidation Kinetics Program Sponsored by the NRC Division Metal-Water Oxidation Kinetics Program, Sponsored by the NRC Division of Reactor Safety Research for October-December 1976," ORNL/NUREG/TM-87 Oak Ridge National Laboratory (1976).
20. L. Baker and C. Just, "Studies of Metal-Water Reactions at High Temperatures III. Experimental and Theoretical Studies of the Zirconium-Water Reaction," ANL-6548 Argonne National Laboratory (May 1962).
21. G. W. Parker, L. J. Ott, and S. A. Hodge, "Small-Scale BWR Core Debris Eutectics Formation and Melting Experiment," Nuclear Engineering and Design, 121, pp. 341-347 (1990).
22. D. A. Powers, "Erosion of Steel Structures by High-Temperature Melts," Nuclear Science and Engineering, 88, pp. 357-366, June 1984.
23. M. Pilch and W. W. Tarbell, High Pressure Vessel—The Discharge Phase, NUREG/CR-4383, SAND85-0012 (September 1985)

BH Package Reference Manual

24. J. L. Rempe et al., Light Water Reactor Lower Head Failure Analysis, NUREG/CR-5642, EGG-2618, Idaho National Engineering Laboratory (October 1993).
25. G. E. Mueller et al., Thermal-Hydraulic and Characteristic Models for Packed Debris Beds, NUREG/CR-4689, ORNL/TM-10117 (December 1986).
26. D. W. Akers et al., Examination of Relocated Fuel Debris Adjacent to the Lower Head of the TMI-2 Reactor Vessel, NUREG/CR-6195, EGG-2732 (March 1994).
27. V. E. Schrock et al., Steam-Water Flooding in Debris Beds and Its Role in Dryout, EPRI NP-3858, University of California at Berkeley, Berkeley, CA (March 1985).
28. D. H. Cho et al., "On the Pattern of Water Penetration into a Hot Particle Bed," Nuclear Technology, 65, p. 23 (April 1984).
29. T. Ginsberg et al., An Experimental and Analytical Investigation of Quenching of Superheated Debris Beds Under Top-Reflow Conditions, NUREG/CR-4493, BNL-NUREG-51951 (January 1986)
30. R. J. Lipinski, "A Coolability Model for Post Accident Nuclear Reactor Debris," Nuclear Technology, Vol. 65 (April 1984).
31. A. W. Reed et al., DCC-1/DCC-2 Degraded Core Coolability Analysis, NUREG/CR-4390, SAND85-1967R3 (October 1985).
32. K. R. Boldt et al., DCC Degraded Core Coolability: Experiment and Analysis, NUREG/CR-4606, SAND86-1033, September 1986.
33. B. W. Spencer et al., Fragmentation and Quench Behavior of Corium Melt Streams in Water, NUREG/CR-6133, ANL-93/32 (February 1994).
34. R. O. Wooten et al., March 2 (Meltdown Accident Response Characteristics) Code Description and Users' Manual, NUREG/CR-3988 (August 1984).
35. G. G. Wallis, One Dimensional Two-Phase Flow, McGraw-Hill Book Company, New York, NY (1969).
36. L. S. Tong, Boiling Heat Transfer and Two-Phase Flow, John Wiley and Sons, Inc., New York, NY (1965).
37. S. A. Hodge, C. R. Hyman, and R. L. Sanders, "BWR-Specific Models for MELCOR," presented at the 1993 Cooperative Severe Accident Research Program (CSARP) Review Meeting, Bethesda, MD (May 6, 1993).

38. R. Siegel and J. R. Howell, Thermal Radiation Heat Transfer, Appendix C, formula 28, p. 828, 2nd edition, McGraw-Hill Book Company, New York, NY (1972).
39. C. R. Hyman et al., "MELCOR Modifications for SBWR Applications," presented at the Twentieth Water Reactor Safety Information Meeting, Bethesda, MD (October 23, 1992).

Burn (BUR) Package Reference Manual

The Burn (BUR) package models the combustion of gases in control volumes. The models consider the effects of burning on a global basis without modeling the actual reaction kinetics or tracking the actual flame front propagation. The BUR package models are based on the deflagration models in the HECTR 1.5 code. New in MELCOR 1.8.5 is a diffusion flame model, also derived from HECTR 1.5.

This Reference Manual describes the models employed in the BUR package. Detailed descriptions of the user input requirements can be found in the BUR Package Users' Guide.

Contents

1.	INTRODUCTION.....	5
2.	DETAILED MODELS	6
2.1	Burn Model Logistics	6
2.2	Ignition Criteria	7
2.3	Combustion Completeness	9
2.4	Burn Duration	10
2.5	Combustion Rate.....	12
2.6	Propagation Criteria	13
2.7	Detonation	15
2.8	Diffusion Flame Model.....	15
3.	TIMESTEP CONTROL	16
4.	REFERENCES.....	16

1. Introduction

The Burn (BUR) package models the combustion of gases in control volumes. These models consider the effects of burning off premixed gases without modeling the actual reaction kinetics or tracking the actual flame front propagation. The models in the BUR package are based on the deflagration models in the HECTR 1.5 code [1]. The only significant modifications made were to provide more direct user control of the models through the implementation of sensitivity coefficients and to include optional model parameters that are used to override the nominal parameters in control volumes in which direct containment heating (DCH) is occurring.

A diffusion flame model is available in MELCOR 1.8.5, also based on HECTR 1.5. The diffusion flame model allows more realistic modeling of DCH phenomena without having to make major adjustments to the nominal bulk burn parameters.

Briefly, a burn is initiated if certain criteria are satisfied in a control volume, causing the reactants (hydrogen, carbon monoxide and oxygen) to be converted during the burn to steam and carbon dioxide. The conversion occurs over a time interval called the burn duration. The reaction may or may not be complete, depending on the conditions in the control volume. After a burn is initiated in a control volume, it can be propagated to adjoining control volumes if a second set of criteria is satisfied. These criteria, as well as the duration and completeness of the burns, are discussed in Section 2. The modeling follows the recommendations of the MELCOR Assessment on Combustible Gas Treatment [2]. The default values and correlations used to calculate burn effects are those used in Reference 1.

For user convenience, the BUR package also prints messages to warn the user when the detonability criteria are satisfied in a control volume. A *detonation* is combustion in which the flame front travels at supersonic speeds, whereas a *deflagration* travels at subsonic speeds. In the BUR package, only deflagrations are modeled; detonations are merely flagged and no other action is taken.

The gases hydrogen (H_2), carbon monoxide (CO), carbon dioxide (CO_2), and oxygen (O_2) must be defined in the NonCondensable Gas (NCG) package whenever the BUR package is active. Steam (H_2O) is automatically present for all MELCOR calculations, so no special action need be taken to include it in a calculation.

The BUR package currently has a limited capability to burn deuterium gas (D_2). For purposes of combustion, D_2 is treated as equivalent to H_2 on a *mole-for-mole basis*. Therefore, one mole of D_2 will combine with one-half mole of O_2 to produce one mole of H_2O (not D_2O), and mass will not be conserved. Some equivalence must be assumed in the absence of a D_2O equation of state comparable in quality to the equation of state used in MELCOR for H_2O . Equivalence on a molar basis was chosen because the equations of state of D_2O and H_2O are much more similar on a molar basis than on a mass basis,

BUR Package Reference Manual

particularly in the gas phase. In addition, the former gives a more accurate value for the heat of combustion.

The same mole-for-mole equivalence is assumed in ignition, detonation, and completeness calculations, and input (or default) data for H_2 will be applied to D_2 and H_2/D_2 mixtures. We believe that the error is small: for example, the ideal combustion limits for D_2 are 5.0 to 95.0 mole percent compared to 4.0 to 94.0 mole percent for H_2 .

2. Detailed Models

In the following equations, variables that are defined by user input are referred to by the same names as described in the Burn Package Users' Guide. Thus, there is a direct correspondence between the variables in the Users' Guide and those in the Reference Manual.

2.1 Burn Model Logistics

A burn is initiated in a control volume if the ignition criteria discussed in Section 2.2 are satisfied. As soon as a burn is initiated, calculations (described in Sections 2.3 and 2.4) are performed to determine the completeness of the burn and its duration. During subsequent timesteps, the reactants are converted to the products of combustion in that control volume according to the reactions.



The rate of burning varies during the burn duration to account for change in composition, e.g., due to inter-compartment flow and gas sources, as described in Section 2.5.

After a burn is initiated in a control volume, it can be propagated to adjoining control volumes if a second set of criteria is satisfied. These criteria are discussed in Section 2.6. After a burn propagates into a control volume, the same steps as outlined above for ignition are followed to calculate the burn effects.

2.2 Ignition Criteria

A deflagration is initiated in a control volume if the mole fraction composition satisfies the criteria described in this section. In addition, control volumes that are specified to contain igniters are tested against different criteria than control volumes without igniters, and a separate criteria may be specified for use when direct containment heating (DCH) is occurring in a control volume. For all cases, LeChatelier's formula (for the effective combustion mole fraction for a mixture containing more than one combustible gas) is used to determine the threshold of ignition. In particular, ignition occurs when the following criteria is satisfied:

$$X_{H_2} + X_{CO} \left(\frac{L_{H_2,ign}}{L_{CO,ign}} \right) \geq L_{H_2,ign} \quad (2.3)$$

where

X_{H_2} = hydrogen mole fraction in the control volume;

X_{CO} = carbon monoxide mole fraction in the volume;

$L_{H_2,ign}$ = XH2IGN, if there are no igniters in the volume and DCH is not occurring,

or

XH2IGY, if there are igniters in the volume and DCH is not occurring,

or

XH2DCH, if DCH is occurring in the volume;

$L_{CO,ign}$ = XCOIGN, if there are no igniters in the volume and DCH is not occurring,

or

XCOIGY, if there are igniters in the volume and DCH is not occurring,

or

XCODCH, if DCH is occurring in the volume;

XH2IGN = hydrogen mole fraction limit for ignition without igniters, when DCH is not occurring, input on record BUR001 (default = 0.10);

BUR Package Reference Manual

XH2IGY = hydrogen mole fraction limit for ignition with igniters, when DCH is not occurring, input on record BUR001 (default = 0.07);

XH2DCH = hydrogen mole fraction limit for ignition during DCH, input on record BUR001 (default = XH2IGY);

XCOIGN = carbon monoxide mole fraction limit for ignition without igniters, when DCH is not occurring, input on record BUR001 (default = 0.167);

XCOIGY = carbon monoxide mole fraction limit for ignition with igniters, when DCH is not occurring, input on record BUR001 (default = 0.129);

XCODCH = carbon monoxide mole fraction limit for ignition during DCH, input on record BUR001 (default = XCOIGY).

The preceding tests are made only for the presence of sufficient combustible gases. Tests are also made to determine whether there is sufficient oxygen and to determine whether the amount of steam and carbon dioxide is below the inerting level. The same values are used when igniters are present as when there are no igniters, but separate values may be specified for use during DCH. The ignition and inerting criteria are

$$X_{O_2} \geq XO2IG \text{ (or } XO2DCH \text{ during DCH)} \quad (2.4)$$

$$X_{H_2O} + X_{CO_2} < XMSCIG \text{ (or } XINDCH \text{ during DCH)} \quad (2.5)$$

where

X_{O_2} = oxygen mole fraction in the control volume;

X_{H_2O} = steam mole fraction in the control volume;

X_{CO_2} = carbon dioxide mole fraction in the volume;

XO2IG = minimum oxygen mole fraction for ignition, input on record BUR001 (default = 0.05);

XO2DCH = minimum oxygen mole fraction for ignition during DCH, input on record BUR001 (default = XO2IG);

XMSCIG = maximum diluent mole fraction for ignition, input on record BUR001 (default = 0.55);

XINDCH = maximum diluent mole fraction for ignition during DCH, input on record BUR001 (default = XMSCIG).

If all three tests are satisfied (Equations (2.3) through (2.5)), i.e., there is enough hydrogen and/or carbon monoxide, enough oxygen, and not too much steam and/or carbon dioxide, a burn is initiated. The burn duration and combustion completeness are discussed in Sections 2.3 and 2.4. If too much steam and carbon dioxide is present, the control volume is considered to be inert, and is identified as such in the printed edits. A message is printed to the output file and to the special message file and a plot dump is written (if specified by the user) when a deflagration begins and ends in any control volume.

2.3 Combustion Completeness

In MELCOR, deflagrations are not required to be complete; that is, all of the combustible gases present in a control volume at the start of a deflagration are not required to be burned during the deflagration. The *combustion completeness* is used to determine the amounts of combustible gases that should be present in a control volume at the end of an incomplete burn. In the BUR package, the combustion completeness, CC, is defined as

$$CC = 1 - \frac{Y_{min}}{Y_{max}} \quad (2.6)$$

where Y is given by the LeChatelier formula,

$$Y = X_{H_2} + X_{CO}(YH_2CC/YCOCC) \quad (2.7)$$

and

Y_{max} = value of LeChatelier formula evaluated at the start of the burn (initial amount of combustibles);

Y_{min} = value of LeChatelier formula that is desired at the end of the burn (final amount of combustibles);

YH2CC = XH2CC, if DCH is not occurring, or
= XH2CCD, if DCH is occurring;

YCOCC = XCOCC, if DCH is not occurring, or
= XCOCCD, if DCH is occurring;

BUR Package Reference Manual

XH2CC = hydrogen mole fraction for calculating combustion completeness, input on record BUR003 (default = 0.08);

XH2CCD = hydrogen mole fraction for calculating combustion completeness during DCH, input on record BUR003 (default = XH2CC);

XCOCC = carbon monoxide mole fraction for calculating combustion completeness, input on record BUR003 (default = 0.148);

XCOCCD = carbon monoxide mole fraction for calculating combustion completeness during DCH, input on record BUR003 (default = XCOCC).

The combustion completeness is first evaluated by the method described below, then it is used to determine the value for Y_{min} for the current deflagration in the control volume. The burning rate is adjusted as necessary (see Section 2.5) to achieve this value at the end of the burn.

The combustion completeness can be input as a constant value, calculated from a user-specified control function, or calculated from a correlation. The default correlation for combustion completeness, which was obtained from the HECTR 1.5 code [1], and derived from experimental data, is dependent on the mole fraction of combustible gases present at the start of the burn, Y_{max} , and is given by

$$CC = 0.0 \text{ for } Y_{max} \leq 0.03746 \quad (2.8)$$

$$= 23.4116(Y_{max} - 0.03746) \text{ for } Y_{max} > 0.03746 \quad (2.9)$$

The constants in this correlation have been implemented in sensitivity coefficient array 2202.

2.4 Burn Duration

The burn duration is calculated by dividing a user-specified characteristic dimension by the *flame speed*. The flame speed can be input as a constant value, calculated from a user-specified control function, or calculated from a correlation. Optional input can be specified to determine the flame speed with a different constant, control function or correlation when DCH is occurring in the control volume. The default correlation, obtained from the HECTR 1.5 code, was derived from experimental data. However, few data were available regarding the effect of large amounts of diluents (steam and carbon dioxide) on flame speed, so the correlation is questionable in mixtures with high diluent concentration. For these mixtures, sensitivity studies should be conducted to bound the expected pressure rises. The default correlation for the flame speed, V , is

$$V = V_{base} \times C_{dil} \quad (2.10)$$

where

$$V_{base} = 59.2Y_{max} + 1.792 \text{ if } 0.0 \leq Y_{max} \leq 0.1, \quad (2.11)$$

$$= 172.88Y_{max} - 9.576 \text{ if } 0.1 < Y_{max} \leq 0.2, \quad (2.12)$$

$$= 50.Y_{max} + 15. \text{ if } 0.2 < Y_{max} \leq 0.3, \quad (2.13)$$

$$= -50.Y_{max} + 45. \text{ if } 0.3 < Y_{max} \leq 0.4, \quad (2.14)$$

$$= -75.Y_{max} + 55. \text{ if } 0.4 < Y_{max} \leq 0.6, \quad (2.15)$$

$$= -64.3Y_{max} + 48.58 \text{ if } 0.6 < Y_{max} \leq 1.0 \quad (2.16)$$

$$C_{dil} = \max(0.05, 1.0 - 4.53XD + 5.37XD^2) \text{ if } 0.0 \leq Y_{max} \leq 0.2 \quad (2.17)$$

$$= \max(0.05, 1.0 - 4.53XD) + 5.37XD^2)(0.3 - Y_{max})/0.1 \\ + \max(0.0, 1.0 - 1.29XD)(Y_{max} - 0.2)/0.1 \text{ if } 0.2 < Y_{max} \leq 0.3 \quad (2.18)$$

$$= \max(0.0, 1.0 - 1.29XD) \text{ if } 0.3 \leq Y_{max} \leq 1.0 \quad (2.19)$$

XD = diluent concentration ($X_{H_2O} + X_{CO_2}$).

The constants in this correlation have been implemented in sensitivity coefficient array 2200. The burn duration time, t_{comb} , is calculated by dividing the flame speed into a user-specified characteristic dimension of the control volume, CDIM (or CDDH when DCH is occurring), input on record BUR1XX:

$$\begin{aligned}
 t_{comb} &= CDIM / V \text{ if DCH is not occurring or} \\
 &= CDDH / V \text{ if DCH is occurring.}
 \end{aligned}
 \tag{2.20}$$

2.5 Combustion Rate

The combustion rate (amount of hydrogen, carbon monoxide, and oxygen converted to steam and carbon dioxide per timestep) is not constant during a burn. Rather, it is adjusted at each timestep to account for inter-compartment flows and gas sources in an effort to match the desired final conditions. In other words, the combustion rate is adjusted so that the mole fractions corresponding to the calculated combustion completeness and the desired burn duration are simultaneously achieved. At each timestep, the burn rate, YRATE, is calculated as

$$YRATE = (Y(t) - Y_{min}) / (t_o + t_{comb} - t) \tag{2.21}$$

where

t_o = time that burn was initiated, and

t = current time in calculation.

Once the rate is calculated, it is used to determine the decrease in the inventory of the combustible gases for the current MELCOR system timestep:

$$DELH2 = X_{H2}(t) \cdot YRATE \cdot \frac{DT}{Y(t)} \tag{2.22}$$

$$DELCO = X_{CO}(t) \cdot YRATE \cdot \frac{DT}{Y(t)} \tag{2.23}$$

where

$DELH2$ = decrease in hydrogen moles in the control volume during the timestep from combustion,

$DELCO$ = decrease in carbon monoxide moles in the control volume during the timestep from combustion, and

DT = MELCOR system timestep (s).

At the end of the burn, the value Y_{\min} would be reached exactly if there were no flow or sources. These values are updated on every timestep to reflect the changing conditions. DELH2 and DELCO are constrained to prevent burning more moles of either gas than are present in the control volume.

The energies of formation are included in the water and noncondensable gas equations of state. With this formulation, simply changing the relative masses of the reactants and products will automatically result in the appropriate pressure and temperature increase. Thus, it is not necessary to calculate a combustion energy release to a control volume. The total mass and energy of a control volume are not changed by the BUR package, but the masses of individual species are changed to reflect the reactions listed in Section 2.1. (That is, DELH2, DELCO, and $0.5 \cdot \text{DELH2} + 0.5 \cdot \text{DELCO}$ moles of hydrogen, carbon monoxide, and oxygen are subtracted from the control volume while DELH2 and DELCO moles of steam and carbon dioxide are added to the control volume.) Because the specific enthalpy of each species properly accounts for the energy of formation, the conversion of the reactants to the products increases the temperature and pressure of the control volume with combustion, even though the total energy remains unchanged.

2.6 Propagation Criteria

Propagation of combustion from a control volume to connected control volumes is allowed after a user-controlled time period has elapsed. This delay is intended to account for the time it would take for a flame to reach the edge of a control volume if a flame front were actually being modeled. Different delay periods may be specified depending upon whether or not DCH is occurring in the control volume. Propagation will then occur if the propagation criteria are satisfied in the connected control volume. The propagation delay, t_{prop} , is calculated to be

$$t_{\text{prp}} = \text{FRAC} \cdot t_{\text{comb}} \quad (2.24)$$

where

FRAC = TFRAC, if DCH is not occurring in the control volume, or
 = TFDH, if DCH is occurring in the control volume; and

TFRAC = propagation time fraction input on record BUR1XX (default = 0)

TFDH = override value of TFRAC during DCH, input on record BUR1XX (default = TFRAC).

BUR Package Reference Manual

Note that if TFRAC equals zero, propagation is possible as soon as a control volume begins burning. If TFRAC equals 1.0, propagation is only considered at the end of the control volume burn.

For propagation, LeChatelier's formula is still applicable if appropriate values are used for the L parameters. Propagation is allowed if the following inequality is satisfied

$$X_{H_2} + X_{CO}(L_{H_2,prp} / L_{CO,prp}) \geq L_{H_2,prp}$$

where

$L_{H_2,prp}$ = XH2PUP, for upward propagation, or
= XH2PHO, for horizontal propagation, or
= XH2PDN, for downward propagation;

$L_{CO,prp}$ = XCOPUP, for upward propagation, or
= XCOPHO, for horizontal propagation, or
= XCOPDN, for downward propagation;

XH2PUP = hydrogen mole fraction limit for upward propagation, input on record BUR003 (default = 0.041).

XH2PHO = hydrogen mole fraction limit for horizontal propagation, input on record BUR003 (default = 0.06).

XH2PDN = hydrogen mole fraction limit for downward propagation, input on record BUR003 (default = 0.09).

XCOPUP = carbon monoxide mole fraction limit for upward propagation, input on record BUR003 (default = 0.125).

XCOPHO = carbon monoxide mole fraction limit for horizontal propagation, input on record BUR003 (default = 0.138).

XCOPDN = carbon monoxide mole fraction limit for downward propagation, input on record BUR003 (default = 0.15).

The propagation direction is determined directly from the flow path input using the *from* and *to* elevations (see the FL Package Users' Guide). If a flow path is not open, or if the flow path is covered by water, propagation is not allowed. Note that the presence of a check valve is not taken into account when determining whether a flow path is open.

A message is printed to the output file and to the special message file and a plot dump is written (if specified by the user) when a deflagration due to propagation begins in any control volume.

2.7 Detonation

MELCOR does not contain a detonation model. However, tests are performed in each control volume, and a warning message is written indicating the possibility of a detonation if all of the following mole fractions limits are satisfied:

$$X_{H_2} > XH2DET \quad (2.25)$$

$$X_{O_2} > XO2DET \quad (2.26)$$

$$X_{H_2O} < XH2ODT \quad (2.27)$$

where

XH2DET = minimum hydrogen mole fraction for detonable mixture, input on record BUR002 (default = 0.14),

XO2DET = minimum oxygen mole fraction for detonable mixture, input on record BUR002 (default = 0.09), and

XH2ODT = maximum steam mole fraction for detonable mixture, input on record BUR002 (default = 0.30).

No detonation calculation is performed when a detonable mixture is detected. The warning message is written, but the calculation continues under the control of the deflagration model. The detonation model is mainly intended as a user convenience to flag potentially dangerous conditions that may require separate analysis.

2.8 Diffusion Flame Model

The diffusion flame model is intended to model the burning of hydrogen entering a control volume under DCH conditions. Under such conditions, the hydrogen enters accompanied by hot melt particles which act as igniters, so that the conditions for ignition and burning are quite different from those for a bulk burn. The diffusion flame implementation is a simple model that burns combustible gas passing through a flow path and entering a control volume containing oxygen, subject to ignition criteria. These are defined on the

BUR Package Reference Manual

BUR005 input records (see BUR Users Guide), new in MELCOR 1.8.5. This general approach is used both in MELCOR and in CONTAIN.

As implemented in MELCOR, a combustion completeness criterion is used as specified on the BURCFxx cards and described in the BUR Users Guide. No flame speed or duration calculation is performed, and the ignition criteria are the same as for deflagration. Additionally, the airborne DCH debris temperature must be greater than a lower limit specified by the C2203 sensitivity coefficient (default = 600K). See BUR Users Guide.

The ignition limits for the diffusion flame model are set to insure virtually complete combustion with any oxygen present in the receiving volume even if large amounts of inerting gases are present. This is done to simulate the expected effect of hot DCH debris in the incoming gas on hydrogen recombination, and is similar to the model used in calculating DCH with CONTAIN3. The diffusion flame implementation assumes burning occurs whenever the ignition criteria are met. The effects of flashback or blowout are not considered. (Note: flashback occurs when the flame is swallowed back into the combustible gas source; blowout occurs when the flame front moves away from the gas source so rapidly that it is extinguished).

3. Timestep Control

When a burn first occurs, the Burn Package requests a fallback after which the calculation continues with the timestep value specified by the BURTIM record. In addition, as the burn approaches completion, tests are included to prevent excessive overshoot of the originally-desired burn completeness values. In particular, a timestep is repeated if the originally-desired burn completeness values are crossed during that timestep and either (a) the combustible gas concentration is more than 0.5% different, or (b) the diluent concentration is more than 1% different from the originally-desired burn completeness values. These maximum overshoots can be adjusted through sensitivity coefficient C2201.

4. References

- 1 S. E. Dingman, et al., HECTR Version 1.5 User's Manual, SAND86-0101, NUREG/CR-4507 (April 1986).
- 2 G. G. Weigand, ed., Thermal-Hydraulic Process Modeling in Risk Analysis: An Assessment of the Relevant Systems, Structures, and Phenomena, SAND84-1219, NUREG/CR-3986 (August 1984).
- 3 K. K. Murata et al., Code Manual for CONTAIN 2.0: A Computer Code for Nuclear Reactor Containment Analysis, SAND97-1735, NUREG/CR-6533 (December 1997).

Cavity (CAV) Package Reference Manual

The MELCOR Cavity (CAV) package models the attack on the basemat concrete by hot (often molten) core materials. The effects of heat transfer, concrete ablation, cavity shape change, and gas generation are included, using models taken from the CORCON-Mod3 code. The coding of the models is identical to that in CORCON-Mod3, but interfaces have been modified for integration into the MELCOR framework. This integration couples the Cavity package models to thermal-hydraulic boundary conditions in the Control Volume Hydrodynamics (CVH) package, to sources of core debris from the Core (COR) and/or Fuel Dispersal Interactions (FDI) package, and to the standard MELCOR input, output, plotting, and restart capabilities. The fission-product release models in CORCON-Mod3—originally developed as the separate VANESA code—are included in MELCOR as part of the RadioNuclide (RN) package.

This Reference Manual provides an overview of modeling in the CAV package. User input for running MELGEN and MELCOR with the CAV package activated is described in the CAV Package Users' Guide. The fission-product release models (VANESA) and available input are described in the RN Reference Manual and Users' Guide, respectively.

Contents

1.	Introduction	5
2.	Phenomenology	6
3.	Models	8
3.1	System Components	8
3.2	Debris Layering and Mixing	10
3.2.1	Enforced Mixing	11
3.2.2	Enforced Stratification	11
3.2.3	Mechanistic Mixing	12
3.3	Energy Generation and Heat Transfer	14
3.4	Concrete Ablation and Cavity Shape Change	16
3.5	Chemistry	17
3.6	Mass Transfer and Associated Heat Effects	18
3.7	Debris Spreading	19
3.8	Energy Conservation	20
3.9	Material Properties	20
4.	Comparison to Stand-Alone CORCON	21
	APPENDIX A: Species List for CORCON in MELCOR CAV Package	25
	References	27

List of Figures

Figure 3.1	Cavity System Components	9
Figure 3.2	Position and Motion of Body Points	17

List of Tables

Table 4.1	Comparison of Stand-Alone CORCON-Mod3 [1] and MELCOR Cavity Package	22
-----------	---------------------------------------------------------------------------	----

1. Introduction

The Cavity (CAV) package in MELCOR models the attack on the basemat concrete by hot, often molten, core materials. The effects of heat transfer, concrete ablation, cavity shape change, gas generation, and debris/gas chemistry are included. The package consists of models taken from the CORCON-Mod3 code [1] together with all necessary interfaces to the MELCOR database and to other packages in MELCOR.

Before the initial release version of CORCON-Mod3 [2] was incorporated into MELCOR and into CONTAIN [3], a number of modifications were made to the coding that had no effect on results calculated by the stand-alone code, but allowed the direct use of all routines containing phenomenological models and properties data *without modification* in the systems codes. These changes involved a restructuring of the internal database and of the interfaces to input and output routines (including diagnostics and plotting) and to routines that provide boundary conditions for the CORCON models.

Boundary conditions for temperature and pressure used by the cavity models are obtained from an associated CVH control volume, rather than from user input as in the stand-alone CORCON. Any overlying coolant (water) pool is considered part of the boundary condition rather than part of the cavity model and is modeled by CVH. Heat and evolved gases are delivered as sources to the associated CVH volume.

Debris from the Core (COR) package, the Fuel Dispersal Interactions (FDI) package, or the External Data File (EDF) package is ordinarily deposited into the cavity through the Transfer Process (TP) package. However, initial contents may also be defined in CAV input and arbitrary addition rates may be prescribed by input to the TP package. When debris is deposited, no spreading calculation is performed because it is assumed to spread instantaneously to the maximum area permitted by the cavity geometry.

The CAV packages uses the CORCON-Mod3 properties routines, which are currently independent of the general Materials Properties (MP) package in MELCOR.

The phenomena modeled by the CAV package may be treated in more than one location in a MELCOR calculation. Transfer of material between cavities is allowed based on three tests: axial rupture, radial rupture, or a transfer triggered by a Control Function. Each of the three types of rupture (axial, radial, and triggered) can overflow to a separate cavity, but only "one-way" transfers are allowed. That is, if material can overflow from cavity 1 to cavity 2, it is not permitted to flow from cavity 2 back to cavity 1, either directly or through intermediate cavities. These ruptures can be used to model such phenomena as failure of the pedestal in a BWR Mk I or of the diaphragm slab in a BWR Mk II. Triggered transfers may also simulate (in a qualitative way) the effects of the spreading of debris across a flat floor.

CAV Package Reference Manual

The VANESA model [4] was integrated into CORCON-Mod3 to calculate the release of fission products and the generation of aerosols from debris in the cavity. The structure of MELCOR requires that radionuclides associated with debris in the cavity be treated by the RadioNuclide (RN) package, which maintains time-dependent inventories for each RN class in each cavity. The relevant subroutines from CORCON-Mod3 were therefore made part of the RN package. They are identical to the routines in the latest stand-alone version of CORCON-Mod3 and in CONTAIN; an interface is provided through a utility entry in the RN package that duplicates the functionality in the stand-alone code. See the RN package Reference Manual for more details.

Several options for direct user input of internal heating of the debris by fission products are allowed, but this heating is ordinarily calculated by the RN and DCH (Decay Heat) packages, based on RN inventories. Therefore, the effects on internal heating of relocation of debris into or between cavities, as well as the effects of RN releases within each cavity, are automatically accounted for.

2. Phenomenology

This section gives a qualitative description of the processes modeled in the CAV package in MELCOR, and the physical picture on which the models are based. The information is largely derived from Section 2.1 of the CORCON-Mod3 Manual [1]. Interfaces to other MELCOR packages are noted in the discussion.

The attack of core debris on concrete in a light water reactor is primarily thermal and may be considered quasi-steady for much of the period of a reactor accident. Decay heat and heat from chemical reactions is generated in the debris and is transferred either through its top surface or to the concrete floor. Boundary conditions at the surface, including temperature and the presence or absence of water, are obtained from the associated control volume in CVH. Heat lost from the cavity top surface is treated by CVH as a source into that control volume.

The quasi-steady partition of the heat transfer to the concrete floor and through the debris top surface is determined by the ratio of the corresponding thermal resistances. Thus, debris behavior and concrete ablation are dominated by conservation of energy, with heat transfer relations providing the most important constitutive relations.

Under the conditions visualized by the CORCON developers, the heat flux to the concrete floor is sufficient to decompose it, releasing water vapor (from both adsorbed water and hydroxides) and carbon dioxide (from carbonates) and to melt the residual oxides. The surface of the concrete is typically ablated at several centimeters per hour and molten oxides and molten steel from reinforcing bars in the concrete are added to the debris pool. The decomposition gases are strongly oxidizing at debris temperatures and will be reduced, primarily to hydrogen and carbon monoxide, on contact with metals in the debris. Ultimately, the reacted and unreacted gases enter the atmosphere above the debris pool,

where they may or may not burn immediately. (Modeling of these containment phenomena is not included in CORCON.) These gases (with appropriate enthalpies) are treated as sources in the associated control volume in CVH. The possibility that the combustible gases will burn is considered by the BUR package.

The full concrete response is extremely complicated, with elements of ablation, transient conduction, decomposition of hydroxides and carbonates in advance of the ablation front, and transport of gases and liquid water through the pores of the concrete. Further, the length scale of the temperature profile is often comparable to the size of the coarse aggregate in concrete, making any assumption of homogeneous properties questionable.

In CORCON and in CAV, concrete response is modeled as quasi-steady ablation. The thermal diffusivity of concrete is extremely small, a few times 10^{-7} m²/s. Over the time scale of interest in cavity phenomena (hours), the amount of heat which can be transferred into concrete (by transient conduction) under nonablative conditions is usually small compared to the amount of heat which must be removed from core debris through other mechanisms to maintain its temperature below the ablation temperature. Therefore, if the debris temperature is below the ablation temperature, the concrete floor surface is modeled as an adiabatic boundary.

Gas released at the bottom of the debris pool is assumed to rise through it as bubbles. Gas released at the side of the pool may also form bubbles that rise to the surface. At sufficiently high gas release rates, a stable gas film may form at either the bottom or side interfaces. Gas bubbles rising through the debris pool increase its volume. This "level swell" increases the depth of the pool and area of its radial interface with the concrete floor.

The rising bubbles also promote the production of aerosols containing fission products stripped from the fuel debris. The processes involved, reactive vaporization and bubble bursting, are treated by the VANESA model [4] in the RN package in MELCOR. This model calculates the removal and relocation of fission products and the resulting sources of aerosols for the MAEROS aerosol physics model (also part of the RN package). All necessary data concerning the temperature and bulk composition of the debris and the gas generation rates are passed by CAV to a utility entry in RN; the fission product inventories themselves are part of the RN database. The subroutines that implement VANESA in the RN package are identical to those that implement it in CORCON-Mod3.

Experimental evidence (cited in Reference 1) shows that the various oxidic species in the melt are highly miscible, as are the metallic species, but that the two groups are mutually immiscible. Previous versions of CORCON assumed that the core debris would stratify into distinct layers based on the relative densities of the phases. The passage of gas bubbles through the interface between layers can overcome this separation if the gas flux is high or the density difference is small by entraining droplets of the lower (denser) material and mixing them into the upper one. If entrainment occurs, the degree of mixing achieved is determined by a balance between entrainment and re-separation as the denser droplets settle out under the influence of gravity. The debris may therefore be fully stratified,

CAV Package Reference Manual

partially mixed, or fully mixed, and the state may change as the densities and gas fluxes change during a debris-concrete interaction.

There is a possibility that an overlying coolant layer (water) could interact with molten debris so as to break it up and form a coolable debris bed. In the MAAP code [5], this breakup and quenching is assumed to occur; it is not considered in CORCON, nor is it included in the current version of the MELCOR CAV model.

As the core-concrete interaction progresses, the debris pool grows as concrete oxides are added to it; its surface area increases, and internal heating decreases. Therefore, debris temperatures and heat fluxes decrease, and the possibility of refreezing arises. Substantial freezing of the metal phase may occur. However, the large internal heating and small thermal conductivity of the oxidic phase prevent the formation of steady, solid crusts thicker than a few centimeters. Therefore, unless the debris is spread over an extremely large area, the interior of the oxidic phase will remain molten for a long time, probably for weeks.

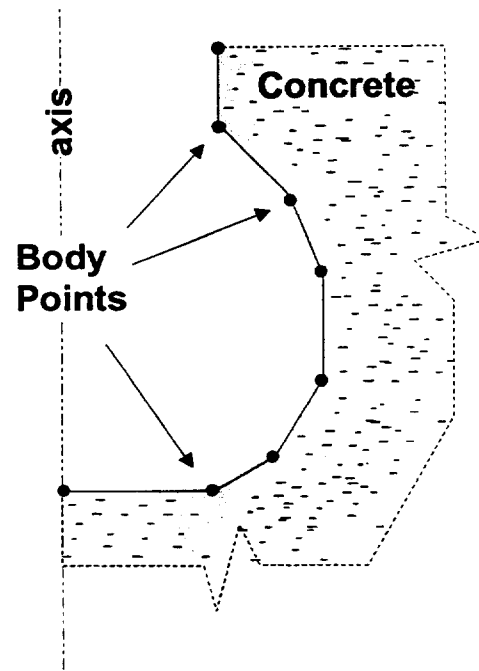
3. Models

Documentation of the CORCON-Mod3 [1] remains the primary reference for most of the submodels in the Cavity package. The following subsections briefly summarize the material contained there, while noting modifications made for incorporation into MELCOR.

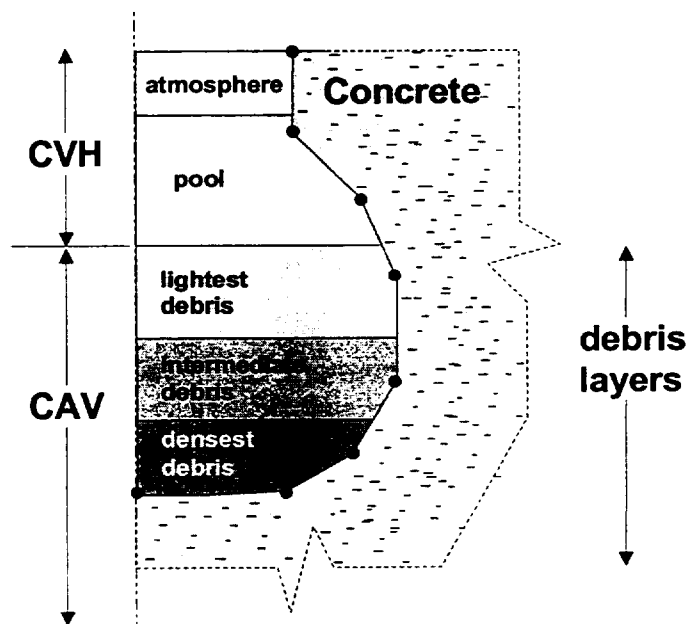
3.1 System Components

The physical system considered by the Cavity package consists of an axisymmetric concrete cavity, a multilayered debris pool, and a set of boundary conditions (provided by CVH) at the top surface of the debris, as illustrated in Figure 3.1.

The shape of the concrete cavity is described by a series of so-called *body points* lying in a vertical cross-section of the concrete surface. The initial shape is defined by user input. The concrete itself is described by specifying an average chemical composition; its thermochemical properties are then obtained from an internal database of properties for the component species. A number of standard compositions are available by name as built-in defaults, or the user may define composition and melting temperatures through input.



(a) Cavity Geometry



(b) Cavity Contents and Boundary Conditions

Figure 3.1 Cavity System Components

The modeling assumes that all oxidic species in the debris are mutually miscible, as are all metallic species, but that oxides are not miscible with metals. If the densities of the phases are different, the debris will tend to separate into distinct oxidic and metallic phases under the influence of gravity, but this stratification may be partially or completely overcome by the stirring effect of gas bubbles. If the density difference is sufficiently small and the gas bubbles sufficiently large, droplets of a lower (denser) layer can be entrained across the interface to mix with a lighter layer above it.

The debris pool is modeled as a number of layers filling some part of the concrete cavity. Pure-phase and mixed-phase layers may be included, and the ordering of the layers is assumed to be determined by their densities, with the densest on the bottom and the lightest on top. Many configurations are possible, as discussed in Section 3.2. Layer volumes, including the swelling effects of gas bubbles, determine the elevations of layer interfaces and of the debris surface.

3.2 Debris Layering and Mixing

Five possible types of debris layers are considered in CORCON; each has a conventional three-letter designation in the associated documentation. In order of increasing density they are:

- LOX: Pure oxide, less dense than the metallic phase;
- LMX: Mixed phases, less dense than the metallic phase;
- MET: Pure metal;
- HMX: Mixed phases, more dense than the metallic phase; and
- HOX: Pure oxide, more dense than the metallic phase.

If only oxides are present, the debris is called LOX by convention. The possibility of creating mixed-phase layers was introduced as part of the enhanced modeling in CORCON-Mod3. The major assumptions concerning these mixed layers is very specific:

The LMX layer is formed by entrainment of metal from MET or HMX into a previously existing LOX layer, and consists of a suspension of discrete droplets of metal in a less-dense continuous oxidic phase. The mixing is assumed to be complete so that the LOX layer is converted to an LMX layer in the process; LMX and LOX cannot exist simultaneously. The entrainment competes with settling of the denser metal droplets from LMX back into the lower layer (or to form a new MET layer if there is no lower metal-containing layer present).

The HMX layer is formed by entrainment of oxides from HOX into a previously existing MET layer, and consists of a suspension of discrete droplets of oxide in a less-dense continuous metallic phase. The mixing is assumed to be complete so that the MET layer is converted to an HMX layer in the process; HMX and MET cannot exist simultaneously. The entrainment competes with settling of the denser

oxide droplets from HMX back into HOX (or to form a new HOX layer if there is none present).

Under these assumptions, there are 15 possible configurations of the debris. These can be summarized as follows:

	1	2	3	4	5	6	7	8	9	10	11	12	13	14	15
LOX				X	X	X					X				X
LMX							X	X	X	X		X	X		
MET	X			X			X				X	X		X	
HMX		X	X		X	X			X	X					
HOX	X	X		X	X		X	X	X						

where "X" denotes the presence of the layer.

Three options are available for the treatment of layering and mixing of debris in CORCON. They are (1) enforcement of complete mixing, (2) enforcement of complete stratification, and (3) mechanistic modeling of the entrainment and separation processes. The first of these (complete mixing) is the default in the CAV package in MELCOR, but the user may specify any of the options by input of MIXING on the CAVnnak record.

3.2.1 Enforced Mixing

This is the simplest of the options, with the debris always considered to form a single layer. If both metals and oxides are present, the layer will be HMX or LMX (configuration 3 or 13), depending on the relative densities of the phases. If there is only a single phase, it will be either MET or LOX (configuration 14 or 15). As noted previously, this is the default treatment in MELCOR.

3.2.2 Enforced Stratification

This was the only option available in CORCON in versions prior to Mod3, in which the possible creation of heterogeneous mixtures of metals and oxides was not considered. It was therefore the only option available in versions of MELCOR prior to 1.8.3.

When this option is specified, the possibility of two oxidic layers, physically separated by a metallic layer, is allowed for. If the initial oxide phase is sufficiently rich in UO₂ (fuel) to be more dense than the initial metallic phase, it is assumed to form an oxidic layer beneath the one containing the metals. An oxide slag, rich in concrete and steel oxides and less dense than the metals will then accumulate on top of the metal layer. Thus, the most

general structure of the debris pool is a light oxide layer (LOX), over a metallic layer (MET), over a heavy oxide layer (HOX).

This three-layer configuration (configuration 4) can persist until dilution by less dense concrete oxides renders the HOX layer less dense than the MET layer. The configuration is then (instantaneously) converted to one containing only MET and LOX (configuration 11), with the latter layer combining the previous contents of HOX and LOX. Addition of UO_2 -rich debris to a debris pool in the LOX-over-MET configuration can result in an oxide mixture that is denser than the contents of MET. When this occurs, the LOX is eliminated and the configuration is (instantaneously) converted to one of MET over HOX (configuration 1). These changes in configuration are effected by checking the relative densities of adjacent layers at every step of the calculation, and relocating and/or combining the layers as appropriate.

3.2.3 Mechanistic Mixing

The most general option uses mechanistic models for entrainment and separation developed by Green [6, 7, 8] to predict the occurrence and extent of mixing. One consequence of this modeling is to eliminate the instantaneous change in debris configuration (often referred to as "layer flip") resulting from an insignificant change in the relative densities of the debris phases. Instead, the phases will become increasingly strongly mixed whenever their densities approach equality (unless there is no gas flow to drive the mixing).

The entrainment model assumes that bubbles passing through the interface between two layers may carry material from the lower layer into the upper one if they are large enough. The critical diameter depends on density ratios and on the surface tension of the liquid-liquid interface; above the threshold, a correlation is used to determine the volume of condensed-phase material entrained by each gas bubble. The separation model is based on the terminal velocity of falling droplets of a size corresponding to the critical Weber number for the onset of droplet oscillations.

Competition between these processes defines the net rate of mixing or separation at the various layer interfaces. The model considers entrainment of oxides from HOX into HMX or LMX, or into MET to form HMX, and of metal from MET or HMX into LMX or into LOX to form LMX. It also considers the possibility that a mixed layer is unstable and will separate to produce a new HOX layer below HMX or a new MET layer below LMX.

After release of the initial version of CORCON-Mod3 [2], the numerical implementation of the models into MELCOR was modified to provide numerical stability with reasonable timesteps. The entrainment rate depends primarily on the gas flux; therefore, over a finite timestep,

$$\dot{m}_e(t) \approx \dot{m}_e(0) \quad (3.1)$$

However, the separation rate is proportional to the mass of the discontinuous phase in the mixed layer, and has the form

$$\dot{m}_s(t) = \frac{M_D(t) v_{\text{settle}}}{L_M} \quad (3.2)$$

where v_{settle} is the settling velocity, M_D is the mass of droplets suspended in the mixed layer, and L_M is thickness of that layer.

The mass of suspended droplets therefore satisfies

$$\frac{dM_D}{dt} = \dot{m}_e(t) - \dot{m}_s(t) \approx \dot{m}_e(0) - \frac{M_D(t)}{\tau_s} \quad (3.3)$$

where

$$\tau_s \equiv \frac{L_M}{v_{\text{settle}}} \quad (3.4)$$

is the time constant for separation. Equation (3.3) has the analytic solution.

$$M_D(t) = M_D(0) + [\dot{m}_e(0)\tau_s - M_D(0)](1 - e^{-t/\tau_s}) \quad (3.5)$$

Equation (3.5) expresses the fact that entrainment and separation approach a balance where the mass of suspended droplets M_D^{ss} is

$$M_D^{ss} = \dot{m}_e \tau_s \quad (3.6)$$

with a characteristic time τ_s . Independent treatment of the competing processes will be numerically unstable unless the timestep, Δt , is less than τ_s , and the results will be dependent on timestep unless Δt is *much* less than τ_s . Because the time constant may be relatively short compared to the rates at which conditions are changing, the revised

version of CORCON-Mod3 applies the analytic solution given by Equation (3.5) over a timestep. This requires moving a net mass

$$\Delta M_e^{net} = (\dot{m}_e^0 \tau_s - M_D^0) (1 - e^{-\Delta t / \tau_s}) \quad (3.7)$$

from the lower layer to the upper layer during the timestep, where superscript 0 denotes evaluation at the start of the step. If the net move is positive, it must be limited to the contents of the lower layer. If it is negative, it cannot—by its very form—exceed the mass of droplets initially suspended in the upper layer. This change in numerical implementation has eliminated almost all of the instabilities observed in layer mixing in the initially released version of CORCON-Mod3.

3.3 Energy Generation and Heat Transfer

The fuel/concrete interaction is driven primarily by decay heat power generated within the debris pool, with heat from oxidation reactions also contributing. In stand-alone CORCON, the decay heating is calculated by an internal model based on an initial fission product inventory and fits to the decay powers for each of the 27 elements in CORCON. In MELCOR, this heating is calculated by the RN and DCH packages; the model is conceptually very similar to that in CORCON (see the RadioNuclide (RN) and Decay Heat (DCH) Package Reference Manuals and Reference 1), but the CAV database contains no information on the location—or relocation—of the fission products. (The exact model used in stand-alone CORCON is therefore not available, even as an option, in MELCOR.) Heat sources based on control functions and/or tabular functions are also permitted, primarily for simulation of experiments.

For the calculation of energy conservation, each debris layer is treated as a lumped mass with a single (average) temperature. The heat flux between the interior of each layer and each of its interfaces (with another layer, with concrete, or with the pool or the atmosphere in the bounding control volume) is treated separately. Continuity of the heat flux determines the temperature of each interface.

The possible heat transfer regimes within each debris layer are conduction and natural convection, based on conventional correlations, and bubble-enhanced convection based on Kutateladze [9] and surface renewal [10] models. The correlations are implemented in such a way that they reproduce correlations for convective heat transfer in internally heated fluid layers (in the absence of gas flows) developed by Kulacki and co-workers [11, 12, 13] with a maximum error of 30 percent and an average error closer to 10 percent. An enhancement factor developed by Farmer [14] is applied at the top surface of the debris (adjacent to the coolant or the atmosphere) to account for the greater surface area of the unstable surface.

The modeling includes the possibility that the interior of a layer may be fluid, with heat transfer by convection, while one or more of its axial and radial surfaces is covered by a solid crust, with heat transfer by conduction [15]. In all cases, only one-dimensional effects are considered, and the situation is assumed to be quasi-steady.

Losses from the surface are calculated, based either on radiation and convection in the absence of overlying water or on a complete pool boiling curve in its presence. The representation of the boiling curve is the one used in CORCON [1], and includes convection, nucleate boiling, transition boiling, and film boiling regimes. In the film boiling regime, the effects of coolant subcooling and of gas barbotage (injection of noncondensable gas at the coolant interface), both of which can greatly increase both the film boiling heat flux and the temperature at which the film collapses (the Leidenfrost point), are also included.

The concrete surface is treated using a quasi-steady ablation model. If concrete is ablating, it presents a constant temperature boundary condition defined by the ablation temperature, T_a . This temperature is obtained either from internal data or user input. Under quasi-steady conditions, changes in the sensible heat content of the preheated region in advance of the ablation front may be neglected. (As mentioned in Section 2, the thermal diffusivity of concrete is extremely small. The *total* heat content of this region is therefore small, and is neglected.) The rate of ablation (in $\text{kg/m}^2\text{-s}$) is then proportional to the heat flux (W/m^2) from the debris to the concrete surface. Their constant of proportionality is simply the inverse of the heat of ablation h_a .

If the heat flux to a concrete surface at an assumed temperature of T_a would be negative, no ablation can be taking place, and heat transfer can affect only the thermal boundary layer in the concrete. Under these conditions, change in the heat content of this boundary layer is neglected and the concrete surface is treated as an adiabatic boundary. Further decomposition of concrete in advance of ablation is also neglected.

An additional thermal resistance is included between the debris and the concrete. CORCON-Mod3 allows this resistance to be calculated using either a gas film or a slag film model. In each case, separate models are provided for the bottom and side surfaces of the debris.

The gas film models are based on the assumption of a gas film between the debris and the concrete. An analog of Taylor-instability-bubbling film boiling is used on nearly horizontal surfaces [16], and an analog of attached-flow film boiling is used on strongly inclined surfaces. A transition from bubbling to flow is made over a range of inclination angles. Details of the model are presented in Reference 1.

A detailed slag film model was developed by Bradley [17], based on a picture of transient growth and removal. He found that when the resulting thermal resistance of the slag film was combined with the resistance within the debris layer, the net heat transfer coefficient between the interior of the debris and the concrete surface could be adequately

CAV Package Reference Manual

represented as a constant multiple (0.29) of the latter coefficient over a wide range of conditions. The heat transfer coefficient for the slag film model is therefore calculated in CORCON as 0.41 times the heat transfer coefficient between the interior of the debris and its surface, for either the bottom and side surfaces of the debris, so that the net heat transfer coefficient is $1.0 \cdot 0.41 / (1.0 + 0.41) = 0.29$ times the internal heat transfer coefficient.

The model to be used may be selected independently for the bottom and side surfaces of the debris. The default in MELCOR 1.8.3 and later versions is to use the gas film model in both places, consistent with previous versions of MELCOR. The user may specify which model is to be used on the bottom and/or side surfaces by input of GFILMBOTT or GFILMSIDE on the CAVnnak record, as described in the CAV Package Users' Guide. (There is no default for the choice of models in stand-alone CORCON-Mod3, and the Manual [1] provides no recommendation.)

3.4 Concrete Ablation and Cavity Shape Change

In steady-state ablation, the incident heat flux and the ablation rate are directly proportional; the ratio is simply the volumetric ablation enthalpy. Therefore, the heat flux to the concrete at each body point in the cavity profile is used to calculate the local ablation rate. A new position of the body point is then calculated, displaced along the local normal to the surface. To maintain calculational stability, the cavity profile is then rezoned, and the body points are interpolated back onto a series of guiding lines called rays, as illustrated in Figure 3.2. The effect of the rezone is that the body points must follow the rays, and their spacing along the cavity profile is constrained. As shown in the figure, all but one of the rays pass through a user-defined origin. The final ray lies parallel to the axis, through the outermost point on the flat bottom of the cavity, and serves to ensure that this flat bottom remains flat. The scheme evolved from the CASCET model [18] written by ACUREX/Aerotherm Corporation under contract to Sandia.

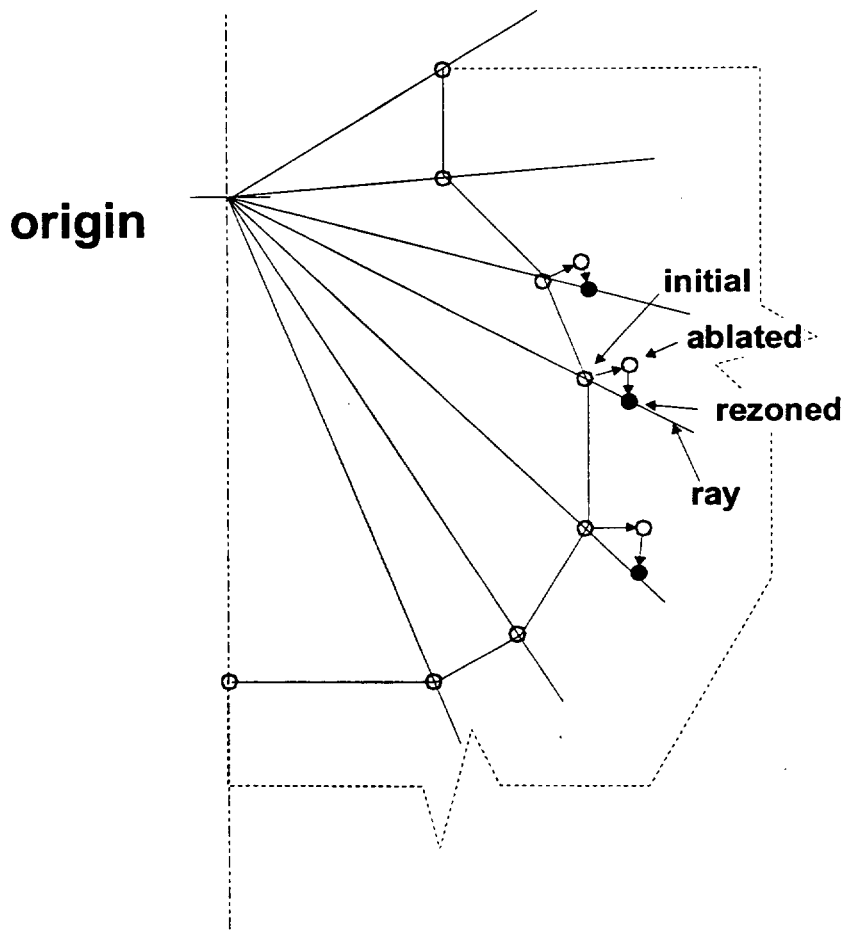


Figure 3.2 Position and Motion of Body Points

3.5 Chemistry

The chemistry considered in the Cavity package of MELCOR involves interactions between concrete decomposition products and metallic species in the debris pool. Equilibrium chemistry is assumed, without consideration of rate limiting effects. The calculational method is very general and is based on minimization of the total Gibbs function for a metallic phase, a gaseous phase, and an oxidic phase. Each of the three phases is treated as an ideal solution; that is, the entropy of mixing is considered, but any heat-of-solution effects are ignored.

Two separate reactions are considered. The first involves reactions in the interior of the debris. For a pure metal layer, it is modeled as mutual equilibrium among the metal layer and the gas bubbles and concrete decomposition oxides passing through it. For a mixed-phase layer, the oxidic constituents of the layer are included as reactants. The primary effect is the oxidation of metals by the H_2O and CO_2 in the bubbles. However, if the metallic phase contains significant amounts of Zr, it can also reduce the concrete oxides

CAV Package Reference Manual

to produce metallic Al, Ca, and Si. The user may specify that these reactions be ignored (as in older versions of CORCON) through input of CTOXYREA on record CAVnnak; in this case, only the products of metal oxidation are included in the oxide phase.

The second reaction involves mutual equilibrium among the metal layer, the gas film at its radial boundary, and the products of metal oxidation. Concrete decomposition (and other) oxides are not included in this reaction.

The gaseous reactants are H_2O and CO_2 , and the principal gaseous products are H_2 and CO . The full equilibrium calculation in CORCON predicts the formation of small amounts of additional gaseous species including hydrocarbons and various dissociation products such as atomic hydrogen. Most, if not all, of these species are predicted to occur in quantities insufficient to warrant their inclusion in the control volume inventories. To ignore them would violate mass conservation, and there is insufficient information to unambiguously convert them to "equivalent" amounts of significant species. The problem can be avoided by imposing constraints in minimization of the Gibbs function to eliminate consideration of any gaseous species other than H_2O , CO_2 , H_2 , and CO . This option was added to stand-alone CORCON-Mod 3 after its initial release, and is used in MELCOR. The results conserve mass and represent a restricted equilibrium state consistent with the modeling of atmosphere chemistry in MELCOR. We believe this to be a reasonable approach. If it were desired to include additional gases such as methane, only a trivial change to coding would be required. This is because the Gibbs function to be minimized has not been changed, but only the domain over which it is minimized.

The equilibrium calculation sometimes predicts the "coking" reaction in which CO_2 is fully reduced to condensed carbon (rather than simply to CO), primarily in the presence of metallic Zr. Because simulant experiments have not provided overwhelming evidence either for or against the occurrence of coking, the user is permitted to specify whether this reaction will be permitted in CORCON. The default in MELCOR is to suppress the production of condensed carbon, but the user may enable this production by input of the COKE parameter on the CAVnnak record.

In stand-alone CORCON, the chemistry includes an extremely simplified consideration of fission products; in MELCOR, this calculation is entirely replaced by the VANESA model [4] in the RN package.

3.6 Mass Transfer and Associated Heat Effects

The processes involved include the injection of concrete decomposition products (condensed and gaseous) into the debris pool, the addition of core and structural materials from other packages through the use of TP, the addition of debris from rupture or overflow of another cavity, and the production of condensed-phase materials from chemical reactions. Also involved is the transport of all these materials to their proper locations, whether within a debris layer in CAV or in a CVH volume. These processes modify both

the mass inventories and the energy contents of the various debris layers and determine the mass source delivered to CVH and its associated enthalpy.

The masses and enthalpies of all debris layers are updated for mass transfer and associated heat transfer in two passes. These passes follow the paths of gaseous and condensed-phase concrete decomposition products, and of the products of chemical reactions involving these materials. The updating procedure is designed to account for successive interactions of transported materials, from the location where they are born to the location where they reside at the conclusion of the advancement procedure.

The first pass, upward through the debris pool, follows the rising gases and rising condensed-phase materials from concrete decomposition or melt/gas reactions. (The direction of motion of condensed-phase materials is determined by its density relative to the density of the local layer material.) The materials are thermally equilibrated with any layers they pass through, and their mass and energy are ultimately added to the layer where they end up (condensed phases) or to the associated CVH volume (gases). For condensed-phase materials, this final layer is assumed to be the first layer encountered that already contains that phase: HMX, MET, or LMX for metals, and any layer *but* MET for oxides. A new LOX layer may be formed to accommodate rising oxides from concrete ablation or metal oxidation or none already exists. Similarly, a new MET layer may be created to accommodate steel from melting reinforcing bars in concrete if the pool contains only a dense oxide layer.

Melt/gas chemical reactions are evaluated during this upward pass, following rising bubbles and flowing films. The composition of the layer involved is modified to reflect the effects of the reaction and, if the reaction takes place in the pure metal layer (MET), the condensed phase oxidic products are added to the rising inventory. The gas composition is modified appropriately, and the heat of reaction is assumed to remain with the layer in which the reactions occurs.

The second pass, downward through the debris pool, is similar; it follows any material entering from above (from another cavity or from a TP), and any sinking reaction and/or concrete ablation products. If the mechanistic mixing model is used, mixing calculations are done during the downward pass. This differs from the initially released version of CORCON-Mod3 [2]. The change was made because separation of a mixed layer can create a new pure-phase layer *below* it, and the revised order of calculations greatly simplifies the logic in treating this possibility.

3.7 Debris Spreading

In general, CORCON assumes that debris will spread uniformly and instantaneously across the full width of any cavity into which it is deposited. CORCON-Mod3 added an optional parametric capability to simulate the finite rate of debris spreading by prescribing a maximum radius of the axially symmetric debris pool as a function of time. This can be

CAV Package Reference Manual

used to confine the debris as a slowly spreading or non-spreading glob on the floor for some period of time and/or to delay its contact with the side walls of the cavity for as long as may be desired. One effect will be to reduce the surface area of the debris, thus reducing the rate at which it can lose heat. This modeling may affect the timing of the debris-concrete interaction in cases where the initial debris is largely solidified, and is incapable of ablating concrete at a significant rate until it has become more fluid as a result of continued heating by internal decay heat.

In stand-alone CORCON, the maximum radius must be specified as a function of time by an input table. In MELCOR, it may be specified by a tabular function, a control function, or a channel in an external data file. In most MELCOR calculations, debris will not appear in the cavity until after the reactor vessel fails, and the time of this event will not be known in advance. The control function option allows the radius to be defined as a function of time *relative to debris deposition*. It could also be used to consider the debris temperature (as an indicator of its viscosity) in estimating the spreading rate.

In the initially released version of CORCON-Mod3, the radial surface of spreading debris was subjected to the same thermal boundary condition as the top surface. A subsequent revision allows optional treatment of this boundary as adiabatic. This capability is available in MELCOR.

3.8 Energy Conservation

CORCON uses a formulation for the energy equation for debris in the cavity in which temperature-driven heat transfers between layers are treated semi-implicitly, as described in Reference 1. Numerical difficulties associated with addition of new debris were observed during incorporation into MELCOR. The implementation of the equation was substantially modified to improve stability by including modifications made to previous versions of CORCON in the CAV package of MELCOR 1.8.2. The revised numerical treatment is now included in the stand-alone code as well as in MELCOR.

3.9 Material Properties

The material properties in the CAV package are those of the stand-alone CORCON code. They include internally consistent specific heats, enthalpies, and chemical potentials for a large number of condensed and gaseous species, based on fits to JANAF [19] and other data. All enthalpies are based on the JANAF thermochemical reference point. All heats of reaction are therefore implicitly contained in the enthalpy data. Also included are data on thermal expansivity and density, thermal conductivity, viscosity, and surface tension.

The list of materials for which properties are defined is contained in Appendix A. These data are independent of the MELCOR data contained in the Water (H₂O), NonCondensable Gas (NCG), and Material Properties (MP) packages. They are retained both for

consistency with the stand-alone CORCON code and to facilitate incorporating future upgrades to CORCON modeling into MELCOR. Appropriate adjustments to enthalpies are made whenever materials are passed into or out of the Cavity package.

Additional models are included for evaluating the properties of mixtures. Details of the material properties models, and further references, are contained in Reference 1. Most are quite conventional, but two deserve further discussion in this Reference Manual.

In determining the enthalpy of a mixture as a function of temperature, a submodel is used to determine its melting range as defined by solidus and liquidus temperatures. Below the solidus temperature of the mixture, properties for the solid phase of each species—extrapolated, if necessary—are used. Similarly, liquid phase properties (possibly extrapolated) are used above the liquidus temperature. Between solidus and liquidus, the enthalpy is interpolated as a linear function of temperature (corresponding to a constant specific heat).

The melting range for the metallic phase is determined from a fit to the ternary phase diagram for Cr-Fe-Ni; other elements (Zr, C) are simply ignored. If the metal phase contains no Cr, Fe, or Ni, however, the melting point of Zr will be used. The melt range for an oxidic phase is determined by reference to a pseudo-binary phase diagram based on an ideal solution model for the liquid and solid phases. One component is high melting and is assumed to consist of fuel (UO_2 and ZrO_2); the second component is low melting and includes everything else. The corresponding melting temperatures and effective latent heats are taken from internal data for fuel for the first component and from the properties of the concrete oxides for the second.

Also modeled is the effect of SiO_2 content on the viscosity of oxidic mixtures, based on a modification of a correlation derived by Shaw [20]. The original correlation was fit to a database containing geologic data for materials with relatively high silica contents; no consideration was given to application of the correlation outside of the range of compositions included in the original database. As implemented in CORCON and in MELCOR, the original correlation has been modified to avoid nonphysical extrapolation characteristics. It is coupled to a conventional Kendell-Monroe [21] mixture model in such a way that the viscosity is a continuous function of composition over an unrestricted range of compositions. Details are given in Reference 22.

4. Comparison to Stand-Alone CORCON

The Cavity (CAV) package in MELCOR consists primarily of the CORCON-Mod3 code [1]. The calculational routines are identical to those in the stand-alone code, but input, output, and interfaces to boundary conditions are different. In addition, the MELCOR implementation includes several sensitivity coefficients to allow user control of submodels in CORCON. The sensitivity coefficients currently available are:

CAV Package Reference Manual

1. an additive modification to the concrete ablation enthalpy, and
2. coefficients in many heat transfer relations.

In future versions, we expect to expand this list to allow access to more of the so-called "user flexibility" options available in CORCON-Mod3.

Additional similarities and differences with respect to CORCON-Mod 3 are summarized in Table 4.1.

Table 4.1 Comparison of Stand-Alone CORCON-Mod3 [1] and MELCOR Cavity Package

Feature	CORCON-Mod3	MELCOR
Concrete Cavity, Layered Debris, Debris/Concrete Heat Transfer, Concrete Ablation	Treatment identical	
Ablation Delay	Not permitted	Optional control function
Overlying Water	Simple equilibration of rising gases	Part of CVH SPARC bubble model
Atmosphere and Surroundings	User-input tabular boundary conditions	Boundary conditions from CVH Package
Debris/Water or Debris/Atmosphere Interface	Models and correlations identical; numerics of solution modified for MELCOR	
Fission Product (F.P.) Inventories	Six "pseudo-species" (coarse grouping) included in CORCON; separate detailed inventory for VANESA	Treated in detail by RN package (not part of CAV package inventory)
Internal Heating	Internal model based on F.P. inventories or input table	From DCH package, based on fission product inventories or input table
Fission Product Release	Models and correlations identical; numerics of solution modified by location of model in RN package in MELCOR	

Table 4.1 Comparison of Stand-Alone CORCON-Mod3 [1] and MELCOR Cavity Package

Feature	CORCON-Mod3	MELCOR
Debris/Gas Chemistry	General equilibrium gases, metals, oxides	Same model, minor gas species suppressed
Cavity Rupture/Debris Overflow	Not modeled	Mechanistic melt-through or "triggered" failure; overflow to lower cavity
Debris Addition	User-input table	Through TP package, from other MELCOR package or table input, or from other cavity overflow or rupture
Debris Spreading	Parametric model; requires user-input table vs. time	Same model, but allows calculation using control functions
Associated F.P. Addition	Based on added UO_2 , or user-input table	Calculated by RN for package providing debris source, or table input
User Control of Modeling	Provided through "user flexibility" options [2]	Provided by user input and sensitivity coefficients; not all "user flexibility" options are enabled
Restart/Fallback Capability	Not available	Provided as part of MELCOR structure
User Input	Fixed format	MELCOR free-field format
Printed Output	Controlled by CORCON input	Essentially identical; controlled by MELCOR input
Plotted Output	Latest version allows use of HISPLTM	Plots available in normal MELCOR manner

The differences between the MELCOR Cavity package and stand-alone CORCON-Mod3 listed in Table 4.1 fall into three distinct groups:

CAV Package Reference Manual

1. Coupling of Phenomena

These differences include the use of calculated boundary conditions such as temperature, pressure, and debris addition rates rather than user-supplied tabular data which must be generated from some independent source, and the provision to allow debris to be relocated between two or more locations when cavity boundaries fail. CAV allows the use of tabular boundary conditions by defining time-specified volumes in CVH and/or tabular debris addition rates through TP and EDF. Both CORCON-Mod3 and MELCOR can calculate internal decay heating based on fission product inventories, with these inventories based on fission product release rates calculated using VANESA. In MELCOR, the decay heat is based directly on the detailed inventories calculated by VANESA; in CORCON-Mod3, these inventories must be approximately mapped back into the coarse group inventories used by the CORCON decay heat model.

2. User Control

MELCOR is intended for use as a PRA code while versions of CORCON prior to Mod3 were developed as best-estimate codes. Therefore, MELCOR 1.8.2 allowed more user control of modeling options than did the then-existing versions of CORCON. User flexibility options were made available in CORCON-Mod3. Although there was some overlap in capabilities, several of the sensitivity coefficients in the MELCOR 1.8.2 CAV package have not been reconnected to CORCON-Mod3, and many of the user flexibility options in that code have not yet been made accessible from MELCOR input. This situation will be corrected in later versions of MELCOR.

3. User Interface, User Convenience

These differences include revised input formats, restart and fallback capabilities, and plot capabilities, which have no effect on modeling of physical phenomena.

Although the CAV package in MELCOR and the stand-alone CORCON-Mod3 code contain identical versions of all subroutines incorporating phenomenological models and materials properties, they should be viewed as distinct entities because of the differences in treatment of interfaces and calculation of boundary conditions. However, because the basic modeling is identical, it is possible to run equivalent calculations with the two codes under appropriate choices of options and restrictions on boundary conditions.

APPENDIX A: Species List for CORCON in MELCOR CAV Package

The following lists the species considered by CORCON and available for use in MELCOR, either as initial contents in the melt or as constituents of concrete:

OXIDES	METALS
SIO2	FE
TIO2	CR
FEO	NI
MNO	ZR
MGO	MN
CAO	C(C)
SRO	NA
BAO	AL
LI2O	U
NA2O	SI
K2O	UAL3
FE2O3	UAL2
ALSO3	CA
UO2	
ZRO2	
CR2O3	
NIO	
FE3O4	
MN3O4	
PUO2	
UO3	
U3O8	

CAV Package Reference Manual

The observant reader may note that several additional species are included in the corresponding list, Table 2.1, in [1]. These include the aluminates, fission products, and element "X", which are (or were) used in internal models in stand-alone versions of CORCON and are not relevant to the implementation in MELCOR.

There are five additional species which may be used in specification of concrete compositions:

CONCRETE CONSTITUENTS
CO ₂
H ₂ O _{CHEM} (chemically bound water)
H ₂ O _{EVAP} (evaporative water)
CaCO ₃
Ca(OH) ₂

These are used only in specification of the concrete composition; in particular, CaCO₃ and Ca(OH)₂ are decomposed during initialization into CaO plus CO₂ and into CaO plus H₂O_{CHEM} respectively. The difference between H₂O_{CHEM} and H₂O_{EVAP} is the binding energy which must be overcome to release the chemically-bound water from the concrete.

The list of gases in Table 2.1 of Reference 1 is not relevant to MELCOR input, as the composition of the control volume above the debris pool is determined by the CVH package. In addition, production of all trace gaseous species has been suppressed in the chemical reaction routines so that the only gases considered by CORCON in MELCOR are H₂, H₂O, CO, and CO₂.

References

1. D. R. Bradley and D. R. Gardner, CORCON-MOD3: An Integrated Computer Model for Analysis of Molten Core-Concrete Interactions. Users Manual, NUREG/CR-5843, SAND92-0167, Sandia National Laboratories, Albuquerque, NM (October 1993).
2. K. E. Washington, Letter Report to Sudhamay Basu, USNRC, "CORCON-Mod3 Code Integration," under FIN L1484 (February 1993).
3. K. K. Murata et al., Code Manual for CONTAIN 2.0: A Computer Code for Nuclear Reactor Containment Analysis, NUREG/CR-6533, SAND97-1735, Sandia National Laboratories, Albuquerque, NM (December 1997).
4. D. A. Powers, J. E. Brockmann, and A. W. Shiver, VANESA: A Mechanistic Model of Radionuclide Release and Aerosol Generation During Core Debris Interactions with Concrete, NUREG/CR-4308, SAND85-1370, Sandia National Laboratories, Albuquerque, NM (July 1986).
5. MAAP, Modular Accident Analysis Program User's Manual, Volumes 1 and 2, IDCOR (undated).
6. G. A. Greene, "Heat, Mass, and Momentum Transfer in a Multi-Fluid Bubbling Pool," Advances in Heat Transfer, Vol. 21, pp. 270-345 (1991).
7. G. A. Greene, J. C. Chen, and M. T. Conklin, "Onset of Entrainment Between Immiscible Liquid Layers Due to Rising Gas Bubbles," International Journal of Heat and Mass Transfer, Vol. 31, p. 1309 (1988).
8. G. A. Greene, J. C. Chen, and M. T. Conklin, "Bubble-Induced Entrainment Between Stratified Liquid Layers," International Journal of Heat and Mass Transfer, Vol. 34, p. 149 (1990).
9. S. S. Kutateladze and I. G. Malenkov, "Boiling and Bubbling Heat Transfer Between a Gas-Liquid System and a Heat Exchange Element," Zhurnal Prikladnoi Khimii (Journal of Applied Chemistry of the USSR), Vol. 35, No. 11 (1962).
10. G. A. Greene and T. F. Irvine, "Heat Transfer Between Stratified Immiscible Liquid Layers Driven by Gas Bubbling Across the Interface," in ANS Proceedings of the 1988 National Heat Transfer Conference, Houston, TX, July 24-27 (1988).
11. F. A. Kulacki and R. J. Goldstein, "Thermal Convection in a Horizontal Fluid Layer with Uniform Volumetric Energy Source," Journal of Fluid Mechanics, Vol. 55, No. 2, p. 271 (1975).

CAV Package Reference Manual

12. F. A. Kulacki and M. E. Nagle, Journal of Heat Transfer, Vol. 97, p. 204 (1975).
13. F. A. Kulacki and A. A. Emara, Trans. ANS, Vol. 22, No. 2, p. 447 (1975).
14. M. T. Farmer, J. J. Sienicki, and B. W. Spencer, "CORQUENCH: A Model for Gas Sparging-Enhanced Melt Water Film Boiling Heat Transfer," ANS Special Session on Thermal Hydraulics of Severe Accidents, November 11-15, 1990.
15. R. K. Cole, Jr., "A Crust Formation and Refreezing Model for Molten-Fuel/Concrete Interaction Codes," Paper 12.5 in Proceedings, International Meeting on Light Water Reactor Severe Accident Evaluation, Cambridge, MA (1983).
16. H. Alsmeyer and M. Reimann, "On the Heat and Mass Transport Processes of Horizontal Melting or Decomposing Layer under a Molten Pool," Nuclear Reactor Safety Heat Transfer, Winter Annual Meeting ASME, Atlanta, GA, pp. 47-53 (1977).
17. D. R. Bradley, "Modeling of Heat Transfer Between Core Debris and Concrete," in ANS Proceedings of the 1988 National Heat Transfer Conference, Houston, TX, p. 37-49 (July 1988).
18. K. C. Kwong, R. A. S. Beck, and T. C. Derbidge, CORCON Program Assistance, FR-79-10/AS, ACUREX Corporation/Aerotherm Aerospace Division, Mt. View, CA (July 1979).
19. JANAF Thermochemical Tables, DOW Chemical Company, Thermal Research Laboratory, Midland, MI (1965).
20. H. R. Shaw, "Viscosities of Magmatic Silicate Liquids: An Empirical Method of Prediction," American Journal of Science, Vol. 272, pp. 870-893 (1972).
21. J. Kendell and K. P. Monroe, "The Viscosity of Liquids, III Ideal Solution of Solids in Liquids," Journal of the American Chem. Soc., Vol. 39, No. 8, p. 1802 (September 1917).
22. R. K. Cole, Jr., D. P. Kelly, and M. A. Ellis, "Molten Fuel/Concrete Interactions Study," in Light Water Reactor Safety Research Program Semiannual Report, April-September 1982, NUREG/CR-3407, SAND83-1576, Nuclear Fuel Cycle Program, Sandia National Laboratories, Albuquerque, NM (October 1983).

Condenser (CND) Package Reference Manual

The purpose of the MELCOR CND Package is to model the effects of the Isolation Condenser System (ICS) and the Passive Containment Cooling System (PCCS), both of which use heat exchangers submerged in large water pools. Several older boiling water reactors (BWRs) and the new proposed simplified boiling water reactor (SBWR) contain isolation condensers to condense steam created in the core and return it to the primary system. Only the simplified boiling water reactor, however, contains the passive containment cooling system to provide steam suppression in the drywell in the event of a LOCA or when the depressurization valves are used to equalize the pressures of the reactor vessel and containment. This equalization is required so that water can drain to the reactor vessel from the gravity-driven cooling system pools located several meters above the top of the core. The CND Package constitutes a subpackage within the ESF Package. The removal or transport of fission product vapors and aerosols is not modeled. The Reference Manual gives a description of the subroutines used in the CND Package.

User input for running MELGEN and MELCOR with the CND Package activated is described separately in the Condenser Package Users' Guide.

Contents

1.	Introduction	5
2.	PCCS Model	5
2.1	Introduction and Concept	5
2.2	General PCCS Performance	6
2.3	Operation of the PCCS Model	7
2.4	The Iterative Procedure	15
2.4.1	Purpose	15
2.4.2	Initial Conditions	15
2.4.3	Iterative Steps	15
2.5	Example Results	18
2.6	Effect of the Drywell Pressure on PCCS Operation	26
3.	ICS Model	29
3.1	Introduction and Concept	29
3.2	Operation of the ICS Model	29
3.3	Example Results	31
4.	Interface with MELCOR	34
	References	35

List of Tables

Table 2.1 Tabular input example for variation of PCCS performance with drywell-wetwell differential pressure	21
Table 2.2 Tabular input example for variation of PCCS performance with the drywell noncondensable gas mole fraction at an ICS/PCC pool temperature of 323.16 K.21	
Table 2.3 Tabular input example for variation of PCCS performance with the drywell noncondensable gas mole fraction at an ICS/PCC pool temperature of 373.16 K.21	
Table 2.4 Variation in PCCS Performance with Pressure in Drywell.	28
Table 3.1 Variation in ICS Performance with Pressure in the Reactor Vessel	32

List of Figures

Figure 2.1 The noncondensable gas mole fraction decreases rapidly when steam is released directly into the drywell atmosphere during the final stage of an SBWR reactor vessel depressurization.	19
Figure 2.2 The drywell-to-wetwell pressure differential delpre and the differential pressure reqpre at which flow through the PCCS vent line is initiated.....	20
Figure 2.3 The available PCCS heat exchanger capacity (dots) is primarily determined by the drywell noncondensable gas mole fraction (solid line).	23
Figure 2.4 The available PCCS (three-unit) heat exchanger capacity pitcet and the power e2adic actually utilized.	24
Figure 2.5 The total mass flow pltifl through the PCCS vent line and the associated flow pltnfl of noncondensable gases.....	25

1. Introduction

This Package describes the Passive Containment Cooling System (PCCS) and Isolation Condenser System (ICS) models developed at Oak Ridge National Laboratory (ORNL) for use with MELCOR. This manual is divided into three sections. Section 2 describes the PCCS model, while Section 3 describes the extension of the basic PCCS model to provide calculational capability for the ICS. Finally, the interface with MELCOR for both the PCCS and ICS models is described in Section 4.

2. PCCS Model

2.1 Introduction and Concept

The PCCS is a safety-related passive system designed to remove the core decay heat that would be introduced into the SBWR containment during a loss-of-coolant accident (LOCA). The PCCS is described in Section 6.2 of the *SBWR Standard Safety Analysis Report (SSAR)* [1].

The basic operation of the PCCS derives from the induced flow of some of the drywell atmosphere to the wetwell airspace via the PCCS whenever the drywell-to-wetwell pressure differential is sufficient to clear the water from the vent line terminus within the pressure suppression pool. The venting pathway through the PCCS includes a heat exchanger in which the gases are cooled and some (or all) of the steam vapor is condensed; the condensate is drained to the Gravity-Driven Cooling System (GDCS) pool within the drywell. The noncondensable gases and any steam carryover through the vent line are released into the pressure suppression pool, where the gas bubbles rise to the pool surface. The intermittent nature of the venting process causes the thermal-hydraulic behavior of the PCCS to be much more complex than the normally encountered heat exchanger-condenser applications for which the flow is continuous.

The PCCS model described here is based upon the concept that the MELCOR code should adequately represent the effects of the PCCS under the boundary conditions that would be imposed by accidents. It is not intended that the MELCOR calculation should attempt to predict the performance of these heat exchanger-condenser systems based upon basic physical considerations; this is done by more sophisticated thermal-hydraulic codes. Furthermore, test calculations performed with MELCOR demonstrate that attempts to use the basic code "building block" approach to connect control volumes, flow paths, and heat sink structures as necessary to directly simulate the PCCS heat exchanger-condensers will result in code difficulties; these include oscillations in the predicted flows and energy exchanges, a demand for extremely small timesteps, and impractically large CPU and wall clock time consumption.

2.2 General PCCS Performance

Based upon the available information in the literature concerning the PCCS design and the results of equipment tests reported by the development consortium to date, it is clear that any PCCS component model must have the following basic attributes:

- (1) Capacity limited to gravity drainage of steam condensing in the tubes until drywell pressure exceeds suppression chamber pressure by a margin [about 7.25 kPa (1.05 psid)] sufficient to overcome PCCS vent line submergence. With normal pressure suppression pool water level, the uppermost vent line exit hole lies at the depth of 0.75 m (2.5 ft). The pool water level may vary during the course of an accident and this must be considered in the model.
- (2) For long-term cooling situations of practical interest for BWR accident calculations, the drywell-to-suppression chamber pressure differential is limited to the submergence of the drywell-to-pressure suppression pool vents.
- (3) Capacity increases as the drywell-to-suppression pool pressure differential (vent line flow) increases over the small range between PCCS vent line clearance and clearance of the main horizontal vents.
- (4) Capacity decreases with increasing partial pressure of noncondensable gases in the upper drywell because of the interference of the gas boundary layer within the PCCS tubes with the steam-to-wall heat transfer.
- (5) Whenever the wetwell pressure approaches (or exceeds) the drywell pressure so that vent line flow is zero, the PCCS heat exchanger-condenser is subject to filling with noncondensable gases as the condensing steam is continuously replaced with a mixture of steam and noncondensable gas from the drywell. The PCCS is said to be "bound" when it contains only cool noncondensable gas so that all heat exchange and condensing operation is terminated.
- (6) The average PCCS capacity over the long term is determined by the heat transfer from the outer surface of the PCCS heat exchanger tubes to the surrounding ICS/PCC pool. For the LOCA analysis presented in Section 6.2 of the SSAR, the General Electric Company has employed a constant heat transfer coefficient of $4500 \text{ W}/(\text{m}^2\text{-K})$ [$792.5 \text{ Btu}/(\text{h}\text{-ft}^2\text{-F})$] for the tube outer surface area.
- (7) Capacity of the PCCS decreases as the pressure in the drywell falls below its optimum operational pressure. As the pressure drops in the drywell, the temperature of the steam and associated condensate drops, thereby lowering the heat transfer between the condenser wall and the steam. Heat transfer is determined by the heat transfer coefficient times the surface area times the difference between the steam temperature and the temperature of the condenser wall, which is very close to the surrounding pool temperature.

A general model interacting with MELCOR has been constructed from the available information and tested satisfactorily. Nevertheless, the most recent detailed information concerning experimental measurements or the results of sophisticated calculations of PCCS performance as a function of the ICS/PCC pool temperature, the drywell-to-wetwell atmosphere pressure differential, atmospheric pressure in the drywell, and the noncondensable gas fraction in the drywell atmosphere should be used to refine the input for this model (described in the CND Package Users' Guide) whenever production calculations are performed.

2.3 Operation of the PCCS Model

The PCCS model is contained within MELCOR Subroutine CNDRN1. In this section, the operation of the model is described as a 28-step process. Not all steps are executed each calculational timestep. One of the steps involves an iterative procedure, which is described in detail in Section 2.4. Those readers not interested in pursuing the level of understanding offered by a detailed discussion of model operation are encouraged to skip to Section 2.5, which provides an overview in the form of an example of calculated results.

It is important to recognize that the PCCS model operates on the assumption that the pressure within the PCCS remains equal to the drywell pressure and constant during a calculational timestep. Whenever material is removed, for example, when steam condenses and the condensate is transferred to the GDCS, a void is considered to be created within the PCCS. An uptake of mixture from the drywell atmosphere is required to fill this void at drywell pressure and the subsequent equilibrium conditions within the PCCS are calculated. This approach is taken to avoid the penalties (described in Section 2.1) of a mechanistic model for which mass transfers between the drywell and the relatively small PCCS would be based upon calculated pressure differentials.

The variable names mentioned in the following discussions and in Section 2.4 are the same as those used within Subroutine CNDRN1. The interested reader is encouraged to compare the stepwise operations described here with the actual FORTRAN in a listing of Subroutine CNDRN1; the COMMENT statements that will be obtained with the program listing will provide additional detailed information.

Before beginning the step-by-step discussion of model operation, it is necessary to define a few of the variable names that will be encountered (the meaning of the others will be obvious from the text).

NUMMAT Is the total number of materials considered present (or potentially present) within a control volume. These include the water pool, fog droplets, steam, and the noncondensable gases.

I I is the index of a particular material within a control volume.

CND Package Reference Manual

Index	Material
1	water pool
2	fog
3	vapor
4 through NUMMAT	noncondensable gas

The control volume atmosphere is comprised of materials 2 through NUMMAT. The control volume total pressure is the sum of the partial pressures of materials 3 through NUMMAT.

CEFIC represents the running total kept within the model of the remaining PCCS heat exchanger capacity in Joules. The available capacity is established at the beginning of each timestep from tabular input supplied by the MELCOR user. This initial value depends upon the current ICS/PCC pool temperature, the current drywell-to-wetwell pressure differential, and the current mole fraction of noncondensable gas in the drywell atmosphere. It should be noted that the reduction in PCCS performance due to a buildup of noncondensable gas within the heat exchanger is not established from the tabular input, but rather is calculated by the PCCS model.

ENGIC(I) is the array containing the internal energies of the materials within the PCCS at the beginning of the timestep. During the timestep, the running values of these internal energies are contained in the array ETOTIC(I), which is copied to the ENGIC(I) array at the end of each timestep.

VLICMT is the volume of the materials (steam, fog, noncondensable gases) that constitute the atmosphere within the PCCS. Since the PCCS atmosphere is constrained to remain at a pressure equal to drywell pressure, this volume can be less than the actual PCCS structural volume if material is removed from the PCCS atmosphere during the calculation.

PCCS Model Steps

Steps 1 – 4: Establish Initial Conditions

These initial steps establish the equilibrium conditions within the PCCS with the volume filled at drywell pressure. Some of the available capacity is utilized to cool any noncondensable gas carried over from the previous timestep. Mixture is taken up from the drywell as required to maintain the PCCS at drywell pressure.

- (1) Set the currently available heat removal capacity CEFIC based upon the drywell-to-wetwell pressure differential, the pressure in the drywell, and the noncondensable gas fraction in the drywell atmosphere. The dependence upon the pressure

differential and the source pressure are obtained from user-input tabular function IPCDPR and IPSRPR, respectively. The dependence upon the noncondensable gas mole fraction is obtained by interpolation between the user-input tabular functions IPLTMP (for 323.16 K) and IPCNCN (for 373.16 K), which correspond to ICS/PCC pool temperatures of 50 °C and 100 °C, respectively. (See Users' Guide for input record ESFCND0200.)

- (2) Cool any noncondensable gases remaining within the PCCS at the end of the previous timestep. The gas temperature is reduced to the ICS/PCC pool temperature TICPL by calling the routine NCGPRO to obtain the internal energy of the gases at the new temperature.
 - Reduce the internal energies ENGIC(I) accordingly.
 - Reduce the available capacity CEFIC.
- (3) Take up enough mixture from the drywell atmosphere to make the calculated PCCS equilibrium pressure equal to the drywell pressure. (Section 2.4 provides a discussion of the iterative procedure used.)
 - Reduce the drywell gas, vapor, and fog masses and energies accordingly.
 - Output of the equilibration routine includes
 - ETOTIC(I) total internal energies and
 - XMSICN(I) masses
 of the fog, vapor, and noncondensable gases.
 - Set the PCCS material volume VLICMT equal to the internal volume of the PCCS structure.
- (4) Determine if there will be vent line flow this timestep.
 - If No, continue with Steps 5 – 9.
 - If Yes, continue with Steps 10 – 27.

Steps 5 – 9: No Vent Line Flow

The PCCS is now full at drywell pressure with its contents at an equilibrium temperature. If there was a void remaining at the end of the previous timestep, or if some cooling of the noncondensable gases occurred, then some steam (and fog) taken up with the mixture from the drywell atmosphere will be included. CEFIC has already been reduced (Step 2) as necessary to account for the cooling of noncondensable gas.

- (5) If no steam exists within the PCCS (No void at the end of the previous timestep and no noncondensable gas cooling or no steam in drywell atmosphere)
 - Energy to ICS/PCC pool limited to that used to cool the noncondensable gases.

Go to Step 28.

- (6) Condense the steam (and cool the fog) within the PCCS.
- May be limited because of insufficient capacity CEFIC remaining after the cooling of the noncondensable gas (Step 2).
 - Add the masses and energies to the GDCS Pool.
 - Reduce ETOTIC(I) and XMSICN(I) for steam and fog accordingly.
 - Set RMVLIC equal to the accumulated void within the PCCS.
 - Reduce the available capacity CEFIC accordingly.
- (7) If CEFIC > 0.0 and RMVLIC > 0.0, take up enough mixture from the drywell atmosphere to use the available capacity and to partially fill the void (with noncondensable gas). On the other hand, it is possible that the noncondensable gas takeup will completely fill the void without using all of the available capacity.
- The steam and fog taken up are never actually added to the PCCS volume within the model but rather are removed from the drywell atmosphere and added directly to the GDCS Pool as saturated liquid.
 - Reduce the available capacity CEFIC by the amount of energy used in condensing the steam and cooling the fog.
 - For the noncondensable gas takeup: Increase XMSICN(I) and ETOTIC(I) for these gases and remove the associated masses and energies from the drywell.
 - Reduce the void RMVLIC according to the takeup of noncondensable gas (only)—note that RMVLIC will remain greater than zero only if the takeup from the drywell atmosphere was limited by the available heat exchange and condensing capacity.
- (8) Set VLICMT = VLICMT - RMVLIC. There will be a void within the PCCS at the beginning of the next timestep if RMVLIC > 0.0 here.
- (9) Add the energy used in cooling the noncondensable gases (Step 2) and in condensing the steam/cooling the fog (Steps 6 and 7) to the ICS/PCC pools.

Go to Step 28.

Steps 10 – 27: With Vent Line Flow

At this point, the PCCS is full at drywell pressure with its contents at an equilibrium temperature. If a void remained at the end of the previous timestep or if some cooling of the noncondensable gases occurred, then some steam (and fog) taken up with the mixture from the drywell atmosphere will be included. CEFIC has already been reduced (Step 2) to account for any cooling of the noncondensable gas.

- (10) Calculate the PCCS vent line mass transfer XMS2FL. The transfer is based upon the pressure differential between the drywell and the vent line terminus, which is submerged in the pressure suppression pool.
- (11) Move noncondensable gases from PCCS to wetwell and reduce the running total for XMS2FL accordingly.
 - RMVLIC is the associated PCCS void.
 - Reduce the values of XMSICN(I) masses and ETOTIC(I) internal energies for the noncondensable gases.
 - At this point, either:
 XMS2FL=0.0; some noncondensable gas remains in PCCS
 or
 XMS2FL>0.0; all noncondensable gas has been removed so that only steam and fog remain within the PCCS.
- (12) Condense the steam within the PCCS up to the limits of the available capacity CEFIC. Place the liquids in the GDSC pool.
 - XMSREM is the mass of steam condensed.
 - Reduce CEFIC accordingly.
 - Reduce XMSICN(I) and ETOTIC(I) for the steam.
- (13) If some steam remains in the PCCS and if some vent line mass transfer remains (XMS2FL > 0.0) then
 - Move the steam (uncondensed) through the vent line to the pressure suppression pool.
 - Reduce XMS2FL accordingly.
 - Increase XMSREM so it now represents both the condensed steam drained to the GDSC and the uncondensed steam moved to the pressure suppression pool.
 - Reduce XMSICN(I) and ETOTIC(I) for the steam.
- (14) Increase RMVLIC to account for the void created by both the steam condensed and drained to the GDSC pool and the steam moved to the pressure suppression pool via the PCCS vent line.

Note: Steps 12 – 14 are actually performed (in sequence) for fog, steam, and any water pool that has formed within the PCCS volume. The handling of steam is demonstrated in this discussion; the fog and water pool (if it exists) are treated in a similar manner.

- (15) Reduce the PCCS material volume VLICMT by subtracting the void RMVLIC.

Set VOLINT = 0.0
VINTNC = 0.0
XMNNST = 0.0

- (16) If both the remaining heat exchanger capacity CEFIC and the remaining vent line mass transfer XMS2FL have been reduced to zero.

Go to Step 28.

Steps 17 – 18: Heat Removal Capacity/Vent Line Mass Transfer Imbalance

It is unlikely that the amount of mixture that must be taken up from the drywell in order to use the remaining heat removal capacity will provide exactly the amount of noncondensable gas required to satisfy the remaining mass transfer requirement. These two steps determine the remaining model logic to be employed, based upon the sign of imbalance.

- (17) Set VOLINT = Mixture volume required from drywell to use all remaining capacity CEFIC in condensing the associated steam and cooling the associated fog.

XMNNST = Mass of noncondensable gas associated with VOLINT.

VL2FL = 0.0

- (18) Will XMNNST satisfy the remaining mass transfer requirement XMS2FL?

If No:

Go to
Steps 19 – 21

If Yes:

Go to
Steps 22 – 25

Steps 19 – 21: Mass Transfer Dominates

XMNNST (based upon use of all of the available heat exchanger-condenser capacity) is insufficient to satisfy the remaining mass transfer requirement XMS2FL.

- (19) Set ADDRVL = mixed volume to be taken up from drywell solely to satisfy the mass transfer requirement.
- (20) Add the steam (uncondensed) and fog associated with ADDRVL directly to the pressure suppression pool and remove them from the drywell atmosphere.

Transfer the noncondensable gases from the drywell to the wetwell atmosphere, while representing the heat transfer to the water that would occur during their bubbly passage through the pressure suppression pool.

- (21) Set VLICMT = 0.0
CEPIC = 0.0

All material originally within the PCCS and all new material taken up from the drywell has been passed through the vent line. Also, all available heat exchanger capacity has been utilized.

Go to Step 26.

Note that VINTNC is 0.0 here while VOLINT is the mixture volume taken up from the drywell to satisfy the heat exchanger capacity.

Steps 22 – 25: Heat Removal Capacity Dominates

XMNNST (based upon satisfying the heat exchanger capacity requirement) exceeds the remaining mass transfer requirement XMS2FL. VOLINT (set in Step 17) is the mixture volume associated with XMNNST.

- (22) Set VINTNC = noncondensable gas volume associated with VOLINT.
- (23) Set VL2FL = noncondensable gas volume associated with XMS2FL. This is the volume that will flow through the PCCS vent line this timestep based upon XMS2FL.
- (24) If $VINTNC > (RMVLIC + VL2FL)$

Cannot take up all of the mass XMNNST (associated with volume VINTNC).

- Reduce the mixed volume to be taken up from the drywell.

$$VOLINT = VOLINT \times \left(\frac{RMVLIC + VL2FL}{VINTNC} \right)$$

- Reduce the available heat capacity by the amount used

$$CEVIC = CEVIC - CEVIC \times \left(\frac{RMVLIC + VL2FL}{VINTNC} \right)$$

- Reduce VINTNC to a value sufficient to fill the available PCCS void plus provide the remaining vent line mass transfer.

$$VINTNC = RMVLIC + VL2FL$$

Else

$$CEFOC = 0.0$$

- (25) Adjust the material volume within the PCCS

$$VLICMT = VLICMT + VINTNC - VL2FL$$

All available energy is utilized if VINTNC is less than or equal to (RMVLIC + VL2FL)

Here VINTNC is the noncondensable gas volume to be taken up from the drywell and added to the PCCS volume.

Steps 26 – 27: Transfer of Steam, Fog, and Gas from the Drywell Atmosphere

- (26) Remove the noncondensable gases associated with VOLINT from the drywell atmosphere and add them to the PCCS volume and the wetwell airspace.

If VINTNC is greater than zero here, then some of the noncondensable gases taken up from the drywell to satisfy the available heat removal capacity are not passed through to the pressure suppression pool, but rather remain within the PCCS.

Increase XMSICN(I) and ETOTIC(I) for the noncondensable gases accordingly.

For the portion of the noncondensable gases (maybe all) that are passed to the pressure suppression pool, add the masses to the wetwell atmosphere and represent the heat transfer from the bubbles to the pool, adding the residual energies to the wetwell atmosphere.

- (27) Remove the steam and fog associated with VOLINT from the drywell atmosphere and add the condensate to the GDCS pool.

Step 28: Set PCCS Internal Energies for the Next Timestep

- (28) Set ENGIC(I) = ETOTIC(I) for the steam, fog, and noncondensable gases within the PCCS.

This is the last step in each calculation of PCCS operation. Any material remaining within the PCCS is considered to remain at drywell pressure and may or may not fill the PCCS volume.

2.4 The Iterative Procedure

2.4.1 Purpose

The objective of this iterative procedure is to fill the PCCS volume with the mixture of gases, fog, and vapor from the drywell atmosphere to make the PCCS pressure equal to the drywell pressure. The iteration constitutes Step 3 of the PCCS operation as described in Section 2.3 and may be performed at the beginning of each timestep, depending upon the initial conditions within the PCCS volume.

2.4.2 Initial Conditions

The initial conditions within the PCCS are those established at the end of the previous timestep, and fall into three categories.

- (a) The PCCS may be bound (filled) with noncondensable gases at the temperature of the ICS/PCC pool and the pressure of the drywell atmosphere.
- (b) The PCCS may be completely voided, or contain only steam and fog; in either event, there are no noncondensable gases within the PCCS.
- (c) The PCCS may contain a mixture of noncondensable gas and steam. If the temperature of the mixture exceeds the temperature of the ICS/PCC pool, then the noncondensable gases are cooled to the pool temperature (as explained in Section 2.3) before the iteration begins.

Initial filling of the PCCS volume from the drywell atmosphere is necessary only for cases (b) and (c), and is accomplished by means of the steps described below:

2.4.3 Iterative Steps

- (1) Call the MELCOR equilibrium routine CVTWGE with input

CVMS(I)	initial masses,
CVEM(I)	internal energies, and
XNMCLS x VOLIC	the total PCCS volume.

The calculated output includes the equilibrium values for

CND Package Reference Manual

XMSICN(I)	masses,
ETOTIC(I)	internal energies,
PRIC	pressure, and
TEMPIC	temperature

For the equilibrium calculation, the index I represents fog (I=2), steam (I=3), and noncondensable gases (I=4, NUMMAT).

The first step is skipped in the first iteration if the PCCS is initially totally voided; in this case, the pressure PRIC is simply set to zero.

- (2) Check to see if the pressure in the PCCS exceeds the pressure in the drywell after the initial equilibration calculation, which would indicate a current drywell pressure less than the pressure at the end of the previous timestep.

If the condition is met, then determine the expanded volume of the noncondensable gases at the new drywell pressure. If the expanded volume is greater than the volume of the condensers plus the source line volume, allow material to flow back from the PCCS to the drywell. The fraction of PCCS noncondensable gases to be removed from the condensers and transferred back to the drywell is:

$$F2FLBK = 1 - \frac{PCCS \text{ VOLUME}}{VICDRY - PCCS \text{ VOLUME} - PCCS \text{ SOURCE LINE VOLUME}}$$

where VICDRY is the expanded volume of the noncondensable gases at the new drywell pressure:

$$VICDRY = \frac{PCCS \text{ PRESSURE} \times PCCS \text{ VOLUME}}{DRYWELL \text{ PRESSURE}}$$

FLMULT is then set to zero and the execution sequence is continued with Step 6.

- (3) The mass transfer multiplier FLMULT is set depending upon the relative values of the PCCS pressure PRIC and the upper and lower boundaries of a pressure range centered on the drywell pressure PRES(IVPCSO) as follows,

.....PRES(IVPCSO) + 100

.....PRES(IVPCSO)

.....PRES(IVPCSO) - 100.

As indicated, the total width of the acceptable pressure range is 200 Pa (about 0.03 psi).

If PRIC is less than the lower boundary limit, then FLMULT is set to a positive value. Conversely, if PRIC is greater than the upper boundary limit, then FLMULT is set to a negative value. In either case, the absolute value of FLMULT is reduced by a factor of two each trip through the iterative loop.

When PRIC finally lies within the acceptable boundaries, FLMULT is simply set to zero.

- (4) The volume to be transferred from the drywell to the PCCS during this iterative step is calculated from

$$\text{VOL2FL} = [\text{PCCS VOLUME} - \text{VLICMT}] \times \text{FLMULT}$$

where VLICMT is the material volume at the end of the previous timestep, reduced by 10 percent. The value of VLICMT set in the initial iterative pass is used without change during all subsequent passages through the loop.

Returning to a consideration of the possible initial conditions, it should be recognized that VLICMT will be zero at the end of the previous timestep if the PCCS is completely voided, in which case taking away ten percent would have no effect. The ten percent reduction is intended for cases in which noncondensable gases are present and are cooled before the iterative procedure is begun; some of the drywell atmospheric mixture must be brought into the PCCS to maintain a pressure equal to drywell pressure, and the iterative procedure accomplishes exactly this.

In fact, for the case with the PCCS completely voided at the end of the previous timestep, there is no need for iteration at all. The PCCS volume is very small in comparison with the drywell volume. Therefore, it is reasonable to assume that the PCCS will be filled with a material mass and energy composition identical to that of the drywell. One pass through the iteration loop is made to confirm that the calculated PCCS pressure after filling is equal (within limits) to the drywell pressure.

What about the case in which the PCCS is bound (filled with cooled noncondensable gas) and at drywell pressure? Reducing VLICMT by ten percent here has no effect since FLMULT is zero and hence VOL2FL is zero regardless of the value of VLICMT.

The upshot of this rather complicated discussion is that VOL2FL will normally be positive during the first pass through the iterative loop. An exception occurs if the PCCS pressure is already equal (within limits) to the drywell pressure. In that case,

CND Package Reference Manual

VOL2FL will be zero and the iteration will not be extended beyond a single pass through the loop.

- (5) At this point, VOL2FL may be negative if the PCCS volume was overfilled during the previous pass through the iterative loop. Depending upon the sign of VOL2FL, the masses ADMS(I) and internal energies ADEM(I) of the steam, fog, and noncondensable gases within this volume of drywell atmosphere are added to (subtracted from) the PCCS volume. These masses and associated enthalpies are subtracted from (added to) the drywell control volume.

In these exchanges, portions of the drywell atmosphere are being transferred. Internal energy is added to or subtracted from the PCCS because a void is being either eliminated or created, as is the associated PV work term. For the drywell, gases entering or leaving do flow work upon (compression) or derive work from (expansion) the remaining gases. Hence enthalpy transfer is appropriate.

- (6) CVEM(I) and CVMS(I) are adjusted depending upon the values of ADEM(I) and ADMS(I) for all materials within the PCCS atmosphere and the calculation returns to iterative step 1 unless FLMULT is zero. [FLMULT = 0 signifies that the PCCS pressure equals (within limits) the drywell pressure.]
- (7) Once convergence is satisfied, VLICMT is set equal to the PCCS structural volume.

2.5 Example Results

This section provides, as an example, a discussion of the calculated PCCS operation for a MELCOR representation of the SBWR station blackout accident sequence. While reading this description, it is important to bear in mind that the available PCCS heat exchanger-condenser capacity (based upon current operation parameters) is assumed to be known each timestep; the purpose of the model is to determine the associated heat transfers and fluid flows, with due consideration of the current status of the PCCS with respect to binding. It is important to note that, for this example, no degradation in performance due to variations in the drywell pressure is assumed.

For an unmitigated station blackout accident sequence, reactor vessel depressurization would automatically occur when the vessel level reached a point about 3.6 m (12 ft) above the top of the core. The SBWR depressurization involves stepped opening of the safety relief valves, which discharge into the pressure suppression pool, followed by stepped opening of the six depressurization valves (DPVs), which discharge directly into the drywell atmosphere. The example results discussed here cover the period from just before the initial DPV actuation to five minutes thereafter.

Figure 2.1 shows the effect of the DPV openings, which begin at time 11161 seconds, upon the noncondensable gas fraction in the drywell. The actual DPV opening sequence is two valves at 11161 seconds, two valves at 11206 seconds, and two valves at 11251 seconds.

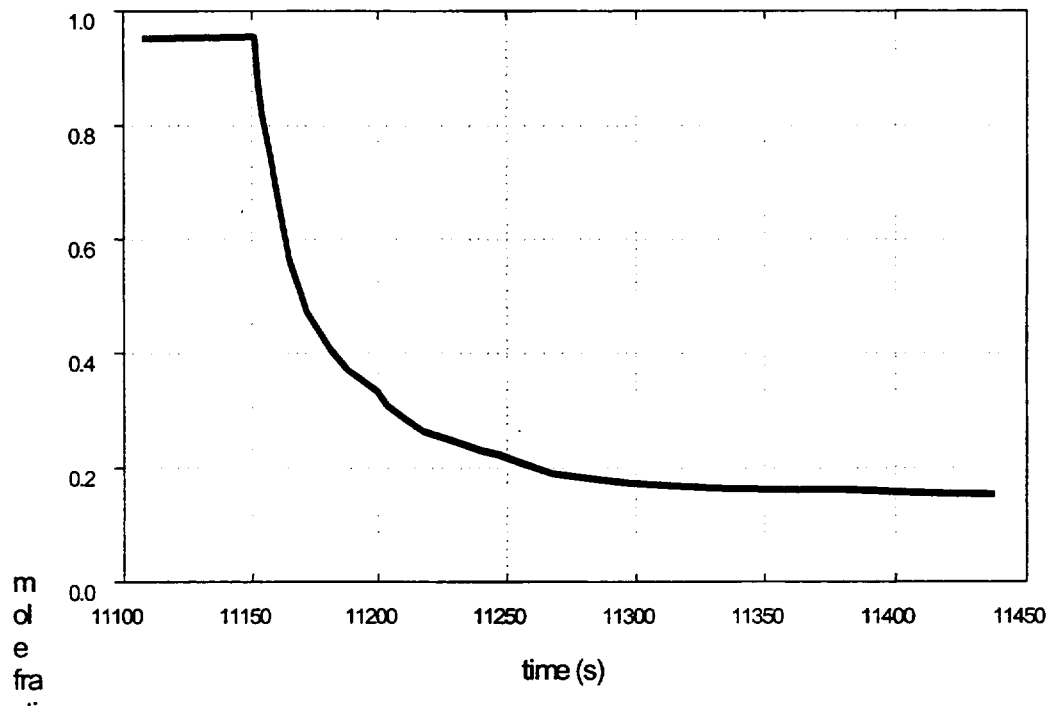


Figure 2.1 The noncondensable gas mole fraction decreases rapidly when steam is released directly into the drywell atmosphere during the final stage of an SBWR reactor vessel depressurization.

The reactor vessel depressurization also increases the drywell-to-wetwell differential pressure, as indicated by the response of variable **delpre**, shown in Figure 2.2. The variable **reqpre**, also plotted on this figure, represents the differential pressure required to induce flow through the PCCS vent line. It increases slightly during the period of the calculation as the height of the pressure suppression pool surface above the vent line terminus increases.

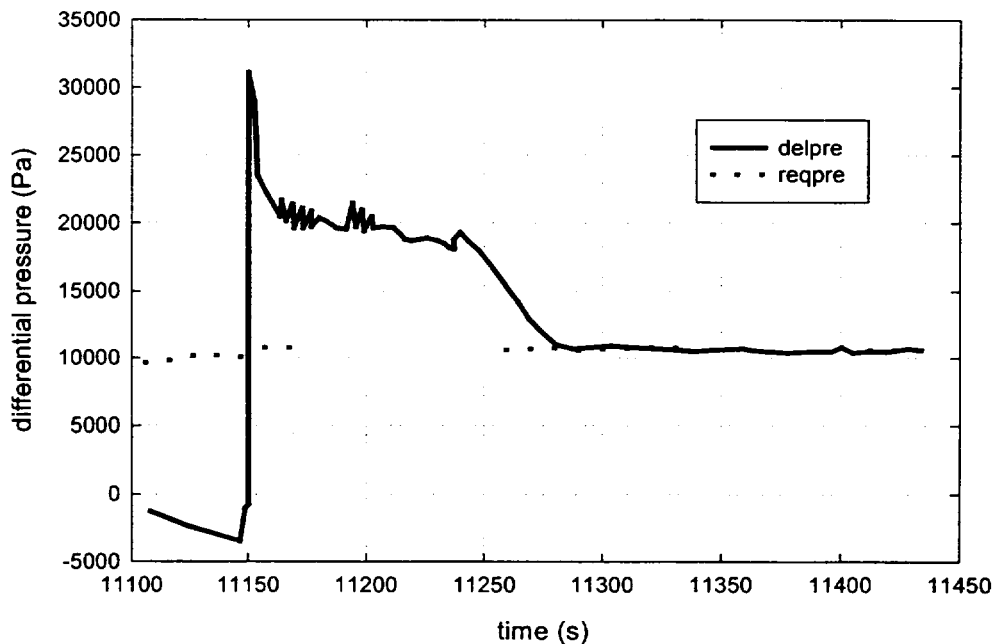


Figure 2.2 The drywell-to-wetwell pressure differential **delpre** and the differential pressure **reqpre** at which flow through the PCCS vent line is initiated.

At this point, it is necessary to consider the variation in PCCS performance in accordance with current conditions. The PCCS heat exchanger capacity is determined at the beginning of each timestep based (in order of increasing importance) upon (1) the current drywell-to-wetwell differential pressure, and (2) the current mole fraction of noncondensable gas in the drywell (considering the current ICS/PCC pool temperature and interpolating between values for two reference pool temperatures). The tabular input employed for this example calculation is listed in Tables 2.1 through 2.3. The basic capacity per PCCS unit is 10 MW_t at an ICS/PCC pool temperature (saturation) of 374.15 K (213.8 F), a drywell-to-wetwell pressure differential of 7239.5 Pa (1.05 psi), and a drywell noncondensable gas fraction of 0.0 (pure saturated steam). As stated above, the performance of the condenser is assumed to be constant over all source volume pressures.

Table 2.1 Tabular input example for variation of PCCS performance with drywell-wetwell differential pressure

Differential Pressure (Pa)	psi	Variation Factor
0.0	0.00	1.000
7239.5	1.05	1.000
8618.5	1.25	1.072
10342.1	1.50	1.153
12065.8	1.75	1.227
13789.5	2.00	1.294
15423.6	2.24	1.353

Table 2.2 Tabular input example for variation of PCCS performance with the drywell noncondensable gas mole fraction at an ICS/PCC pool temperature of 323.16 K

Noncondensable Gas Mole Fraction	Variation Factor
1.00	0.00
0.10	0.60
0.05	0.82
0.02	0.90
0.01	0.96
0.00	1.00

Table 2.3 Tabular input example for variation of PCCS performance with the drywell noncondensable gas mole fraction at an ICS/PCC pool temperature of 373.16 K

Noncondensable Gas Mole Fraction	Variation Factor
1.00	0.00
0.10	0.60
0.05	0.82
0.02	0.90
0.01	0.96
0.00	1.00

The example calculation represents the operation of all three PCCS units. Changes in the ICS/PCC pool temperature are assumed to have no effect upon the PCCS system performance, chiefly because the pool is sufficiently large that its temperature increase is small during the period of the calculation. It may be noted by comparing the variation factors listed in Table 2.2 and Table 2.3 that no credit has been given for an enhancement

CND Package Reference Manual

of the PCCS heat exchanger capacity for ICS/PCCS pool temperatures below saturation. At the time that this example calculation was performed, no information concerning this enhancement was available. Subsequently, it has become apparent that such enhancement should be represented by providing different values in Table 2.2 and Table 2.3. Similarly, the variation in performance due to source volume pressure changes were added when the need for such a reduction became apparent. (See the BH Package Users' Guide with respect to input card ESFCND0200 for additional information.)

The drywell-to-wetwell differential pressure affects the heat exchanger performance because it determines the (forced-convection) velocity within the heat exchanger tubes. The velocity, in turn, affects the heat transfer coefficient (h) at the inner surface of the tubes. A conventional expression commonly used has the form

$$h = (\text{const.}) \times \text{Re}^{0.8},$$

where Re (the Reynolds number) includes the velocity. As a result, the heat transfer coefficient for various differential pressures between the drywell and the wetwell can be represented (assuming all other variables are constant) by

$$h = (\text{const.}) \times (\text{differential pressure})^{0.4}.$$

Thus, as indicated in Table 2.1, the PCCS capacity is enhanced as the differential pressure increases.

By far the largest effect upon PCCS capacity derives from changes in the noncondensable gas fraction of the gas entering the PCCS from the drywell. This large influence can be observed in Figure 2.3, which compares the current (three-unit) PCCS capacity to the drywell noncondensable gas mole fraction (also shown in Figure 2.1). It is obvious that the increase in available capacity shown in Figure 2.3 is inversely proportional to the decrease in noncondensable gas mole fraction. This large effect of the noncondensable gas fraction in reducing the condensation effectiveness is well known. The tabular input reproduced in Table 2.2 and Table 2.3 is derived from information provided in the paper, Heat Removal of Isolation Condenser Applied as a Passive Containment Cooling System by H. Nagasaka et al., of the Nuclear Energy Group, Toshiba Corporation. [2]

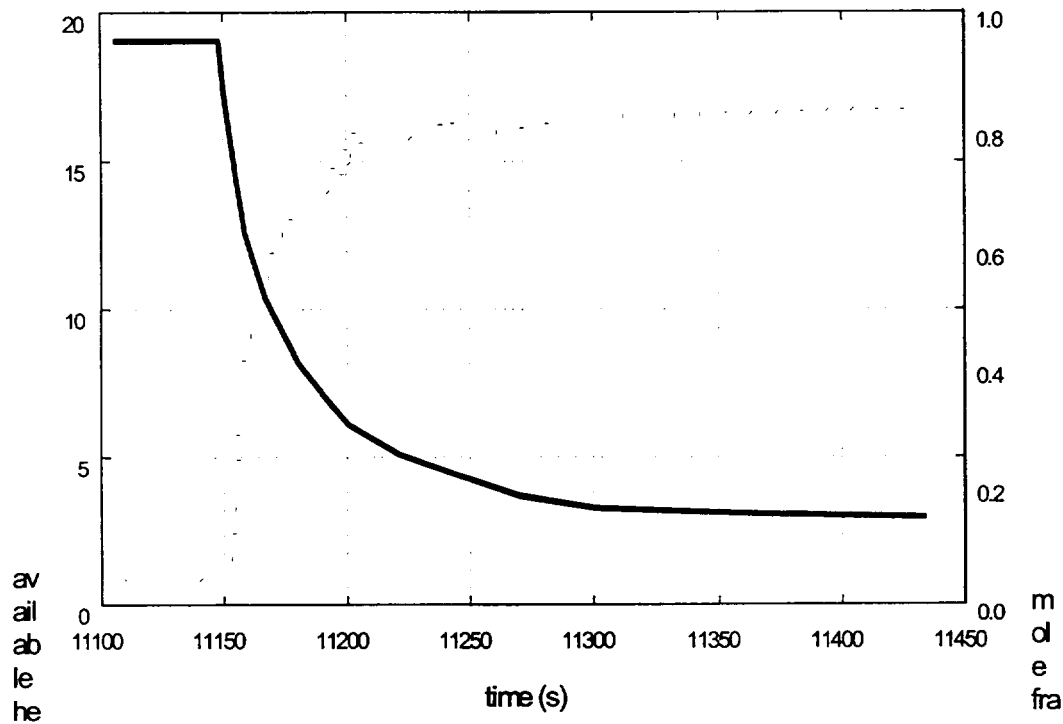


Figure 2.3 The available PCCS heat exchanger capacity (dots) is primarily determined by the drywell noncondensable gas mole fraction (solid line).

The available (three-unit) PCCS capacity is shown again, as variable **pitcef** on Figure 2.4. It should be recognized that three PCCS units operating under base conditions would have a combined capacity of 30 MW_t, whereas the maximum value of **pitcef** shown on Figure 2.4 is about 17 MW_t. Again, this reduction is primarily due to the presence of noncondensable gas in the drywell atmosphere, which will always be the case.

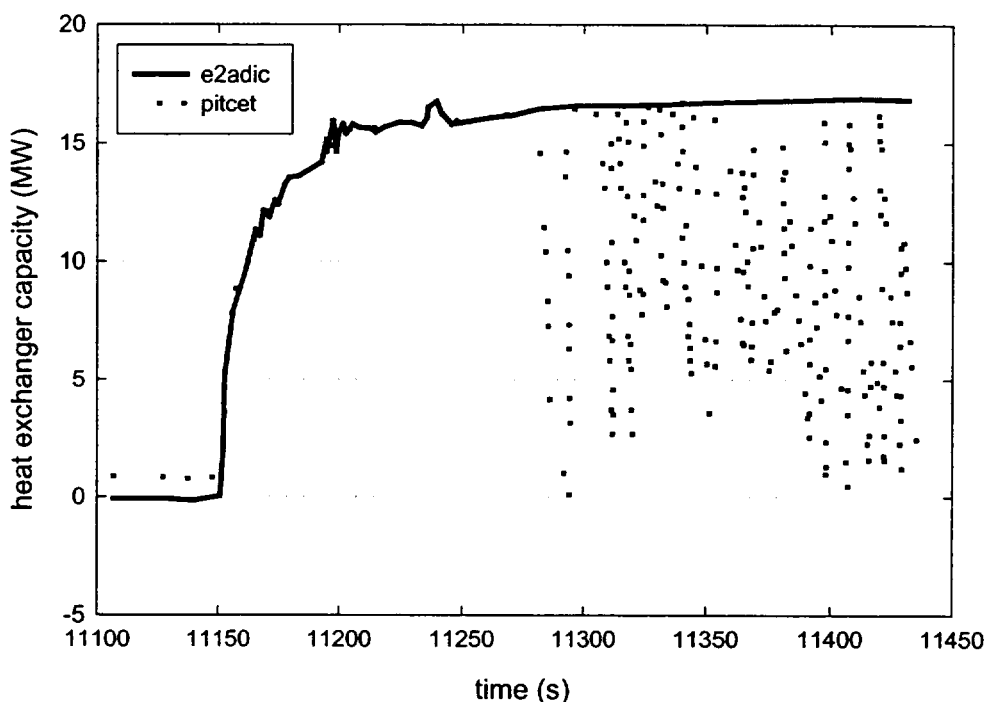


Figure 2.4 The available PCCS (three-unit) heat exchanger capacity **pitcet** and the power **e2adic** actually utilized.

Also shown in Figure 2.4 is the variable **e2adic**, which is the heat exchanger power actually being used. As indicated, none of the available capacity is utilized before the reactor vessel depressurization begins. This is because the PCCS heat exchanger tubes are "bound," or filled with noncondensable gas. Once reactor vessel depressurization begins, however, (1) the available heat exchanger capacity greatly increases, and (2) all of this capacity is used.

The reason that all of the available capacity is used during the period immediately after DPV opening is that the vent line flow induced by the increasing drywell pressure now sweeps the noncondensable gases from the PCCS each timestep, permitting the mixture of gases and steam within the drywell to enter. The total vent line flow **pltifl** and the noncondensable gas vent line flow **pltnfl** are shown in Figure 2.5. It should be noted that the vent line flow initially consists entirely of noncondensable gas; all of the steam entering the PCCS during this initial period is condensed.

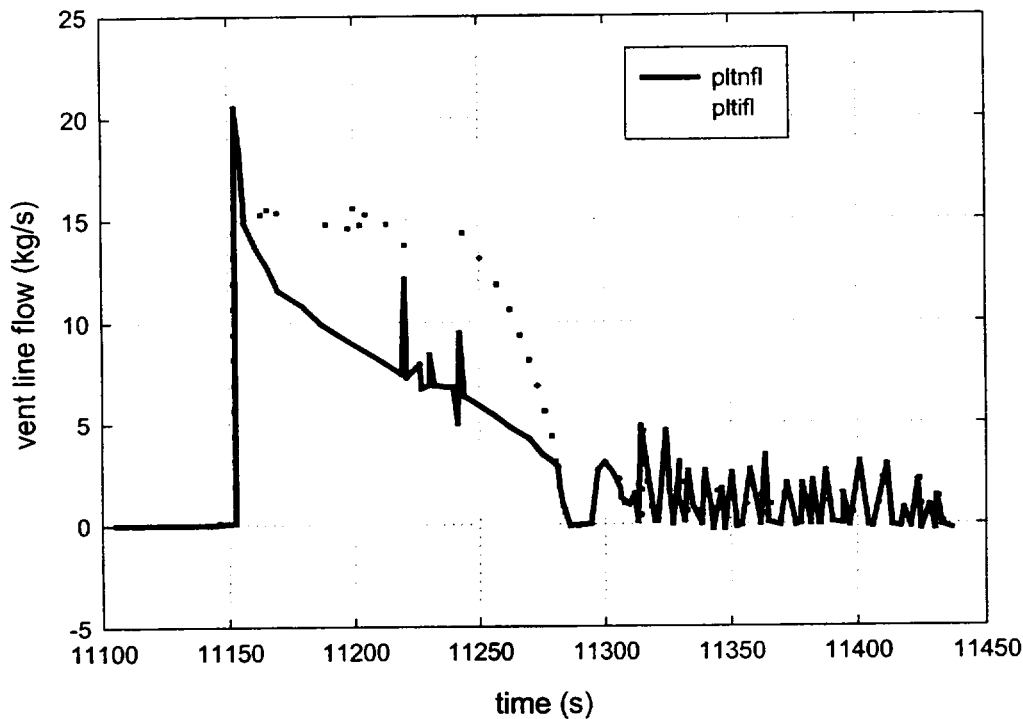


Figure 2.5 The total mass flow **pltifl** through the PCCS vent line and the associated flow **pltnfl** of noncondensable gases.

Steam flow through the vent (the difference between the two plotted variables) does not begin until about 20 seconds after vent line flow begins. Carryover of steam begins at this time because the concentration of steam in the drywell atmosphere has reached a level beyond the available heat exchanger capacity (even though the available capacity is also increasing; see Figure 2.3).

It is instructive to consider the events illustrated in these figures that occur just prior to time 11300 seconds. As shown on Figure 2.2, the drywell-to-wetwell differential pressure drops below the value needed to sustain PCCS vent line flow. This is substantiated by Figure 2.5, where the vent line flow is shown to be zero during this period. Figure 2.4 shows that the portion of available PCCS heat exchanger capacity actually used during this period decreases toward and ultimately reaches zero. This demonstrates that some time is required for the PCCS to fill with noncondensable gases and become bound after vent line flow ceases.

Almost exactly at time 11300 seconds, the drywell-to-wetwell differential pressure becomes sufficient to restore vent line flow (Figure 2.2), vent line flow (all noncondensable gas) is restored (Figure 2.5), and all available capacity is used (Figure 2.4) to condense the steam brought in with the mixed atmosphere from the drywell.

CND Package Reference Manual

After time 11300 seconds, the drywell-to-wetwell differential pressure oscillates about the value required to induce vent line flow (Figure 2.2). During the periods when vent line flow occurs, this flow consists entirely of noncondensable gas (Figure 2.5). During the periods when vent line flow does not occur, the portion of the available capacity that is actually used decreases (Figure 2.4) as the PCCS tends to fill with cooled noncondensable gas. However, a fully bound condition is never attained.

That a fully bound condition is never attained during this final period of the example calculation is a testimony to the effectiveness of the PCCS system in controlling the drywell-to-wetwell differential pressure. Whenever the PCCS performance falters, this differential pressure increases, clearing the vent line and restoring the PCCS performance.

2.6 Effect of the Drywell Pressure on PCCS Operation

The nominal capacity of each PCCS heat exchanger-condenser is reported in the SSAR (Section 6.2.2.1) as 10 MW_t for conditions where the tubes are filled with pure saturated steam at 308 kPa (45 psia) and 407 K (273 °F), and the ICS/PCC pool temperature is 374 K (214 °F). The available capacity under accident conditions is, however, never more than about sixty percent of this because of the presence of noncondensable gases in the drywell atmosphere.

To estimate the variation in performance of the PCCS as a result of changes in the drywell pressure, the heat transfer (q) at the base condition is compared to the heat transfer rates at different pressures. The performance variation factor is thus calculated by dividing the heat transfer at the new condition by the heat transfer at the base condition. Ratios greater than one signify an improvement in performance.

The variation in performance $= q \text{ (new condition)} / q \text{ (base condition)}$

$$= \frac{h_{\text{new}} A (T_{\text{steam}}(\text{new}) - T_{\text{wall}})}{h_{\text{base}} A (T_{\text{steam}}(\text{base}) - T_{\text{wall}})}$$

where

h = heat transfer coefficient,

A = the surface area,

T_{steam} = temperature of the steam (saturation temperature at the pressure of the drywell), and

T_{wall} = temperature of the tube wall (assumed to be same as the temperature of the condenser pool, which is the saturation temperature at atmospheric conditions).

The heat transfer coefficient [3] for condensing steam in various geometries is examined next:

$$h = C \left[\frac{\rho_f (\rho_f - \rho_{steam}) k_f^3 g \sin \theta h_{fg}}{\mu_f L (T_{steam} - T_{wall})} \right]^{1/4}$$

where

- ρ_f = the density of the liquid film,
- ρ_{steam} = the density of the steam,
- T_{steam} = temperature of the saturated steam,
- T_{wall} = temperature of the wall, the temperature of the condenser pool,
- $\sin \theta$ = sine of the angle of the tubes with the horizontal; for vertical tubes, the value is one,
- h_{fg} = latent heat of the steam being condensed,
- μ_f = viscosity of the film,
- k_f = thermal conductivity of the film,
- L = equivalent length,
- g = gravitational constant, and
- C = a constant value that must be calculated depending on the geometry, being either a vertical plate or a cylindrical tube.

It is important to note that this equation for the heat transfer coefficient is for condensers with relatively low vapor Reynolds numbers, less than 35,000. This equation will underestimate the heat transfer coefficient for condensers with a higher value; however, since the primary purpose of the equation as used here is to determine the variation in performance (and not the absolute value of the heat transfer) at low pressures, the use of the equation is appropriate.

The variation in performance becomes:

$$\begin{aligned}
&= \frac{h_{new}(T_{steam}(new) - T_{wall})}{h_{base}(T_{steam}(base) - T_{wall})} \\
&= \frac{\left[\frac{\rho_f(\rho_f - \rho_{steam})k_f^3 h_{fg}}{\mu_f(T_{steam} - T_{wall})} \right]_{(new)}^{1/4} (T_{steam}(new) - T_{wall})}{\left[\frac{\rho_f(\rho_f - \rho_{steam})k_f^3 h_{fg}}{\mu_f(T_{steam} - T_{wall})} \right]_{(base)}^{1/4} (T_{steam}(base) - T_{wall})}
\end{aligned}$$

The performance variation factors for pressures are shown in Table 2.4. The base operating condition for the PCCS is at 0.3 MPa as noted in Table 2.4 by a value of unity for the multiplication factor. Also, as the pressure increases the performance of the PCCS improves. Thus, it is obvious why the ICS (which operates at a pressure of 7.4 MPa versus 0.3 MPa for the PCCS) has an energy removal capacity that is three times larger than the PCCS but has a smaller heat transfer surface area.

Table 2.4 Variation in PCCS Performance with Pressure in Drywell.

Pressure (Pa)	Multiplication Factors for PCCS Performance
0.000E + 00	0.0000
6.113E + 02	0.0000
5.000E + 04	0.0000
1.000E + 05	0.0000
1.500E + 05	0.4250
2.000E + 05	0.6660
2.500E + 05	0.8495
3.000E + 05	1.0000
3.500E + 05	1.1289
4.000E + 05	1.2425
4.500E + 05	1.3450
5.000E + 05	1.4386
6.500E + 05	1.6807
7.000E + 05	1.7518

Table 2.4 provides multiplication factors for performance variation for drywell pressures up to 0.7 MPa; however, it is recognized that the SBWR containment is predicted to fail at pressures greater than 0.65 MPa.

3. ICS Model

3.1 Introduction and Concept

The ICS (Isolation Condenser System) is a safety-related passive operating system designed to remove the core decay heat directly from the reactor vessel following reactor shutdown and isolation. It is described in Section 5.4.6 of the SBWR Standard Safety Analysis Report (SSAR) [1]. Unlike the PCCS, the ICS is not continuously in operation. A motor-operated valve must be opened (or, if power is lost, a nitrogen-operated bypass valve must open) in order to initiate operation of the ICS.

Flow through the ICS is first induced by the action of condensate draining from the condenser tubes into the reactor vessel annulus. The drainage draws in steam from the upper portion of the reactor vessel; this steam is condensed and returned to the vessel annulus. In the event that the ICS becomes "bound" by noncondensable gases, a vent line is provided to permit release of the gases trapped within the ICS to the pressure suppression pool.

The flow through the vent line is started and stopped by an active control system that continuously monitors the reactor vessel pressure. Once the vessel pressure reaches the vent opening setpoint (implying the ICS is bound), the valves on the vent line open allowing the accumulated noncondensable gases to escape to the pressure suppression pool, thereby reinitiating operation of the ICS.

The vent line valves are signaled to close once the vessel pressure has decreased below the reset (closing) setpoint for the vent. A time delay circuit is integrated into the logic to protect the vent valves from excessive cycling.

The ICS modeling concept is the same as for the PCCS in that it is recognized that it is not a purpose of the MELCOR code to predict ICS performance based upon first principles. Rather, based upon the available experiment evidence, MELCOR should adequately represent the effects of the ICS heat exchanger-condenser system under the boundary conditions that would be imposed by accidents.

3.2 Operation of the ICS Model

The same basic algorithms, contained in Subroutine CNDRN1, are used to model both the ICS and the PCCS. There is, however, a block of coding specific to the ICS. This coding block mimics the operation of the ICS vent line control logic, which has no counterpart within the PCCS (the flow through the PCCS vent line is limited only by the submergence depth of the vent line in the pressure suppression pool). The following is a description of the significant differences between the operating characteristics of the ICS and the PCCS and the logic enhancements required to represent the ICS.

CND Package Reference Manual

The ICS operates at pressures near normal reactor vessel pressure, approximately 7 MPa, as compared to the PCCS, which operates at post accident drywell pressures of less than 0.50 MPa.

Because of the difference in operating pressures, allowances had to be made in the calculation of the vent line capacity to limit the flow to sonic velocity (choked flow) at the exit conditions. This was done by the use of the Modified Darcy Formula taken from the Crane Technical Paper No. 410.[4] The Darcy Formula estimates a mass flow rate for compressible flow using a net expansion factor through the pipe and the differential pressure between the reactor vessel and the choke point at the pipe exit. (The pressure at the exit condition can be easily determined if the flow is choked.) The determination of the net expansion factor serves to limit the flow through the pipe to sonic velocity at the pipe exit conditions.

The mass flow rate is determined in a subroutine CNDICF, which is used for both the PCCS and the ICS vent line flow calculations. CNDICF first determines the resistance coefficient for the vent line. Using the resistance coefficient, the maximum net expansion factor and the maximum $\Delta P/P$ for sonic velocity are found by interpolating between the values found on page A-22 of the Crane Technical Paper for a k value of 1.4. If the pressure in the PCCS/ICS minus the wetwell pressure divided by the PCCS/ICS pressure is greater than the value found for $(\Delta P)/P$, then the flow is choked. If the flow is not choked, then a linear interpolation is performed between zero and the calculated differential pressure to determine the net expansion factor. If the flow is choked, then the maximum $(\Delta P)/P$ is used to determine the pressure at the exit condition, and the net expansion factor is simply equal to its maximum value. The mass flow rate can then be estimated.

Because of the higher pressures at which the ICS condensers operate, the condenser tube walls are significantly thicker than for the PCCS condensers. This greater tube wall thickness may require a different performance degradation curve to represent system response to increases in noncondensable gas mole fractions. Provision is made for this new curve, when available, to be represented in the ICS set of user-input tabular functions, which are applied in a manner identical to the PCCS tabular functions described in detail in Section 2.3.

The heat removal capacity of a single ICS unit is at least 30 MW_t at a reactor pressure of 7.420 MPa (1050 psig) when fed by pure saturated steam. The large (factor of 3) increase in capacity over the PCCS is a direct result of the increase in steam density at reactor vessel pressure (where 1 m³ of steam contains approximately 8 times the mass of the same volume at drywell conditions). Therefore, the ICS has a greater amount of stored energy within the fluid contained in the condenser tubes.

As described in Section 3.1, the vent line for each ICS unit contains a motor-operated valve, which is actuated upon a high pressure within the reactor vessel such as would occur whenever the condenser tubes become bound with noncondensable gases.

Unlike the PCCS, the ICS condensers are not expected to operate after the equalization of reactor vessel and drywell pressures that would occur under accident conditions as a result of ADS actuation and DPV sequencing. This conclusion is not stated explicitly in the SSAR, but follows from information contained in Section 5.4.6 and the control diagrams provided in Volume 15 of the SSAR. The control diagrams indicate that the controllers for the vent line valves receive their signals for automatic operation from reactor vessel pressure sensors exclusively.

After blowdown, these controllers would no longer receive a high pressure signal since the vessel would be at the same pressure as the drywell. Thus, the ICS would quickly become bound by noncondensable gases with no provision for venting except by means of operator intervention. However, no guidance to the operator concerning this action can be found in the SBWR Emergency Procedure Guidelines (EPGs).

The drain line from the ICS returns condensate directly to the reactor vessel annulus. The elevation of the ICS condensers provides a sufficient gravity head so that the condensate will drain to the vessel annulus even though the annulus water level may be several meters above the condensate return line. A loop seal is provided in the drain line to prevent steam from entering the condensers via this line should the water level fall below the connection point to the reactor vessel.

3.3 Example Results

Several test calculations have been performed using the ICS model with two units in operation for various accident sequences. The accident sequences considered are loss of offsite power (station blackout), a main steam line LOCA, and a break in the bottom head drain line. For the station blackout calculation, the ICS was predicted to operate continuously and to cause depressurization of the reactor vessel without SRV or ADS actuation, thus preventing loss of reactor coolant inventory and circumventing core degradation.

For the bottom head LOCA calculation, the ICS was predicted to operate until shortly after ADS actuation, when drywell atmosphere begins to be pulled into the reactor vessel (through the open DPVs) as the water drains from the bottom of the vessel. Subsequently, the presence of noncondensable gases within the reactor vessel causes rapid binding of the IC condenser tubes and without vent actuation, ICS operation terminates. The main steam line LOCA calculation shows a similar behavior with the ICS slowly becoming bound with the noncondensable gases that arise from hydrogen generation in the core and from the small amount of drywell atmosphere that mixes with the reactor vessel atmosphere after vessel depressurization.

CND Package Reference Manual

To test the logic of the vent line control valve, additional calculations were performed in which a large amount of nitrogen was arbitrarily placed into the reactor vessel upper head for the station blackout and for the main steam line LOCA accident sequences. This provides an overpressure of noncondensable gas such that the vessel water is initially subcooled. The large noncondensable gas mole fraction at the isolation condenser inlet limits the ICS capacity (while operating) to a value insufficient to remove the decay heat. These test calculations show a very short period of ICS operation prior to binding.

Because of the inability of the ICS to remove any energy while bound, the calculated pressure in the reactor vessel increases until the vent valve opening setpoint is reached. The vent valve then opens to remove noncondensable gases from the ICS tubes to the wetwell and thereby restore ICS operation. While the vent line is open, the pressure in the reactor vessel decreases slightly, which leads to closing of the vent valve.

This predicted cyclic behavior continues with increasing frequency until the water within the reactor vessel reaches the saturation temperature and the rate of vessel pressurization increases markedly. Subsequent ICS vent actuation does not provide sufficient gas release through the small vent line to prevent the increasing vessel pressure from reaching the SRV opening setpoint. The action of opening the SRVs forces most of the nitrogen out of the reactor vessel and reduces the noncondensable gas mole fraction from approximately fifty percent to less than one percent. This produces a steam-rich environment within the ICS so that operation can resume.

For the main steam line LOCA, the ICS also becomes quickly bound, but flow through the break removes most of the imposed nitrogen from the reactor vessel. However, the break flow also serves to prevent the reactor vessel pressure from ever increasing above the vent valve opening setpoint; therefore, the ICS remains bound after operating for only a short time after the accident is initiated. (Possible operator action to remote-manually open the vent valve was not considered in this calculation.)

Similar to the PCCS, the ICS efficiency will degrade as the pressure in the reactor vessel decreases. To estimate this degradation, the same methodology described in Section 2.6 is utilized.

The multiplication factors for variation in performance for pressures are shown in Table 3.1. (Factors greater than unity signify an improvement in performance.) The base operating condition for the ICS is at 7.4 MPa as noted in Table 3.1 by a value of unity for the multiplication factor.

Table 3.1 Variation in ICS Performance with Pressure in the Reactor Vessel

Pressure (Pa)	Multiplication Factors for ICS Performance
0.000E + 00	0.0000
6.113E + 02	0.0000

CND Package Reference Manual

Pressure (Pa)	Multiplication Factors for ICS Performance
5.000E + 04	0.0000
1.000E + 05	0.0000
1.500E + 05	0.1080
2.000E + 05	0.1692
2.500E + 05	0.2159
3.000E + 05	0.2541
3.500E + 05	0.2869
4.000E + 05	0.3157
4.500E + 05	0.3418
5.000E + 05	0.3655
6.500E + 05	0.4271
7.000E + 05	0.4451
7.500E + 05	0.4624
8.000E + 05	0.4787
8.500E + 05	0.4943
9.000E + 05	0.5092
9.500E + 05	0.5237
1.000E + 06	0.5376
1.100E + 06	0.5643
1.200E + 06	0.6507
1.300E + 06	0.6139
1.400E + 06	0.6368
1.500E + 06	0.6591
1.750E + 06	0.6661
2.000E + 06	0.6980
2.250E + 06	0.7259
2.500E + 06	0.7512
3.000E + 06	0.7956
3.500E + 06	0.8328
4.000E + 06	0.8645
5.000E + 06	0.9159
6.000E + 06	0.9556
7.000E + 06	0.9883
7.200E + 06	0.9942
7.400E + 06	1.0000
7.600E + 06	1.0054
7.800E + 06	1.0106
8.000E + 06	1.0156
8.200E + 06	1.0204
8.400E + 06	1.0252
8.600E + 06	1.0298
8.800E + 06	1.0340
9.000E + 06	1.0381
1.000E + 07	1.0568

4. Interface with MELCOR

The information for the condensers is stored in the ESF Package of the MELCOR database contiguous to the information for the FCL Package. A special routine to process PCCS/ICS model input has also been added for use in calculations for which these models are to be exercised. These modifications to the MELCOR database are bypassed (as are the PCCS/ICS model routine CNDRN1) unless the PCCS and/or ICS input cards are included in the MELGEN input deck.

If the user requests that the PCCS model be invoked for a calculation, then it is necessary that the control volume numbers representing the drywell, wetwell, ICS/PCC pool, and the Gravity-Driven Cooling System (GDCS) be provided on a dedicated MELGEN input card. If the user does not provide this card, the PCCS model will be bypassed. An additional dedicated card is required to indicate the tabular functions that represent the PCCS performance adjustments (depending upon operating parameters).

If the ICS model is to be exercised in a calculation, the user must provide the control volume numbers for the reactor vessel upper head and annulus, ICS/PCC pool(s), and the wetwell. Similar to the case for the PCCS, if the input card carrying this information is not provided, the ICS model will be bypassed.

A few simple descriptive input numbers for the PCCS and/or ICS are also required when these models are to be exercised. This special input consists of the volume of the condensers, the source line volume, the basic capacity of one unit of the condensers, and the dimensions of the vent line (minimum diameter and equivalent length) used in determining the mass flow. The user also inputs the number of units (maximum of three) that are to be considered to be operating.

For the ICS, the setpoints for the vent valve control logic are also required. The number of operating condensers may be changed during the course of a calculation. The CND Package Users' Guide describes the input to both MELGEN and MELCOR required for operation of the PCCS and/or ICS models, and the plot variables and associated special external data files that may be created.

Because the condenser is part of the ESF Package, the condenser energy balance does not have a separate listing under the GLOBAL energy balance edit, but rather is combined with the FCL Package so that an overall ESF energy balance is given. Currently, however, the FCL Package does not have a separate energy balance so the energy balance for the ESF Package represents the condenser package exclusively. For a typical calculation, a relative energy error of approximately 1×10^{-7} percent is produced.

References

1. SBWR Standard Safety Analysis Report (SSAR), GE Nuclear Energy, 25A5113 Rev. A, (1992).
2. H. Nagasaka et al., *Heat Removal of Isolation Condenser Applied as a Passive Containment Cooling System*, of the Nuclear Energy Group, Toshiba Corporation (1990).
- 3 J.P. Holman, *Heat Transfer*, McGraw-Hill, Inc., New York, (1963).
4. "Flow of Fluids through Valves, Pipes, and Fittings," Technical Paper 410, Crane Co., Chicago, IL (1969).